Graduate School ETD Form 9
(Revised 12/07)

PURDUE UNIVERSITY
GRADUATE SCHOOL
Thesis/Dissertation Acceptance

This is to certify that the thesis/dissertation prepared

By Matthew L. Garner

Entitled
Design, Synthesis and Study of DNA-Targeted Benzimidazole-Amino Acid Conjugates

For the degree of Master of Science

Is approved by the final examining committee:

Dr. Eric C. Long
Chair

Dr. Martin J. O'Donnell

Dr. Rob E. Minto

To the best of my knowledge and as understood by the student in the *Research Integrity and Copyright Disclaimer (Graduate School Form 20)*, this thesis/dissertation adheres to the provisions of Purdue University's "Policy on Integrity in Research" and the use of copyrighted material.

Approved by Major Professor(s): Dr. Eric C. Long

Approved by: Dr. Martin J. O'Donnell 09/13/2012
Head of the Graduate Program Date

Graduate School Form 20
(Revised 9/10)

PURDUE UNIVERSITY
GRADUATE SCHOOL

Research Integrity and Copyright Disclaimer

Title of Thesis/Dissertation:

Design, Synthesis and Study of DNA-Targeted Benzimidazole-Amino Acid Conjugates

For the degree of Master of Science

I certify that in the preparation of this thesis, I have observed the provisions of *Purdue University Executive Memorandum No. C-22,* September 6, 1991, *Policy on Integrity in Research.**

Further, I certify that this work is free of plagiarism and all materials appearing in this thesis/dissertation have been properly quoted and attributed.

I certify that all copyrighted material incorporated into this thesis/dissertation is in compliance with the United States' copyright law and that I have received written permission from the copyright owners for my use of their work, which is beyond the scope of the law. I agree to indemnify and save harmless Purdue University from any and all claims that may be asserted or that may arise from any copyright violation.

Matthew L. Garner

Printed Name and Signature of Candidate

09/13/2012

Date (month/day/year)

*Located at http://www.purdue.edu/policies/pages/teach_res_outreach/c_22.html

DESIGN, SYNTHESIS AND STUDY OF DNA-TARGETED BENZIMIDAZOLE-AMINO ACID CONJUGATES

A Thesis

Submitted to the Faculty

of

Purdue University

by

Matthew L. Garner

In Partial Fulfillment of the

Requirements for the Degree

of

Master of Science

December 2012

Purdue University

Indianapolis, Indiana

Dedicated to my family and friends

ACKNOWLEDGMENTS

I would like to acknowledge my mentor Dr. Eric C. Long and thank him for assisting and directing my trip through graduate school. I would also like to specially thank Dr. Tax Georgiadis for his friendship and all his assistance in the laboratory performing syntheses, purification, and analysis. My friend and fellow graduate student, David Ames, was also very helpful through the process of purifying my compounds as well as our trip through graduate courses, I am grateful to have him as a friend.

I would like to thank Dr. Martin J. O'Donnell and Dr. Robert E. Minto for serving on my graduate committee. Dr. Karl Dria and Cary Pritchard were also both helpful in training, advising, and troubleshooting instrumentation and are due considerable thanks. Also, I would like to thank Kitty O'Doherty and Beverly Hewitt for all their assistance through my time at IUPUI.

Dr. Ryan Denton was also a great friend and advisor through the time I spent teaching labs for him and is due considerable thanks as well. Wai Ping Kam is another friend gained during my time in graduate school that helped and offered me advice throughout the process of teaching labs.

I would like to thank my parents, sister, family, and friends for all their love, support, and encouragement throughout my time in graduate school. Finally, I would like to thank my lovely girlfriend, Amanda Hardwick, for all her support and belief in me throughout my time at IUPUI. I am truly blessed to have such wonderful people in my life and without them I wouldn't have been able to obtain this degree.

TABLE OF CONTENTS

Page

Page

LIST OF TABLES

LIST OF FIGURES

Figure Page

LIST OF ABBREVIATIONS

ACN	acetonitrile
Ala	alanine
Arg	arginine
Asn	asparagine
Asp	aspartic acid
BI	benzimidazole
Boc	di-tert-butyl dicarbonate
bp	base pair
CT-DNA	calf thymus DNA
Cys	cysteine
DCM	dichloromethane
DIC	diisopropylcarbodiimide
DMF	dimethylformamide
DMSO	dimethyl sulfoxide
DNA	deoxyribonucleic acid
EtBr	ethidium bromide
EtOAc	ethyl acetate
EtOH	ethanol
Fmoc	fluorenylmethoxycarbonyl
FID	fluorescence intercalator displacement

Gln	glutamine
Glu	glutamic acid
Gly	glycine
His	histidine
HOBt	1-hydroxybenzotriazole
HPLC	high performance liquid chromatography
HT-FID	high-throughput fluorescence intercalator displacement assay
Ile	isoleucine
LC/MS	liquid chromatography mass spectrometry
Leu	leucine
Lys	lysine
MeOH	methanol
Met	methionine
mRNA	messenger ribonucleic acid
NMR	nuclear magnetic resonance
Phe	phenylalanine
Pro	proline
Ser	serine
TFA	trifluoroacetic acid
Thr	threonine
TLC	thin-layer chromatography
TRIS	tris(hydroxymethyl)aminomethane
Trp	tryptophan
Tyr	tyrosine

UV	ultraviolet
Val	valine
Xaa(s)	any amino acid(s)
Xaa-BI-(+)	any amino acid-benzimidazole-amidine

ABSTRACT

Garner, Matthew L. M.S., Purdue University, December 2012. Design, Synthesis and Study of DNA-Targeted Benzimidazole-Amino Acid Conjugates. Major Professor: Eric C. Long.

The DNA minor groove continues to be an important biological target in the development of anticancer, antiviral, and antimicrobial compounds. Among agents that target the minor groove, studies of well-established benzimidazole-based DNA binders such as Hoechst 33258 have made it clear that the benzimidazole-amidine portion of these molecules promotes an efficient, site-selective DNA association. Building on the beneficial attributes of existing benzimidazole-based DNA binding agents, a series of benzimidazole-amino acid conjugates was synthesized to investigate their DNA recognition and binding properties. In this series of compounds, the benzimidazole-amidine moiety was utilized as a core DNA "anchoring" element accompanied by different amino acids to provide structural diversity that may influence DNA binding affinity and site-selectivity. Single amino acid conjugates of benzimidazole-amidines were synthesized, as well as a series of conjugates containing 20 dipeptides with the general structure Xaa-Gly. These conjugates were synthesized through a solid-phase synthetic route building from a resin-bound amino acid (or dipeptide). The synthetic steps involved: (1) the coupling of 4-formylbenzoic acid to the resin-bound amino acid (via diisopropylcarbodiimide and hydroxybenzotriazole); followed by (2) introduction of a 3,4-diaminobenzamidoxime in the presence of 1,4-benzoquinone to construct the benzimidazole ring; and, finally, (3) reduction of the resin-bound amidoxime functionality to an amidine via treatment with 1M $SnCl_2 \cdot 2H_2O$ in DMF before cleavage of final product from the resin. The synthetic route developed and employed was simple and straightforward except for the final reduction that proved to be very arduous. All target compounds were obtained in good yield (based upon weight), averaging 73% mono-amino acid and 78% di-amino acid final compound upon cleavage from resin.

Ultimately, the DNA binding activities of the amino acid-benzimidazole-amidine conjugates were analyzed using a fluorescent intercalator displacement (FID) assay and calf thymus DNA as a substrate. The relative DNA binding affinities of both the mono- and di-amino acid-benzimidazole-amidine conjugates were generally weaker than that of netropsin and distamycin with the dipeptide conjugates showing stronger binding affinities than the mono-amino acid conjugates. The dipeptide conjugates containing amino acids with positively charged side chains, Lys-Gly-BI-(+) and Arg-Gly-BI-(+), showed the strongest DNA binding affinities amongst all our synthesized conjugates.

CHAPTER 1. STRUCTURE OF B-FORM DNA AND MINOR GROOVE RECOGNITION BY LOW MOLECULAR WEIGHT COMPOUNDS

1.1. Overview

The DNA minor groove has been an important focus of chemical and biological studies since the elucidation of the structure of DNA and an understanding of the role of DNA in the life cycle of a cell. The interaction of small molecules with DNA is also a prolific area of study because many therapeutically important molecules bind reversibly to nucleic acids.[1-6] It is commonly believed that minor groove binding compounds disrupt normal cellular functions by binding near or at promoter regions of genes, altering transcription[7] or disrupting DNA replication. Thus, much effort has been directed toward the discovery of low molecular weight compounds that recognize and bind to DNA due to their potential use as anticancer, antiviral, and antimicrobial drugs.[7-10] In addition, the development of sequence-specific and sequence-selective DNA binding molecules is a research goal that is important for understanding nucleic acid molecular recognition due to the ability of these agents to act as nucleic acid conformational probes and footprinting reagents.[11,12] In general, low molecular weight ligands recognize DNA using a combination of weak intermolecular forces such as electrostatics, van der Waals forces, and hydrogen bonding; DNA binding can ultimately occur through ligand interactions with the minor groove, phosphodiester backbone, and stacked Watson-Crick base pairs.

As will be discussed, the structural basis for the design of many man-made DNA minor groove binding ligands originates from naturally occurring peptide-based compounds such as netropsin, distamycin, actinomycin, and echinomycin.[13-16] These compounds have provided a starting point for many drug design efforts including synthetic polyamides.[17] Also, benzimidazole derivates[18] have displayed exceptional DNA binding abilities and may provide a useful moiety for drug design. Some important features of molecules that bind to the minor groove of B-DNA like those mentioned above are: (1) a crescent shape complementary to the curvature of the minor groove; (2)

positive charges that enhance electrostatic interactions; (3) inward-facing hydrogen-bonding groups for sequence recognition; and (4) an unfused heterocyclic structure that allows flexible structural optimization of the compound for minor groove interactions.[19] These guidelines have aided in the design of minor groove binding heterocycles with strong minor groove binding interactions and biological activities.[20-21] While we note the importance of shape complementarity, more recent studies also emphasize that the shapes of compounds do not have to exactly match the curvature of the minor groove to yield strong sequence-specific binding, as well as the usefulness of nitrogen containing heterocycles for minor groove recognition.[22] All of these factors were considered in the design of our minor groove binding agents to be described herein.

This thesis will describe a series of mono- and di-amino acid-benzimidazole-amidine conjugates designed to target the minor groove of B-form DNA. A phenyl-benzimidazole core structure will be included to provide hydrogen-bonding sites as well as allowing an overall molecular curvature that closely resembles that of the minor groove. In addition, by introducing amino acids, we will place in position: (1) amide bonds that can serve as auxiliary hydrogen-bonding sites to interact with the DNA minor groove, and (2) side-chains that introduce structural and chemical diversity. Finally, an amidine group will provide a positively charged moiety that can interact electrostatically with the negatively charged phosphodiester backbone of DNA. Positively charged moieties are usually attracted to A/T-rich regions of DNA that have a slightly increased electrostatic potential than regions of G•C base pairs.

1.2. Introduction to DNA Structure

1.2.1. Overview

The “Central Dogma of Molecular Biology” (Figure 1.1) outlines the role of DNA in living organisms[23] and the role of DNA in replication and protein expression. DNA contains all the genetic information that controls the synthesis and regulation of protein expression in a cell. DNA has two main functions: (1) to provide a template for its own replication during cell division and (2) to direct transcription of complementary strands of messenger ribonucleic acid (mRNA) and other RNAs.[24] Upon the initiation of protein expression, DNA is initially transcribed into an mRNA template that is processed and

transported to a ribosome where the mRNA is used as a direct read-out template containing a triplet code specifying the amino acids of a specific protein. DNA thus encodes all of the sequence information of a protein and dictates the sequences where proteins bind to regulate these processes.[25] Therefore, DNA is a vital "database" of all genetic information, and this information must be duplicated during replication every time a cell undergoes mitosis. The central roles played by DNA makes it a very good target for low molecular weight ligands that may be able to alter or inhibit these processes due to their potential ability to bind to DNA. To better understand what molecular characteristics would be favorable for targeting DNA as a drug receptor, it is important to understand the structure of DNA itself.

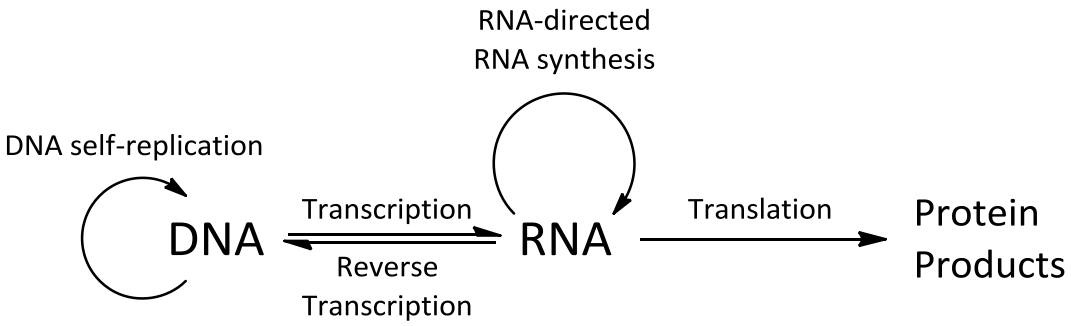

Figure 1.1. The "Central Dogma of Molecular Biology."

1.2.2. Structure of B-Form DNA

DNA is composed of two phosphodiester-linked nucleotide strands that align in an anti-parallel fashion and ultimately form a double helical structure.[23] The interior of the DNA helix contains stacked base pairs of purines and pyrimidines that are attached to the C1′ of the ribose ring via an *N*-glycosidic bond and interact with each other via hydrogen bonds to form Watson-Crick base pairs (Figure 1.2). Watson-Crick base pairs are composed of a purine (adenine or guanine) and a pyrimidine (thymine or cytosine) nucleobase. More specifically, adenine (A) and thymine (T) are hydrogen-bonding partners and cytosine (C) and guanine (G) are hydrogen-bonding partners. A•T pairs are formed via two hydrogen bonds, and G•C pairs are formed via three hydrogen bonds (Figure 1.3). These base pairs are isostructural and can replace one another without altering the position of the C1′ atom in the sugar-phosphate backbone.[24] Also, Watson-Crick base pairs can be exchanged without disturbing the double helix (change G•C to

C•G or A•T to T•A). As a consequence of helix formation, the bases occupy the core of the helix and the sugar-phosphate chains are coiled about its periphery, thereby minimizing the repulsions between charged phosphate groups. The negative charges of each phosphodiester bond result in an anionic polymer backbone. Thus, electrostatics play a major role in the binding of low molecular weight ligands and proteins to DNA.

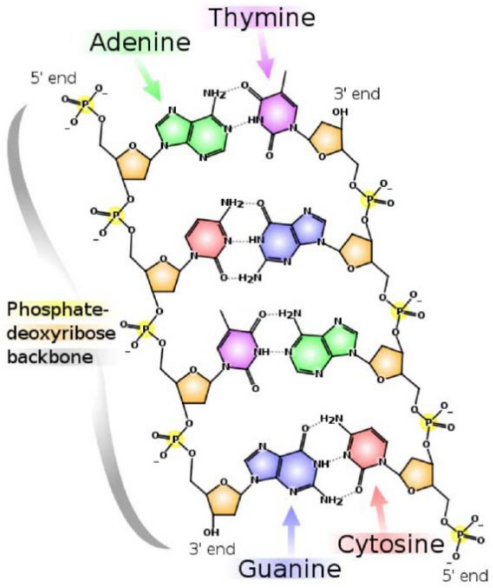

Figure 1.2. Primary structure of DNA.

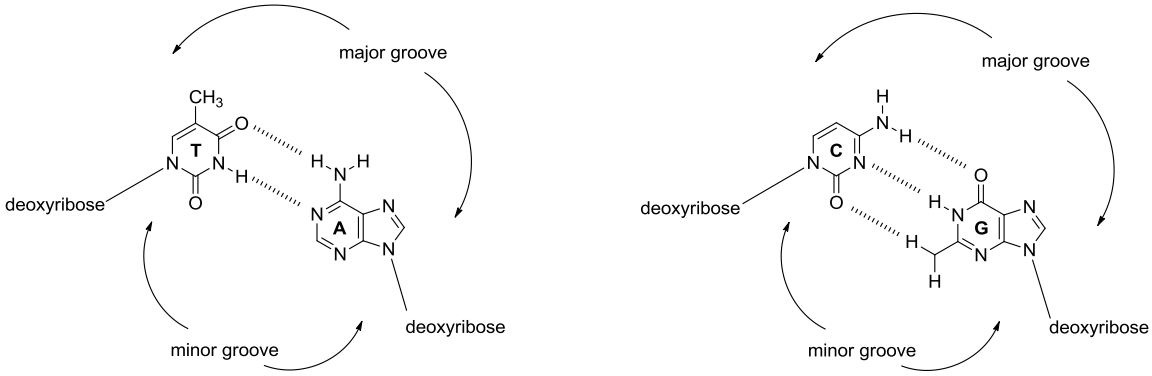

Figure 1.3. A•T and G•C Watson-Crick base pairs of DNA.

DNA can adopt three major polymorphs: A-form, B-form, and Z-form (Figure 1.4)[25], of which B-form is the most relevant under physiological conditions (pH 7.2, 0.15 M NaCl). B-DNA is a right-handed double helix with approximately 10 nucleotides per helical turn. The π-π stacked nucleobases are nearly perpendicular to the helix axis of B-DNA. In comparison, A-DNA is wider than B-DNA and has base pairs inclined to its helix axis instead of perpendicular to it; and Z-DNA is a left-handed helix whose repeat units are dinucleotides that lead to a "zigzag" backbone.[25] The conformation adopted by DNA depends upon the hydration level, DNA nucleotide sequence, and chemical modification of the bases. Overall, DNA can exhibit several different conformations in different sequence segments.[25,26]

Figure 1.4. Structures of A, B, and Z-DNA (left to right).[25]

The double helix structure of DNA leads to two asymmetrical exterior grooves that run between the anionic backbones and constitute opposite sides of each base pair plane. In B-DNA, there is a wide and deep major groove and a narrow and deep minor groove (Figure 1.5) that results from the asymmetric connection of the Watson-Crick base pairs to the phosphate backbone.[27] The edges of the stacked base pairs constitute the floor of the grooves and present different hydrogen-bond acceptors and donors to ligands. In general, the major groove is the preferred recognition site for proteins because its width accommodates bulkier ligands and makes the groove floor accessible

for the binding functionalities of a protein to interact with the stacked edges of the base pairs. The edges of A•T and G•C base pairs provide three possible hydrogen-bonding sites within the DNA major groove. There are two hydrogen-bond acceptors (adenine-N7 and thymine-O4) and one hydrogen-bond donor (adenine-N6) for A•T base pairs, and there are two hydrogen-bond acceptors (guanine-N7 and guanine-O4) and one hydrogen-bond donor (cytosine-N4) for G•C base pairs.[28] Bulky proteins generally identify bases in the major groove for their site-specific binding, often using α-helical structural elements in their binding and DNA recognition.

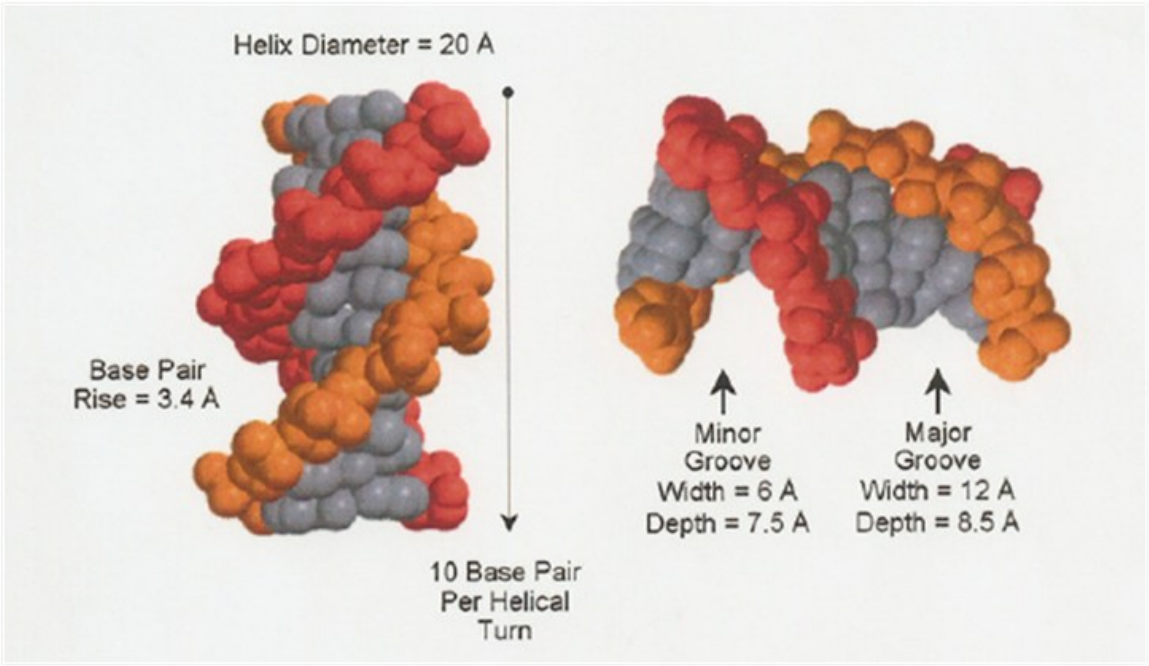

Figure 1.5. Structure of the B-form DNA double helix.[25]

The narrower minor groove is most often the target for small molecules as opposed to bulkier proteins. Small molecules can fit snuggly into the minor groove, which is narrower in regions of high A•T content (6 Å), than regions of high G•C content (12 Å), allowing for increased surface contact and enhanced binding affinity. There are, however, fewer functionalities for nucleobase recognition in comparison to the major groove: G•C base pairs contain only three accessible hydrogen-bonding sites in the minor groove and A•T base pairs contain two hydrogen-bond acceptors (adenine-N3 and thymine-O2).[28] X-ray studies have shown that the exocyclic N2 amino group of guanine

is often a hydrogen-bond donor group.[29] However, this same amino group also appears to disrupt the association of DNA minor groove binders in G/C-rich regions by protruding from the floor of the groove, preventing a close association that would otherwise occur in deeper A/T-rich regions. Conceptually, the three sites in G•C base pairs would compare favorably to the two of A•T base pairs, but studies have demonstrated that many binders prefer A•T sites. This suggests that hydrogen bonding is not the sole determinant for sequence recognition within the DNA minor groove. It is likely that electrostatic potential is of great importance for minor groove recognition as a series of A•T base pairs has a greater negative electrostatic potential at the floor of the groove than that of G•C base pairs.[7] The more negative electrostatic potential of A•T base pairs is likely the reason positively charged ligands prefer A/T-rich regions to G/C-rich regions.

Much effort has been expended towards understanding the structure of DNA and its potential drug binding sites. It has been established that ligand-DNA binding commonly occurs through a combination of electrostatics, van der Waals forces, and hydrogen bonding. The negatively charged phosphodiester backbone forms complexes with low molecular weight ligands with positive charges through electrostatic interactions; the formation of the Watson-Crick base pairs results in the presence of hydrophobic features along the walls of the groove. Knowledge of the numerous binding sites in DNA and the methods known DNA binders use to bind to DNA aids our attempts to develop new molecules with increased binding affinity and specificity. This thesis will focus on utilizing low molecular weight ligand-DNA interactions of the minor groove in our design of amino acid-benzimidazole-amidine conjugates as possible DNA minor groove binding ligands.

1.3. DNA Ligand Binding Modes

There are several DNA-ligand binding modes, including (1) exterior surface binding which is mainly electrostatically driven, (2) intercalation, and (3) groove binding to either the major or minor groove. DNA intercalators are typically positively-charged, rigid, planar aromatic compounds that insert between two adjacent stacked Watson-Crick base pairs (Figure 1.6)[30] resulting in the DNA and binder undergoing conformational changes upon their interaction, often leading to distortion of the DNA helix in DNA-ligand complexes.[31] In DNA, intercalation is a two-stage process including

(1) an initial diffusion-controlled association of the intercalator with the exterior of the helix followed by (2) a slower insertion of the intercalator between stacked base pairs. When intercalation occurs, the flanking base pairs must separate approximately 0.3 nm, causing structural changes in the DNA which can lead to inhibition of transcription and replication. Intercalators can also resemble another base pair and cause enzymes to make errors in transcription, resulting in the addition of an extra base that alters the triplet code generating an altered sequence. Therefore, many intercalators are powerful mutagens and in some cases can be used in chemotherapeutic treatments to inhibit cancer cell replication.[12,32,33] Ethidium bromide and thiazole orange (Figure 1.7) are two common intercalating dyes that display enhanced fluorescence upon DNA binding. These agents are also important dyes for measuring DNA binding affinity of ligands in fluorescent intercalator displacement (FID) experiments[34,35] or to visualize DNA fragments in agarose gel electrophoresis.[36,37]

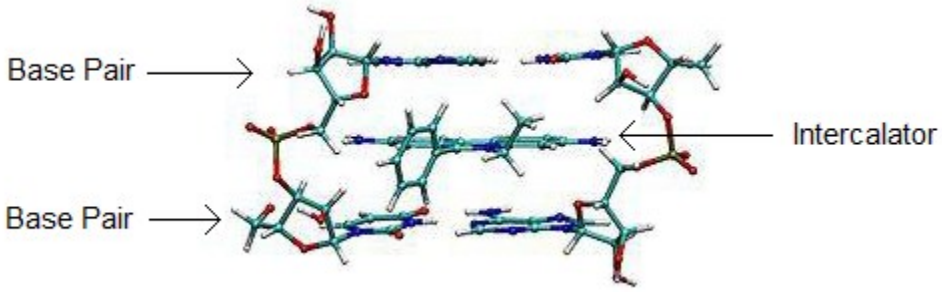

Figure 1.6. Ethidium bromide intercalated between two DNA base pairs.

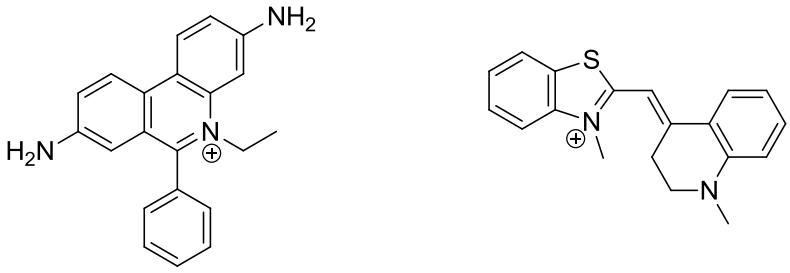

Ethidium Bromide Thiazole Orange

Figure 1.7. Structures of ethidium bromide and thiazole orange.

There are many factors involved in DNA minor groove binding, thus only the major influences will be discussed. The natural products netropsin and distamycin have played an integral role in understanding these mechanisms of small molecule-DNA minor groove recognition. An early crystal structure of netropsin bound to DNA revealed that minor groove binding occurs when netropsin aligns along the groove cleft of B-DNA and forms hydrogen bonds with the floor of the groove.[38] Overall, small molecule DNA recognition occurs through a combination of electrostatic interactions with the phosphodiester backbone, hydrogen bonding to the nucleobases, van der Waals contact with the walls of the groove, hydrophobic interactions, and steric hindrance to influence the mode of ligand binding to DNA.[39] The sugar-phosphate backbone of DNA, which is negatively charged, is attractive to positively charged ligands which results in an increase of ligand concentration near DNA from bulk solution. As stated earlier, A•T regions of B-DNA have greater negative potential than those of G•C regions due to the presence of electron rich thymine-O2 and adenine-N3 as well as the narrowed groove width, making A•T regions targets for positively charged ligands. Therefore, minor groove binding ligands typically have at least one positively charged group to enhance its A•T site selectivity as well as binding affinity.

The width, structurally, of the groove around the helix can also play a part in the minor groove binding of ligands to DNA. In regions of high A•T content, the groove is narrower, whereas regions of high G•C content have a wider groove due, as noted earlier, to the exocyclic group of guanine. An x-ray structure of netropsin bound to DNA suggest the exocyclic group protrudes from the floor of the minor groove and causes steric hindrance that interferes with binding in regions of high G•C content.[40] Many minor groove binders are elongated structures that contain multiple hydrogen-bonding functionalities, therefore the narrower groove in A/T-rich regions contributes to the hydrophobic contacts made with the surfaces of small molecules.[41] The narrower groove in A/T-rich regions aids in aligning small molecules so that hydrogen-bonding groups are directly exposed to the floor of the groove, whereas the wider groove in G/C-rich regions does not provide the tight fit to aid in binding by planar ligands.

1.4. Examples of DNA Minor Groove Binding Ligands

1.4.1. Netropsin

Netropsin, a natural product observed to bind to the minor groove of B-DNA, is a polyamide that has been shown to display *in vitro* antiviral activity, but is not administered clinically due to its high toxicity.[42] Netropsin (Figure 1.8) consists of two carboxamide-linked *N*-methylpyrrole units with two positively-charged terminal groups, a guanidinium and an amidinium that aid in binding to the DNA minor groove.[43,44]

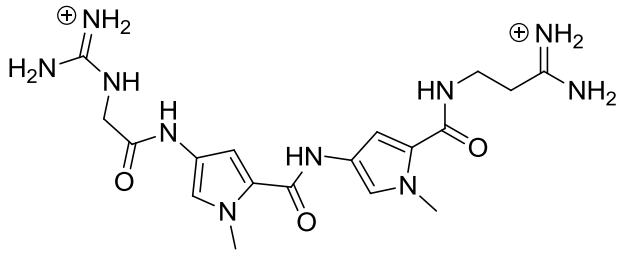

Netropsin

Figure 1.8. Structure of netropsin.

Crystal structures of netropsin bound to A/T-rich regions of DNA have shown that binding occurs when netropsin aligns in the minor groove of DNA and forms hydrogen bonds within the groove (Figure 1.9).[10,45-47] When bound to DNA, netropsin adopts a crescent shape that nicely complements the curvature of the minor groove for a span of four base pairs and there is a combination of non-covalent interactions that further contribute to binding; these have been confirmed by NMR and X-ray studies.[8,9] The positively charged amidinium and guanidinium facilitate delivery of the ligand to the minor groove. Upon docking, hydrophobic contacts between the ligand and the minor groove walls leads to an affinity-enhancing interaction and hydrogen bonding occurs between the amide hydrogens and the adenine-N3 or thymine-O2. An illustration of the hydrogen bonds formed between netropsin and the minor groove is presented in Figure 1.10.[48] The roles of the positively charged ends of the ligand as well as the hydrogen bonding that occurs in the groove are both ideas that are central to the development of our amino acid-benzimidazole-amidine conjugates.

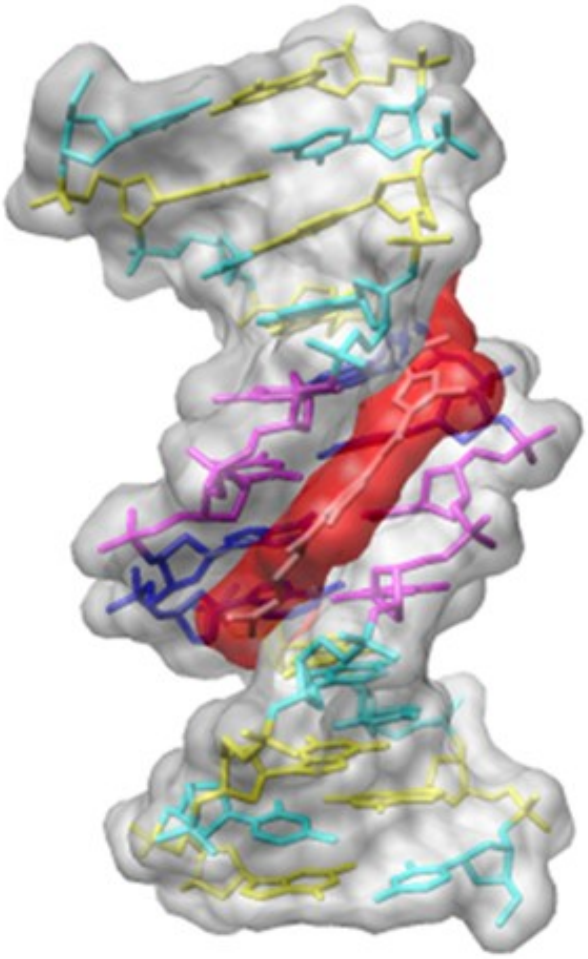

Figure 1.9. Netropsin bound to the minor groove of 5′-AATT DNA.[10]

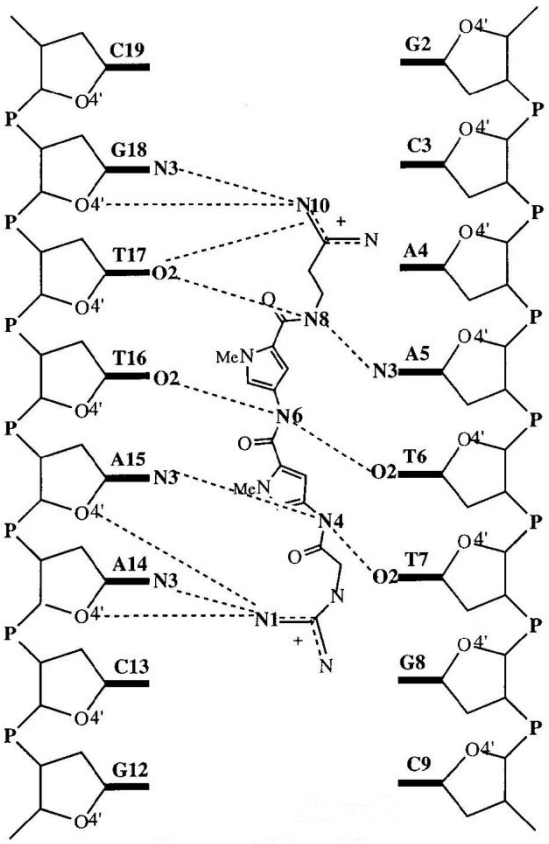

Figure 1.10. Hydrogen bonding observed between netropsin and the AATT oligonucleotide.[48]

It has been established that netropsin prefers to bind to A/T-rich regions of the DNA minor groove, and FID studies have given further details about the preferred binding sites of netropsin to DNA (Figure 1.11).[49] The FID analysis of netropsin yielded merged-bar histograms of the rank-ordered 136 hairpin, four-base pair library with a steep plot curvature associated with sequences that provide preferred binding sites as well as the expected horizontal and vertical displacement of the FID profile with increased netropsin concentration.[49] As expected, the A/T-only sequences were the preferred binding sites and 9 of 10 possible sequences were found within the first 11 sequences in the rank-order, further underscoring the A/T-preference of netropsin.

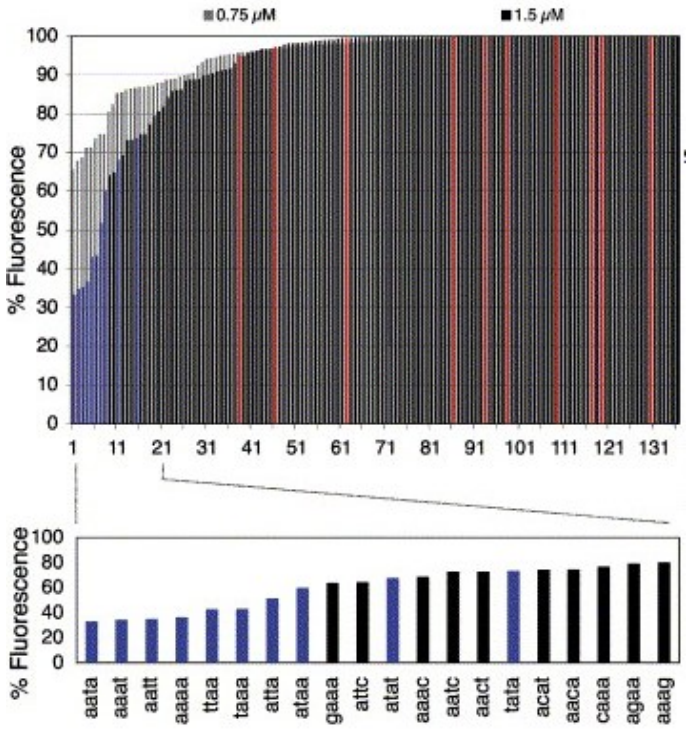

Figure 1.11. Merged-bar FID histogram of netropsin at 0.75 and 1.5 μM.[49]

1.4.2. Distamycin

Another example of a polyamide that binds preferentially to A/T-rich regions of the DNA minor groove is distamycin (Figure 1.12).[9] The structure of distamycin includes pyrrole groups linked by amide bonds with an N-terminal formyl group and a positively charged amidinium. Distamycin binds to DNA very similar to netropsin. Distamycin requires four A/T base pairs as established by NMR and X-ray studies.[49,50] DNA-distamycin binding at asymmetric sites is directional with the N-terminal formyl group pointing toward the 5' end of the A/T-rich strand. Along with 1:1 binding, two distamycin ligands can bind simultaneously to sites with at least five A•T base pairs. In these 2:1 complexes (Figure 1.13), two distamycin ligands are stacked side by side, and the positively charged end groups point in opposite directions.[51] The formyl group of each ligand lies at the 5' end of the adjacent strand. To accommodate the second ligand in this 2:1 motif, the minor groove must be widened by approximately 3.5 Å relative to the 1:1 complex. The 2:1 motif spans five base pairs, and in six-base-pair sites, 2:1 complexes rapidly slide between overlapping five-base-pair sites.[52-54] The relative

binding constants of the ligands and the preference for the 2:1 over the 1:1 mode varies significantly with the DNA sequence.

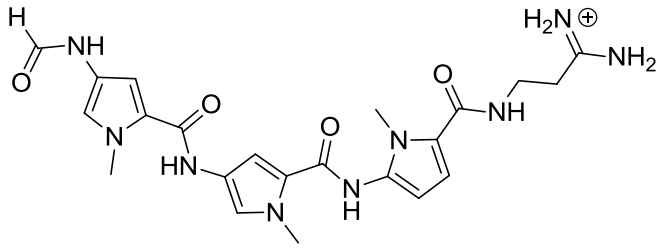

Distamycin

Figure 1.12. Structure of distamycin.

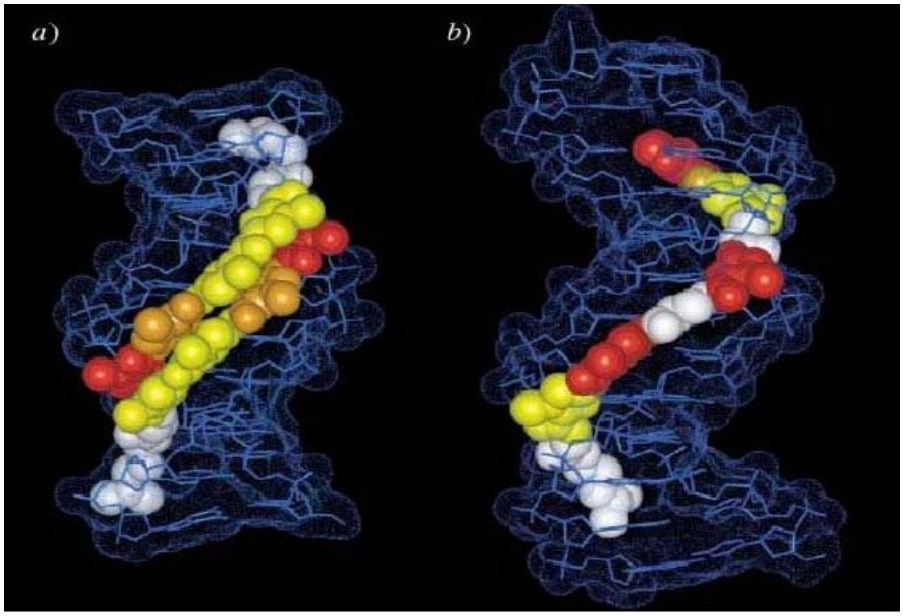

Figure 1.13. Structures of polyamides bound to DNA: (A) 2:1 motif, (B) 1:1 motif.[51]

Similar to netropsin, FID studies of distamycin show an expected increased affinity for regions rich in A•T bases in a 512-member library containing all possible 5 base pair combinations of nucleobases (Figure 1.14).[55] The FID histogram showed the presence of all but two five-bp A/T-sites in the top 45 sequences and all but two four-bp A/T-sites in the top 151 sequences. The top 50 sequences were comprised of 14 (of 16

possible, 88%) five-bp A/T-sites, 15 (of 32 possible, 47%) four-bp A/T-sites, 10 (of 80 possible, 13%) three bp A/T-sites, and 11 (of 176 possible, 6%) two bp A/T-sites, illustrating a preference for sites containing four or five A•T base pairs over sites with two or three base pairs.[55] These findings for distamycin, like those of netropsin, also point to the importance of having a positively charged moiety and many different hydrogen-bonding groups present in A•T selective minor groove binders.

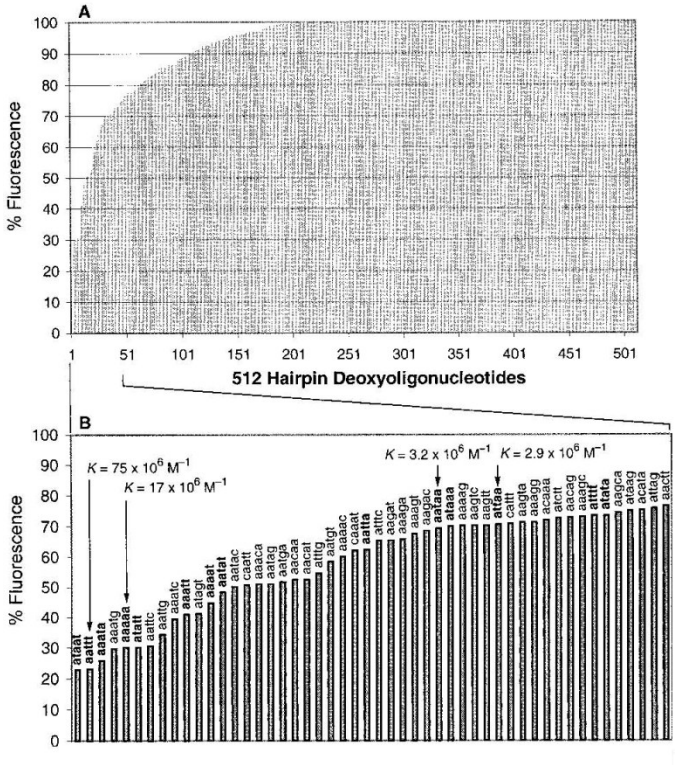

Figure 1.14. Merged-bar FID histogram of distamycin at 2.0 μM: (A) all 512 oligonucleotide sequences, (B) top 50 sequences showing highest affinity.[55]

1.4.3. Synthetic Polyamides

The natural products netropsin and distamycin and their A•T site selectivities have inspired the development of synthetic minor groove binders. It was proposed early on that netropsin and distamycin-like molecules could be developed to specifically recognize the guanidine exocyclic amino group through hydrogen bonding, thus expanding the DNA recognition of these agents to G•C containing regions.[56,57] Many such so-called lexitropsins, where methylimidazole rings are substituted for

methylpyrrole rings (Figure 1.15) were developed to introduce a guanidine-specific hydrogen-bond acceptor.[58-64] Unfortunately, these lexitropsins did not become G•C specific despite losing their preference for A•T sites. This is likely because there is still considerable A/T-site recognition inherent to the structure due to amide hydrogens and the positively charged terminal moiety as well as the overall shape of the ligand.

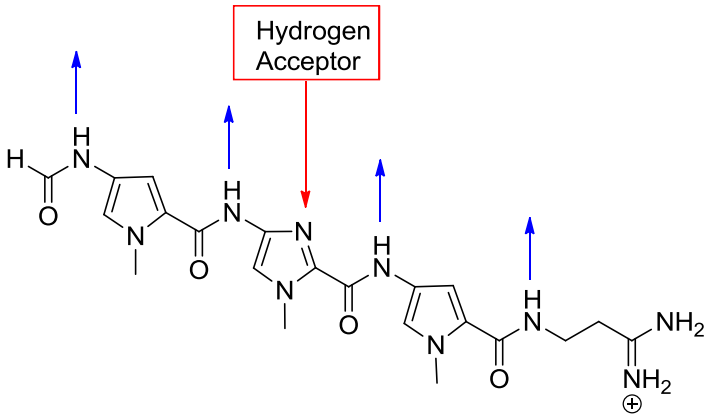

Figure 1.15. Lexitropsin 2-imidazole-distamycin with arrows indicating hydrogen accepting and donating groups in red and blue, respecitively.

Building upon the lexitropsins, a more recent polyamide design arose from the discovery of the 2:1 binding mode displayed by distamycin within the minor groove.[10] It was shown by NMR studies that two distamycin molecules could align in an antiparallel orientation in A/T-rich regions of the DNA minor groove,[65] and, similarily, two synthetic polyamides can fit side by side and form hydrogen bonds within the minor groove. This antiparallel side-by-side arrangement aligned the five-membered heterocycles against each other, allowing contact within the walls of the minor groove. Crystal structures of the DNA-polyamide complexes have shown that the spacing of polyamide rings matches the spacing of DNA base pairs.[66-68] Importantly, given this arrangement, the four Watson-Crick base pairs can be differentiated in the minor groove by the specific positions of their hydrogen-bond donors and acceptors.[69] A•T can be distinguished from T•A by utilizing the lone pairs of electrons on the thymine-O2. Therefore, side-by-side pairing allows for a specific pattern of hydrogen bonding.

Employing the above, Dervan *et al*. have shown that polyamides are amenable to synthetic manipulation, allowing their physical properties and minor groove interactions

to be controlled. Moreover, over two decades of work has gone into the development of hairpin polyamides and what has become known as the "Pairing Code."[10] This has led to a new model of sequence-specific recognition in the DNA minor groove. Polyamides are comprised of combinations of methylimidazole (Im), methylpyrrole (Py), and methyl-3-hydroxypyrrole (Hp) units to form molecules that bind to the minor groove as antiparallel dimers. Covalently linking the amino- and carboxyl-termini of two antiparallel dimers with an aliphatic γ-aminobutyric acid resulted in hairpin polyamides that could recognize all combinations of base pairs as illustrated for one sequence in Figure 1.16.[10,65]

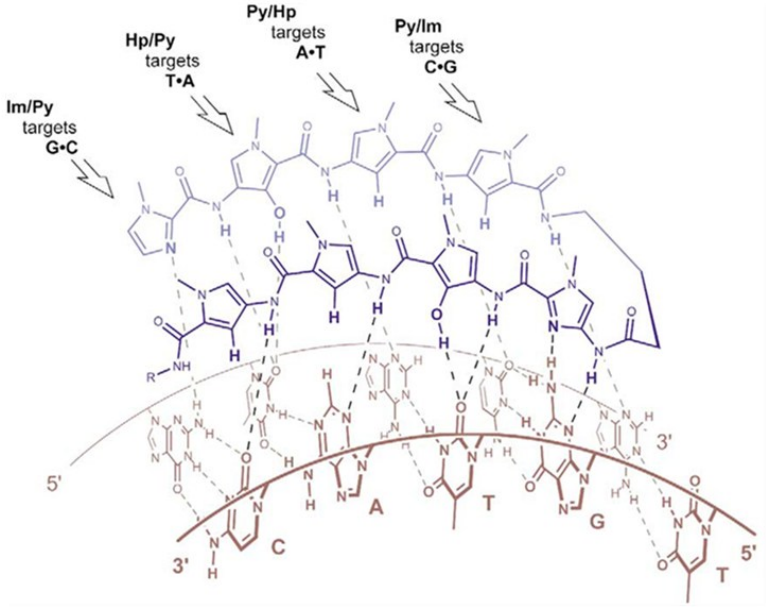

Figure 1.16. Pairing code illustrating the contacts of polyamides with minor groove. Note, the structure of the Hp extends a hydrogen deep into the groove to interact with sterically hindered thymine-O2 lone pair.[65]

Although the Pairing Code has aided the successful targeting of many DNA sequences, there are many more sequences that are difficult to target with high affinity and specificity. In addition, the Hp residue noted above degrades over time in the presence of acid or free radicals. Therefore a more stable thymine-selective moiety is desired. Because of this, research in the area of minor groove binding polyamides has been directed toward developing heterocycles with improved stability and recognition capability.[10] Phenyl-benzimidazoles exhibit several of these desired qualities due to

their slightly different curvature and ability to recognize DNA through two sets of hydrogen-bond donating groups.[70] This curvature, as well as the possible hydrogen bonding that can occur in the minor groove with the benzimidazole are key to including benzimidazoles in our design of minor groove binding ligands.

1.5. Benzimidazole-Based DNA Minor Groove Binders

Phenyl-benzimidazole ring systems represent a structural framework that is amenable to functionalization and imparts a curvature that complements the DNA minor groove. Benzimidazole derivatives have been incorporated into the backbones of polyamides in a manner that preserves hydrogen bonding contact with the minor groove.[71] Indeed, (1) the classic minor groove-binding Hoechst dyes are composed of benzimidazole units and (2) hydroxybenzimidazole (Hz) and imidazopyridine (Ip) rings have been included in polyamides without an amide linker between the rings. It has been shown that Py-Hz and Py-Ip pairs are functionally identical to the five-membered ring pairs Py-Hp and Py-Im.[72] The Py-Hz pair has been shown to distinguish T/A from A/T base pairs while the Py-Ip pair has been shown to distinguish G/C from C/G base pairs. The benzimidazole containing polyamides have proven to be more chemically stable and have been incorporated into effective minor groove binding DNA ligands.

1.5.1. Hoechst 33258

Hoechst 33258 (Figure 1.17) is a bis-benzimidazole comprised of two linked benzimidazole groups with a phenol and methylpiperazine at either end. Hoechst 33258 has been employed as a chromosomal stain[73] and a fluorescence indicator[74] due to its ability to be excited by ultraviolet light at ~350 nm and to exhibit enhanced fluorescence upon binding to DNA. DNA footprinting and biophysical studies have shown Hoechst 33258 binds selectively to A•T sequences.[74] Hoechst has been shown to exhibit antitumor activity and was in phase I/II clincal trials against pancreatic carcinomas before being abandoned due to its toxicity.[75,76]

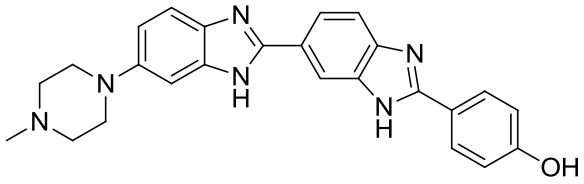

Hoechst 33258

Figure 1.17. Structure of Hoechst 33258.

Hoechst 33258 and its interactions with DNA have been extensively studied using a number of techniques including NMR and X-ray crystallographic analysis.[72,77-79] Similar to netropsin and distamycin, Hoechst 33258 binds preferentially to A/T-rich regions of the DNA minor groove.[80] These results are confirmed by FID analysis (Figure 1.18).[55] The FID histogram showed the presence of 16 (of 16 possible, 100%) five-bp A/T-sites and 19 (of 32 possible, 59%) four-bp A/T-sites within the top 50 sequences with the top 20 sequences being exclusively four- or five-bp A/T-sites.[55] When Hoechst 33258 is bound to A/T-rich DNA, hydrogen bonds form between the benzimidazole nitrogen atoms and the minor groove of DNA when the benzimidazole donor can contact the thymine-O2 or adenine-N3 atoms in a conformation similar to that of netropsin.[81] The bulky N-methylpiperazine ring of Hoechst is usually located in a wider G•C portion of the minor groove flanking A/T-rich sequences without participating in hydrogen bonding.

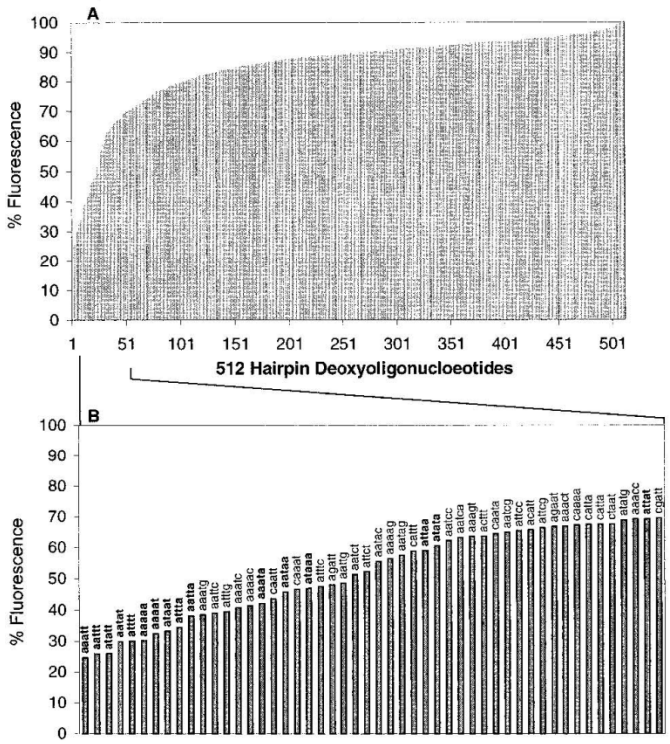

Figure 1.18. Merged-bar FID histogram of Hoechst 33258 at 2.0 μM: (A) all 512 oligonucleotide sequences, (B) top 50 sequences showing highest affinity.[55]

The effect of amino acids on the binding affinity of Hoechst 33258 was explored by incorporating the full structure of Hoechst 33258 into peptides and testing their binding affinity and site selectivity.[82] The results of simple Hoechst 33258 conjugates (Figure 1.19) show nearly the same binding preference for A/T-rich regions of DNA as that for the parent Hoechst 33258 while increasing up to 60 times the binding affinity for the peptide-Hoechst 33258 conjugate.[82] This shows the benzimidazole moiety is important for DNA minor groove recognition and that conjugation with amino acids can increase the binding affinity without altering the sequence preference of the parent structure, showing us that amino acid-benzimidazole-amidine conjugates can also be strong DNA minor groove binders. As will be described, we incorporated amino acids into our benzimidazoles as has been done with some Hoechst systems, although we elected to use fewer amino acids and only included a single benzimidazole moiety in our design compared to the di-benzimidazole-amino acid Hoechst systems to keep our molecules small and compact while increasing their binding affinity over non-amino acid containing benzimidazole-amidine systems.

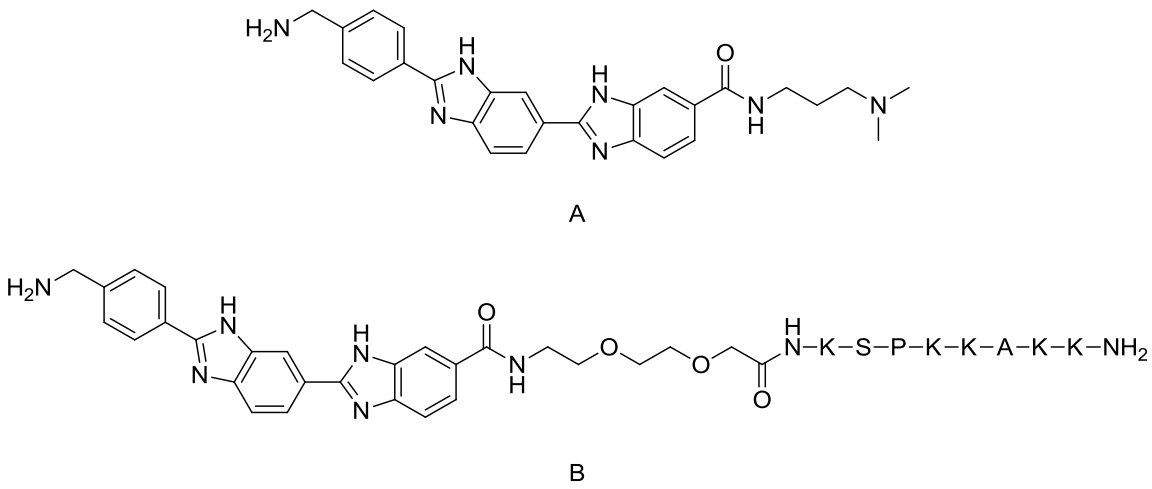

Figure 1.19. Structures of (A) a simple Hoechst 33258 analogue and (B) a Hoechst-peptide conjugate.

1.5.2. Benzimidazole-Amidine Systems

In addition to Hoechst, benzimidazole-amidine systems such as RT29 (Figure 1.20) and a series of furamidine and related diamidine dication compounds, refered to as the DB series (Figure 1.21), provide a favorable and flexible DNA recognition element.[17,83-87] RT 29 is a benzimidazole diphenyl ether core that is capped by amidine groups. FID analysis of RT 29 shows a similar rank order to what has previously been reported for netropsin, proving RT 29 to be another A/T-rich minor groove DNA binder.[17,83] Crystallographic results for the DNA complex with RT29 shows the compound undergoes significant conformational changes and incorporates a water molecule directly into the complex to allow it to adopt a crescent shape and complete the compound-DNA interface.[17,83] RT 29 is attractive to the minor groove of A/T-rich regions due to the positive charge character of the two cationic amidine groups, and the nitrogens also participate in hydrogen bonding with A/T bases.[88-90]

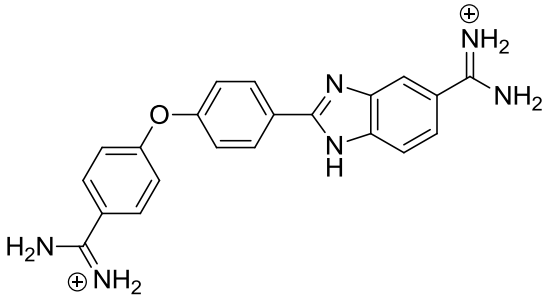

Figure 1.20. Structure of RT 29.

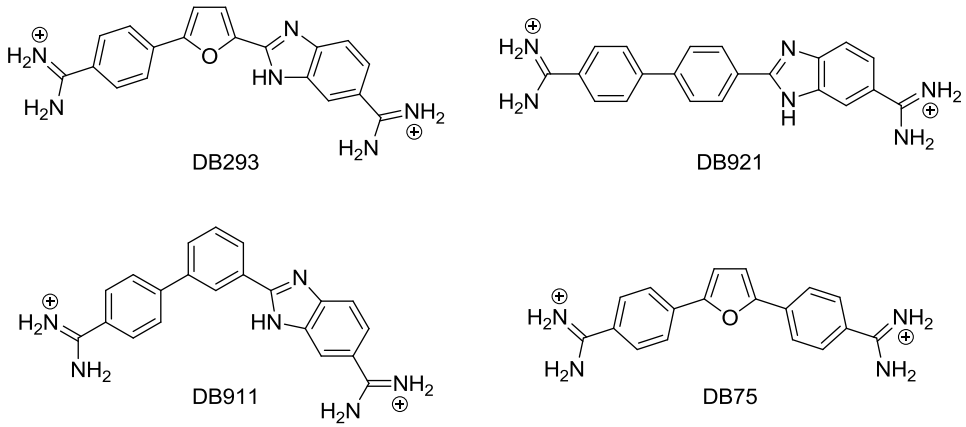

Figure 1.21. Structures of DB Series Compounds.

Among heterocyclic diamidines, DB293 has been shown to bind to A/T-rich sites as a monomer and as a stacked dimer similar to distamycin.[91] X-ray crystallographic analysis of DB921 bound to an AATT sequence suggests a water molecule is also able to complete the curvature of DB921 for minor groove interactions,[87] and DB921 binds to A/T-rich DNA sequences stronger than the rest of the DB series with a binding constant of greater than $10^8\,M^{-1}$ under physiological conditions.[18] Finally, the prodrug DB75 has shown activity against eukaryotic parasitic diseases and is in Phase III clincal trials against sleeping sickness.[92] Aromatic diamidines have drawn interest due to their antimicrobial activity which is believed to be a result of their minor groove binding affinity.[93] The combination of extra hydrogen bonding from amidines along with that of

the benzimidazole make compounds containing these moieties strong targets for the development of DNA minor groove binding agents.

In summary, we have introduced benzimidazole compounds, benzimidazole-amidine systems, and benzimidazole-peptide conjugates. Benzimidazoles are good minor groove A/T-rich region binding moieties due to their ability to hydrogen bond with the floor of the the minor groove and that their size is not too bulky to be accommodated by the minor groove. The positively charged amidine moiety is drawn to the more negatively charged A/T regions of DNA and provides excellent affinity for these regions. Peptides conjugated with these moieties can enhance the binding affinity. Therefore, we hypothesize that amino acid-benzimidazole-amidine conjugates should be good DNA minor groove binders due to the combination of these advantageous features.

1.6. Plan of Study

The subsequent chapters of this thesis will describe a new series of amino acid-phenyl-benzimidazole-amidine conjugates designed in our laboratory. These compounds consist of a phenyl-benzimidazole-amidine core conjugated to different amino acids (Figure 1.22). The structural basis for the design of minor groove binding ligands and key features that are important to minor groove binding ligands include: (1) incorporating amino acids to provide structural diversity, (2) positive charges that enhance electrostatic interactions, (3) and hydrogen-bonding groups for sequence recognition. By incorporating many key features from different binders as introduced here, it was anticipated that a series of selective and high affinity minor groove binding agents would emerge. The phenyl-benzimidazole is a stable and strong binder to A/T-rich regions of the DNA minor groove; the positively charged amidine group is attracted to the negative potential of the DNA minor groove, which is highest in A/T-rich regions; and amino acids provide subtle structural diversity to perhaps drive different conjugates toward different DNA sites. The combination of these groups should yield a strong and selective binder to A/T-rich regions, and perhaps other sequences, of the DNA minor groove.

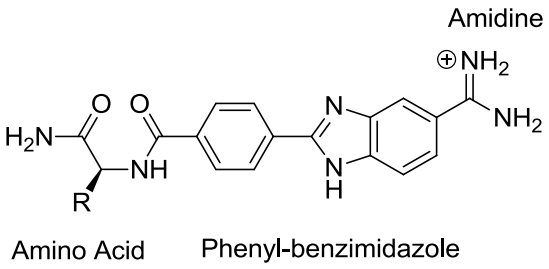

Figure 1.22. Structure of model amino acid-phenyl-benzimidazole-amidine system.

The focus of this study was to develop the synthesis of the amino acid-benzimidazole-amidine system that we have designed and to determine their relative DNA binding affinities. All conjugates will be synthesized on solid-phase support and their relative binding will be measured with the FID assay. Conjugates of this form have never been explored, and the solid-phase synthesis of benzimidazole-amidine systems has not been reported. Therefore, the synthetic protocol will be useful to supplement solid-phase synthesis.

1.7. List of References

1. McKnight, R. E.; Gleason, A. B.; Keyes, J. A.; Sahabi, S. *Bioorg. Med. Chem. Lett*. **2007**, *17*, 1013.
2. Tse, W. C.; Boger, D. L. *Chem. Biol*. **2004**, *11*, 1607.
3. Haq, I. *Arch. Biochem. Biophys*. **2002**, *403*, 1.
4. Yang, X. L.; Wang, A. H-J. *Pharmacol. Ther*. **1999**, *83*, 181.
5. Chaires, I. B. *Biopolymers* **1997**, *44*, 201.
6. Hutchins, R. A.; Crenshaw, J. M.; Graves, D. E.; Denny, W. A. *Biochemistry* **2003**, *42*, 13754.
7. Neidle, S. *Nat. Prod. Rep*. **2001**, *18*, 291.
8. Neidle, S. *Biopolymers* **1997**, *44*, 105.
9. Geierstanger, B. H.; Wemmer, D. E. *Ann. Rev. Biophys. Biomol. Struct*. **1995**, *24*, 463.
10. Dervan, P. B. *Bioorg. Med. Chem.* **2001**, *9*, 2215.
11. Munde, M.; Ismail, M. A.; Arafa, R.; Peixoto, P.; Catharine J.; Collar, C. J.; Liu, Y.; Hu, L. X.; David-Cordonnier, M.; Lansiaux, A.; Bailly, C.; Boykin, D. W.; Wilson, W. D. *J. Am. Chem. Soc.* **2007**, *129*, 13732.
12. Hurley, L. H. *Nat. Rev. Cancer* **2002**, *2*, 188.
13. Gale, E. F.; Cundliffe, E.; Reynolds, P. E.; Richmond, M. H.; Waring, M. J. in: *The Molecular Basis of Antibitoic Action, 2nd Ed.,* Wiley & Sons, **1981**.
14. Ughetto, G.; Wang, A. H-J.; Quigley, G. J.; va der Marel, G. A.; van Boom, J. H.; Rich, A. *Nucleic Acids Res.* **1985**, *13*, 2305.
15. Wang, A. H-J.; Ughetto, G.; Quigley, G. J.; Hakoshima, T.; van der Marel, G. A.; *Science* **1984**, *225*, 1115
16. Wang, A. H-J.; Ughetto, G.; Quigley, G. J.; Rich, A.; *J. Biomol. Struct. Dyn.* **1986**, *4*, 319.
17. Bremer, R. E.; Baird, E. E.; Dervan, P. B. *Chem. Biol.* **1998**, *5, 119.*
18. Tanious, F. A.; Laine, W.; Peixoto, P.; Bailly, C.; Goodwin, K. D.; Lewis, M. A.; Long, E. C.; Georgiadis, M. M.; Tidwell, R. R.; Wilson, W. D. *Biochemistry* **2007**, *46*, 6944.
19. Bailly, C.; Waring, M. J. *Nucleic Acids Res.* **1998**, *26*, 4309.
20. Mathis, A. M.; Holman, J. L.; Sturk, L. M.; Boykin, D. W.; Tidwell, R. R.; Hall, J. E. *Antimicrobial Agents Chemother.* **2006**, *50*, 2185.

21. Wilson, W. D.; Nguyen, B.; Tanious, F. A.; Mathis, A.; Hall, J.E.; Stephens, C. E.; Boykin, D. W. *Curr. Med. Chem. Anti-Cancer Agents* **2005**, *5*, 389.
22. Nguyen, B.; Hamelberg, D.; Bailly, C.; Colson, P.; Stanek, J.; Brun, R.; Neidle, S.; Wilson, W. D. *Biophys. J.* **2004**, *86*, 1028.
23. Crick, F. *Nature* **1970**, *227*, 561.
24. Voet, D.; Voet, J. G. *Biochemistry, 2nd Ed.,* Wiley & Sons, **1995**.
25. Ghosh, A.; Bansal, M. *Acta. Crystallogr. D. Biol. Crystallogr.* **2003**, *59*, 620.
26. Basu, H. S.; Feuerstein, B. G.; Zarling, D. A.; Shafer, R. H.; Marton, L. J. *J. Biomol. Struct. Dyn.* **1988**, 6, 299.
27. Steitz, T. A. *Q. Rev. Biophys.* **1990**, *23*, 205.
28. Seeman, N. C.; Rosenberg, J.M.; Rich, A. *Proc. Natl. Acad. Sci. U.S.A*. **1976**, *73*, 804.
29. Marky, L.A.; Breslauer, K. J. *Proc. Natl. Acad. Sci. U.S.A.* **1987**, *84*, 4359.
30. Lerman, L. S. *J. Mol. Biol.* **1961**, 3, 18.
31. Huang, X.; Shullenberger, D. F.; Long, E. C. *Biochem. Biophys. Res. Commun.* **1994**, *198*, 712.
32. Waring, M. J. *Annu. Rev. Biochem.* **1981**, *50*, 159.
33. Chen, J.; Stubbe, J. *Nat. Rev.* **2005**, *5*, 102.
34. Boger, D. L.; Tse, W. C. *Bioorg. Med. Chem.* **2001**, *9*, 2511.
35. Tse, W. C.; Boger, D. L. *Acc. Chem. Res.* **2004**, *37*, 61.
36. Waring, M. J. *J. Mol. Biol.* **1965**, *13*, 269.
37. Crawford, L. V.; Waring, M. J. *J. Mol. Biol.* **1967**, *25*, 23.
38. Neidle, S. Ed. *Oxford Handbook of Nucleic Acid Structure*, Oxford University Press, **1984**.
39. Neto, B. A.; Lapis, A. A. *Molecules* **2009**, 14, 1725.
40. Kopka, M. L.; Yoon, C.; Goodsell, D.; Pjura, P.; Dickerson, R.E. *J. Mol. Biol.* **1985**, *183*, 553.
41. Koo, H-S.; Wu, H-M.; Crothers, D. M. *Nature* **1986**, *320,* 501.
42. Zimmer, C.; Wähnert, U. *Prog. Biophys. Mol. Biol*. **1986**, *47*, 31.
43. Patel, N.; Berglund, H.: Nilsson, L.; Rigler, R.; McLaughlin, L. W.; Gräslund, A. *Eur. J. Biochem*. **1992**, *203*, 361.
44. Bailly, C.; Chaires, J. B. *Bioconjugate Chem.* **1998**, *9*, 513.

45. Zimmer, C. *Prog. Nucleic Acid Res. Mol. Biol*. **1975**, *15*, 285.
46. Taylor, J. S.; Schultz, P. G.; Dervan, P. B. *Tetrahedron* **1984**, *40*, 457.
47. Dervan, P. B. *Science* **1986**, *232*, 464.
48. Nunn, M. C.; Garman, E.; Neidle, S. *Biochemistry* **1997**, *36*, 4792.
49. Lewis, M. A.; Long, E. C. *Bioorg. Med. Chem*. **2006**, *14*, 3481.
50. Pelton, J. G.; Wemmer, D. E. *Biochemistry* **1988**, *27*, 8088.
51. Marques, M. A.; Doss, R. M.; Urbach, A. R.; Dervan, P. B.; *Helvetica Chimica. Acta.* **2002**, *85*, 4485.
52. Coil, M.; Fredrick, C. A.; Wang, A. H-J.; Rich, A. *Proc. Natl. Acad. Sci. USA* **1987**, *84*, 8385.
53. Fagan, P. A.; Wemmer, D. E. *J. Am. Chem. Soc*. **1992**, *114*, 1080.
54. Geierstanger, B. H.; Jacobsen, J. P.; Mrksich, M.; Dervan, P. B.; Wemmer, D. E. *Biochemistry* **1994**, *33*, 3055.
55. Boger, D. L.; Fink, B. E.; Brunette, S. R.; Tse, W. C.; Hedrick, M. P. *J. Am. Chem. Soc.* **2001**, *123*, 5878.
56. Kopka, M. L.; Yoon, C.; Goodsell, D.; Pjura, P.; Dickerson, R. E. *Proc. Natl. Acad. Sci. USA* **1985**, *82*, 1376.
57. Burckhardt, G.; Luck, G.; Zimmer, C.; Shirl, J.; Krowicki, K.; Lown, J. W. *Biochem. Biophys. Acta.* **1989**, *1009*, 11
58. Kissinger, K.; Krowicki, K.; Dabrowiak, J. C.; Lown, J. W. *Biochemistry* **1987**, *26*, 5590.
59. Lee, M.; Chang, D. K.; Hartley, J. A.; Pon, R. T.; Krowicki, K.; Lown, J. W. *Biochemistry* **1988**, *27*, 445.
60. Lee, M.; Coulter, D. M.; Pon, R. T.; Krowicki, K.; Lown, J. W. *Biomol. Struct. Dyn*. **1988**, *5*, 1059.
61. Lee, M.; Hartley, J. A.; Pon, R. T.; Krowicki, K.; Lown, J. W. *Nucleic Acids Res*. **1988**, *16*, 665.
62. Lee, M.; Krowicki, K.; Hartley, J. A.; Pon, R. T.; Lown, J. W. *J. Am. Chem. Soc*. **1988**, *110*, 3641.
63. Lee, M.; Rhodes, A. L.; Wyatt, M. D.; Hartley, F. S. J. *Biochemistry* **1993**, *32*, 4237.
64. Kielkopf, C. L.; Baird, E. E.; Dervan, P. B.; Rees, D. C. *Nat. Struct. Biol.* **1998**, *5*, 104.

65. Dervan, P. B. *Curr. Opin. Struct. Biol.* **2003**, *13*, 284.
66. Kielkopf, C. L.; White, S.; Szewczyk, J. W.; Turner, J. M.; Baird, E. E.; Dervan, P. B.; Rees, D. C. *Science* **1998**, *282*, 111.
67. Kielkopf, C. L.; Bremer, R. E.; White, S.; Szewczyk, J. W.; Turner, J. M.; Baird, E. E.; Dervan, P. B.; Rees, C. C. *J. Mol. Biol.* **2000**, *295*, 557.
68. White, S.; Szewczyk, J. W.; Turner, J. M.; Baird, E. E.; Dervan, P. B. *Nature* **1998**, *391*, 468.
69. Fede, A.; Labhardt, A.; Bannwarth, W.; Leupin, W. *Biochemistry* **1991**, *30*, 11377.
70. Morgan, A. R.; Lee, J. S.; Pulleyblank, D. E.; Murray, N. L; Evans, D. H. *Nucleic Acids Res.* **1979**, *7*, 3.
71. Renneberg D.; Dervan, P. B. *J. Am. Chem. Soc*. **2003**, *125*, 5707.
72. Harshman, K. D.; Dervan, P. B. *Nucleic Acid Res.* **1985**, *13*, 4825.
73. Coll, M.; Frederick, C. A.; Wang, A. H-J.; Rich, A. *Proc. Natl. Acad. Sci. U.S.A.* **1987**, *84*, 8385.
74. Teng, M.; Ladbury, J.E.; Chowdhry, B. Z.; Jenkins, T. C.; Chaires, J. B. *J. Mol. Biol.* **1997**, *271*, 244.
75. Chen, A. Y.; Yu, C.; Gatto, B.; Liu, L. F. *Proc. Natl. Acad. Sci.* **1993***, 90*, 8131.
76. Kraut, E. H.; Fleming, T.; Segal, M.; Neidhart, J. A.; Behrens, B. C.; MacDonald, J. *Invest. New Drugs* **1991**, *9*, 95.
77. Spink, N.; Brown, D. G.; Skelly, J. V.; Neidle, S. *Nucleic Acid Res*. **1994**, *22*, 1607.
78. Searle, M. S.; Embrey, K. J. *Nucleic Acid Res.* **1990**, *18*, 3753.
79. Teng, M. K.; Usman, N.; Frederick, C. A.; Wang, J. *Nucleic Acid Res.* **2000***, 16*, 2671.
80. Quintana, J. R.; Lipanov, A. A.; Dickerson, R. E. *Biochemistry* **1991**, *30*, 10294.
81. Haq, I.; Ladbury, J. E.; Chowdhry, B. Z.; Jenkins, T. C.; Chaires, J. B. *J. Mol. Biol*. **1997**, *271*, 244.
82. Behrens, C.; Harrit, N.; Nielsen, P. E. *Bioconj. Chem*. **2001**, *12*, 1021.
83. Goodwin, K. D.; Lewis, M. A.; Tanious, F. A.; Tidwell, R. R.; Wilson, W. D.; Georgiadis, M. M.; Long, E. C. *J. Am. Chem. Soc.* **2006**, *128*, 7846.
84. Lombardy, R. L.; Tanious, F. A.; Ramachandran, K.; Tidwell, R. R.; Wilson, W. D. *J. Med. Chem.* **1996**, *39*, 1452.

85. Peixoto, P.; Liu, Y.; Depauw, S.; Hildebrand, M-P.; Boykin, D. W.; Bailly, C.; Wilson, W. D.; David-Cordonnier, M. *Nucleic Acids Res.* **2008**, *36*, 3341.
86. Rahimian, M.; Kumar, A.; Say, M.; Bakunov, S. A.; Boykin, D. W.; Tidwell, R. R.; Wilson, W. D. *Biochemistry* **2009**, *48*, 1573.
87. Miao, Y.; Lee, M. P. H.; Parkinson, G. N.; Batista-Parra, A.; Ismail, M. A.; Neidle, S.; Boykin, D. W.; Wilson, W. D. *Biochemistry* **2005**, *44*, 14701.
88. Goodwin, K. D.; Long, E. C.; Georgiadis, M. M. *Nucleic Acids Res.* **2005**, *33*, 4106.
89. Clark, G. R.; Boykin, D. W.; Czarny, A.; Neidle, S. *Nucleic Acids Res.* **1997**, *25*, 1510.
90. Ismail, M. A.; Batista-Parra, A.; Miao, Y.; Wilson, W. D.; Wenzler, T.; Brun, R.; Boykin, D. W. *Bioorg. Med. Chem.* **2005**, 13, 6718.
91. Bailly, C.; Chessari, G.; Carrasco, C.; Joubert, A.; Mann, J.; Wilson, W. D.; Neidle, S. *Nucleic Acids Res.* **2003**, *31*, 1514.
92. Ismail, M. A.; Arafa, R. K.; Brun, R.; Wenzler, T.; Miao, Y.; Wilson, W. D.; Generaux, C.; Bridges, A.; Hall, J. E.; Boykin, D. W. *J. Med. Chem.* **2006**, *49*, 5324.
93. Ismail, M. A.; Brun, R.; Wenzler, T.; Tanious, F. A.; Wilson, W. D.; Boykin, D. W. *Bioorg. Med. Chem.* **2004**, *12*, 5405.

CHAPTER 2. DESIGN AND SYNTHESIS OF AMINO ACID-BENZIMIDAZOLE-AMIDINE CONJUGATES

2.1. Design of Amino Acid-Benzimidazole-Amidine Conjugates

Benzimidazoles and their derivatives are powerful antitumor, antifungal, and antiviral compounds[1-4] that have been employed extensively in the design of DNA minor groove targeted compounds.[5] The structure of the benzimidazole ring system has been shown to be a good design element for recognition of the DNA minor groove due to the presence of heteroatoms in the ring that promote hydrogen bonding and, as part of a phenyl-benzimidazole, the overall curvature of these systems can closely resemble that of the minor groove itself.[6-9] Therefore, benzimidazoles provide a building block for further structural variability, and they have been shown to exhibit excellent interactions with the minor groove of DNA in many systems.[10-17] Because of these qualities, benzimidazoles were included in the design of our DNA minor groove targeted compounds.

In addition to the benzimidazole moiety, amidines have been shown to be an important pharmacophore in medicinal chemistry. More specifically, aromatic amidines have been shown to function as arginine side-chain mimetics due to their favorable spatial and cationic properties.[18,19] Many of the previously mentioned DNA minor groove binders, such as netropsin, distamycin, RT 29, and the DB series, include amidine moieties. An amidine contributes a positive charge which aids in recognition of the minor groove, more specifically, A/T-rich sites that have a greater negative electrostatic potential.[11,19-25] These desirable qualities led to the inclusion of the amidine moiety in our design of DNA minor groove binding targets.

Amino acids were also included in our design to provide structural diversity to the basic phenyl-benzimidazole structure. The differing side chains of each amino acid provide subtle structural differences to the overall molecule which may lead to the targeting of different DNA sequences. Individual amino acids or small chains of amino acids should be compact enough to fit into the DNA minor groove, and these will contain

multiple amide bonds similar to the structures of netropsin, distamycin, and the lexitropsins[11,19-21,26-29] Because of these qualities, we have designed benzimidazole-amidine systems that include a single amino acid and systems that include two amino acids. The basic structures of our resin bound benzimidazole-amidine systems are shown in Figure 2.1.

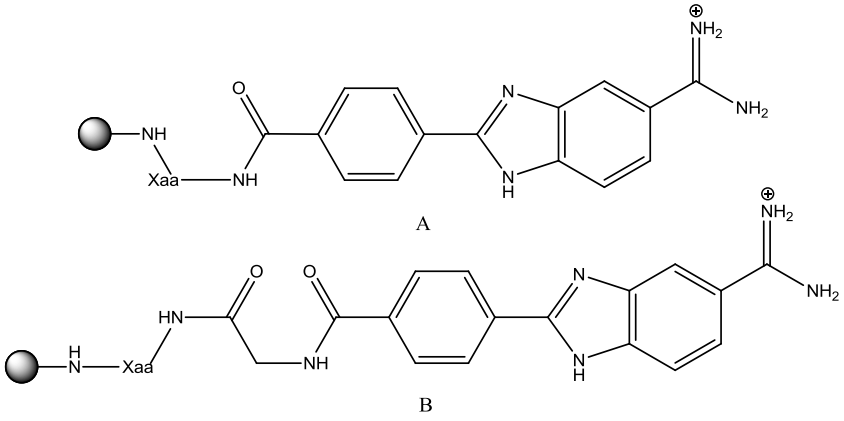

Figure 2.1. Resin-bound benzimidazole amidine systems: (A) single amino acid- and (B) di-amino acid-benzimidazole-amidine conjugates where Xaa is any one of 20 naturally occurring amino acids (except Trp, Ser, Cys, or His for structure A).

2.2. Synthesis – General Considerations

Solid-phase synthetic methods for the generation of amino acid conjugates have become increasingly important since the development of solid-phase peptide synthesis.[30] As such, all of our planned syntheses were carried out via solid-phase synthetic protocols because they are amenable to quickly and easily assembling peptide bonds as well as their ease of purification. Numerous solid-phase resins have been developed over the years to yield desirable terminal functionalities after product cleavage, and a couple of the most commonly used resins in solid-phase chemistry are Rink amide resin and Wang resin (Figure 2.2). Rink amide resin was specifically used to build our compounds because upon final cleavage of product from the resin an amide terminal group is formed whereas Wang resins result in a terminal carboxylic acid. In our case, the resulting amide termini will not possess a charge under physiological conditions and can act as a hydrogen bond donor to potentially aid in the recognition of the DNA minor groove. In contrast, a carboxylic acid would generate a product with a

negative charge which would repel the negatively charged DNA phosphodiester backbone. Base-labile Fmoc-group protected amino acids were coupled to the deprotected Rink amide resin through their C-termini via established peptide bond forming solid-phase synthetic protocols (Figure 2.3).[31-33] Amino acids containing side-chain protecting groups that can be easily removed during TFA resin cleavage were used to avoid extra steps to remove the protecting group.

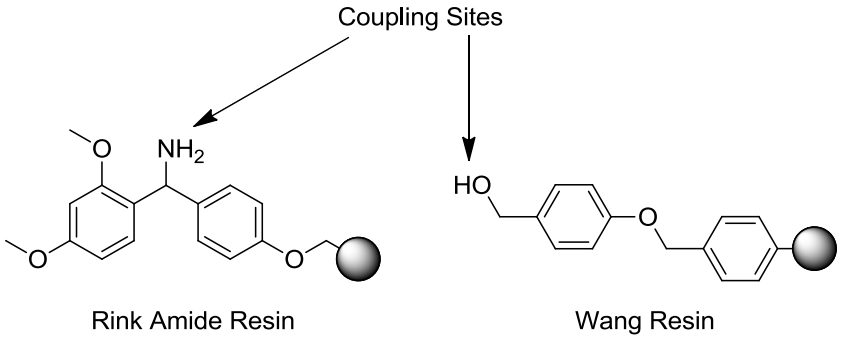

Figure 2.2. Structures of Rink amide resin and Wang resin, arrows indicate coupling sites.

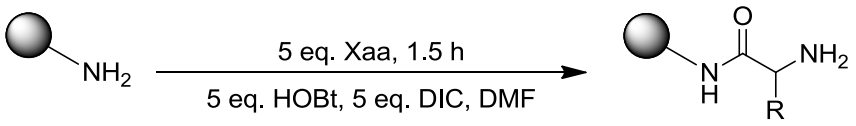

Figure 2.3. Solid-phase coupling of amino acid to Rink amide resin.

Due to the importance of the amidine group to the recognition of minor groove binding agents, we sought to include this moiety into our systems. Earlier, our group had attempted to incorporate amidines into resin-bound benzimidazole structures via the Pinner conversion[34-37] of a nitrile with an alcohol in gaseous HCl to form an alkyl imidate which can then be treated with an amine and the catalytic hydrogenation of an amidoxime with palladium on charcoal,[25,38-40] but neither of these reactions was successful on resin. However, it has also been shown that $SnCl_2 \cdot 2H_2O$ can reduce aromatic nitro compounds to amines on solid support.[41] To overcome the lack of an

efficient method to synthesize an amidine on resin, a milder procedure using $SnCl_2 \bullet 2H_2O$ (Figure 2.4) to reduce the amidoxime moiety was employed in this new work.

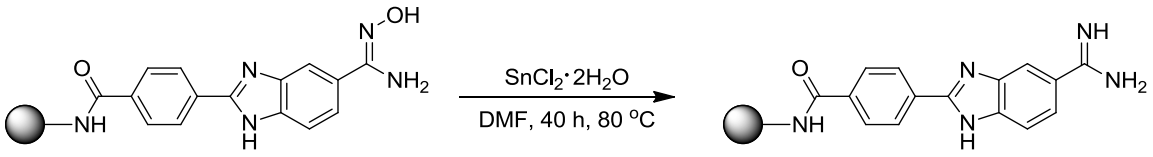

Figure 2.4. Solid-phase amidoxime reduction.

As a means to monitor coupling efficiency during the course of the synthesis, the Kaiser test was employed to quickly and efficiently check for the presence of amines to avoid incomplete peptide chain synthesis.[42] Typically, a few resin beads are removed from the reaction mixture, washed, and dried, then placed in a test tube. 2-3 drops of (1) 500 mg ninhydrin dissolved in 10 mL EtOH, (2) 80 g phenol in 20 mL EtOH, and (3) 2 mL 0.001 M KCN diluted to 100 mL in pyridine are added to the resin and placed in a heating block at 100 °C for 5 minutes. A negative test for free amine yields no color change to the resin, whereas a positive test yields a deep purple color change to the resin. The Kaiser test was used extensively throughout the synthesis of our amino acid-benzimidazole-amidine conjugates to check the progress of each coupling.

2.2.1. Synthesis of 3,4-Diaminobenzamidoxime

To provide us with a group that could be reduced to form an amidine moiety on resin, we synthesized a benzamidoxime group that can be coupled easily to a free aldehyde on resin. The synthesis of our amidoxime group was not performed on resin, but was instead synthesized in solution by heating 3,4-diaminobenzonitrile in the presence of 10 equivalents of 50% aqueous hydroxylamine for 5 hours (Figure 2.5). This reaction was carried out initially at room temperature overnight before optimization determined that performing the reaction under reflux provided much higher yield (up to 90%) than allowing the reaction to stir overnight without heating. Product was characterized by LC/MS and ^{1}H NMR (Figure 2.6 & Table 2.1).

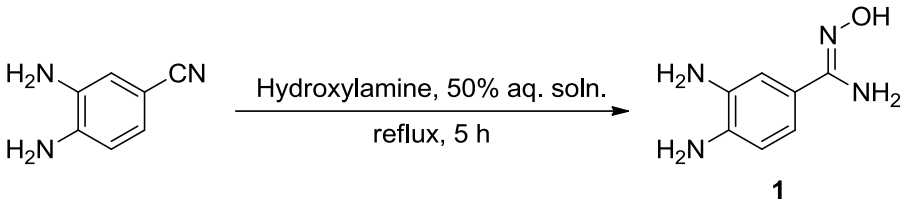

Figure 2.5. Synthesis of 3,4-diaminobenzamidoxime (**1**).

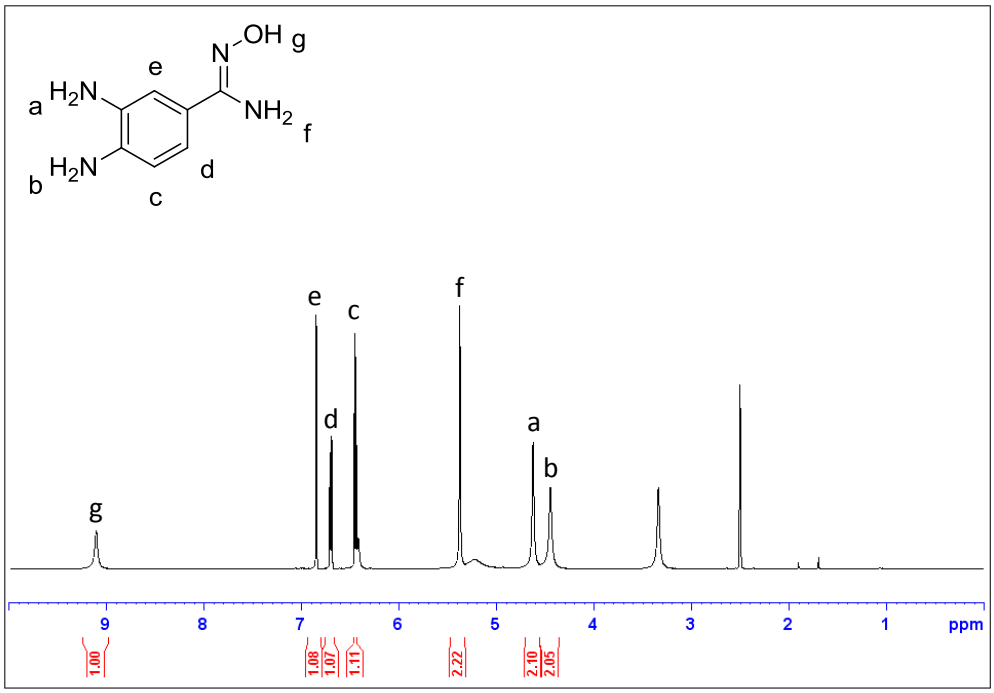

Figure 2.6. ^{1}H NMR of purified 3,4-diaminobenzamidoxime (**1**) in DMSO-d_6.

2.2.2. Benzimidazole-Amidines Lacking Amino Acid Diversity

The benzimidazole-amidine system was initially developed without including amino acids. These model systems were studied to optimize the synthesis of the benzimidazole-amidine core, more specifically to improve the problematic synthesis of the amidine. Past attempts to reduce the amidoxime group to an amidine yielded no or very little desired product upon cleavage, thus the reaction conditions of this step required optimization to produce desirable products. These attempts will be touched upon in the following section.

Initially, we explored the synthesis of phenyl-benzimidazole-amidines on resin (Figure 2.7). First, 4-carboxybenzaldehyde was coupled to deprotected Rink amide resin under conditions similar to those used in the coupling of amino acids to the resin. The Fmoc protecting group of commercial Rink amide resin was removed by allowing the resin to shake for 30 min at room temperature in a 1:4 (v/v) mixture of piperidine and DMF. Increased piperidine concentrations were tried but they did not appear to shorten reaction time and shorter reaction times at 20% piperidine did not always yield complete deprotection. The resin was washed with DMF, methanol, DCM, and diethyl ether and the presence of a terminal amino group was confirmed using a Kaiser test.

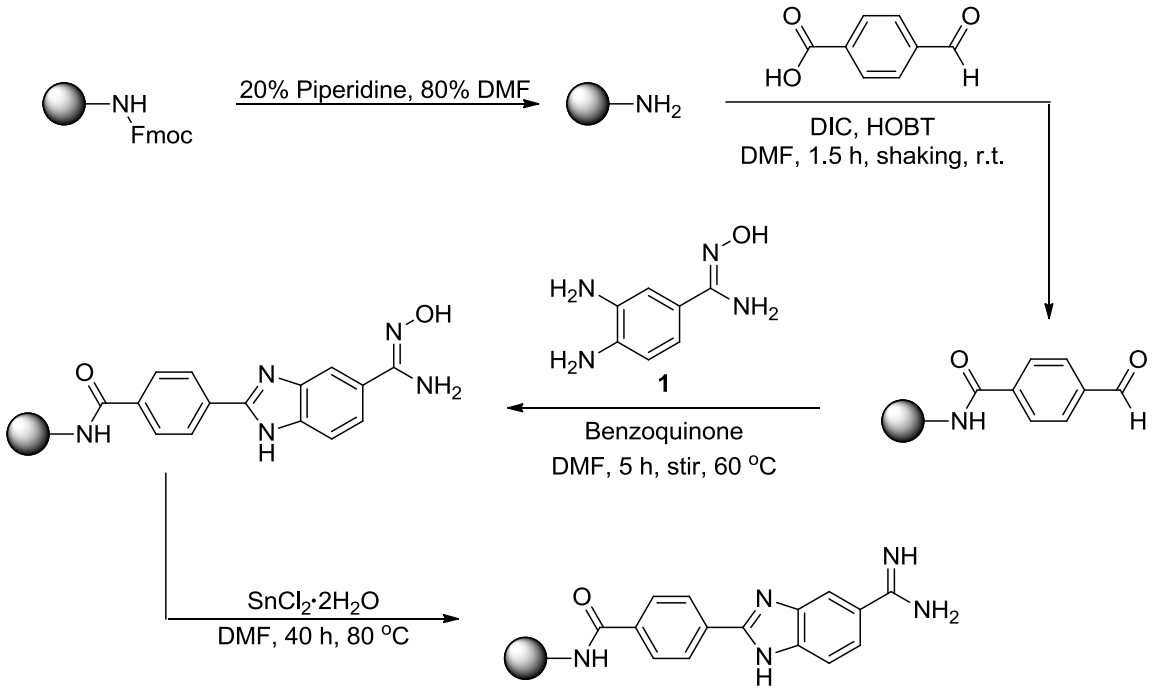

Figure 2.7. Solid-phase synthesis of phenyl-benzimidazole-amidine.

Upon deprotection of the resin, 5 equivalents of 4-carboxybenzaldehyde, 1-hydroxybenzotriazole (HOBt), and diisopropylcarbodiimide (DIC) were added, based upon 0.25 g of resin at 0.66 mmol/g resin loading. To allow the formation of an amide bond between the free amine of the resin and the carboxylic acid group of the carboxybenzaldehyde, the reaction was shaken at room temperature for 1.5 hours and

monitored via Kaiser test. When purple resin beads were present, indicating an incomplete coupling, a second coupling of five equivalents of 4-carboxybenzaldehyde was performed. Initially, the amount of 4-carboxybenzaldehyde added was increased up to 10 times excess in an attempt to complete the coupling in the initial 1.5 hours, or shorter if possible, but there was no discernible difference observed versus using five equivalents. Reaction times up to 5 hours were also attempted, but the coupling was still incomplete. Finally, it was decided that doing a double coupling with 1.5 hour reaction times was the most efficient way to proceed with this step of the reaction. The resin was again washed with DMF, methanol, DCM, and diethyl ether and the completed coupling of the carboxybenzaldehyde to the resin was confirmed by Kaiser test.

Next, the benzimidazole ring was formed via the condensation of the aldehyde (from 4-carboxybenzaldehyde) with 3,4-diaminobenzamidoxime. Ten equivalents of the amidoxime-containing diaminobenzene **1** was allowed to react with the resin-linked aldehyde for five hours at 60 °C. In an attempt to conserve the diaminobenzene, syntheses using five equivalents were attempted but did not yield complete coupling in five hours and required overnight reactions to reach completion. Also, differing reaction times were attempted with shorter times showing incomplete coupling via LC/MS (mixture of product and starting material) and longer reaction times showing no difference to five hours. The reaction was also conducted at room temperature but would typically take up to 24 hours to show complete coupling. After the formation of the benzimidazole was complete, resins were washed with DMF, methanol, DCM, and diethyl ether and the amidoxime group was reduced to the desired amidine moiety.

The reduction of resin-bound amidoxime to resin-bound amidine proved to be the most difficult reaction leading to final product, but was eventually achieved by adding 15 equivalents of 1 M $SnCl_2 \bullet 2H_2O$ in DMF to the resin-bound benzimidazole amidoxime and allowing the reaction to proceed at 70 °C for over 40 hours. To increase the reaction yield, a new aliquot of the $SnCl_2$ solution was added to the reaction mixture every 4 hours. Initially performing the reaction with only one aliquot of 1 M $SnCl_2 \bullet 2H_2O$ led to the reaction mixture thickening to the point that stirring would no longer occur and upon cleavage, very little or no desired product was seen. Increasing the concentration and/or volume of 1 M $SnCl_2 \bullet 2H_2O$ did not alleviate this problem and usually resulted in less than 25% yield. Eventually, additional aliquots of 1 M $SnCl_2 \bullet 2H_2O$ were added to the

reaction vessel and it was determined that adding a new aliquot every four hours throughout the day would prevent the reaction mixture from thickening and yielded desired product upon cleavage. Shorter durations of the entire reaction were attempted but at 24 hours there was still a large amount of unreacted amidoxime present, so 40 hours remained the overall length of reaction time.

Upon the final amidine formation, the phenyl-benzimidazole-amidine was cleaved from the resin with a 1:1 solution of TFA:DCM. The TFA and DCM were evaporated under a flow of nitrogen gas and the resulting residue was dissolved in methanol and passed through silica then concentrated leading to a 76% yield. Product was characterized by LC/MS and ^{1}H NMR (Figure 2.8 & Table 2.2).

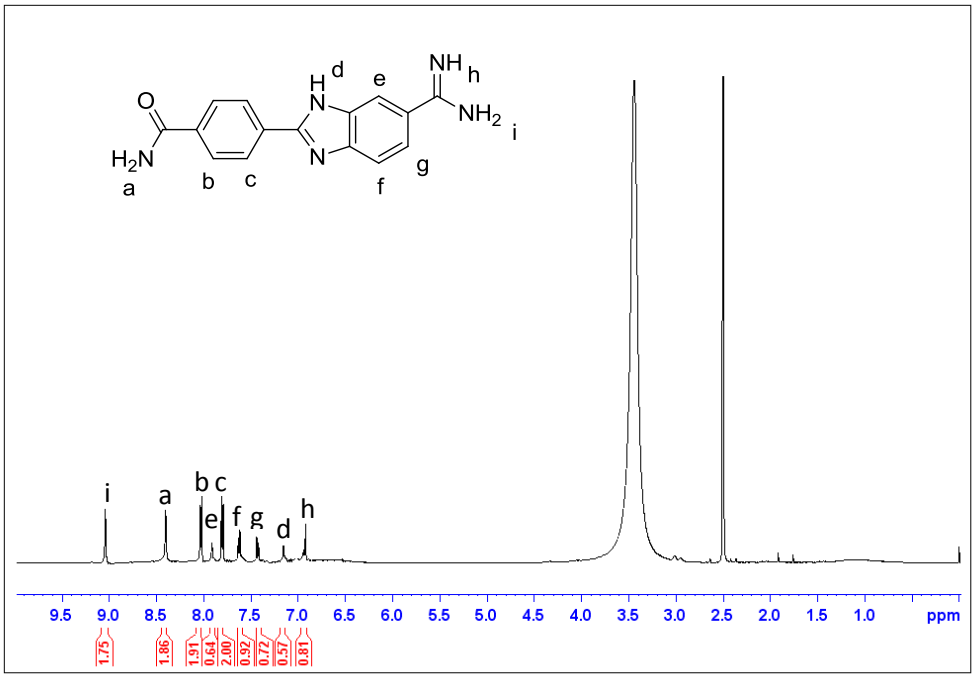

Figure 2.8. ^{1}H NMR of model-benzimidazole-amidine (**2**) in DMSO-d_6.

2.2.3. Amino Acid-Benzimidazole-Amidine Conjugates

Having confirmed the ability to synthesize phenyl-benzimidazole-amidines on resin in good yield, we proceeded to synthesize amino acid-containing benzimidazole-amidines. Two classes of amino acid-benzimidazole-amidines were synthesized: (1) containing only a single amino acid (Xaa) and (2) a dipeptide containing an amino acid linked via a glycine to the benzimidazole-amidine portion (Xaa-Gly). The glycine residue

was added to provide space between the benzimidazole-amidine portion and the varied amino acid.

2.2.3.1. Single Amino Acid-Benzimidazole-Amidine Conjugates

The syntheses of these conjugates followed the same route described previously with the addition of amino acid couplings directly to Rink amide resin preceding the coupling of 4-carboxybenzaldehyde (Figure 2.9). Once resin deprotection was confirmed via Kaiser test, five equivalents of the desired amino acid, based upon 0.25 g of resin at 0.66 mmol/g resin loading was shaken at room temperature for 1.5 hours. Reaction times and reagent concentrations that were tested with 4-carboxybenzaldehyde were also used with the amino acids but it was also seen that higher concentrations did not make the reaction proceed faster. After washing the resin, a Kaiser test was performed to verify the coupling of the amino acid to the resin. If free amine was present, a second coupling of five equivalents of amino acid was performed for another 1.5 hours. Generally, amino acids with side chains that contained protecting groups (Trp, Ser, Thr, Asn, Gln, Tyr, Cys, Lys, Arg, His, Asp, and Glu) required a double coupling, whereas amino acids with no protecting groups (Gly, Ala, Val, Leu, Ile, Met, Pro, and Phe) on their side chains did not require a double coupling. Once the Kaiser test was negative for free amine, the resin-bound amino acid was liberated of its protecting Fmoc group via shaking in 20% piperidine, 80% DMF for 30 minutes. Once deprotection was confirmed via Kaiser test, 4-carboxybenzaldehyde was coupled to the resin and the benzimidazole and amidine moieties were formed as previously described. After cleavage from resin, the Xaa-benzimidazole-amidines were characterized via LC/MS and ^{1}H NMR. Isolated, lyophilized product yields and LC/MS results are reported in Table 2.3. A sample ^{1}H NMR of glycine-benzimidazole-amidine is shown in Figure 2.10 and Table 2.4.

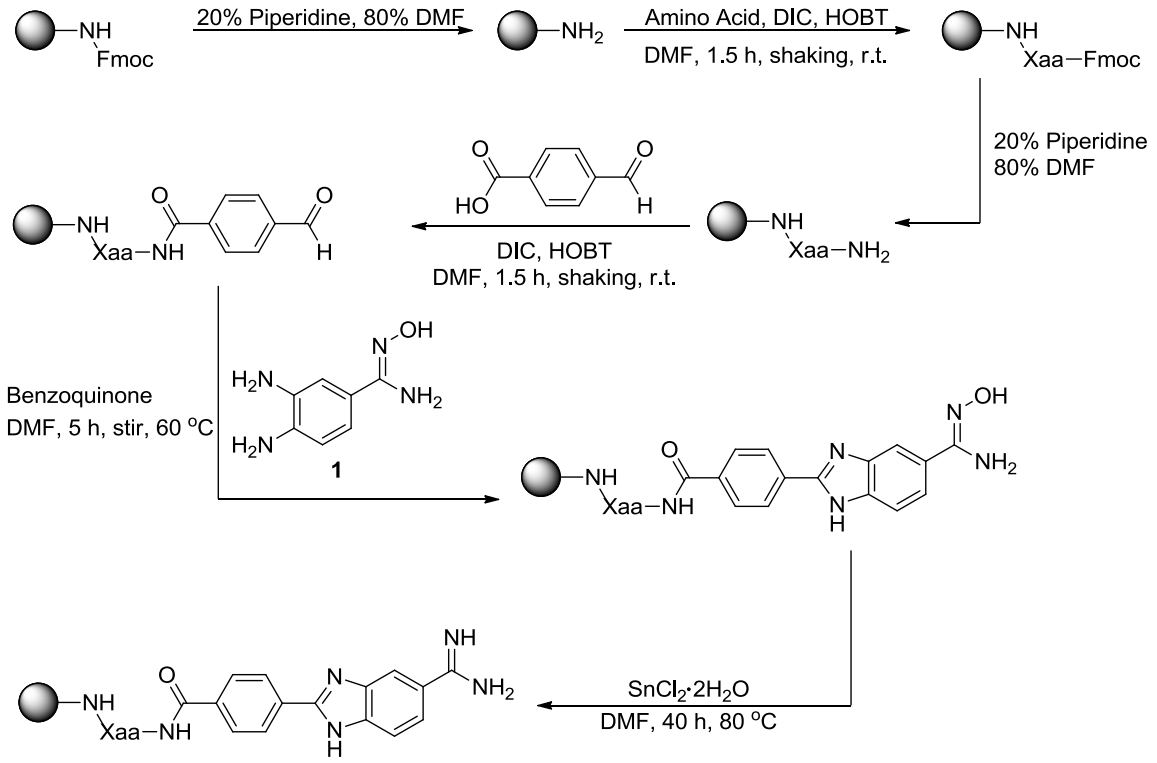

Figure 2.9. Solid-phase synthesis of single amino acid-benzimidazole-amidine conjugates.

Table 2.1. Mono-amino acid-benzimidazole-amidine conjugate *m/z* and yields.

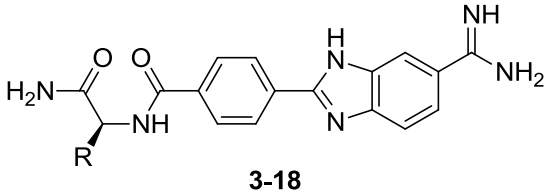

3-18

Compound	R	$[M+H]^+$ *m/z*	Yield	Compound	R	$[M+H]^+$ *m/z*	Yield
3	Gly	337.3	88%	**11**	Thr	381.4	77%
4	Ala	351.4	74%	**12**	Asn	394.3	79%
5	Val	379.3	81%	**13**	Gln	408.5	73%
6	Leu	393.2	76%	**14**	Tyr	443.5	61%
7	Ile	393.2	73%	**15**	Lys	408.5	64%
8	Met	411.5	73%	**16**	Arg	436.5	58%
9	Pro	377.5	79%	**17**	Asp	395.1	78%
10	Phe	427.4	64%	**18**	Glu	409.4	72%

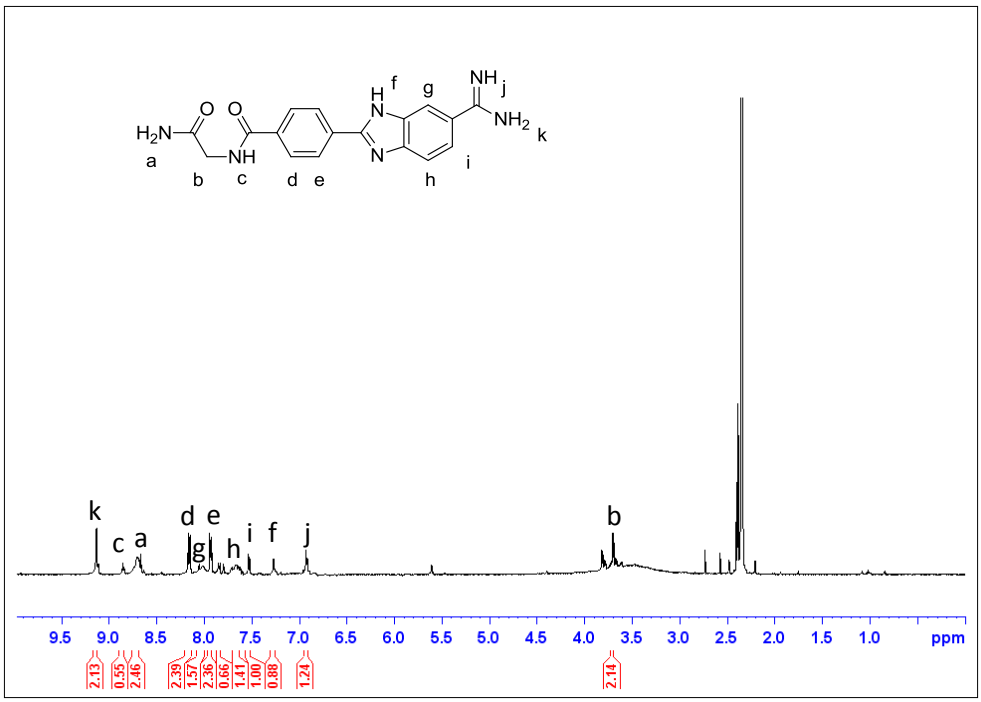

Figure 2.10. Example ^{1}H NMR of glycine-benzimidazole-amidine (**3**) in DMSO-d_6.

2.2.3.2. Dipeptide-Benzimidazole-Amidine Conjugates

The second series of amino acid-containing benzimidazole-amidine conjugates were synthesized following the same technique as the single amino acid-containing series. After the initial resin coupling of one of the twenty naturally occurring amino acids, a glycine residue was coupled to the resin-bound amino acid, resulting in a dipeptide of the sequence Xaa-Gly. Following the formation of the dipeptide, 4-carboxybenzaldehyde was coupled to glycine and the formation of the benzimidazole and amidine groups was completed. After cleavage from resin, the Xaa-Gly-benzimidazole-amidines were characterized via LC/MS and ^{1}H NMR. Isolated, lyophilized product yields and LC/MS results are reported in Table 2.5. A sample ^{1}H NMR of glycine-glycine-benzimidazole-amidine is shown in Figure 2.11 and Table 2.6.

Table 2.2. Di-amino acid-benzimidazole-amidine conjugate *m/z* and yields.

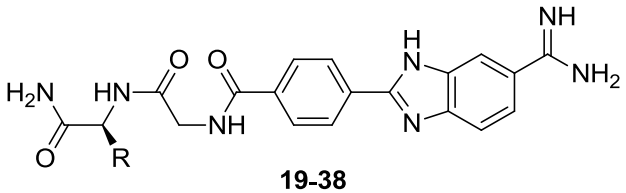

19-38

Compound	R	$[M+H]^+$ *m/z*	Yield	Compound	R	$[M+H]^+$ *m/z*	Yield
19	Gly	394.3	93%	**29**	Thr	438.2	89%
20	Ala	408.2	82%	**30**	Asn	451.3	69%
21	Val	436.3	87%	**31**	Gln	465.2	73%
22	Leu	450.2	85%	**32**	Tyr	500.3	65%
23	Ile	450.4	91%	**33**	Cys	440.1	44%
24	Met	468.2	90%	**34**	Lys	465.2	94%
25	Pro	434.3	91%	**35**	Arg	493.3	78%
26	Phe	484.3	77%	**36**	His	474.4	61%
27	Trp	523.3	74%	**37**	Asp	452.1	85%
28	Ser	424.3	59%	**38**	Glu	466.3	71%

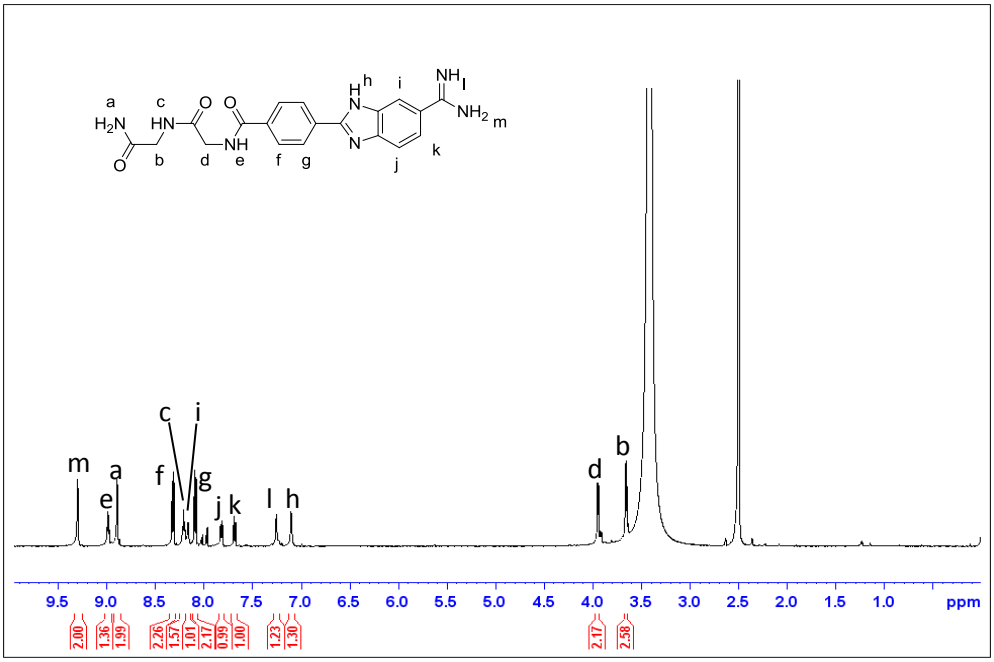

Figure 2.11. Example ^{1}H NMR of glycine-glycine-benzimidazole-amidine (**19**) in DMSO-d_6.

2.3. Summary

A new protocol for synthesizing amino acid-benzimidazole-amidine conjugates via solid-phase chemistry was developed. Sixteen single amino acid-containing phenyl-benzimidazole-amidine conjugates and 20 dipeptide phenyl-benzimidazole-amidine conjugates were synthesized using this method. Despite numerous attempts, tryptophan-, serine-, cysteine-, and histidine-containing single amino acid conjugates could not be successfully synthesized. The likely cause for failure in the synthesis of these amino acid conjugates occurred during the reduction step. All of the Kaiser tests throughout the synthesis of these conjugates showed the couplings were going to completion as expected, and LC/MS of several intermediate products showed the desired masses were present and confirmed that the amino acid, aldehyde, and diaminobenzene-amidoxime couplings went to completion. There was no sign of failed coupling until cleavage after the reduction. Also, the quality of the amino acids should not be of concern as the same sources were used to synthesize the dipeptides without issue. It is possible that complex side chains were not stable to the reduction conditions without another amino acid stabilizing them or that steric hindrance prevented the reduction from proceeding.

The most difficult aspect of the synthesis was the formation of the amidine group. The Pinner synthesis and the catalytic hydrogenation of an amidoxime were not successful on resin. To overcome this, a milder procedure using $SnCl_2 \bullet 2H_2O$ to reduce the amidoxime moiety was employed. The synthesis of our amidoxime group was not performed on resin, but was instead synthesized in solution by heating 3,4-diaminobenzonitrile in the presence of 10 equivalents of 50% aqueous hydroxylamine for 5 hours. The resulting diamino-amidoxime was coupled to the resin and reduced using $SnCl_2 \bullet 2H_2O$. Although the reaction was time-consuming, this proved to be a much more efficient method of forming the desired amidine on resin than previously described methods.

2.4. Experimental Protocols

2.4.1. Materials

All chemicals and organic solvents were reagent grade and used directly without further purification. 3,4-Diaminobenzonitrile, 4-carboxybenzaldehyde, 50% aqueous hydroxylamine, piperidine, 1,4-benzoquinone, tin(II) chloride dihydrate, hydroxybenzotriazole, diisopropylcarbodiimide, DMSO-d_6, acetonitrile, tetrahydrofuran, dichloromethane, methanol, ethanol, diethyl ether, hexanes, dimethylformamide, and acetone were purchased from Sigma-Aldrich. Trifluoroacetic acid was purchased from Fisher Scientific. The amino acids were purchased from Bachem and the Rink amide resin was purchased from EMD Millipore.

2.4.2. Instruments

The NMR used was a 500-MHz Bruker Avance III NMR spectrometer with a 5-mm broadband probe. The LC/MS used was an Agilent 1100 series HPLC with a binary pump, auto-sampler, and diode array detector with a C18 column of a length-by-width of 150mm x 4.6mm and 5-micron particle size. The MS was an Agilent 1946D mass spectrometry detector with electrospray ionization.

2.4.3. Syntheses

2.4.3.1. General Synthetic Considerations

All solid-phase synthetic routes carried out at r.t. were performed in a fritted SPE column reservoir (15 mL) fitted with a Teflon stopcock and septa and shaken on a mechanical stirrer. Solid-phase synthetic routes carried out at elevated temperature were performed in glass scintillation vials (40 mL) containing a stir bar in a reaction block fitted to a hot plate stirrer. Rink amid resin was distributed to each reaction vessel by weight and swelled in 1:1 DCM:DMF for 30 min to 1 h. Fmoc deprotection of Rink amide resin and amino acids was performed by shaking the resin in 1:4 (v/v) piperidine:DMF for 30 minutes at r.t. Deprotection was monitored via Kaiser test. A second coupling of amino acid or 4-carboxybenzaldehyde was performed after 1.5 hours if the Kaiser test revealed free amine was still present. After completion of each synthetic step, reactants

were drained and the resin was washed with DMF (3 x 5 mL), methanol (3 x 5 mL), DCM (3 x 5 mL), and diethyl ether (3 x 5 mL) and the solvents were removed by filtration using a vacuum system. All reactions were performed under the presence of nitrogen.

2.4.3.2. General Procedure for Synthesis of Model-BI-(+)

Deprotected Rink amide resin (0.25 g, 0.66 mmol/g) was treated with 4-carboxybenzaldehyde (0.8250 mmol, 123.8 mg), HOBt (0.8250 mmol, 111.5 mg), and DIC (0.8250 mmol, 104.1 mg) in 15 mL DMF and coupled to the deprotected Rink amide resin. The mixture was shaken on a mechanical stirrer at room temperature for 1.5 h. Completion of the coupling was confirmed by the Kaiser test. 3,4-Diaminobenzamidoxime (1.650 mmol, 274.2 mg) and 1,4-benzoquinone (0.165 mmol, 17.8 mg) were dissolved in 15 mL DMF and coupled to resin-bound phenylaldehyde in a scintillation vial for 5 h at 60 °C using an IKA-Werke mechanical stirrer and heating block. Tin(II) chloride dehydrate (2.475 mmol, 558.5 mg) was dissolved in DMF (2.5 mL) and reacted with the resin-linked amidoxime using an IKA-Werke mechanical stirrer and heating block at 80 °C over 40 h with new aliquots of the Tin(II) chloride solution being added to the reaction mixture every 4 h. The product was cleaved from the resin via shaking in a 1:1 solution of TFA:DCM for 1.5 h. The resin was removed by filtration and rinsed with TFA and the filtrate-containing product was collected in tared vials, then the TFA and DCM were evaporated with a stream of nitrogen until only a couple of mL remained, which was then precipitated into cold ether. The resulting solid was dissolved in MeOH and initially purified via flushing through a silica column (MeOH) to remove bulk impurities and then HPLC purified (A: H_2O, 0.1% TFA; B: ACN, 0.1% TFA. Gradient: 0 min, 80% A; 2 min, 80% A; 20 min, 20% A; 25 min, 0% A; 30 min, 0% A; 32 min, 80% A; 35 min, 80% A). Product was confirmed via LC/MS and ^{1}H NMR.

2.4.3.3. General Procedure for Synthesis of Xaa-BI-(+) Conjugates

Deprotected Rink amide resin (0.25 g, 0.66 mmol/g) was treated with an amino acid (0.825 mmol), HOBt (0.8250 mmol, 111.5 mg), and DIC (0.8250 mmol, 104.1 mg) in 15 mL DMF. The mixture was shaken on a mechanical stirrer at room temperature for 1.5 h. Completion of the coupling was confirmed by the Kaiser test. 4-Carboxybenzaldehyde (0.8250 mmol, 123.8 mg), HOBt (0.8250 mmol, 111.5 mg), and

DIC (0.8250 mmol, 104.1 mg) were dissolved in 15 mL DMF and coupled to deprotected resin-bound amino acid on a mechanical stirrer at room temperature for 1.5 h. Completion of the coupling was confirmed by the Kaiser test. 3,4-Diaminobenzamidoxime (1.650 mmol, 274.2 mg) and 1,4-benzoquinone (0.165 mmol, 17.8 mg) were dissolved in 15 mL DMF and coupled to resin-bound phenylaldehyde in a scintillation vial for 5 h at 60 °C using an IKA-Werke mechanical stirrer and heating block. Tin(II) chloride dehydrate (2.475 mmol, 558.5 mg) was dissolved in DMF (2.5 mL) and reacted with the resin-linked amidoxime using an IKA-Werke mechanical stirrer and heating block at 80 °C over 40 h with new aliquots of the Tin(II) chloride solution being added to the reaction mixture every 4 h. The product was cleaved from the resin via shaking in a 1:1 solution of TFA:DCM for 1.5 h. The resin was removed by filtration and rinsed with TFA and the filtrate-containing product was collected in tared vials, then the TFA and DCM were evaporated with a stream of nitrogen until only a couple of mL remained, which was then precipitated into cold ether. The resulting solid was dissolved in MeOH and initially purified via flushing through a silica column (MeOH) to remove bulk impurities and then HPLC purified (A: H_2O, 0.1% TFA; B: ACN, 0.1% TFA. Gradient: 0 min, 80% A; 2 min, 80% A; 20 min, 20% A; 25 min, 0% A; 30 min, 0% A; 32 min, 80% A; 35 min, 80% A). Product was confirmed via LC/MS and ^{1}H NMR.

2.4.3.4. General Procedure for Synthesis of Xaa-Gly-BI-(+) Conjugates

Deprotected Rink amide resin (0.25 g, 0.66 mmol/g) was treated with an amino acid (0.825 mmol), HOBt (0.8250 mmol, 111.5 mg), and DIC (0.8250 mmol, 104.1 mg) in 15 mL DMF for 1.5 h. The mixture was shaken on a mechanical stirrer at room temperature for 1.5 h. Completion of the coupling was confirmed by the Kaiser test. Glycine (0.8250 mmol, 254.3 mg), HOBt (0.8250 mmol, 111.5 mg), and DIC (0.8250 mmol, 104.1 mg) were dissolved in 15 mL DMF and coupled to deprotected resin-bound amino acid on a mechanical stirrer at room temperature for 1.5 h. 4-Carboxybenzaldehyde (0.8250 mmol, 123.8 mg), HOBt (0.8250 mmol, 111.5 mg), and DIC (0.8250 mmol, 104.1 mg) were dissolved in 15 mL DMF and coupled to the deprotected terminal glycine on a mechanical stirrer at room temperature for 1.5 h. 3,4-Diaminobenzamidoxime (1.650 mmol, 274.2 mg) and 1,4-benzoquinone (0.165 mmol, 17.8 mg) were dissolved in 15 mL DMF and coupled to resin-bound phenylaldehyde in a

scintillation vial for 5 h at 60 °C using an IKA-Werke mechanical stirrer and heating block. Tin(II) chloride dehydrate (2.475 mmol, 558.5 mg) was dissolved in DMF (2.5 mL) and reacted with the resin-linked amidoxime using an IKA-Werke mechanical stirrer and heating block at 80 °C over 40 h with new aliquots of the Tin(II) chloride solution being added to the reaction mixture every 4 h. The product was cleaved from the resin via shaking in a 1:1 solution of TFA:DCM for 1.5 h. The resin was removed by filtration and rinsed with TFA and the filtrate-containing product was collected in tared vials, then the TFA and DCM were evaporated with a stream of nitrogen until only a couple of mL remained, which was then precipitated into cold ether. The resulting solid was dissolved in MeOH and initially purified via flushing through a silica column (MeOH) to remove bulk impurities and then HPLC purified (A: H_2O, 0.1% TFA; B: ACN, 0.1% TFA. Gradient: 0 min, 80% A; 2 min, 80% A; 20 min, 20% A; 25 min, 0% A; 30 min, 0% A; 32 min, 80% A; 35 min, 80% A). Product was confirmed via LC/MS and ^{1}H NMR.

2.4.3.5. Synthesis of Diaminobenzamidoxime

3,4-Diamino-*N*'-hydroxybenzimidamide, (1)

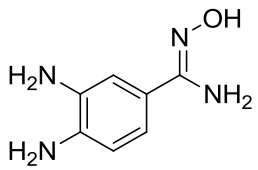

1

Compound **1** was synthesized by mixing 3,4-diaminobenzonitrile (7.5 mmol, 1.0 g) in ethanol (20 mL) and 20 equivalents 50% aqueous hydroxylamine (150 mmol, 4.95 g) and refluxing for 5 hours. The ethanol was evaporated under reduced pressure. The compound was purified via column chromatography [EtOAc:MeOH (90:10)] and confirmed via LC/MS and ^{1}H NMR. (1.06 g, 85%); ^{1}H NMR (DMSO-d_6); δ4.45 (s, 2H), 4.63 (s, 2H), 5.38 (s, 2H), 6.46 (d, J = 8 Hz, 1H), 6.71 (dd, J = 8.5 Hz, 1H), 6.85 (s, 1H), 9.11 (s, 1H); LC/MS calcd for $[M+H]^+$: $C_7H_{10}N_4O$ 167.1, found 167.3.

4-(6-Carbamimidoyl-1*H*-benzo[d]imidazol-2-yl)benzamide, Model-BI-(+), (2)

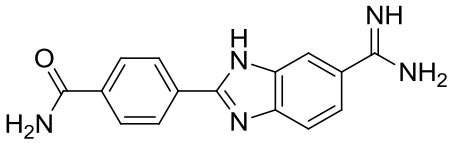

2

Compound **2** was synthesized by General Procedure 2.4.3.2. (35 mg, 76%); ^{1}H NMR (DMSO-d_6); δ6.92 (s, 1H), 7.14 (s, 1H), 7.42 (dd, *J* = 9 Hz, 1H), 7.67 (d, *J* = 9 Hz, 1H), 7.81 (d, *J* = 6 Hz, 2H), 7.90 (s, 1H), 8.06 (d, *J* = 9Hz, 2H), 8.39 (s, 2H), 9.05 (s, 2H); LC/MS calcd for $[M+H]^+$: $C_{15}H_{13}N_5O$ 280.1, found 280.2.

***N*-(2-amino-2-oxoethyl)-4-(6-carbamimidoyl-1*H*-benzo[d]imidazol-2-yl)benzamide, Gly-BI-(+), (3)**

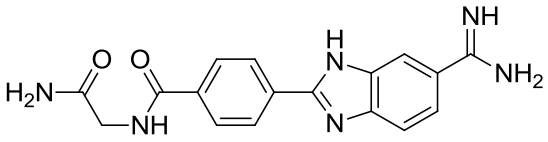

3

Compound **3** was obtained from **2** and Rink-Gly-Fmoc by General Procedure 2.4.3.3. (48 mg, 88%); ^{1}H NMR (DMSO-d_6); δ3.71 (d, *J* = 6 Hz, 2H), 6.93 (d, *J* = 8.5 Hz, 1H), 7.28 (s, 1H), 7.55 (dd, *J* = 8 Hz, 1H), 7.67 (d, *J* = 7.5 Hz, 1H), 7.94 (t, *J* = 14 Hz, 2H), 8.03 (s, 1H), 8.18 (d, *J* = 15 Hz, 2H), 8.69 (s, 2H), 8.86 (s, 1H), 9.14 (s, 2H); LC/MS calcd for $[M+H]^+$: $C_{17}H_{16}N_6O_2$ 337.1, found 337.3.

***N*-(1-amino-1-oxopropan-2-yl)-4-(6-carbamimidoyl-1*H*-benzo[d]imidazol-2-yl)benzamide, Ala-BI-(+), (4)**

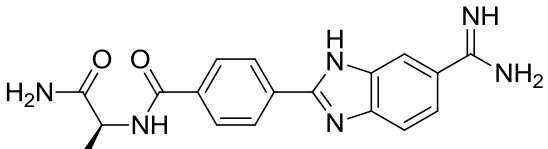

4

Compound **4** was obtained from **2** and Rink-Ala-Fmoc by General Procedure 2.4.3.3. (42 mg, 74%); ^{1}H NMR (DMSO-d_6); δ1.43 (d, *J* = 7 Hz, 3H), 4.46 (m, 1H), 7.03 (s, 1H), 7.43 (s, 1H), 7.70 (dd, *J* = 9 Hz, 1H), 7.83 (d, *J* = 8 Hz, 1H), 8.11 (d, *J* = 9 Hz, 2H), 8.17 (s, 1H), 8.31 (d, *J* = 9 Hz, 2H), 8.58 (d, *J* = 7 Hz, 1H), 8.93 (s, 2H), 9.30 (s, 1H); LC/MS calcd for $[M+H]^+$: $C_{18}H_{18}N_6O_2$ 351.1, found 351.4.

***N*-(1-amino-3-methyl-1-oxobutan-2-yl)-4-(6-carbamimidoyl-1*H*-benzo[d]imidazol-2-yl)benzamide, Val-BI-(+), (5)**

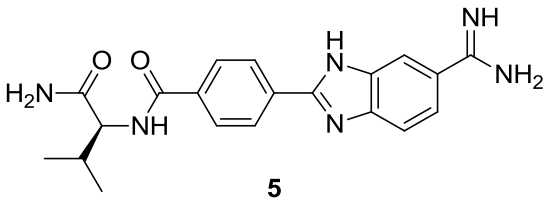

5

Compound **5** was obtained from **2** and Rink-Val-Fmoc by General Procedure 2.4.3.3. (50 mg, 81%); ^{1}H NMR (DMSO-d_6); δ0.94 (d, *J* = 3Hz, 3H), 0.96 (d, *J* = 3 Hz, 3H), 2.13 (m, 1H), 4.31 (m, 1H), 7.11 (s, 1H), 7.52 (s, 1H), 7.68 (dd, *J* = 10 Hz, 1H), 7.82 (d, *J* = 8 Hz, 1H), 8.09 (d, *J* = 9 Hz, 2H), 8.17 (s, 1H), 8.30 (d, *J* = 8 Hz, 2H), 8.34 (s, 1H), 8.95 (s, 1H), 9.30 (s, 1H); LC/MS calcd for $[M+H]^+$: $C_{20}H_{22}N_6O_2$ 379.2, found 379.3.

***N*-(1-amino-4-methyl-1-oxopentan-2-yl)-4-(6-carbamimidoyl-1*H*-benzo[d]imidazol-2-yl)benzamide, Leu-BI-(+), (6)**

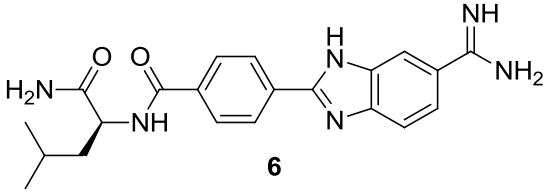

6

Compound **6** was obtained from **2** and Rink-Leu-Fmoc by General Procedure 2.4.3.3. (49 mg, 76%); ^{1}H NMR (DMSO-d_6); δ0.90 (d, *J* = 6.5 Hz, 3H), 0.94 (d, *J* = 6.5 Hz, 3H), 1.23 (t, *J* = 14 Hz, 2H), 1.73 (m, 1H), 4.48 (m, 1H), 6.93 (s, 1H), 7.28 (s, 1H), 7.69 (dd, *J* = 9.5 Hz, 1H), 7.82 (d, *J* = 8.5 Hz, 1H), 8.10 (d, *J* = 8.5 Hz, 2H), 8.17 (s, 1H), 8.32 (d, *J* = 8.5 Hz, 2H), 8.76 (d, *J* = 8 Hz, 1H), 9.12 (s, 2H), 9.30 (s, 2H); LC/MS calcd for $[M+H]^+$: $C_{21}H_{24}N_6O_2$ 393.2, found 393.2.

***N*-(1-amino-3-methyl-1-oxopentan-2-yl)-4-(6-carbamimidoyl-1*H*-benzo[d]imidazol-2-yl)benzamide, Ile-BI-(+), (7)**

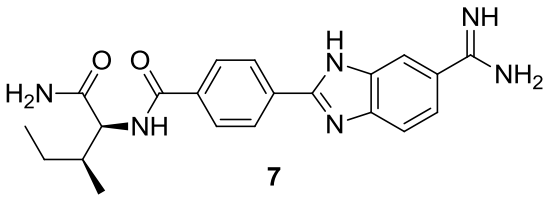

7

Compound **7** was obtained from **2** and Rink-Ile-Fmoc by General Procedure 2.4.3.3. (47 mg, 73%); ^{1}H NMR (DMSO-d_6); δ0.80 (t, *J* = 13 Hz, 3H), 0.87 (d, *J* = 6.5 Hz, 3H), 1.15 (m, 2H), 1.47 (m, 1H), 4.28 (t, *J* = 15 Hz, 1H), 7.04 (s, 1H), 7.47 (s, 1H), 7.52 (d, *J* = 8 Hz, 1H), 7.63 (d, *J* = 8.5 Hz, 1H), 7.93 (d, *J* = 8 Hz, 1H), 8.05 (d, *J* = 8.5 Hz, 2H), 8.26 (d, *J* = 8.5 Hz, 2H), 8.30 (d, *J* = 8.5 Hz, 1H), 8.80 (s, 2H), 9.24 (s, 2H); LC/MS calcd for $[M+H]^+$: $C_{21}H_{24}N_6O_2$ 393.2, found 393.2.

***N*-(1-amino-4-(methylthio)-1-oxobutan-2-yl)-4-(6-carbamimidoyl-1*H*-benzo[d]imidazol-2-yl)benzamide, Met-BI-(+), (8)**

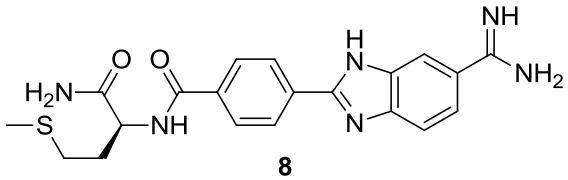

8

Compound **8** was obtained from **2** and Rink-Met-Fmoc by General Procedure 2.4.3.3. (49 mg, 73%); ^{1}H NMR (DMSO-d_6); δ1.94 (s, 3H), 2.44 (t, *J* = 11 Hz, 2H), 3.19 (q, *J* = 15.5 Hz, 2H), 4.40 (m, 1H), 6.97 (s, 1H), 7.35 (s, 1H), 7.56 (dd, *J* = 10 Hz, 1H), 7.70 (d, *J* = 8.5 Hz, 1H), 7.98 (t, *J* = 15.5 Hz, 2H), 8.04 (s, 1H), 8.19 (t, *J* = 15 Hz, 2H), 8.48 (d, *J* = 12 Hz, 1H), 8.83 (s, 2H), 9.17 (s, 2H); LC/MS calcd for $[M+H]^+$: $C_{20}H_{22}N_6O_2S$ 411.2, found 411.5.

1-(4-(6-Carbamimidoyl-1*H*-benzo[d]imidazol-2-yl)benzoyl)pyrrolidine-2-carboxamide, Pro-BI-(+), (9)

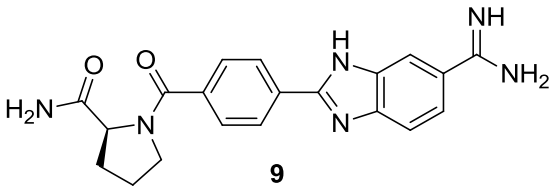

9

Compound **9** was obtained from **2** and Rink-Pro-Fmoc by General Procedure 2.4.3.3. (49 mg, 79%); ^{1}H NMR (DMSO-d_6); δ1.24 (m, 2H), 1.88 (m, 2H), 3.62 (t, *J* = 14 Hz, 2H), 4.40 (t, *J* = 14 Hz, 1H), 7.17 (s, 1H), 7.69 (d, *J* = 8.5 Hz, 1H), 7.76 (d, *J* = 8 Hz, 1H), 7.81 (d, *J* = 8.5 Hz, 2H), 8.17 (s, 1H), 8.24 (t, *J* = 15.5 Hz, 1H), 8.30 (t, *J* = 14.5 Hz, 2H), 9.08 (s, 1H), 9.30 (s, 1H); LC/MS calcd for $[M+H]^+$: $C_{20}H_{20}N_6O_2$ 377.2, found 377.5.

***N*-(1-amino-1-oxo-3-phenylpropan-2-yl)-4-(6-carbamimidoyl-1*H*-benzo[d]imidazol-2-yl)benzamide, Phe-BI-(+), (10)**

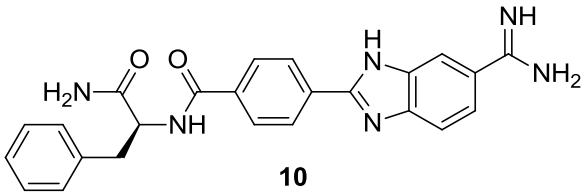

10

Compound **10** was obtained from **2** and Rink-Phe-Fmoc by General Procedure 2.4.3.3. (45 mg, 64%); ^{1}H NMR (DMSO-d_6); δ2.55 (t, *J* = 11 Hz, 2H), 4.68 (m, 1H), 7.02 (s, 1H), 7.17 (m, 1H), 7.22 (q, *J* = 8 Hz, 2H), 7.27 (t, *J* = 15 Hz, 2H), 7.61 (s, 1H), 7.69 (dd, *J* = 8.5 Hz, 1H), 7.82 (d, *J* = 8.5 Hz, 1H), 8.01 (d, *J* = 7.5 Hz, 2H), 8.17 (s, 1H), 8.29 (t, *J* = 15 Hz, 2H), 8.88 (d, *J* = 8 Hz, 1H), 8.98 (s, 2H), 9.30 (s, 2H); LC/MS calcd for $[M+H]^+$: $C_{24}H_{22}N_6O_2$ 427.2, found 427.4.

***N*-(1-amino-3-hydroxy-1-oxobutan-2-yl)-4-(6-carbamimidoyl-1*H*-benzo[d]imidazol-2-yl)benzamide, Thr-BI-(+), (11)**

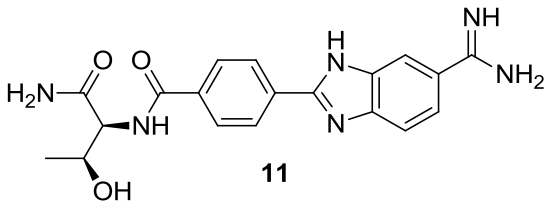

11

Compound **11** was obtained from **2** and Rink-Thr(tBu)-Fmoc by General Procedure 2.4.3.3. (48 mg, 77%); ^{1}H NMR (DMSO-d_6); δ1.13 (d, *J* = 6.5 Hz, 3H), 4.12 (t, *J* = 10.5 Hz, 1H), 4.38 (q, *J* = 8.7 Hz, 1H), 6.94 (s, 1H), 7.27 (s, 1H), 7.45 (s, 1H), 7.69 (d, *J* = 8 Hz, 1H), 8.08 (d, *J* = 8.5 Hz, 1H), 8.13 (d, *J* = 8.5 Hz, 2H), 8.26 (d, *J* = 8.5 Hz, 1H), 8.34 (d, *J* = 8 Hz, 2H), 8.43 (s, 1H), 8.88 (s, 2H), 9.30 (s, 2H); LC/MS calcd for $[M+H]^+$: $C_{19}H_{20}N_6O_3$ 381.2, found 381.4.

2-(4-(6-Carbamimidoyl-1*H*-benzo[d]imidazol-2-yl)benzamido)succinamide, Asn-BI-(+), (12)

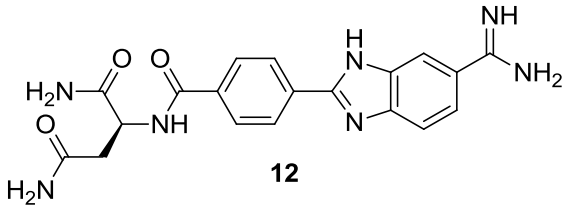

12

Compound **12** was obtained from **2** and Rink-Asn(Trt)-Fmoc by General Procedure 2.4.3.3. (51 mg, 79%); ^{1}H NMR (DMSO-d_6); δ2.61 (d, *J* = 8.5 Hz, 2H), 4.73 (m, 1H), 7.04 (s, 1H), 7.14 (s, 1H), 7.24 (s, 2H), 7.69 (dd, *J* = 8.5 Hz, 1H), 7.83 (d, *J* = 8.5 Hz, 1H), 8.07 (d, *J* = 8.5 Hz, 2H), 8.17 (s, 1H), 8.32 (d, *J* = 8 Hz, 2H), 8.67 (d, *J* = 8 Hz, 2H), 9.06 (s, 2H), 9.30 (s, 2H); LC/MS calcd for $[M+H]^+$: $C_{19}H_{19}N_7O_3$ 394.2, found 394.3.

2-(4-(6-Carbamimidoyl-1*H*-benzo[d]imidazol-2-yl)benzamido)pentanediamide, Gln-BI-(+), (13)

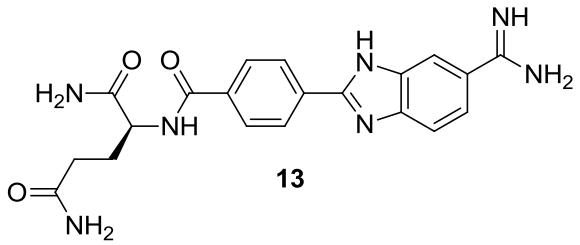

13

Compound **13** was obtained from **2** and Rink-Gln(Trt)-Fmoc by General Procedure 2.4.3.3. (49 mg, 73%); ^{1}H NMR (DMSO-d_6); δ1.95 (m, 2H), 2.36 (m, 2H), 4.41 (m, 1H), 7.02 (s, 1H), 7.12 (s, 2H), 7.22 (s, 1H), 7.69 (d, *J* = 9.5 Hz, 1H), 7.83 (d, *J* = 8.5 Hz, 1H), 8.11 (t, *J* = 14 Hz, 2H), 8.17 (s, 1H), 8.32 (t, *J* = 14.5 Hz, 2H), 8.97 (s, 2H), 9.28 (s, 1H), 9.30 (s, 2H); %). LC/MS calcd for $[M+H]^+$: $C_{20}H_{21}N_7O_3$ 408.2, found 408.5.

***N*-(1-amino-3-(4-hydroxyphenyl)-1-oxopropan-2-yl)-4-(6-carbamimidoyl-1*H*-benzo[d]imidazol-2-yl)benzamide, Tyr-BI-(+), (14)**

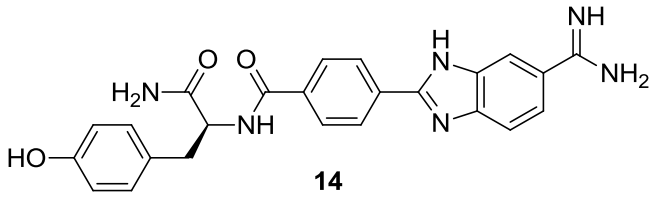

14

Compound **14** was obtained from **2** and Rink-Tyr(tBu)-Fmoc by General Procedure 2.4.3.3. (44 mg, 61%); ^{1}H NMR (DMSO-d_6); δ2.55 (t, *J* = 11 Hz, 2H), 4.58 (m, 1H), 6.65 (t, *J* = 18 Hz, 2H), 7.13 (t, *J* = 18 Hz, 2H), 7.25 (s, 1H), 7.57 (s, 1H), 7.69 (d, *J* = 8.5 Hz, 1H), 7.83 (d, *J* = 8 Hz, 1H), 8.02 (d, *J* = 8 Hz, 2H), 8.17 (s, 1H), 8.29 (t, *J* = 17 Hz, 2H), 8.59 (d, *J* = 8.5 Hz, 1H), 9.07 (s, 2H), 9.30 (s, 2H); LC/MS calcd for $[M+H]^+$: $C_{24}H_{22}N_6O_3$ 443.2, found 443.5.

4-(6-Carbamimidoyl-1*H*-benzo[d]imidazol-2-yl)-*N*-(1,6-diamino-1-oxohexan-2-yl)benzamide, Lys-BI-(+), (15)

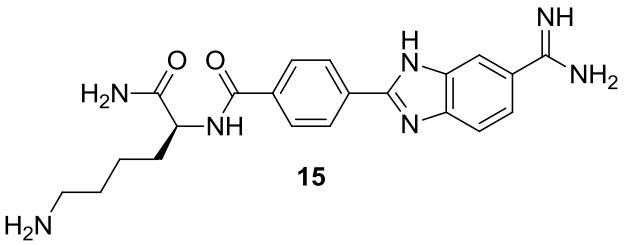

15

Compound **15** was obtained from **2** and Rink-Lys(Boc)-Fmoc by General Procedure 2.4.3.3. (43 mg, 64%); ^{1}H NMR (DMSO-d_6); δ1.44 (m, 2H), 1.58 (t, *J* = 14 Hz, 2H), 1.78 (m, 2H), 2.79 (q, *J* = 8.5 Hz, 2H), 4.40 (q, *J* = 8.5 Hz, 1H), 7.23 (s, 1H), 7.33 (s, 1H), 7.71 (dd, *J* = 8.5 Hz, 1H), 7.83 (s, 2H), 7.89 (d, *J* = 8 Hz, 1H), 8.11 (d, *J* = 8.5 Hz, 2H), 8.19 (s, 1H), 8.35 (d, *J* = 8 Hz, 2H), 8.59 (d, *J* = 8.5 Hz, 1H), 8.95 (s, 2H), 9.34 (s, 2H); LC/MS calcd for $[M+H]^+$: $C_{21}H_{25}N_7O_2$ 408.2, found 408.5.

***N*-(1-amino-5-guanidino-1-oxopentan-2-yl)-4-(6-carbamimidoyl-1*H*-benzo[d]imidazol-2-yl)benzamide, Arg-BI-(+), (16)**

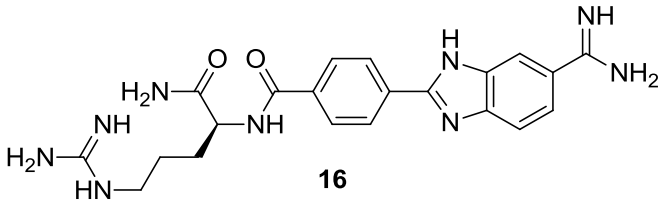

16

Compound **16** was obtained from **2** and Rink-Arg(Pbf)-Fmoc by General Procedure 2.4.3.3. (41 mg, 58%); ^{1}H NMR (DMSO-d_6); δ1.58 (m, 2H), 1.75 (m, 2H), 3.12 (q, *J* = 12.2 Hz, 2H), 4.40 (m, 1H), 7.06 (s, 1H), 7.12 (s, 1H), 7.23 (s, 1H), 7.33 (s, 1H), 7.58 (s, 2H), 7.68 (dd, *J* = 9 Hz, 1H), 7.82 (d, *J* = 8.5 Hz, 1H), 8.05 (t, *J* = 14 Hz, 2H), 8.15 (s, 1H), 8.26 (t, *J* = 13 Hz, 2H), 8.62 (d, *J* = 7.5 Hz, 1H), 8.92 (s, 2H), 9.34 (s, 2H); LC/MS calcd for $[M+H]^+$: $C_{21}H_{25}N_9O_2$ 436.2, found 436.5.

4-Amino-3-(4-(6-carbamimidoyl-1*H*-benzo[d]imidazol-2-yl)benzamido)-4-oxobutanoic acid, Asp-BI-(+), (17)

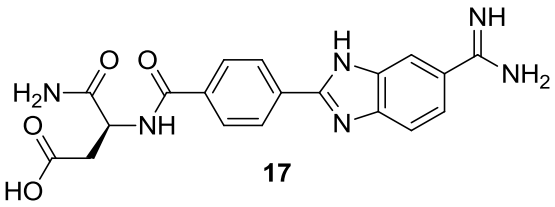

17

Compound **17** was obtained from **2** and Rink-Asp(OtBu)-Fmoc by General Procedure 2.4.3.3. (50 mg, 78%); ^{1}H NMR (DMSO-d_6); δ2.20 (m, 2H), 4.63 (m, 1H), 6.75 (s, 1H), 6.96 (s, 1H), 7.05 (s, 1H), 7.47 (dd, *J* = 8 Hz, 1H), 7.62 (d, *J* = 10 Hz, 1H), 7.88 (d, *J* = 8 Hz, 2H), 7.97 (s, 1H), 8.11 (d, *J* = 7.5 Hz, 2H), 8.36 (d, *J* = 6.5 Hz, 1H), 8.75 (s, 2H), 9.12 (s, 2H); LC/MS calcd for $[M+H]^+$: $C_{19}H_{18}N_6O_4$ 395.1, found 395.1.

5-Amino-4-(4-(6-carbamimidoyl-1*H*-benzo[d]imidazol-2-yl)benzamido)-5-oxopentanoic acid, Glu-BI-(+), (18)

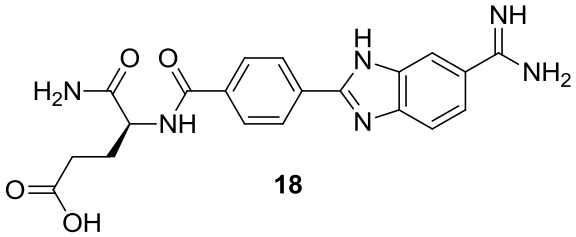

18

Compound **18** was obtained from **2** and Rink-Glu(OtBu)-Fmoc by General Procedure 2.4.3.3. (48 mg, 72%); ^{1}H NMR (DMSO-d_6); δ1.75 (m, 2H), 2.14 (m, 2H), 4.22 (m, 1H), 6.85 (s, 1H), 6.95 (s, 1H), 7.05 (s, 1H), 7.48 (dd, *J* = 8.5 Hz, 1H), 7.61 (d, *J* = 8.5 Hz, 1H), 7.88 (t, *J* = 14 Hz, 2H), 7.96 (s, 1H), 8.11 (t, *J* = 14.5 Hz, 2H), 8.58 (d, *J* = 7.5 Hz, 1H), 8.95 (s, 2H), 9.09 (s, 2H); LC/MS calcd for $[M+H]^+$: $C_{20}H_{20}N_6O_4$ 409.2, found 409.4.

***N*-(2-((2-amino-2-oxoethyl)amino)-2-oxoethyl)-4-(6-carbamimidoyl-1*H*-benzo[d]imidazol-2-yl)benzamide, Gly-Gly-BI-(+), (19)**

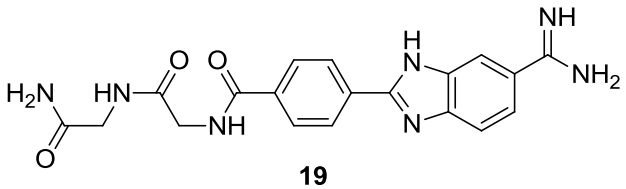

19

Compound **19** was obtained from **2** and Rink-Gly-Gly-Fmoc by General Procedure 2.4.3.4. (60 mg, 93%); ^{1}H NMR (DMSO-d_6); δ3.66 (d, *J* = 6 Hz, 2H), 3.95 (d, *J* = 6.5 Hz, 2H), 7.11 (s, 1H), 7.26 (s, 1H), 7.68 (dd, *J* = 8.5 Hz, 1H), 7.82 (d, *J* = 8.5 Hz, 1H), 8.10 (d, *J* = 8.5 Hz, 2H), 8.17 (s, 1H), 8.21 (t, *J* = 12 Hz, 1H), 8.32 (d, *J* = 8.5 Hz, 2H), 8.88 (s, 2H), 8.97 (t, *J* = 11.5 Hz, 1H), 9.29 (s, 2H); LC/MS calcd for $[M+H]^+$: $C_{19}H_{19}N_7O_3$ 394.2, found 394.3.

***N*-(2-((1-amino-1-oxopropan-2-yl)amino)-2-oxoethyl)-4-(6-carbamimidoyl-1*H*-benzo[d]imidazol-2-yl)benzamide, Ala-Gly-BI-(+), (20)**

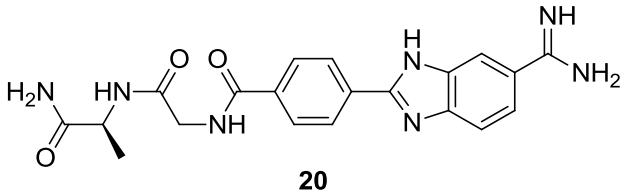

20

Compound **20** was obtained from **2** and Rink-Ala-Gly-Fmoc by General Procedure 2.4.3.4. (55 mg, 82%); ^{1}H NMR (DMSO-d_6); δ1.23 (d, *J* = 8 Hz, 3H), 3.94 (d, *J* = 8.5 Hz, 2H), 4.24 (p, 1H), 7.05 (s, 1H), 7.32 (s, 1H), 7.69 (dd, *J* = 8.5 Hz, 1H), 7.82 (d, *J* = 8.5 Hz, 1H), 8.08 (d, *J* = 8.5 Hz, 2H), 8.10 (t, *J* = 12 Hz, 1H), 8.17 (s, 1H), 8.32 (d, *J* = 8.5 Hz, 2H), 8.92 (t, *J* = 11.5 Hz, 1H), 9.01 (s, 2H), 9.30 (s, 2H); LC/MS calcd for $[M+H]^+$: $C_{20}H_{21}N_7O_3$ 408.2, found 408.2.

***N*-(2-((1-amino-3-methyl-1-oxobutan-2-yl)amino)-2-oxoethyl)-4-(6-carbamimidoyl-1*H*-benzo[d]imidazol-2-yl)benzamide, Val-Gly-BI-(+), (21)**

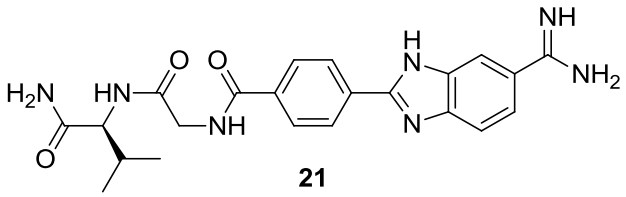

21

Compound **21** was obtained from **2** and Rink-Val-Gly-Fmoc by General Procedure 2.4.3.4. (62 mg, 87%); ^{1}H NMR (DMSO-d_6); δ0.84 (d, *J* = 7 Hz, 3H), 0.87 (d, *J* = 7 Hz, 3H), 1.99 (m, 1H), 3.99 (d, *J* = 7.5 Hz, 2H), 4.16 (t, *J* = 15 Hz, 1H), 7.07 (s, 1H), 7.42 (s, 1H), 7.68 (dd, *J* = 8.5 Hz, 1H), 7.82 (t, *J* = 13.5 Hz, 1H), 7.84 (s, 1H), 8.08 (d, *J* = 8.5 Hz, 2H), 8.17 (s, 1H), 8.32 (d, *J* = 8.5 Hz, 2H), 8.90 (s, 2H), 8.91 (s, 1H), 9.29 (s, 2H); LC/MS calcd for $[M+H]^+$: $C_{22}H_{25}N_7O_3$ 436.2, found 436.3.

***N*-(2-((1-amino-4-methyl-1-oxopentan-2-yl)amino)-2-oxoethyl)-4-(6-carbamimidoyl-1*H*-benzo[d]imidazol-2-yl)benzamide, Leu-Gly-BI-(+), (22)**

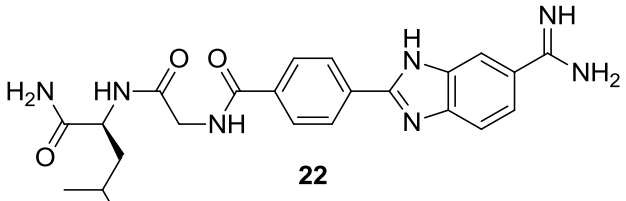

22

Compound **22** was obtained from **2** and Rink-Leu-Gly-Fmoc by General Procedure 2.4.3.4. (63 mg, 85%); ^{1}H NMR (DMSO-d_6); δ0.86 (d, *J* = 9.5 Hz, 3H), 0.89 (d, *J* = 9.5 Hz, 3H), 1.48 (t, *J* = 10 Hz, 2H), 1.60 (m, 1H), 3.96 (d, *J* = 5.5 Hz, 2H), 4.25 (q, *J* = 14.5 Hz, 1H), 7.02 (s, 1H), 7.34 (s, 1H), 7.68 (dd, *J* = 8 Hz, 1H), 7.82 (s, 1H), 8.04 (d, *J* = 8.5 Hz, 1H), 8.08 (d, *J* = 8.5 Hz, 2H), 8.17 (s, 1H), 8.32 (d, *J* = 8.5 Hz, 2H), 8.91 (t, *J* = 12.5 Hz, 1H), 8.96 (s, 2H), 9.29 (s, 2H); LC/MS calcd for $[M+H]^+$: $C_{23}H_{27}N_7O_3$ 450.2, found 450.2.

***N*-(2-((1-amino-3-methyl-1-oxopentan-2-yl)amino)-2-oxoethyl)-4-(6-carbamimidoyl-1*H*-benzo[d]imidazol-2-yl)benzamide, Ile-Gly-BI-(+), (23)**

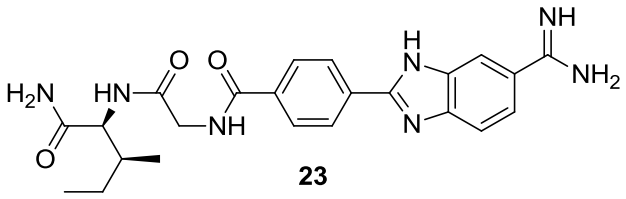

23

Compound **23** was obtained from **2** and Rink-Ile-Gly-Fmoc by General Procedure 2.4.3.4. (67 mg, 91%); ^{1}H NMR (DMSO-d_6); δ0.82 (t, *J* = 13 Hz, 3H), 0.86 (d, *J* = 9 Hz, 3H), 1.08 (m, 2H), 1.44 (m, 1H), 3.99 (t, *J* = 11 Hz, 2H), 4.19 (t, *J* = 15.5 Hz, 1H), 7.07 (s, 1H), 7.43 (s, 1H), 7.69 (d, *J* = 9 Hz, 1H), 7.82 (s, 1H), 7.86 (d, *J* = 9 Hz, 1H), 8.08 (d, *J* = 8.5 Hz, 2H), 8.17 (s, 1H), 8.32 (d, *J* = 8.5 Hz, 2H), 8.89 (s, 2H), 8.91 (t, *J* = 11.5 Hz, 1H), 9.30 (s, 2H); LC/MS calcd for $[M+H]^+$: $C_{23}H_{27}N_7O_3$ 450.2, found 450.4.

***N*-(2-((1-amino-4-(methylthio)-1-oxobutan-2-yl)amino)-2-oxoethyl)-4-(6-carbamimidoyl-1*H*-benzo[d]imidazol-2-yl)benzamide, Met-Gly-BI-(+), (24)**

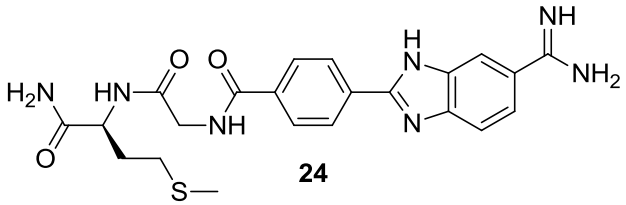

24

Compound **24** was obtained from **2** and Rink-Met-Gly-Fmoc by General Procedure 2.4.3.4. (69 mg, 90%); ^{1}H NMR (DMSO-d_6); δ3.88 (m, 2H), 3.97 (m, 2H), 4.50 (m, 2H), 6.89 (s, 1H), 7.14 (s, 1H), 7.18 (s, 1H), 7.34 (s, 1H), 7.69 (dd, *J* = 8.5 Hz, 1H), 7.83 (d, *J* = 8.5 Hz, 1H), 8.08 (d, *J* = 8.5 Hz, 2H), 8.18 (s, 1H), 8.26 (d, *J* = 8 Hz, 1H), 8.33 (d, *J* = 8.5 Hz, 2H), 8.96 (s, 2H), 9.00 (t, *J* = 11.5 Hz, 1H), 9.30 (s, 2H); LC/MS calcd for $[M+H]^+$: $C_{22}H_{25}N_7O_3S$ 468.1, found 468.2.

1-(2-(4-(6-Carbamimidoyl-1*H*-benzo[d]imidazol-2-yl)benzamido)acetyl)pyrrolidine-2-carboxamide, Pro-Gly-BI-(+), (25)

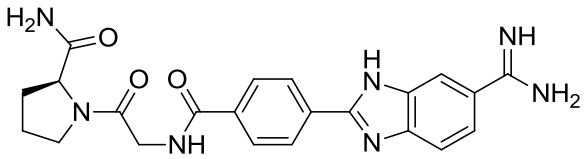

25

Compound **25** was obtained from **2** and Rink-Pro-Gly-Fmoc by General Procedure 2.4.3.4. (65 mg, 91%); ^{1}H NMR (DMSO-d_6); δ1.76 (m, 2H), 1.88 (m, 2H), 3.39 (q, *J* = 17 Hz, 2H), 3.95 (d, *J* = 5.5 Hz, 2H), 4.08 (d, *J* = 8.5 Hz, 1H), 6.80 (s, 1H), 7.11 (s, 1H), 7.53 (dd, *J* = 8.5 Hz, 1H), 7.66 (d, *J* = 8.5 Hz, 1H), 7.93 (d, *J* = 8.5 Hz, 2H), 8.01 (s, 1H), 8.16 (d, *J* = 8 Hz, 2H), 8.61 (t, *J* = 11 Hz, 1H), 8.82 (s, 2H), 9.14 (s, 2H); LC/MS calcd for $[M+H]^+$: $C_{22}H_{23}N_7O_3$ 434.2, found 434.3.

***N*-(2-((1-amino-1-oxo-3-phenylpropan-2-yl)amino)-2-oxoethyl)-4-(6-carbamimidoyl-1*H*-benzo[d]imidazol-2-yl)benzamide, Phe-Gly-BI-(+), (26)**

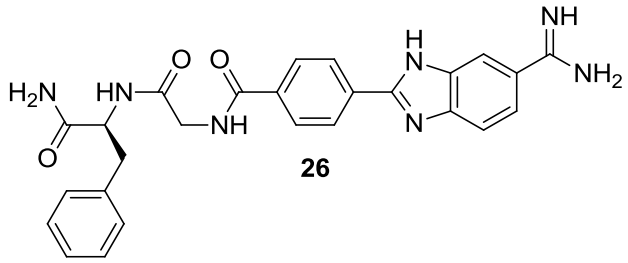

26

Compound **26** was obtained from **2** and Rink-Phe-Gly-Fmoc by General Procedure 2.4.3.4. (61 mg, 77%); ^{1}H NMR (DMSO-d_6); δ3.04 (dd, *J* = 14 Hz, 2H), 3.81 (d, *J* = 10.5 Hz, 2H), 4.46, 4.48 (ABd, *J* = 8.8 Hz, 1H), 7.14 (s, 1H), 7.18 (d, *J* = 5 Hz, 1H), 7.24 (d, *J* = 4 Hz, 4H), 7.45 (s, 1H), 7.70 (dd, *J* = 8.5 Hz, 1H), 7.82 (d, *J* = 7 Hz, 1H), 8.06 (d, *J* = 8.5 Hz, 2H), 8.12 (d, *J* = 8.5 Hz, 1H), 8.18 (s, 1H), 8.32 (d, *J* = 8 Hz, 2H), 8.83 (s, 2H), 8.88 (t, *J* = 12 Hz, 1H), 9.29 (s, 2H); LC/MS calcd for $[M+H]^+$: $C_{26}H_{25}N_7O_3$ 484.2, found 484.3.

***N*-(2-((1-amino-3-(1H-indol-3-yl)-1-oxopropan-2-yl)amino)-2-oxoethyl)-4-(6-carbamimidoyl-1*H*-benzo[d]imidazol-2-yl)benzamide, Trp-Gly-BI-(+), (27)**

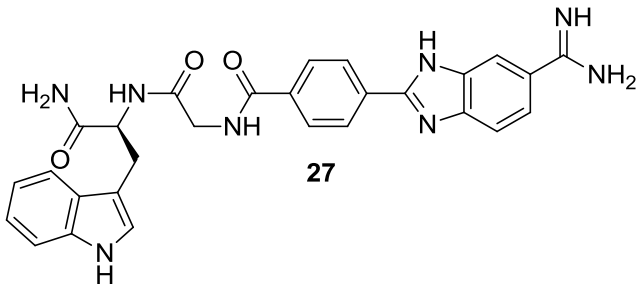

27

Compound **27** was obtained from **2** and Rink-Trp(Boc)-Gly-Fmoc by General Procedure 2.4.3.4. (63 mg, 74%); ^{1}H NMR (DMSO-d_6); δ2.93 (m, 2H), 3.92 (d, *J* = 9 Hz, 2H), 4.43 (q, *J* = 9.2 Hz, 1H), 6.89 (t, *J* = 15 Hz, 1H), 6.96 (t, *J* = 16 Hz, 1H), 7.05 (d, *J* = 13 Hz, 2H), 7.24 (d, *J* = 8 Hz, 1H), 7.36 (s, 1H), 7.52 (d, *J* =7.5 Hz, 1H), 7.61 (dd, *J* = 8.5 Hz, 1H), 7.75 (d, *J* = 8.5 Hz, 1H), 7.99 (d, *J* = 8.5 Hz, 2H), 8.02 (d, *J* = 8.5 Hz, 1H), 8.10 (s, 1H), 8.25 (d, *J* = 8.5 Hz, 2H), 8.81 (t, *J* = 13 Hz, 1H), 8.91 (s, 2H), 9.22 (s, 2H), 10.71 (s, 1H); LC/MS calcd for $[M+H]^+$: $C_{28}H_{26}N_8O_3$ 523.2, found 523.3.

***N*-(2-((1-amino-3-hydroxy-1-oxopropan-2-yl)amino)-2-oxoethyl)-4-(6-carbamimidoyl-1*H*-benzo[d]imidazol-2-yl)benzamide, Ser-Gly-BI-(+), (28)**

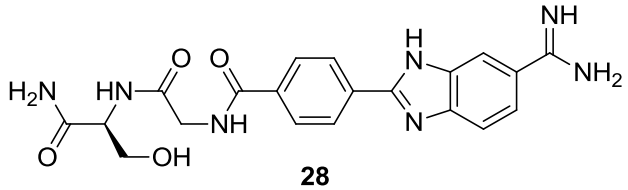

28

Compound **28** was obtained from **2** and Rink-Ser(tBu)-Gly-Fmoc by General Procedure 2.4.3.4. (41 mg, 59%); ^{1}H NMR (DMSO-d_6); δ3.61 (m, 2H), 3.98 (m, 2H), 4.24 (q, *J* = 8.5 Hz, 1H), 7.15 (s, 1H), 7.31 (s, 1H), 7.69 (dd, *J* = 8.5 Hz, 1H), 7.82 (d, *J* = 8.5 Hz, 1H), 7.98 (d, *J* = 8.5 Hz, 1H), 8.08 (d, *J* = 8.5 Hz, 2H), 8.18 (s, 1H), 8.33 (d, *J* = 8.5 Hz, 2H), 8.95 (t, *J* = 10.5 Hz, 1H), 8.97 (s, 1H), 9.30 (s, 2H); LC/MS calcd for $[M+H]^+$: $C_{20}H_{21}N_7O_4$ 424.2, found 424.3.

***N*-(2-((1-amino-3-hydroxy-1-oxobutan-2-yl)amino)-2-oxoethyl)-4-(6-carbamimidoyl-1*H*-benzo[d]imidazol-2-yl)benzamide, Thr-Gly-BI-(+), (29)**

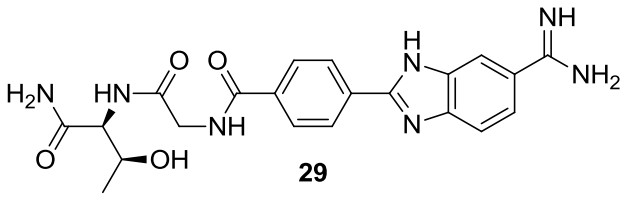

29

Compound **29** was obtained from **2** and Rink-Thr(tBu)-Gly-Fmoc by General Procedure 2.4.3.4. (64 mg, 89%); ^{1}H NMR (DMSO-d_6); δ0.88 (d, *J* = 6.5 Hz, 3H), 1.14 (m, 1H), 3.96 (m, 2H), 5.02 (t, *J* = 12 Hz, 1H), 6.97 (s, 1H), 7.06 (s, 1H), 7.53 (dd, *J* = 9.5 Hz, 1H), 7.62 (s, 1H), 7.66 (d, *J* = 8.5 Hz, 1H), 7.81 (d, *J* = 9 Hz, 1H), 7.93 (d, *J* = 8.5 Hz, 2H), 8.01 (s, 1H), 8.16 (d, *J* = 8 Hz, 2H), 8.19 (s, 1H), 8.81 (t, *J* = 11.5 Hz, 2H), 9.13 (s, 2H); LC/MS calcd for $[M+H]^+$: $C_{21}H_{23}N_7O_4$ 438.2, found 438.2.

2-(2-(4-(6-Carbamimidoyl-1*H*-benzo[d]imidazol-2-yl)benzamido)acetamido)succinamide, Asn-Gly-BI-(+), (30)

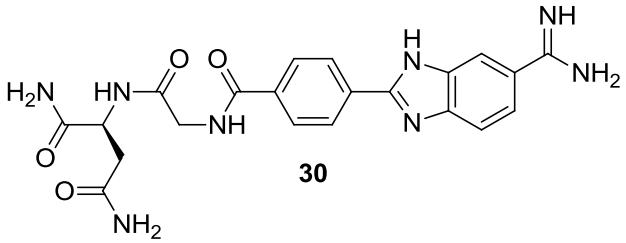

30

Compound **30** was obtained from **2** and Rink-Asn(Trt)-Gly-Fmoc by General Procedure 2.4.3.4. (51 mg, 69%); ^{1}H NMR (DMSO-d_6); δ1.74 (m, 2H), 3.89 (m, 2H), 4.24 (q, *J* = 10.5 Hz, 1H), 7.06 (s, 1H), 7.29 (s, 1H), 7.61 (dd, *J* = 8.5 Hz, 1H), 7.75 (d, *J* = 8.5 Hz, 1H), 8.01 (d, *J* = 8.5 Hz, 2H), 8.06 (d, *J* = 8.5 Hz, 1H), 8.10 (s, 1H), 8.25 (d, *J* = 8.5 Hz, 2H), 8.87 (t, *J* = 11.5 Hz, 1H), 8.92 (s, 2H), 9.23 (s, 2H); LC/MS calcd for $[M+H]^+$: $C_{21}H_{22}N_8O_4$ 451.2, found 451.3.

2-(2-(4-(6-Carbamimidoyl-1*H*-benzo[d]imidazol-2-yl)benzamido)acetamido)pentanediamide, Gln-Gly-BI-(+), (31)

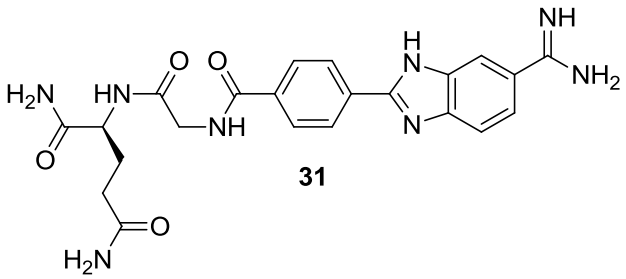

31

Compound **31** was obtained from **2** and Rink-Gln(Trt)-Gly-Fmoc by General Procedure 2.4.3.4. (56 mg, 73%); ^{1}H NMR (DMSO-d_6); δ1.83 (m, 2H), 2.00 (t, *J* = 14 Hz, 2H), 4.01 (t, *J* = 10 Hz, 2H), 4.24 (q, *J* = 8.2 Hz, 1H), 6.80 (s, 1H), 7.15 (s, 1H), 7.33 (s, 2H), 7.73 (dd, *J* = 8.5 Hz, 1H), 7.87 (d, *J* = 8 Hz, 1H), 8.13 (d, *J* = 8.5 Hz, 2H), 8.17 (d, *J* = 8.5 Hz, 1H), 8.22 (s, 1H), 8.37 (d, *J* = 8.5 Hz, 2H), 8.93 (s, 2H), 8.98 (t, *J* = 11.5 Hz, 1H), 9.34 (s, 2H); LC/MS calcd for $[M+H]^+$: $C_{22}H_{24}N_8O_4$ 465.2, found 465.2.

***N*-(2-((1-amino-3-(4-hydroxyphenyl)-1-oxopropan-2-yl)amino)-2-oxoethyl)-4-(6-carbamimidoyl-1*H*-benzo[d]imidazol-2-yl)benzamide, Tyr-Gly-BI-(+), (32)**

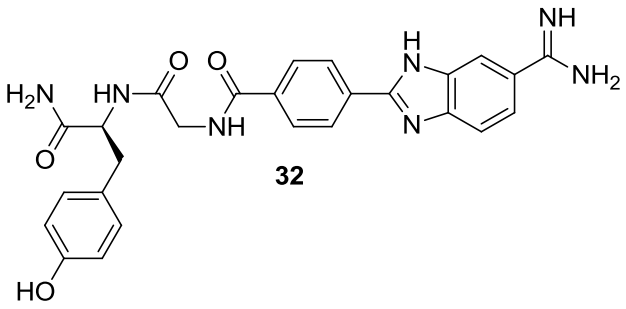

32

Compound **32** was obtained from **2** and Rink-Tyr(tBu)-Gly-Fmoc by General Procedure 2.4.3.4. (53 mg, 65%); ^{1}H NMR (DMSO-d_6); δ2.67 (d, *J* = 9 Hz, 1H), 3.56 (d, *J* = 11 Hz, 2H), 3.74 (d, *J* = 10.5 Hz, 2H), 4.12 (m, 1H), 6.37 (d, *J* = 8.5 Hz, 2H), 6.77 (d, *J* = 8.5 Hz, 2H), 6.85 (s, 1H), 7.16 (s, 1H), 7.45 (dd, *J* = 8.5 Hz, 1H), 7.58 (d, *J* = 8 Hz, 1H), 7.80 (d, *J* = 8 Hz, 1H), 7.83 (d, *J* = 8.5 Hz, 2H), 7.93 (s, 1H), 8.09 (d, *J* = 8.5 Hz, 2H), 8.65 (t, *J* = 12 Hz, 1H), 8.74 (s, 2H), 9.06 (s, 2H); LC/MS calcd for $[M+H]^+$: $C_{26}H_{25}N_7O_4$ 500.2, found 500.3.

***N*-(2-((1-amino-3-mercapto-1-oxopropan-2-yl)amino)-2-oxoethyl)-4-(6-carbamimidoyl-1*H*-benzo[d]imidazol-2-yl)benzamide, Cys-Gly-BI-(+), (33)**

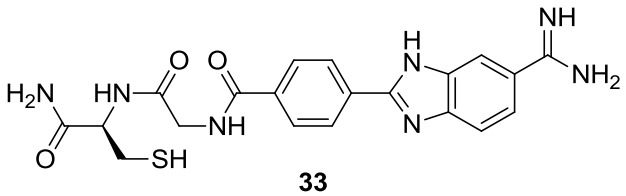

33

Compound **33** was obtained from **2** and Rink-Cys(Trt)-Gly-Fmoc by General Procedure 2.4.3.4. (31 mg, 44%); ^{1}H NMR (DMSO-d_6); δ2.11 (t, *J* = 17.5 Hz, 1H), 2.65 (m, 2H), 3.81 (d, *J* = 7.7 Hz, 2H), 4.18 (m, 1H), 7.07 (s, 1H), 7.25 (s, 1H), 7.50 (dd, *J* = 8.5 Hz, 1H), 7.65 (d, *J* = 8.5 Hz, 1H), 7.91 (d, *J* = 8.5 Hz, 2H), 7.97 (s, 1H), 7.99 (s, 1H), 8.14 (d, *J* = 8.5 Hz, 2H), 8.79 (s, 2H), 8.81 (s, 1H), 9.11 (s, 2H); LC/MS calcd for $[M+H]^+$: $C_{20}H_{21}N_7O_3S$ 440.1, found 440.1.

4-(6-Carbamimidoyl-1*H*-benzo[d]imidazol-2-yl)-*N*-(2-((1,6-diamino-1-oxohexan-2-yl)amino)-2-oxoethyl)benzamide, Lys-Gly-BI-(+), (34)

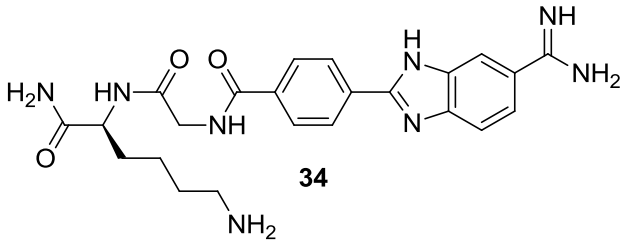

34

Compound **34** was obtained from **2** and Rink-Lys(Boc)-Gly-Fmoc by General Procedure 2.4.3.4. (72 mg, 94%); ^{1}H NMR (DMSO-d_6); δ1.10 (m, 2H), 1.30 (m, 2H), 1.49 (m, 2H), 2.54 (t, *J* = 12 Hz, 2H), 3.74 (d, *J* = 5.5 Hz, 2H), 3.97 (q, *J* = 8.5 Hz, 1H), 6.88 (s, 1H), 7.14 (s, 1H), 7.40 (s, 2H), 7.47 (dd, *J* = 8.5 Hz, 1H), 7.60 (d, *J* = 8.5 Hz, 1H), 7.80 (s, 1H), 7.86 (d, *J* = 8 Hz, 2H), 7.95 (s, 1H), 8.10 (d, *J* = 8.5 Hz, 2H), 8.72 (t, *J* = 11.5 Hz, 1H), 8.75 (s, 2H), 9.07 (s, 2H); %). LC/MS calcd for $[M+H]^+$: $C_{23}H_{28}N_8O_3$ 465.2, found 465.2.

***N*-(2-((1-amino-5-guanidino-1-oxopentan-2-yl)amino)-2-oxoethyl)-4-(6-carbamimidoyl-1*H*-benzo[d]imidazol-2-yl)benzamide, Arg-Gly-BI-(+), (35)**

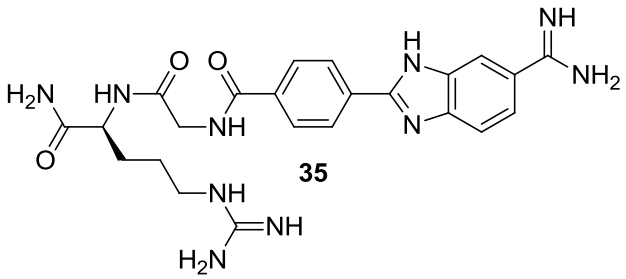

35

Compound **35** was obtained from **2** and Rink-Arg(Pbf)-Gly-Fmoc by General Procedure 2.4.3.4. (63 mg, 78%); ^{1}H NMR (DMSO-d_6); δ1.30 (m, 2H), 1.53 (m, 2H), 2.89 (t, *J* = 12.5 Hz, 2H), 3.75 (d, *J* = 5.5 Hz, 2H), 4.03 (m, 1H), 6.93 (s, 1H), 7.19 (s, 1H), 7.38 (s, 1H), 7.48 (dd, *J* = 8.5 Hz, 1H), 7.62 (d, *J* = 8.5 Hz, 1H), 7.88 (d, *J* = 8.5 Hz, 2H), 7.91 (d, *J* = 8 Hz, 1H), 7.97 (s, 1H), 8.12 (d, *J* = 8.5 Hz, 2H), 8.74 (t, *J* = 11.5 Hz, 1H), 8.84 (s, 2H), 9.09 (s, 2H); LC/MS calcd for $[M+H]^+$: $C_{23}H_{28}N_{10}O_3$ 493.2, found 493.3.

***N*-(2-((1-amino-3-(1H-imidazol-5-yl)-1-oxopropan-2-yl)amino)-2-oxoethyl)-4-(6-carbamimidoyl-1*H*-benzo[d]imidazol-2-yl)benzamide, His-Gly-BI-(+), (36)**

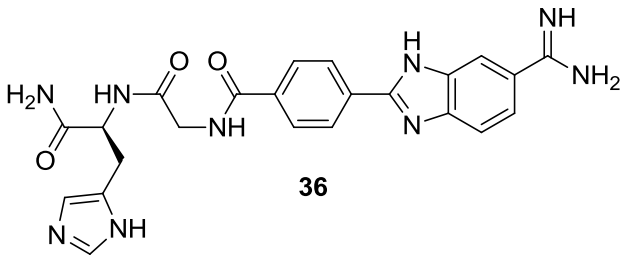

36

Compound **36** was obtained from **2** and Rink-His(Trt)-Gly-Fmoc by General Procedure 2.4.3.4. (47 mg, 61%); ^{1}H NMR (DMSO-d_6); δ2.95 (m, 1H), 3.18 (d, *J* = 10.5 Hz, 2H), 3.89 (d, *J* = 5.5 Hz, 1H), 3.93 (d, *J* = 6 Hz, 2H), 4.54 (m, 1H), 7.33 (s, 1H), 7.38 (s, 1H), 7.44 (s, 1H), 7.69 (dd, *J* = 8.5 Hz, 1H), 7.83 (d, *J* = 8.5 Hz, 1H), 8.08 (d, *J* = 8.5 Hz, 2H), 8.18 (s, 1H), 8.34 (d, *J* = 8.5 Hz, 2H), 8.99 (s, 1H), 9.00 (s, 1H), 9.30 (s, 1H), 14.20 (s, 1H); LC/MS calcd for $[M+H]^+$: $C_{23}H_{23}N_9O_3$ 474.2, found 474.4.

4-Amino-3-(2-(4-(6-carbamimidoyl-1*H*-benzo[d]imidazol-2-yl)benzamido)acetamido)-4-oxobutanoic acid, Asp-Gly-BI-(+), (37)

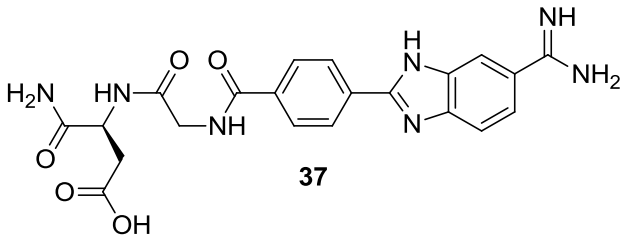

37

Compound **37** was obtained from **2** and Rink-Asp(OtBu)-Gly-Fmoc by General Procedure 2.4.3.4. (63 mg, 85%); ^{1}H NMR (DMSO-d_6); δ2.62 (m, 2H), 3.87 (m, 2H), 4.46 (q, *J* = 13. 5 Hz, 1H), 7.10 (s, 1H), 7.15 (s, 1H), 7.60 (dd, *J* = 8.5 Hz, 1H), 7.73 (d, *J* = 8.5 Hz, 1H), 7.99 (d, *J* = 8.5 Hz, 2H), 8.08 (s, 1H), 8.19 (d, *J* = 8.5 Hz, 1H), 8.23 (d, *J* = 8 Hz, 2H), 8.85 (s, 2H), 8.89 (t, *J* = 11 Hz, 1H), 9.21 (s, 2H), 12.27 (s, 1H); LC/MS calcd for $[M+H]^+$: $C_{21}H_{21}N_7O_5$ 452.2, found 452.1.

5-Amino-4-(2-(4-(6-carbamimidoyl-1*H*-benzo[d]imidazol-2-yl)benzamido)acetamido)-5-oxopentanoic acid, Glu-Gly-BI-(+), (38)

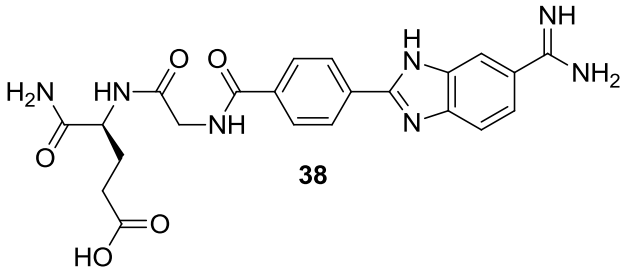

38

Compound **38** was obtained from **2** and Rink-Glu(OtBu)-Gly-Fmoc by General Procedure 2.4.3.4. (54 mg, 71%); ^{1}H NMR (DMSO-d_6); δ1.79 (m, 2H), 2.24 (t, *J* = 15 Hz, 2H), 3.95 (m, 2H), 4.23 (q, *J* = 8 Hz, 1H), 7.13 (s, 1H), 7.36 (s, 1H), 7.70 (dd, *J* = 8.5 Hz, 1H), 7.83 (d, *J* = 8.5 Hz, 1H), 8.08 (d, *J* = 7.5 Hz, 2H), 8.11 (s, 1H), 8.18 (s, 1H), 8.33 (d, *J* = 8.5 Hz, 2H), 8.94 (t, *J* = 11 Hz, 1H), 9.00 (s, 2H), 9.32 (s, 2H), 12.2 (s, 1H); LC/MS calcd for $[M+H]^+$: $C_{22}H_{23}N_7O_5$ 466.2, found 466.3.

2.5. List of References

1. Denny, W. A.; Rewcastle, G. W.; Baguly, B. C. *J. Med. Chem*. **1990**, *33*, 814.
2. Goker, H.; Kus, C.; Boykin, D. W.; Yildiz, S.; Altanlar, N. *Bioorg. Med. Chem*. **2002**, *10*, 2589.
3. Seth, P. P.; Jefferson, E. A.; Risen, L. M.; Osgood, S. A. *Bioorg. Med. Chem. Lett*. **2003**, *13*, 1669.
4. Nare, B.; Liu, Z.; Prichard, R. K.; George, E. *Biochem. Pharmacol*. **1994**, *48*, 2215.
5. Mahaimeed, H. A. *Int. Med. Res*. **1997**, *25*, 175.
6. Renneberg D; Dervan, P. B. *J. Am. Chem. Soc*. **2003**, *125*, 5707.
7. Harshman, K. D.; Dervan, P. B. *Nucleic Acid Res.* **1985**, *13*, 4825.
8. Marques, M. A.; Doss, R. M.; Foister, S.; Dervan, P. B. *J. Am. Chem. Soc*. **2004**, *126*, 10339.
9. Viger, A.; Dervan, P. B. *Bioorg. Med. Chem*. **2006**, *14*, 853.
10. Wilson, W. D.; Nguyen, B.; Tanious, F. A.; Mathis, A.; Hall, J. E.; Stephens, C. E.; Boykin, D. W. *Curr. Med. Chem. Anti-Cancer Agents* **2005**, *5*, 389.
11. Miao, Y.; Michael P. H. Lee, M. P. H.; Parkinson, G. N.; Batista-Parra, A.; Ismail, M. A.; Neidle, S.; Boykin, D. W.; Wilson, W. D. *Biochemistry* **2005**, *44*, 14701.
12. Neidle, S. *Nat. Prod. Rep.* **2001***, 18*, 291.
13. Joubert, A.; Sun, X. W.; Johansson, E.; Bailly, C.; Mann, J.; Neidle, S. *Biochemistry* **2003**, *42*, 5984.
14. Tanious, F. A.; Hamelberg, D.; Bailly, C.; Czarny, A.; Boykin, D. W.; Wilson, W. D. *J. Am. Chem. Soc.* **2004**, *126*, 143.
15. Haq, I.; Ladbury, J. E.; Chowdhry, B. Z.; Jenkins, T. C.; Chaires, J. B. *J. Mol. Biol.* **1997**, *271*, 244.
16. Satz, A. L.; Bruice, T. C. *Acc. Chem. Res.* **2002**, *35*, 86.
17. Haq, I. *Arch. Biochem. Biophys.* **2002**, *403*, 1.
18. Zablocki, J. A.; Miyano, M.; Garland, R. B.; Pireh, D.; Schretzman, L.; Rao, S. N.; Lindmark, R. J.; Panzer-Knodle, S. G.; Nicholson, N. S.; Taite, B. B.; Salyers, A. K.; King, L. W.; Campion, J. G.; Feigen, L. P. *J. Med. Chem.* **1993**, *36*, 1811.
19. Peterlin-Mašič, L.; D. Kikelj, D. *Tetrahedron* **2001**, *57*, 7073.
20. Patel, N.; Berglund, H.: Nilsson, L.; Rigler, R.; McLaughlin, L. W.; Gräslund, A. *Eur. J. Biochem*. **1992**, *203*, 361.

21. Bailly, C.; Chaires, J. B. *Bioconj. Chem.* **1998**, *9*, 513.
22. Geierstanger, B. H.; Jacobsen, J. P.; Mrksich, M.; Dervan, P. B.; Wemmer, D. E. *Biochemistry* **1994**, *33*, 3055.
23. Goodwin, K. D.; Long, E. C.; Georgiadis, M. M. *Nucleic Acids Res.* **2005**, *33*, 4106.
24. Clark, G. R.; Boykin, D. W.; Czarny, A.; Neidle, S. *Nucleic Acids Res.* **1997**, *25*, 1510.
25. Ismail, M. A.; Batista-Parra, A.; Miao, Y.; Wilson, W. D.; Wenzler, T.; Brun, R.; Boykin, D. W. *Bioorg. Med. Chem.* **2005**, 13, 6718.
26. Dervan, P. B. *Curr. Opin. Struct. Biol.* **2003**, *13*, 284.
27. Kielkopf, C. L.; White, S.; Szewczyk, J. W.; Turner, J. M.; Baird, E. E.; Dervan, P. B.; Rees, D. C. *Science* **1998**, *282*, 111.
28. Kielkopf, C. L.; Bremer, R. E.; White, S.; Szewczyk, J. W.; Turner, J. M.; Baird, E. E.; Dervan, P. B.; Rees, C. C. *J. Mol Biol.* **2000**, *295*, 557.
29. White, S.; Szewczyk, J. W.; Turner, J. M.; Baird, E. E.; Dervan, P. B. *Nature* **1998**, *391*, 468.
30. Merrifield, R. B. *J. Amer. Chem. Soc.* **1963**, *85*, 2149.
31. Chan, W. C.; White, P. D. *Fmoc Solid Phase Peptide Synthesis*, Oxford University Press, **2000**.
32. Stewart, J. M.; Young, J. D.; *Solid Phase Peptide Synthesis*, 2nd Ed, Pierce Chemical Company, **1984**.
33. *Peptide Synthesis,* Merck, **2009**.
34. Parrish, R. F.; Straus, J. W.; Paulson, J. D.; Polakoski, K. L.; Tidwell, R. R.; Geratz, J. D.; Stevens, F. M. *J. Med. Chem*. **1978**, *21*, 1132.
35. Goker, H.; Alp, M.; Yĭldĭz, S. *Molecules* **2005**, *10*, 1377.
36. Wendt, M. D.; Rockway, T. W.; Geyer, A.; McClellan, W.; Weitzberg, M.; Zhao, X. M.; Mantei, R.; Nienaber, V. L.; Stewart, K.; Klinghofer, V.; Giranda, V. L. *J. Med. Chem.* **2004**, *47*, 303.
37. Xue, C. B.; Rafalski, M.; Roderick, J.; Eyermann, C. J.; Mousa, S.; Olson, R. E.; DeGrado, W. F. *Bioorg. Med. Chem. Lett.* **1996**, *6*, 339.
38. Ismail, M. A.; Brun, R.; Wenzler, T.; Tanious, F. A.; Wilson, W. D.; Boykin, D. W. *Bioorg. Med. Chem.* **2004**, *12*, 5405.
39. Anbazhagan, M.; Boykin, D. W.; Chad E. Stephens, C. E.; *Synthesis* **2003**, *16*, 2467.

40. Judkins, B. D.; Allen, D. G.; Cook, T. A.; Evans, B.; Sardharwala, T. E. *Synth. Commun*. **1996**, *26*, 4351.
41. Dörwald, Z. F.; *Organic Synthesis on Solid Phase*, 2nd ed., Wiley-VCH: Weinheim, **2002**.
42. Kaiser, E.; Colescott, R. L.; Bossinger, C. D.; Cook, P. I. *Anal. Biochem.* **1970**, *34*, 595.

CHAPTER 3. PRELIMINARY SCREENING OF DNA BINDING ACTIVITY

3.1. Overview

A new series of amino acid-benzimidazole-amidine and di-amino acid-benzimidazole-amidine conjugates were designed and synthesized in our laboratory. To analyze the relative DNA binding affinity of these compounds, a microplate-based fluorescence intercalator displacement (HT-FID) assay was used. This chapter will introduce the HT-FID assay developed by Boger et al. and illustrate its validation process. We will use calf thymus DNA along with ethidium bromide as a fluorescence indicator to establish the relative binding affinity of our amino acid-benzimidazole-amidine conjugates.[1-5]

3.2. HT-FID Assay

There are a number of techniques such as footprinting and affinity cleavage[6] used to analyze the DNA-binding interactions of small molecules; unfortunately, most of these methods are challenging and time-consuming,[7] making analysis of large catalogs of compounds difficult. The HT-FID assay (Figure 3.1)[8], addresses the ease-of-use challenges of other methods and utilizes DNA treated with ethidium bromide to yield fluorescence upon DNA-ethidium bromide binding. Addition of DNA-binding compound displaces the ethidium bromide, resulting in a decrease in the fluorescence. The percent fluorescence decrease is directly related to the extent of DNA-ligand binding and can show the relative binding affinity of our synthesized compounds. FID is commonly employed using a library of all possible 4- or 5-bp hairpin oligonucleotides to establish the DNA-ligand binding site-selectivity of the target compound, but calf thymus DNA (CT-DNA) has the advantage of being a cost-effective high-throughput substrate approximating all possible combinations of base pairs and can be used to establish the relative DNA binding of a group of compounds.[1] It is important to note the analysis of our amino acid-benzimidazole-amidine conjugates is preliminary, and as such, the focus of this section is on the relative binding as determined using CT-DNA rather than

determining the site-selectivity or absolute $K_{binding}$ of our conjugates with a 4- or 5-basepair library. The resulting DNA-binding discussed henceforth shows the relative rank-order of the amino acid-benzimidazole-amidine conjugates as compared to each other in calf thymus DNA, allowing our group to establish the order of DNA-binding activity for the conjugates.

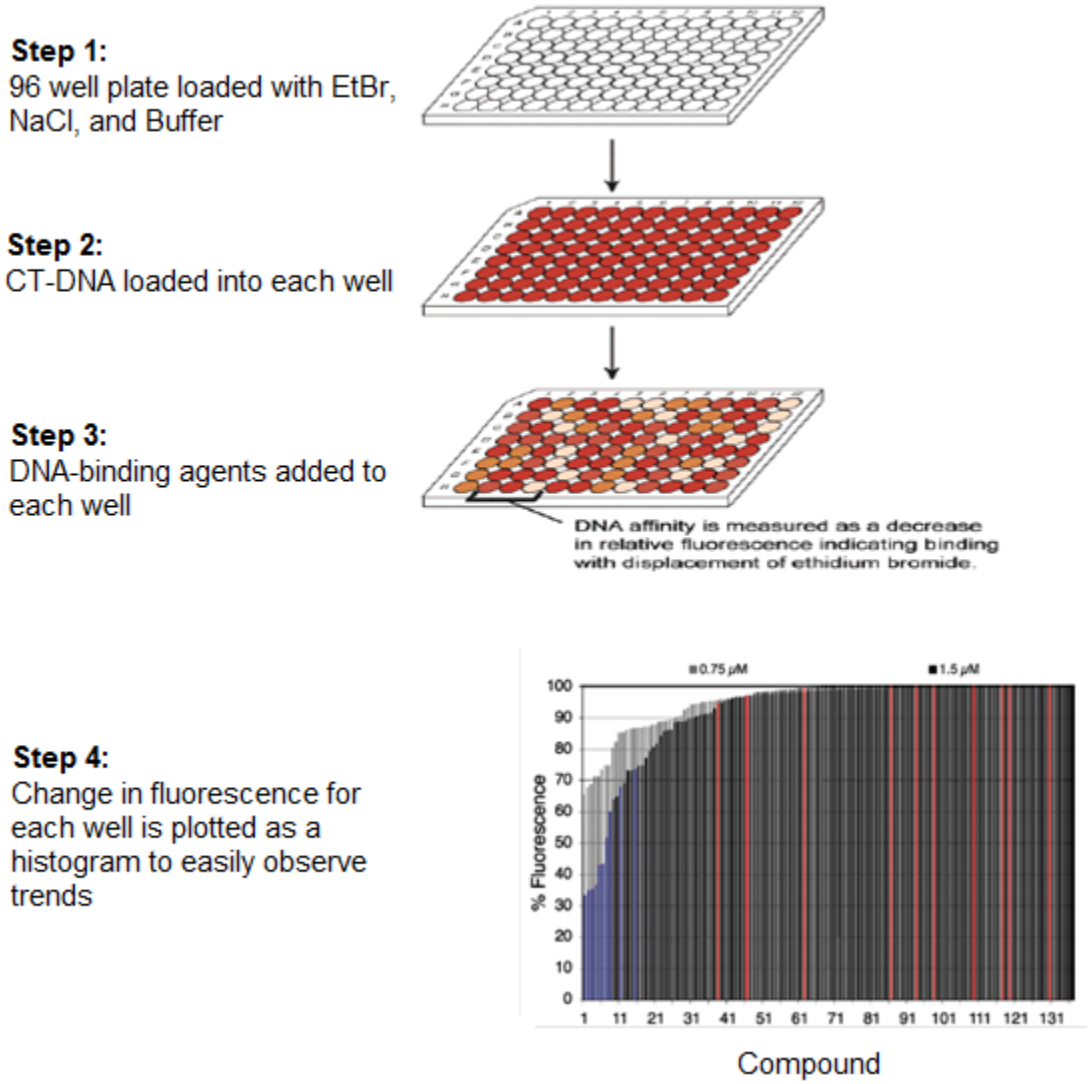

Figure 3.1. Depiction of the HT-FID assay process.

The HT-FID assay using CT-DNA has been used to analyze a commercially-available chemical library of 60,000 compounds to determine which of the compounds exhibited DNA-binding ability.[1] Although a determination of site selectivity was not our focus, the FID assay has been validated by analyzing the DNA binding site selectivity of several well studied A/T-rich minor groove binding agents such as netropsin, distamycin, Hoechst 33258, and RT 29[4] and the assay could be used in the future to further analyze the specific binding sites of our compounds. The HT-FID assay using CT-DNA has the potential to be widely applicable in the discovery of new DNA binding agents, making it an ideal choice to quickly establish the relative binding of our amino acid-benzimidazole-amidine conjugates.

3.2.1. HT-FID Assay Validation

Due to its well-behaved performance in the FID assay, netropsin can be used as a compound in the validation of the assay.[8,9] Netropsin has previously been evaluated using the FID assay with both 4- and 5-bp libraries of oligonucleotides as well as with CT-DNA using ethidium bromide as the reporting fluorophores, thus providing sufficient information to validate the assay. Therefore, netropsin was analyzed along with our amino acid-benzimidazole-amidine conjugates to validate the assay. Distamycin, another compound that has been extensively studied using the 4- and 5-bp libraries was also used in our validation to provide a second well-studied DNA binder for comparison of our conjugates. For our validation, netropsin and distamycin were carried out in the assay side-by-side with our conjugates at concentrations of 0.75, 1.5, and 3.0 μM with 10 μM CT-DNA and 4.5 μM ethidium bromide, as previously described.[1]

To assess the validity of our assay using ethidium bromide-bound calf thymus DNA, Z' scores[10] were determined using netropsin and distamycin as positive controls due to their well understood binding and wells containing a buffer blank were used as a negative control. To define a screening window for the HT-FID assay, μ_{c-} and μ_{c+} are denoted as the means of the negative control signal and positive control signal, respectively. The standard deviations of the signals are denoted as σ_{c-} and σ_{c+}, respectively. The Z'-factor can be used for quality assessment in assay development and optimization and is appropriate for evaluating the overall quality of the assay. For example, if the Z' value is small (negative or near zero), the assay conditions have not

been optimized or the assay is not feasible for generating useful data. An excellent assay has a Z′ score of 0.5 to 1, with 1 being an ideal assay and scores ranging down to 0 only being applicable as a "yes or no" type of assay.[10] In our Z′ analysis, the negative controls provide a maximum percent fluorescence possible from the assay and the positive controls provide a maximum decrease in fluorescence possible from a strong DNA binding agent, therefore determining the dynamic range of the assay. The observed data for netropsin and distamycin is summarized in Table 3.1.

Table 3.1. Z′-score analysis of netropsin and distamycin.

$$Z' = 1 - \frac{(3\sigma_{c+} + 3\sigma_{c-})}{|\mu_{c+} - \mu_{c-}|}$$

Netropsin			Distamycin		
Concentration	Percent F	Z′-score	Concentration	Percent F	Z′-score
0.75 μM	77%	0.75	0.75 μM	84%	0.66
1.50 μM	64%	0.60	1.50 μM	70%	0.50
3.00 μM	59%	0.47	3.00 μM	63%	0.43

Using the data above, it was determined that netropsin could serve as a positive control for the assay when analyzing our conjugates due to the Z′-score generally falling into the acceptable range of 0.5 to 1. Distamycin also appeared to be a suitable control, presenting similar Z′-scores as netropsin, and was also run in parallel with netropsin and our compounds to provide another control. As well as being positive controls, it is interesting to see how our amino acid-benzimidazole-amidine conjugates compare to netropsin and distamycin since they were principal molecules in the design of our conjugates.

3.3. HT-FID Analysis of Amino Acid-Benzimidazole-Amidine Conjugates

The HT-FID assay clearly provides a rapid approach to the detection of ligand-DNA binding that is applicable to a wide range of structurally diverse ligands including peptide-derived agents such as netropsin and distamycin. Thus, the assay is valuable in the examination of our amino acid-benzimidazole-amidine conjugates.

3.3.1. HT-FID Analysis of Mono-Amino Acid-Benzimidazole-Amidine Conjugates

To determine the relative binding affinity of our mono-amino acid-benzimidazole-amidine conjugates to that of our model-benzimidazole and model-benzimidazole-amidine compounds (as well as netropsin and distamycin), all of the compounds were analyzed with the FID assay using CT-DNA. Figure 3.2 shows the merged-bar histogram of 0.75 μM, 1.50 μM, and 3.00 μM concentration of our mono-amino acid-benzimidazole-amidine conjugates. The graph shows that the two well-known DNA-binding agents, netropsin and distamycin, exhibit better binding than any of the mono-amino acid-benzimidazole-amidine conjugates. While the positively charged arginine-containing conjugate is present in the top five of our novel compounds in this assay, the conjugate containing lysine does not appear near the front of the graph, and in fact shows similar binding to the model compound without an amidine group present. This is a surprising result given their similar charged nature, the added positive charge of these two side chains would aid in delivering conjugates containing arginine and lysine to DNA.

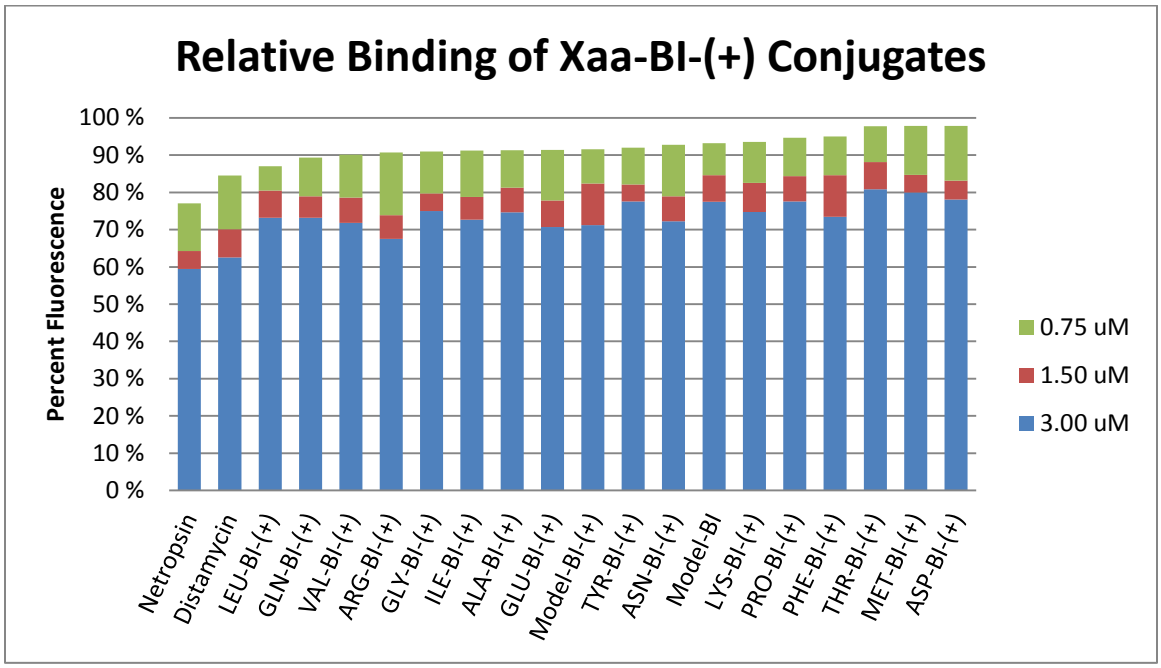

Figure 3.2. Relative binding of Xaa-BI-(+) conjugates in CT-DNA.

3.3.2. HT-FID Analysis of Dipeptide-Benzimidazole-Amidine Conjugates

We also determined the relative binding affinity of our dipeptide-benzimidazole-amidine conjugates using the FID assay in comparison to netropsin, distamycin, model-benzimidazole, and the model-benzimidazole-amidine compounds. The results of the experiment using 0.75 μM, 1.50 μM, and 3.00 μM concentrations of the dipeptide conjugates are shown in Figure 3.3. Initially, the compound that presented the best binding to CT-DNA was the cysteine-containing dipeptide-benzimidazole-amidine, Cys-Gly-BI-(+). This conjugate even outperformed netropsin, which was a very surprising result. There was a suspicion that perhaps the conditions of the assay were causing the sulfur of cysteine to oxidize and form a sulfone or sulfoxide. A sample of the reaction mixture was removed an analyzed by LC/MS, yielding a peak of +16 (*m/z* 456) which suggests that a sulfoxide was forming on cysteine, thus altering our conjugate's binding ability, perhaps in an advantageous fashion.

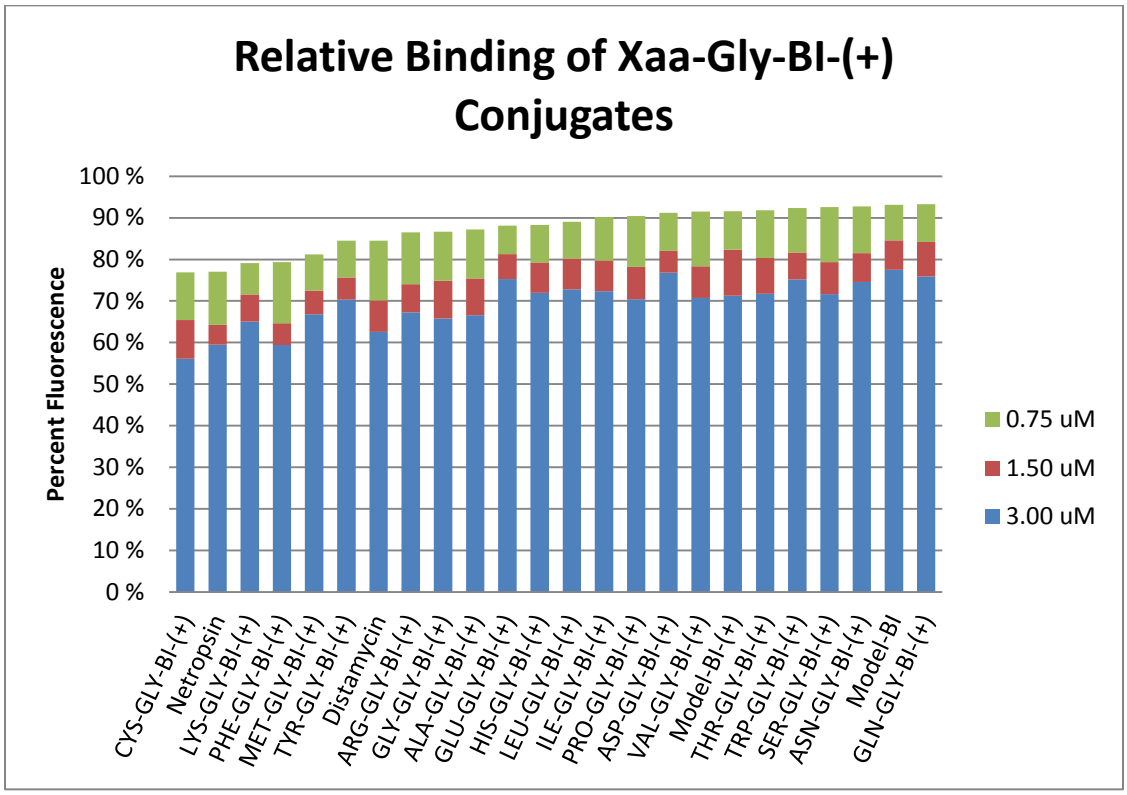

Figure 3.3. Relative binding of Xaa-Gly-BI-(+) conjugates in CT-DNA.

In analyzing our relative binding results, four of our conjugates, Lys-Gly-BI-(+), Phe-Gly-BI-(+), Met-Gly-BI-(+), and Tyr-Gly-BI-(+) presented stronger binding than distamycin with Arg-Gly-BI-(+) being a slightly less potent binder than distamycin. Out of this subset, Lys-Gly-BI-(+) and Arg-Gly-BI-(+) are conjugates that we expected to present strong binding in large part due to their positively charged side-arms. The large planar aromatic rings of Phe-Gly-BI-(+) and Tyr-Gly-BI-(+) can also insert into DNA,[11] so their presence at the front of the histogram is not surprising. Methionine-containing peptides have also been shown to enhance DNA cleavage[12] which may explain the presence of Met-Gly-BI-(+) near the front of the histogram and its outperforming the well-known binder, distamycin.

After our initial results, we sought to further analyze the compounds which presented the best binding. We also included Gly-Gly-BI-(+) in the analysis since it is the most elementary of our conjugates as a comparison. The results of the further analysis of the conjugates at 0.75 μM, 1.50 μM, 2.25 μM, 3.00 μM, 3.75 μM, and 4.50 μM concentrations is shown in Figure 3.4.

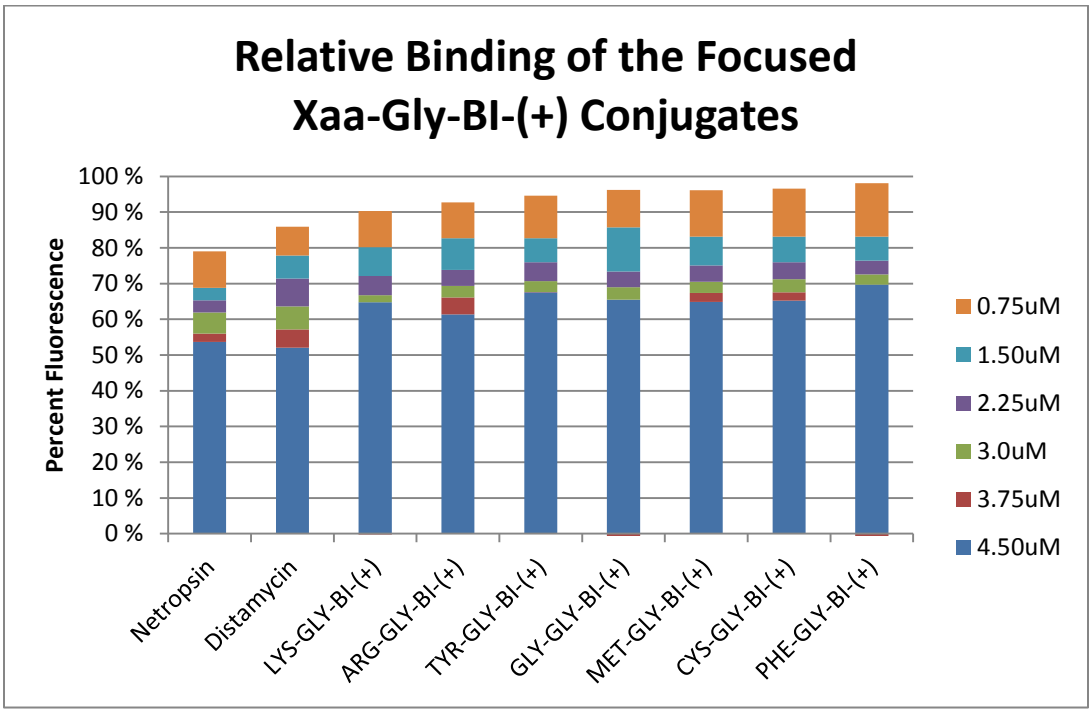

Figure 3.4. Focused relative FID binding analysis of the most potent binders.

Upon further analysis, netropsin and distamycin present the strongest DNA-binding ability as expected and the two conjugates containing positively-charged side arms, Lys-Gly-BI-(+) and Arg-Gly-BI-(+), have the strongest binding of all our conjugates. The presence of lysine- and arginine-containing conjugates at the front of the histogram, outperforming all of our other dipeptide-conjugates is expected as they both contain a positively charged side-arm that should aid in delivering the conjugate to A/T-rich regions of DNA. It is possible that our initial analysis did not show these expected results due to an operator error in addition of the compounds to the well or that over the course of the incubation, the conjugates were oxidized as seen with Cys-Gly-BI-(+) or they decomposed in some manner, skewing the expected results.

3.4. Summary

The dipeptide-benzimidazole-amidine conjugates appear to have better DNA-binding ability than the mono-amino acid-benzimidazole-amidine conjugates as a couple of these conjugates actually outperformed distamycin in the FID assay. Upon further review, it does appear that both netropsin and distamycin are superior to any of our conjugates, as is expected. However, having conjugates that even come close to the DNA binding ability of these two compounds speaks to the great power of the amino acid-benzimidazole-amidine system and may warrant further synthesis and analysis to find stronger dipeptides and possibly tripeptides. It also needs to be noted that the assay using CT-DNA only shows relative binding compared to each other compound and in no way shows site preference since CT-DNA is made up of a mixture of possible base-pair sequences. Also, CT-DNA is a mixture of A/T base-pairs to G/C base-pairs, thus the known A/T-binders netropsin and distamycin will only be able to bind to a portion of the available DNA. This may also apply to our conjugates as they are designed to be A/T-binders, but further analysis of the site-selectivity of each conjugate will be needed and is beyond the scope of the analysis that we intended to perform.

3.5. Experimental Protocols

3.5.1. Materials

Netropsin (ε_{296} = 21,500 $M^{-1}cm^{-1}$) and distamycin (ε_{303} = 37,000 $M^{-1}cm^{-1}$) were purchased from Sigma-Aldrich and quantitated spectroscopically and materials used in buffer solution, NaCl and tris(hydroxymethyl)-aminomethane (TRIS), were also purchased from Sigma-Aldrich. Ethidium bromide (ε_{476} = 5680 $M^{-1}cm^{-1}$) was purchased from Fluka and quantitated spectroscopically. Calf thymus DNA (ε_{260} = 6300 $M^{-1}cm^{-1}$) was purchased from Invitrogen and the concentration of the CT-DNA was confirmed by ultraviolet-visible spectroscopy. All amino acid-benzimidazole-amidine conjugates were synthesized through previously detailed solid-phase protocols in our laboratory. All experiments were carried out on a Varian Cary Eclipse Spectrophotometer fluorescence plate reader.

3.5.2. HT-FID Assay

Each well of a Costar black 96-well plate was loaded with TRIS buffer along with ethidium bromide (150 µL of 5.5 µM EtBr, 120 mM NaCl, and 12 mM TRIS). Calf thymus DNA was then added to each well (25 µL of 11.1 µM CT-DNA in H_2O). Final concentrations in each well were 1.5 µM CT-DNA, 4.5 µM EtBr, and 0.75 to 3.00 µM of DNA-binding agent. The final buffer solution consists of 100 mM NaCl, 10 mM TRIS, pH 7.4. After incubation at 25 °C for 30 minutes, each well was read (average of three readings) on the fluorescence plate reader (λ_{Ex} 545 nm, λ_{Em} 595 nm). Compound assessments were conducted in triplicate with each well acting as its own control well (no agent = 100% fluorescence, no DNA = 0% fluorescence) and fluorescence readings are reported as a percent fluorescence decrease relative to the control wells.

The above protocol was followed for the focused analysis of dipeptide-benzimidazole-amidine conjugates except for the range of compound concentrations was 0.75 to 4.50 µM.

3.6. List of References

1. Glass, L. S.; Bapat, A.; Kelley, M. R.; Georgiadis, M. M.; Long, E. C.; *Bioorg. Med. Chem. Lett.* **2010**, *20*, 1685.
2. Goodwin, K. D.; Lewis, M. A.; Tanious F. A.; Tidwell, R. R.; Wilson, W. D.; Georgiadis, M. M.; Long, E. C. *J. Am. Chem. Soc.* **2006**, *128*, 7846.
3. Lewis, M. A.; Long, E. C. *Bioorg. Med. Chem.* **2006**, *14*, 3481.
4. Tanious, F. A.; Laine, W.; Peixoto, P.; Bailly, C.; Goodwin, K. D.; Lewis, M. A.; Long, E. C.; Georgiadis, M. M.; Tidwell, R. R.; Wilson, W. D. *Biochemistry* **2007**, *46*, 6944.
5. Glass, L. S.; Nguyen, B.; Goodwin, K. D.; Dardonville, C.; Wilson, W. D.; Long, E. C.; Georgiadis, M. M. *Biochemistry* **2009**, *48*, 5943.
6. Boger, D. L.; Tse, W. C. *Bioorg. Med. Chem.* **2001**, *9*, 2511.
7. Boger, D. L.; Fink, B. E.; Hedrick, M. P. *J. Am. Chem. Soc.* **2000**, *122*, 6382.
8. Tse, W. C.; Boger, D. L. *Acc. Chem. Res*. **2004**, *37*, 61.
9. Boger, D. L.; Fink, B. E.; Brunette, S. R.; Tse, W. C.; Hedrick, M. P. *J. Am. Chem. Soc.* **2001**, *123*, 5878.
10. Zhang, J. H.; Chung, T. D.; Oldenburg, K. R. *J. Biomol. Screen.* **1999**, *4*, 67.
11. Chen, Y.; Rice, P. A. *Annu. Rev. Biophys. Biomol. Struct.* **2003**, *32*, 135.
12. Huang, X.; Pieczko, M. E.; Long, E. C. *Biochemistry* **1999**, *38*, 2160.

APPENDICES

Appendix A. ^{1}H NMR Spectra

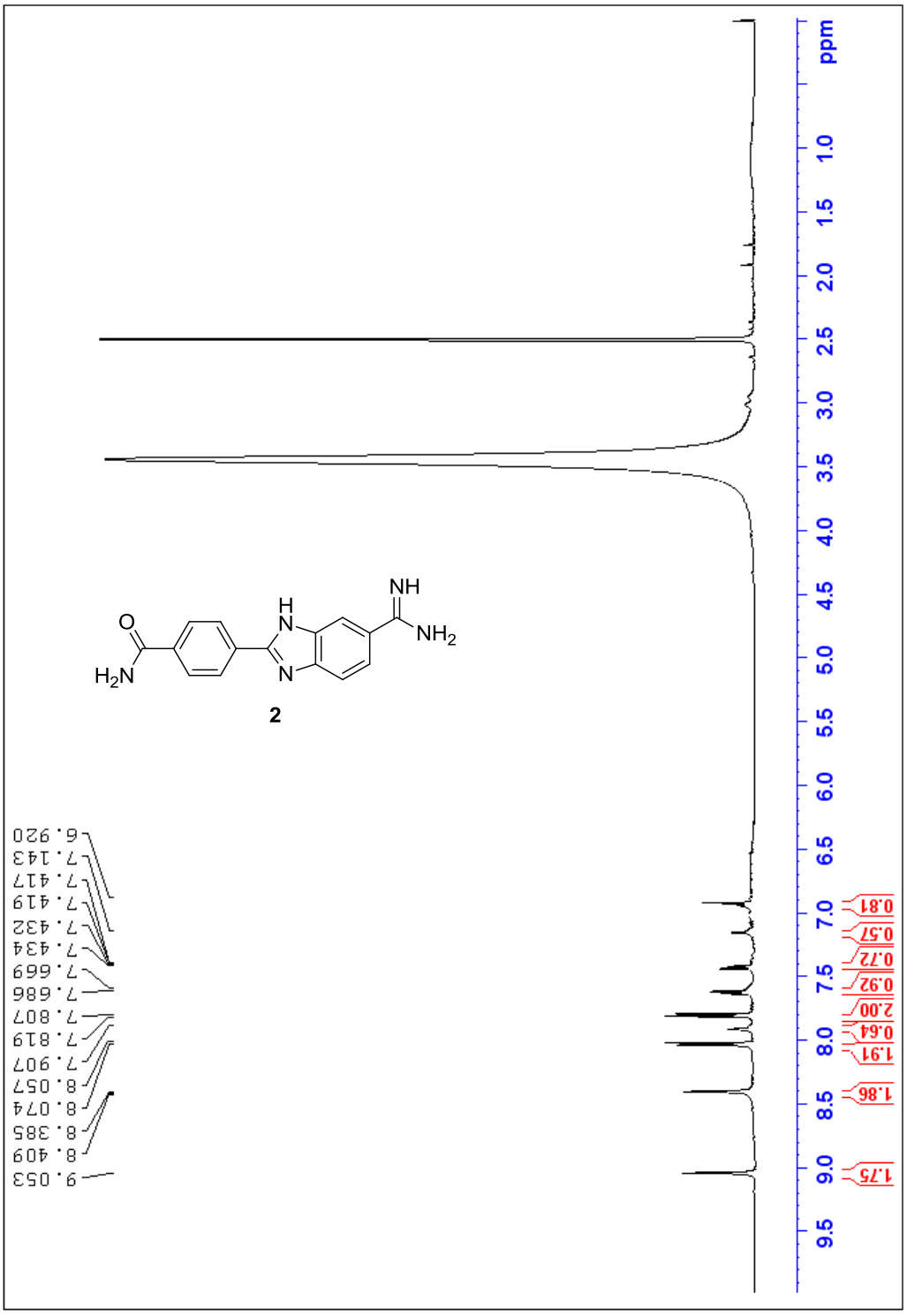

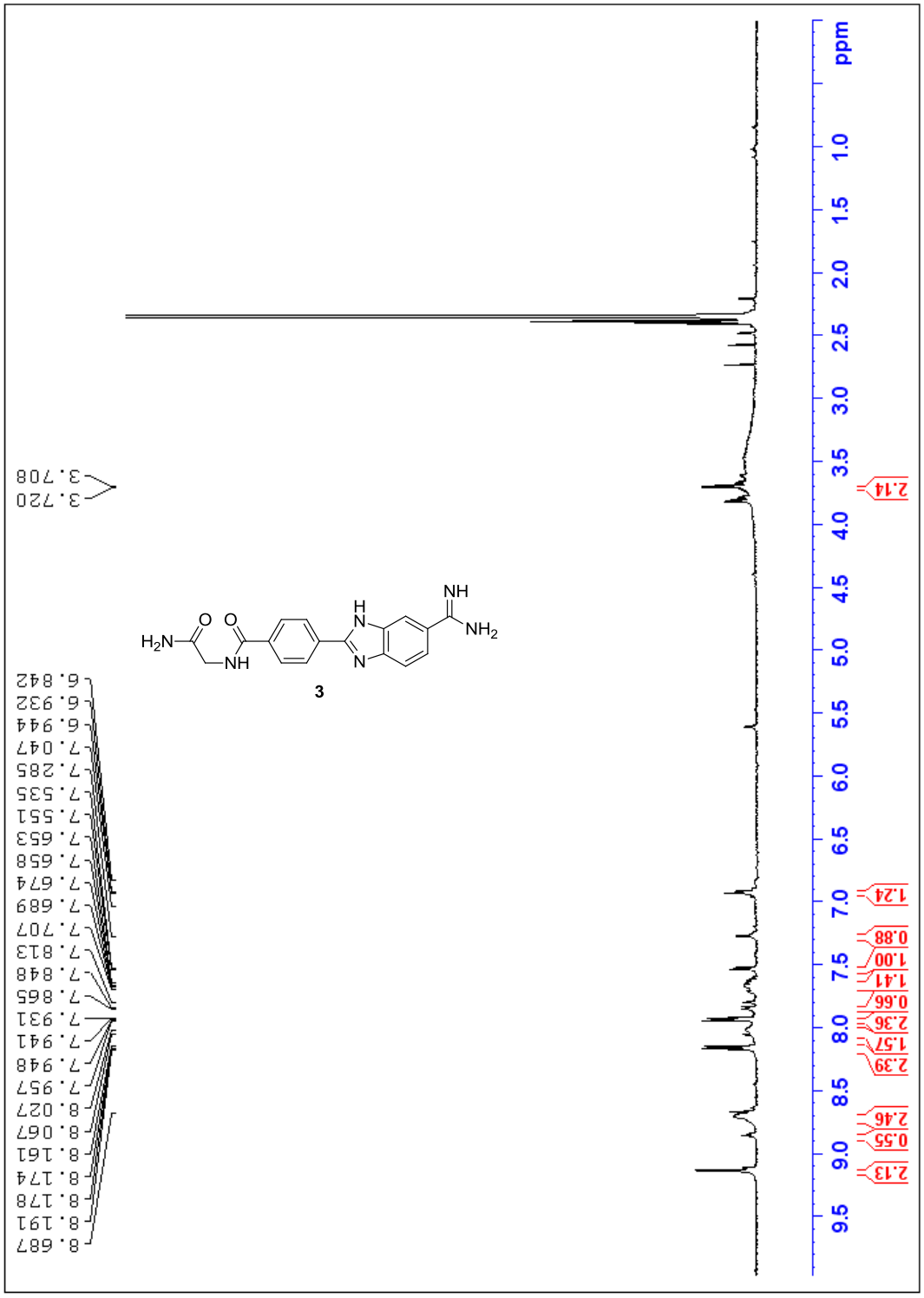
3
ppm
9.5
9.0
8.5
8.0
7.5
7.0
6.5
6.0
5.5
5.0
4.5
4.0
3.5
3.0
2.5
2.0
1.5
1.0
2.13
0.55
2.46
2.39
1.57
2.36
0.66
1.41
1.00
0.88
1.24
2.14
8.687
8.191
8.178
8.174
8.161
8.067
8.027
7.957
7.948
7.941
7.931
7.865
7.848
7.813
7.707
7.689
7.674
7.658
7.653
7.551
7.535
7.285
7.047
6.944
6.932
6.842
3.720
3.708

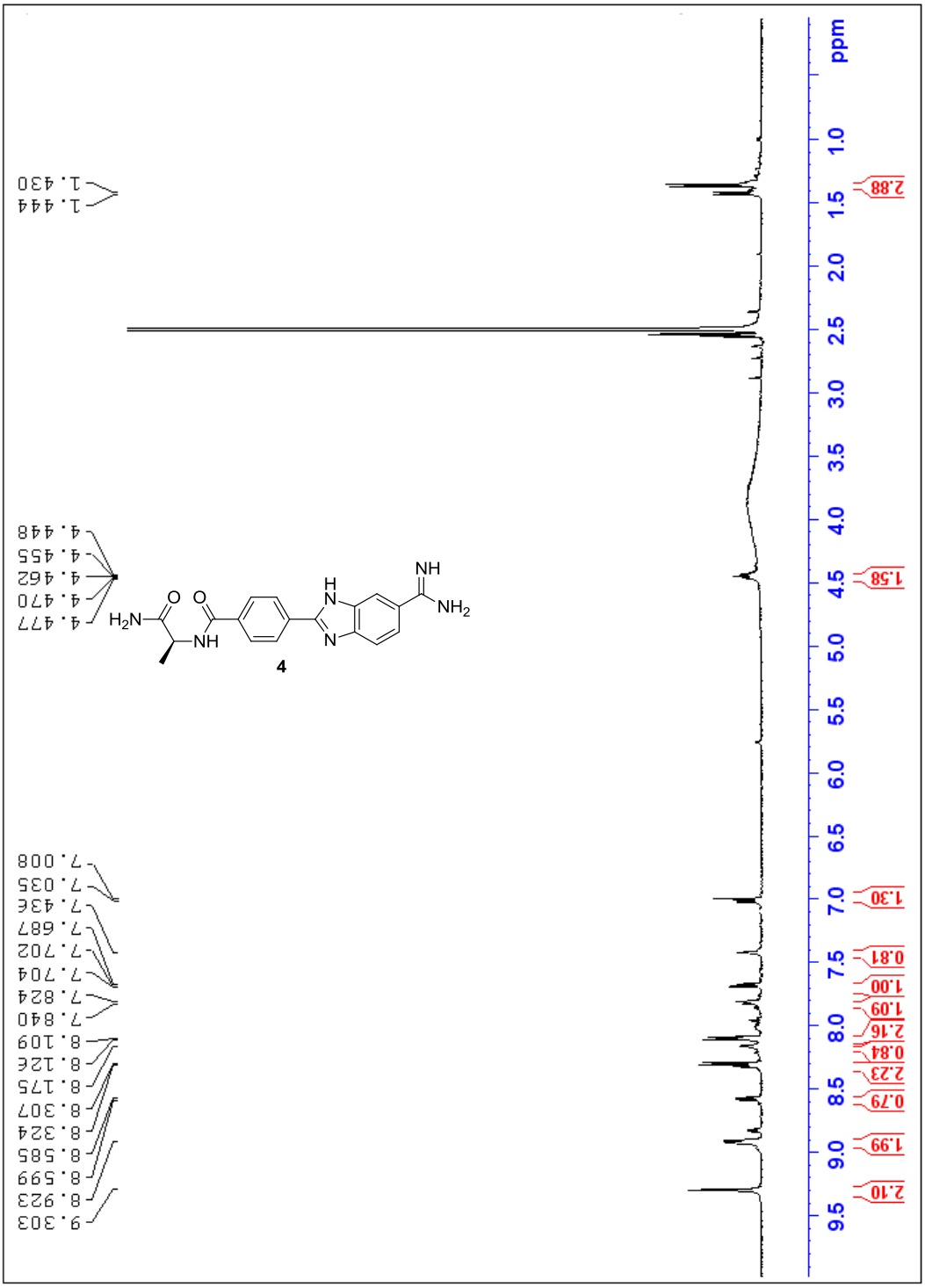
9.303
8.923
8.599
8.585
8.324
8.307
8.175
8.126
8.109
7.840
7.824
7.704
7.702
7.687
7.436
7.035
7.008
4.477
4.470
4.462
4.455
4.448
1.444
1.430
4
ppm
9.5
9.0
8.5
8.0
7.5
7.0
6.5
6.0
5.5
5.0
4.5
4.0
3.5
3.0
2.5
2.0
1.5
1.0
2.10
1.99
0.79
2.23
0.84
2.16
1.09
1.00
0.81
1.30
1.58
2.88

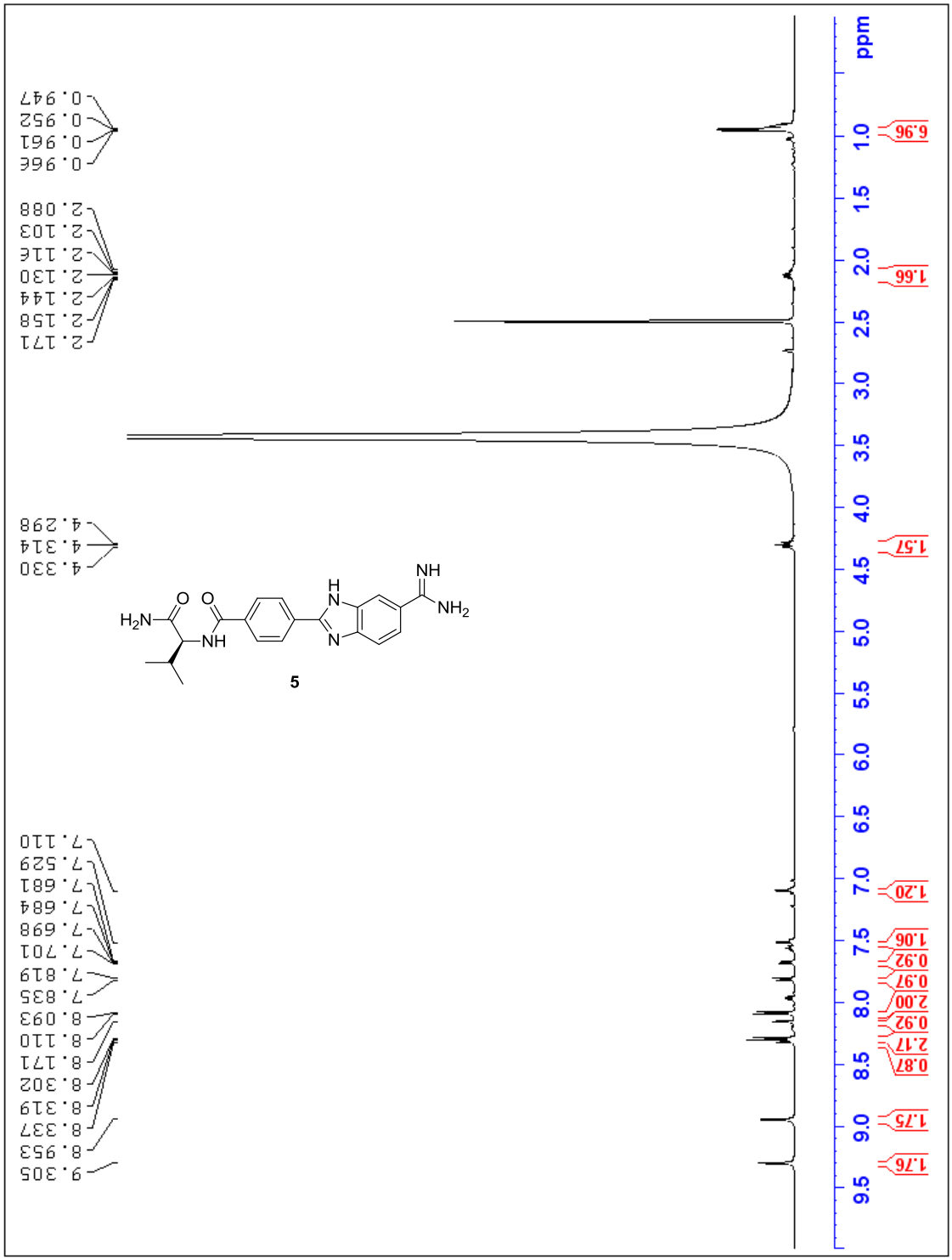
0.947
0.952
0.961
0.966
2.088
2.103
2.116
2.130
2.144
2.158
2.171
4.298
4.314
4.330
7.110
7.529
7.681
7.684
7.698
7.701
7.819
7.835
8.093
8.110
8.171
8.302
8.319
8.337
8.953
9.305
NH
NH2
H2N
O
O
NH
H
N
N
5
ppm
6.96
1.66
1.57
1.20
1.06
0.92
0.97
2.00
0.92
2.17
0.87
1.75
1.76

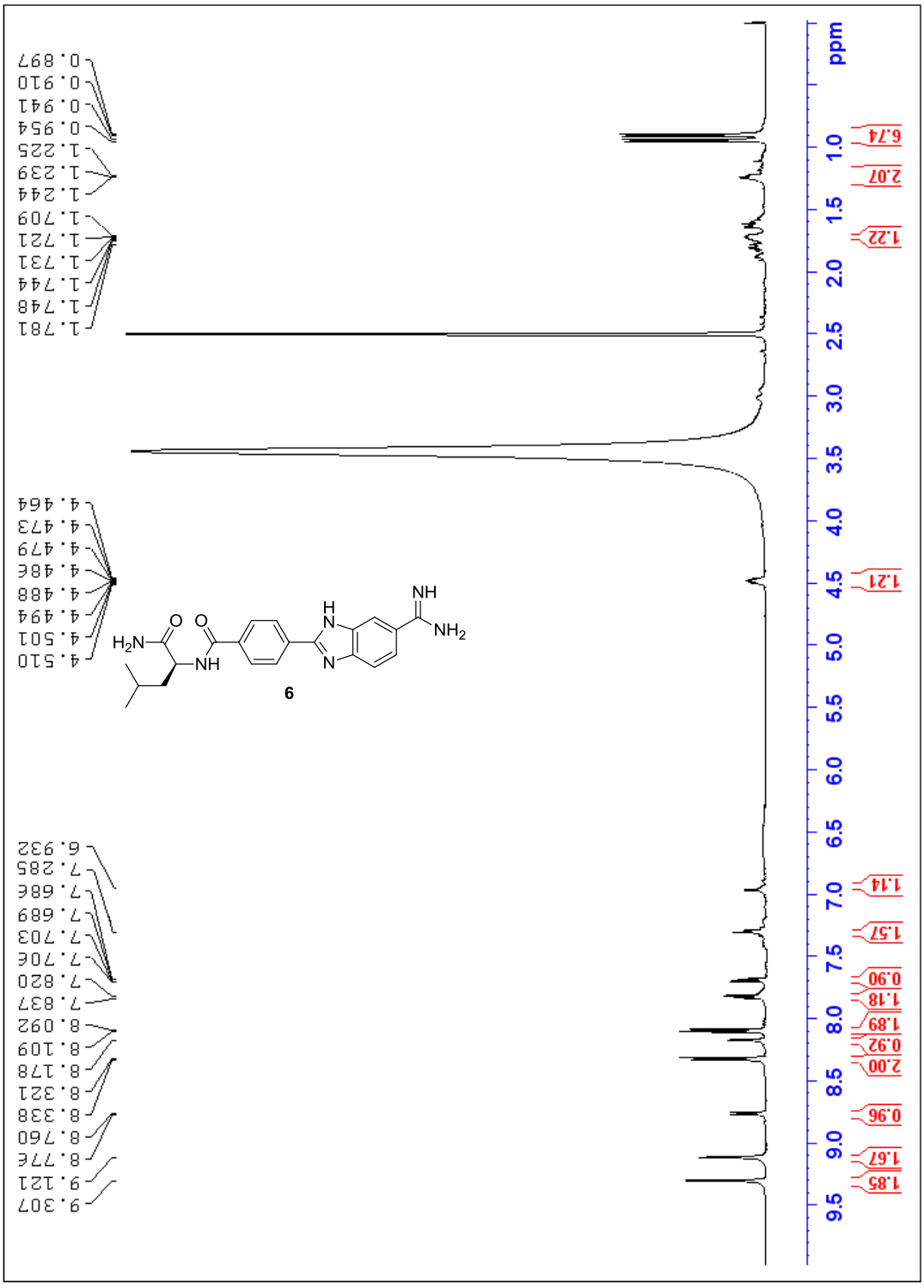
0.897
0.910
0.941
0.954
1.225
1.239
1.244
1.709
1.721
1.731
1.744
1.748
1.781
4.464
4.473
4.479
4.486
4.488
4.494
4.501
4.510
6.932
7.285
7.686
7.689
7.703
7.706
7.820
7.837
8.092
8.109
8.178
8.321
8.338
8.760
8.776
9.121
9.307
H2N
O
O
NH
H
N
N
NH
NH2
6
ppm
9.5
9.0
8.5
8.0
7.5
7.0
6.5
6.0
5.5
5.0
4.5
4.0
3.5
3.0
2.5
2.0
1.5
1.0
6.74
2.07
1.22
1.21
1.14
1.57
0.90
1.18
1.89
0.92
2.00
0.96
1.67
1.85

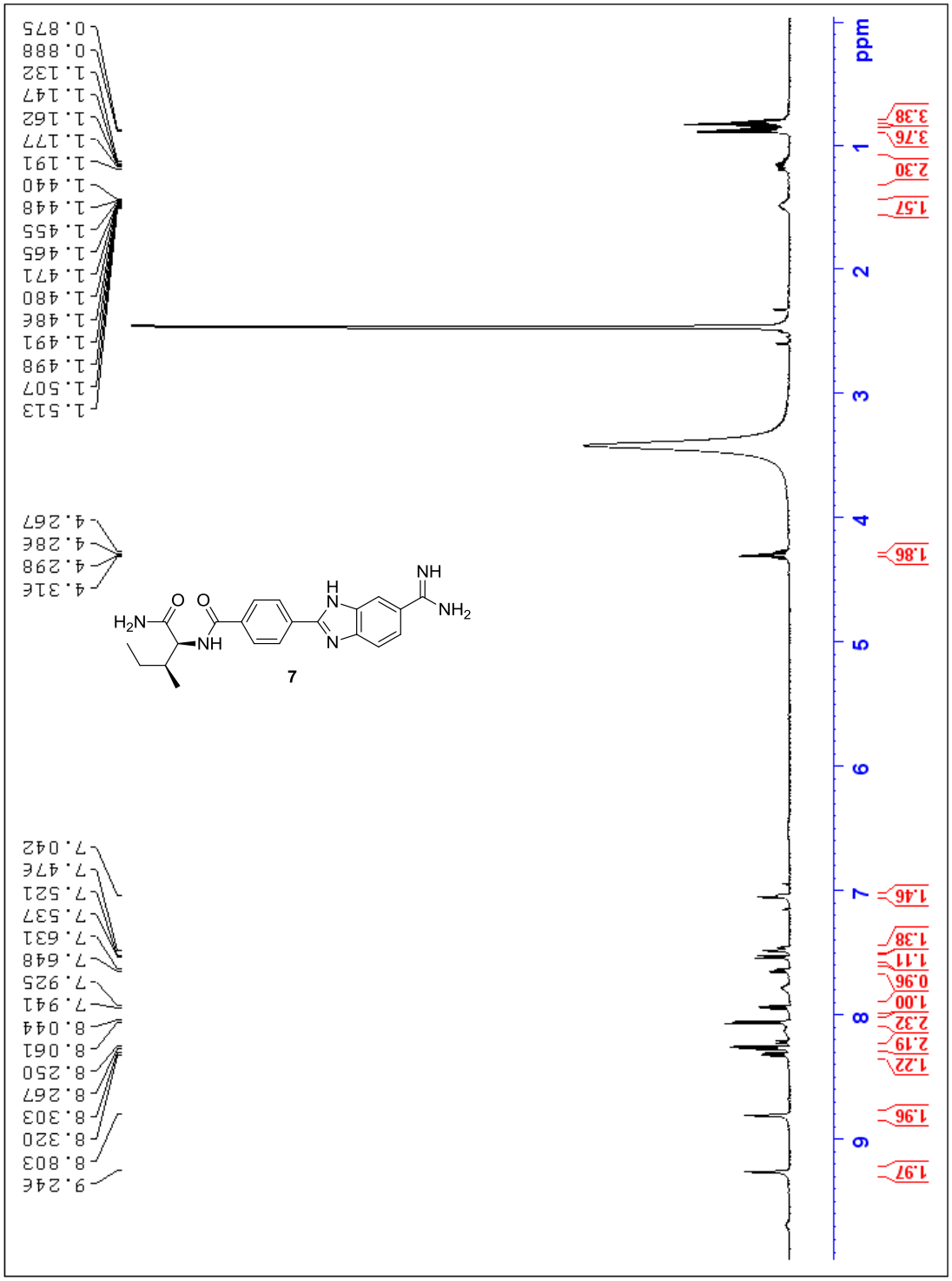
ppm
1
2
3
4
5
6
7
8
9
3.38
3.76
2.30
1.57
1.86
1.46
1.38
1.11
0.96
1.00
2.32
2.19
1.22
1.96
1.97
0.875
0.888
1.132
1.147
1.162
1.177
1.191
1.440
1.448
1.455
1.465
1.471
1.480
1.486
1.491
1.498
1.507
1.513
4.267
4.286
4.298
4.316
7.042
7.476
7.521
7.537
7.631
7.648
7.925
7.941
8.044
8.061
8.250
8.267
8.303
8.320
8.803
9.246
O
O
H2N
NH
H
N
N
NH
NH2
7

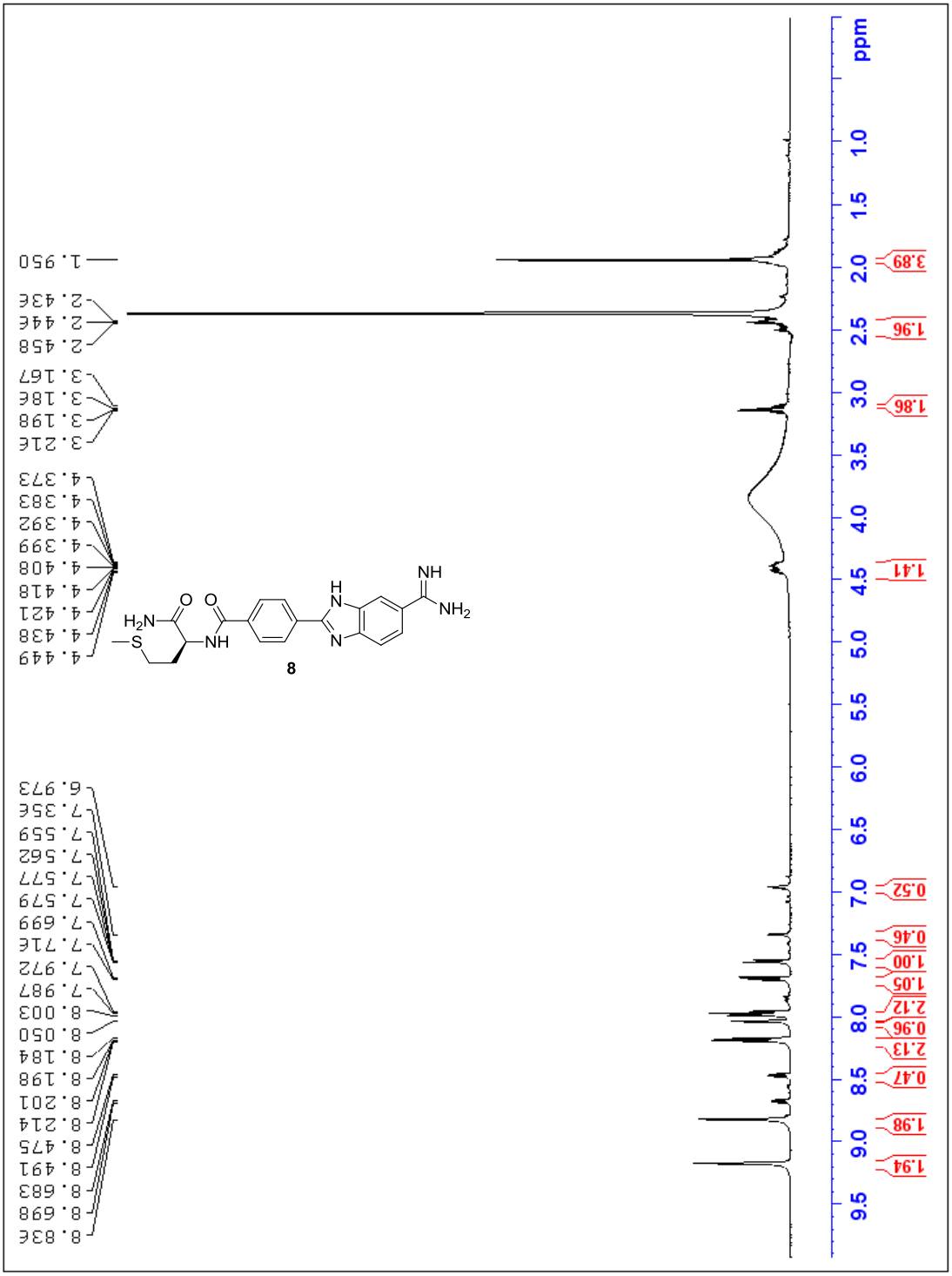
8
ppm
1.950
2.436
2.446
2.458
3.167
3.186
3.198
3.216
4.373
4.383
4.392
4.399
4.408
4.418
4.421
4.438
4.449
6.973
7.356
7.559
7.562
7.577
7.579
7.699
7.716
7.972
7.987
8.003
8.050
8.184
8.198
8.201
8.214
8.475
8.491
8.683
8.698
8.836
3.89
1.96
1.86
1.41
0.52
0.46
1.00
1.05
2.12
0.96
2.13
0.47
1.98
1.94

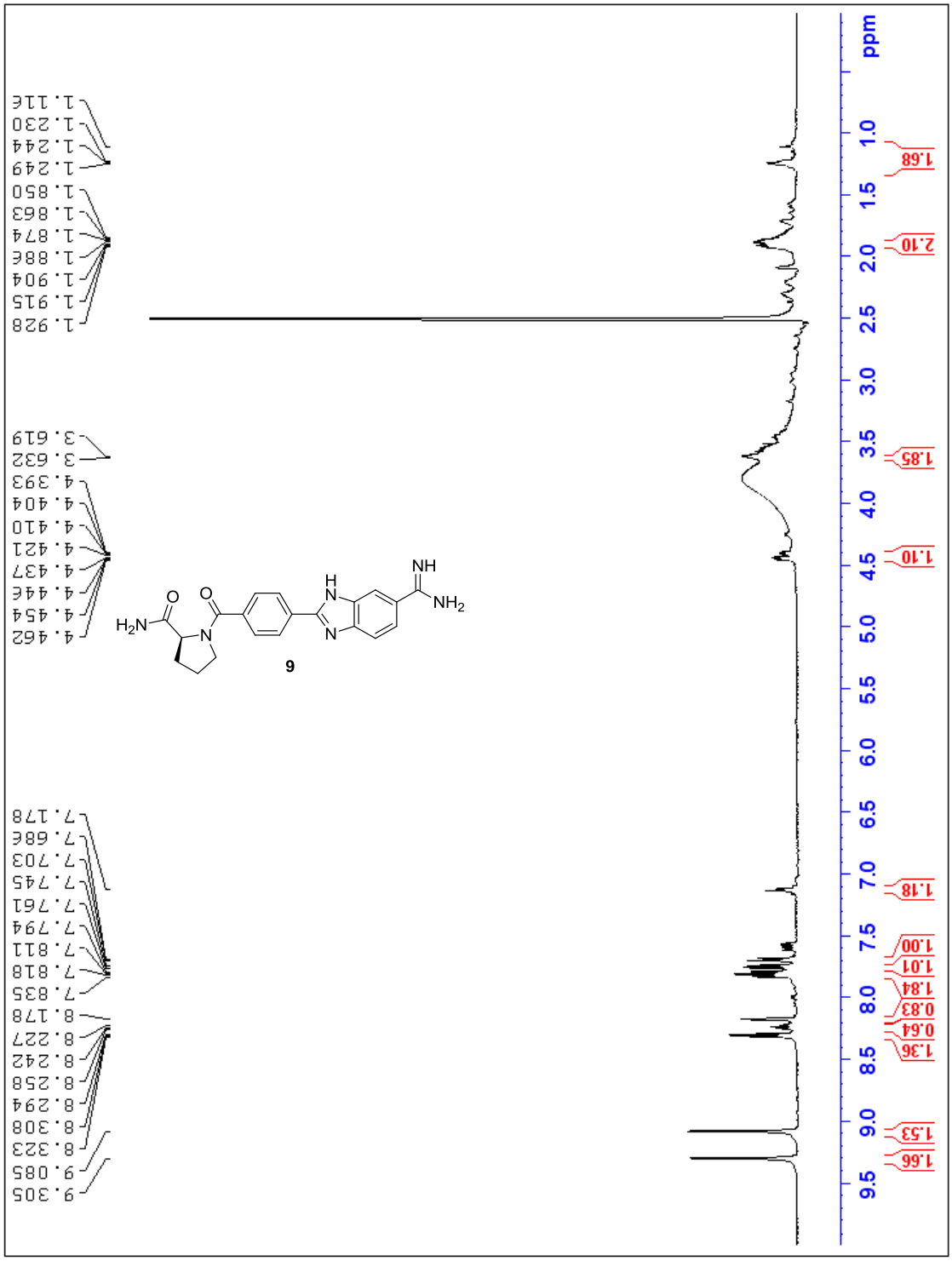
9.305
9.085
8.323
8.308
8.294
8.258
8.242
8.227
8.178
7.835
7.818
7.811
7.794
7.761
7.745
7.703
7.686
7.178
4.462
4.454
4.446
4.437
4.421
4.410
4.404
4.393
3.632
3.619
1.928
1.915
1.904
1.886
1.874
1.863
1.850
1.249
1.244
1.230
1.116
ppm
9.5
9.0
8.5
8.0
7.5
7.0
6.5
6.0
5.5
5.0
4.5
4.0
3.5
3.0
2.5
2.0
1.5
1.0
1.66
1.53
1.36
0.64
0.83
1.84
1.01
1.00
1.18
1.10
1.85
2.10
1.68
NH
NH2
H2N
O
O
N
H
N
N
9

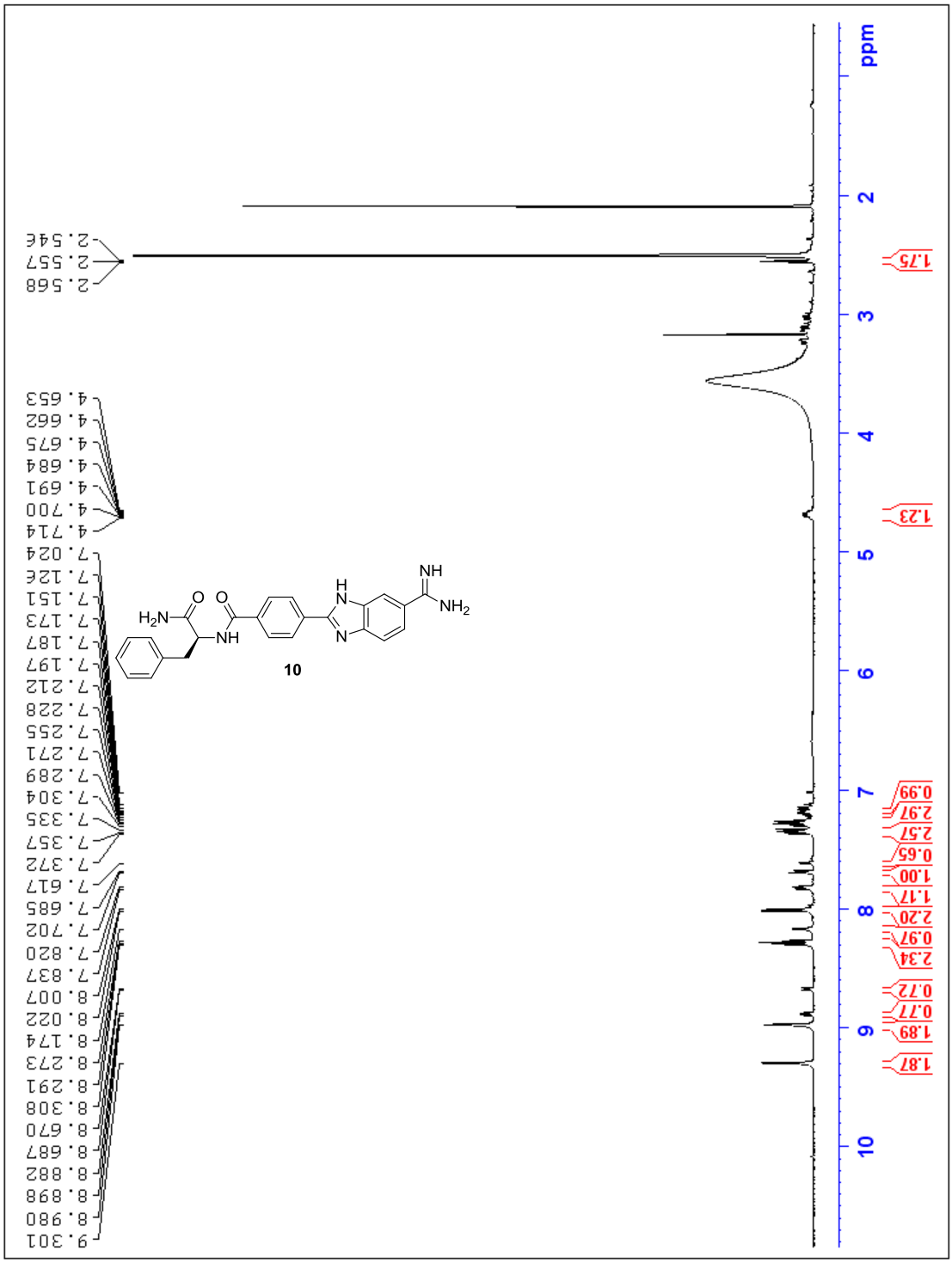
9.301
8.980
8.898
8.882
8.687
8.670
8.308
8.291
8.273
8.174
8.022
8.007
7.837
7.820
7.702
7.685
7.617
7.372
7.357
7.335
7.304
7.289
7.271
7.255
7.228
7.212
7.197
7.187
7.173
7.151
7.126
7.024
4.714
4.700
4.691
4.684
4.675
4.662
4.653
2.568
2.557
2.546
H2N
O
O
NH
NH
N
H
N
NH2
10
ppm
1.87
1.89
0.77
0.72
2.34
0.97
2.20
1.17
1.00
0.65
2.57
2.97
0.99
1.23
1.75

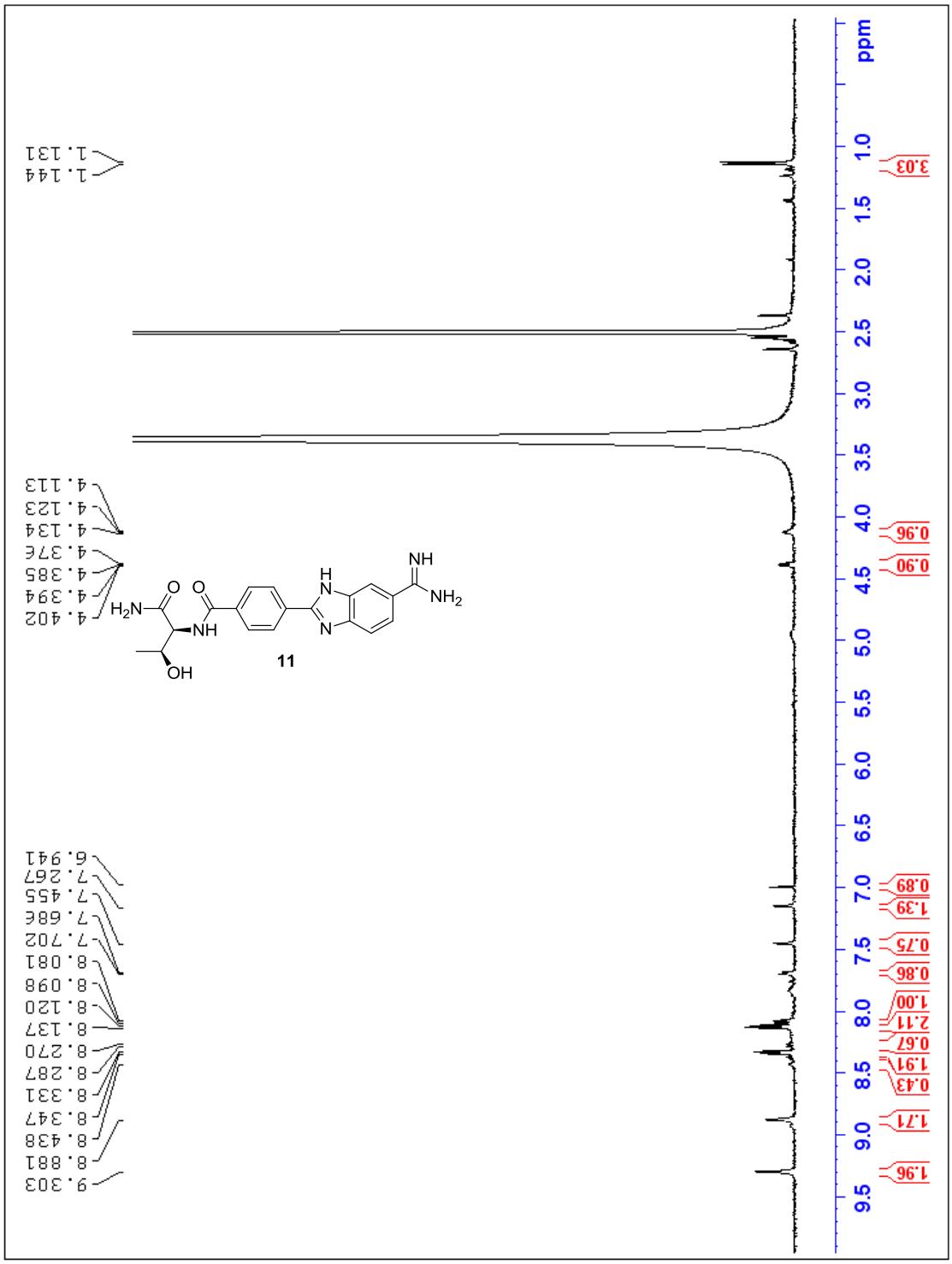
1.131
1.144
4.113
4.123
4.134
4.376
4.385
4.394
4.402
6.941
7.267
7.455
7.686
7.702
8.081
8.098
8.120
8.137
8.270
8.287
8.331
8.347
8.438
8.881
9.303
H2N
O
O
NH
NH
H
N
N
NH2
OH
11
ppm
1.0
1.5
2.0
2.5
3.0
3.5
4.0
4.5
5.0
5.5
6.0
6.5
7.0
7.5
8.0
8.5
9.0
9.5
3.03
0.96
0.90
0.89
1.39
0.75
0.86
1.00
2.11
0.67
1.91
0.43
1.71
1.96

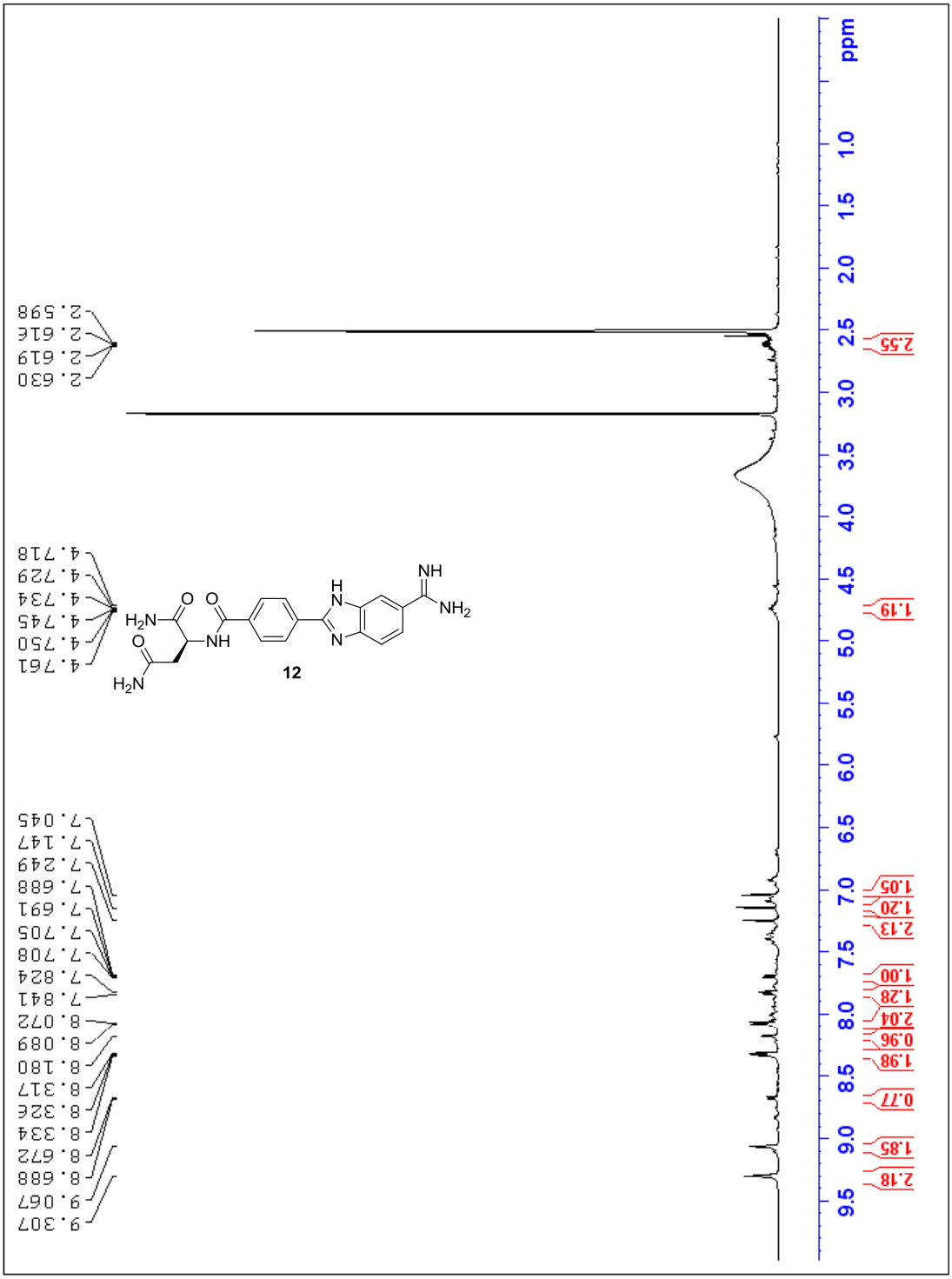
ppm
9.5
9.0
8.5
8.0
7.5
7.0
6.5
6.0
5.5
5.0
4.5
4.0
3.5
3.0
2.5
2.0
1.5
1.0
2.18
1.85
0.77
1.98
0.96
2.04
1.28
1.00
2.13
1.20
1.05
1.19
2.55
9.307
9.067
8.688
8.672
8.334
8.326
8.317
8.180
8.089
8.072
7.841
7.824
7.708
7.705
7.691
7.688
7.249
7.147
7.045
4.761
4.750
4.745
4.734
4.729
4.718
2.630
2.619
2.616
2.598
H2N
O
O
NH
O
H2N
H
N
N
NH
NH2
12

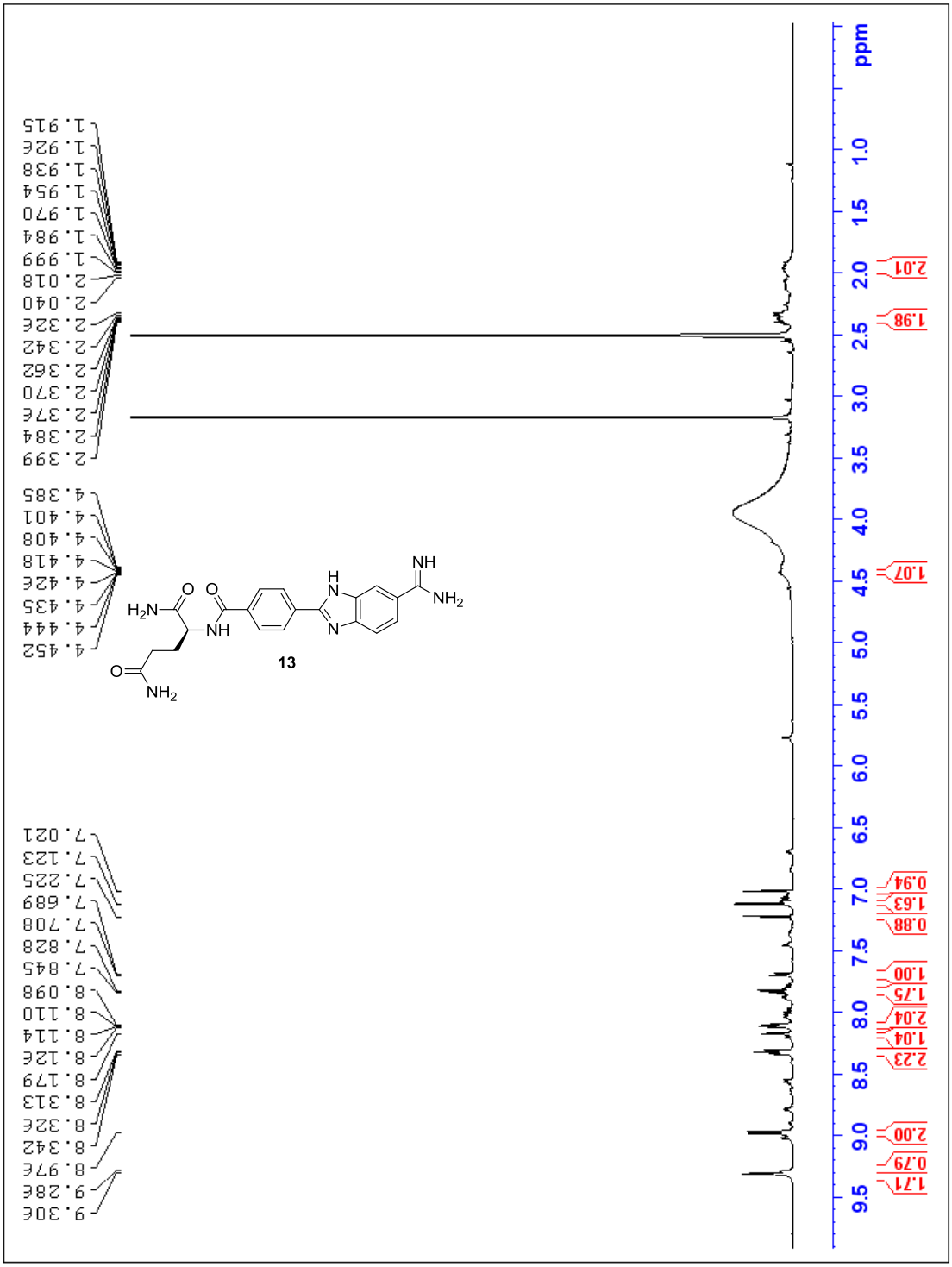
13
ppm
9.306
9.286
8.976
8.342
8.326
8.313
8.179
8.126
8.114
8.110
8.098
7.845
7.828
7.708
7.689
7.225
7.123
7.021
4.452
4.444
4.435
4.426
4.418
4.408
4.401
4.385
2.399
2.384
2.376
2.370
2.362
2.342
2.326
2.040
2.018
1.999
1.984
1.970
1.954
1.938
1.926
1.915
9.5
9.0
8.5
8.0
7.5
7.0
6.5
6.0
5.5
5.0
4.5
4.0
3.5
3.0
2.5
2.0
1.5
1.0
1.71
0.79
2.00
2.23
1.04
2.04
1.75
1.00
0.88
1.63
0.94
1.07
1.98
2.01

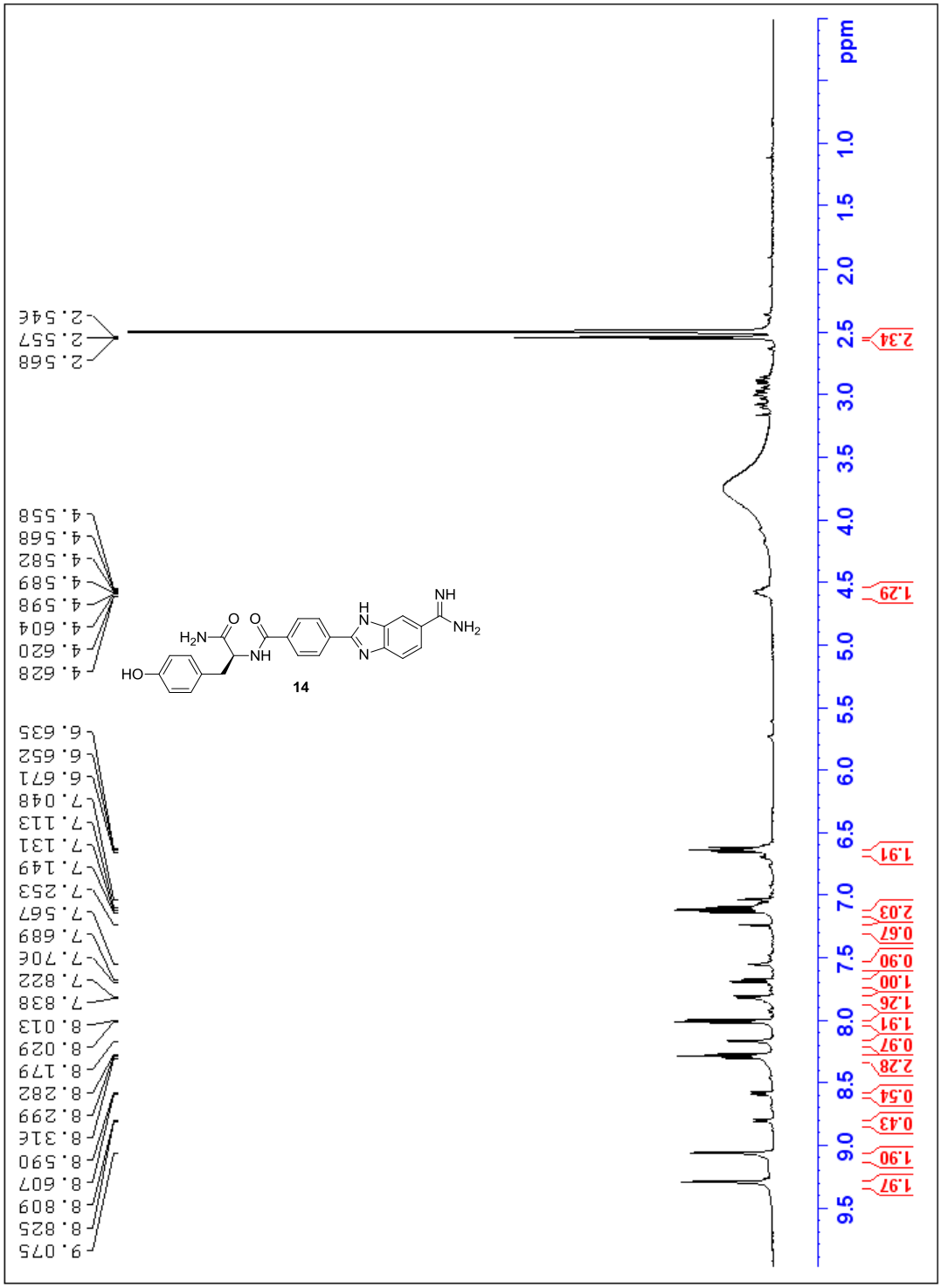
ppm
14

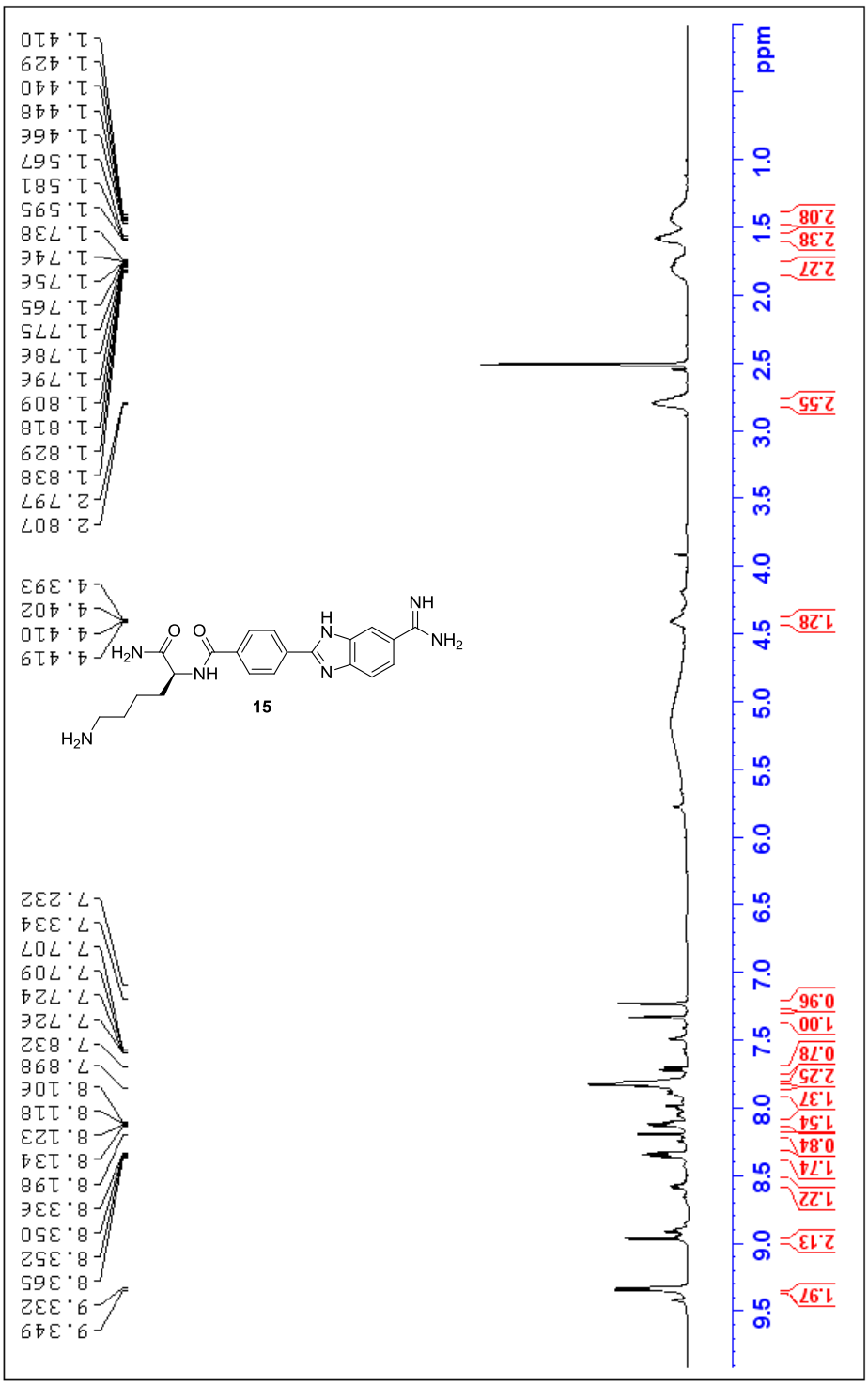
9.349
9.332
8.365
8.352
8.350
8.336
8.198
8.134
8.123
8.118
8.106
7.898
7.832
7.726
7.724
7.709
7.707
7.334
7.232
4.419
4.410
4.402
4.393
2.807
2.797
1.838
1.829
1.818
1.809
1.796
1.786
1.775
1.765
1.756
1.746
1.738
1.595
1.581
1.567
1.466
1.448
1.440
1.429
1.410
15
ppm
1.97
2.13
1.22
1.74
0.84
1.54
1.37
2.25
0.78
1.00
0.96
1.28
2.55
2.27
2.38
2.08

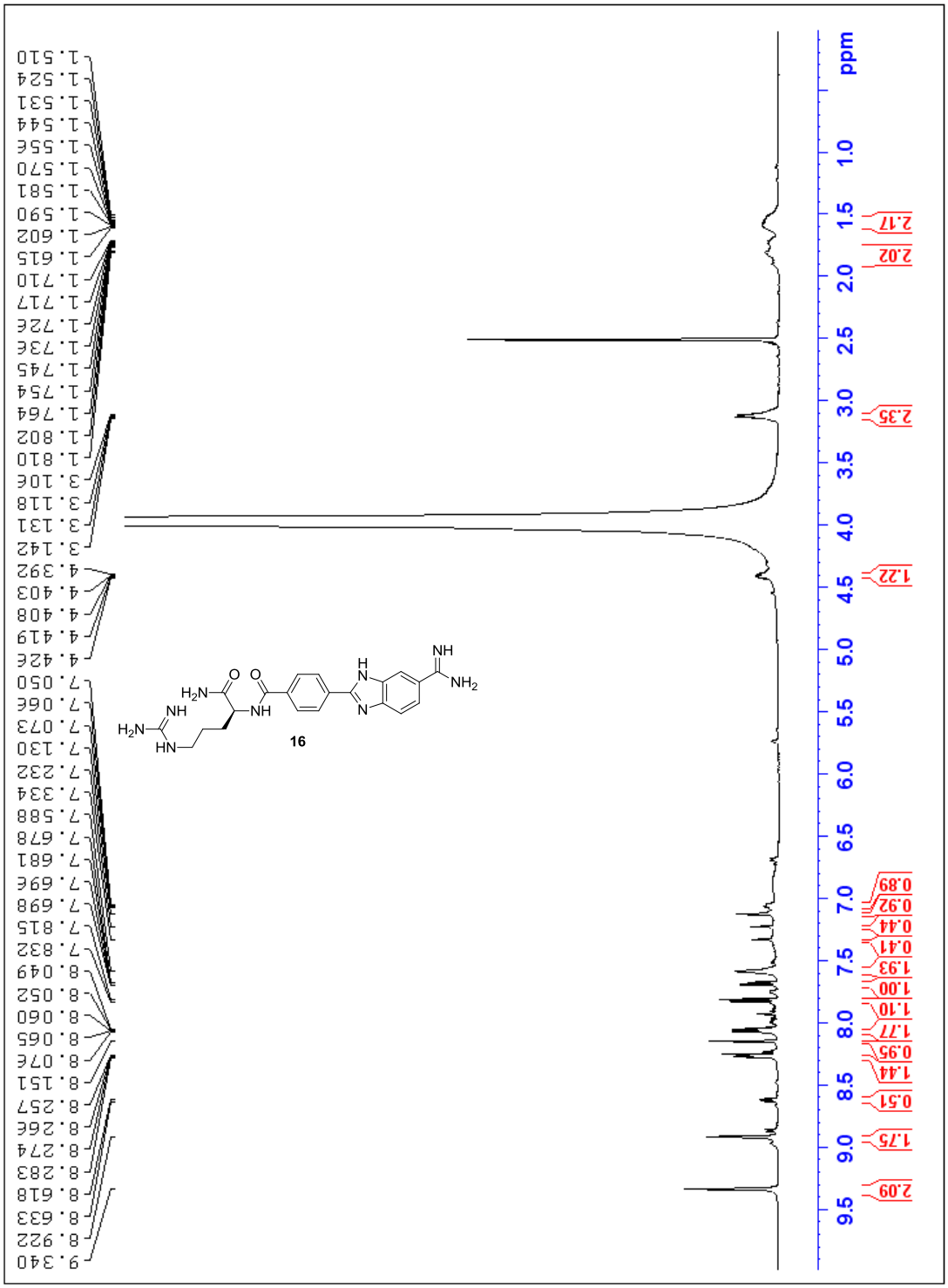
16
ppm
9.340
8.922
8.633
8.618
8.283
8.274
8.266
8.257
8.151
8.076
8.065
8.060
8.052
8.049
7.832
7.815
7.698
7.696
7.681
7.678
7.588
7.334
7.232
7.130
7.073
7.066
7.050
4.426
4.419
4.408
4.403
4.392
3.142
3.131
3.118
3.106
1.810
1.802
1.764
1.754
1.745
1.736
1.726
1.717
1.710
1.615
1.602
1.590
1.581
1.570
1.556
1.544
1.531
1.524
1.510
2.09
1.75
0.51
1.44
0.95
1.77
1.10
1.00
1.93
0.41
0.44
0.92
0.89
1.22
2.35
2.02
2.17

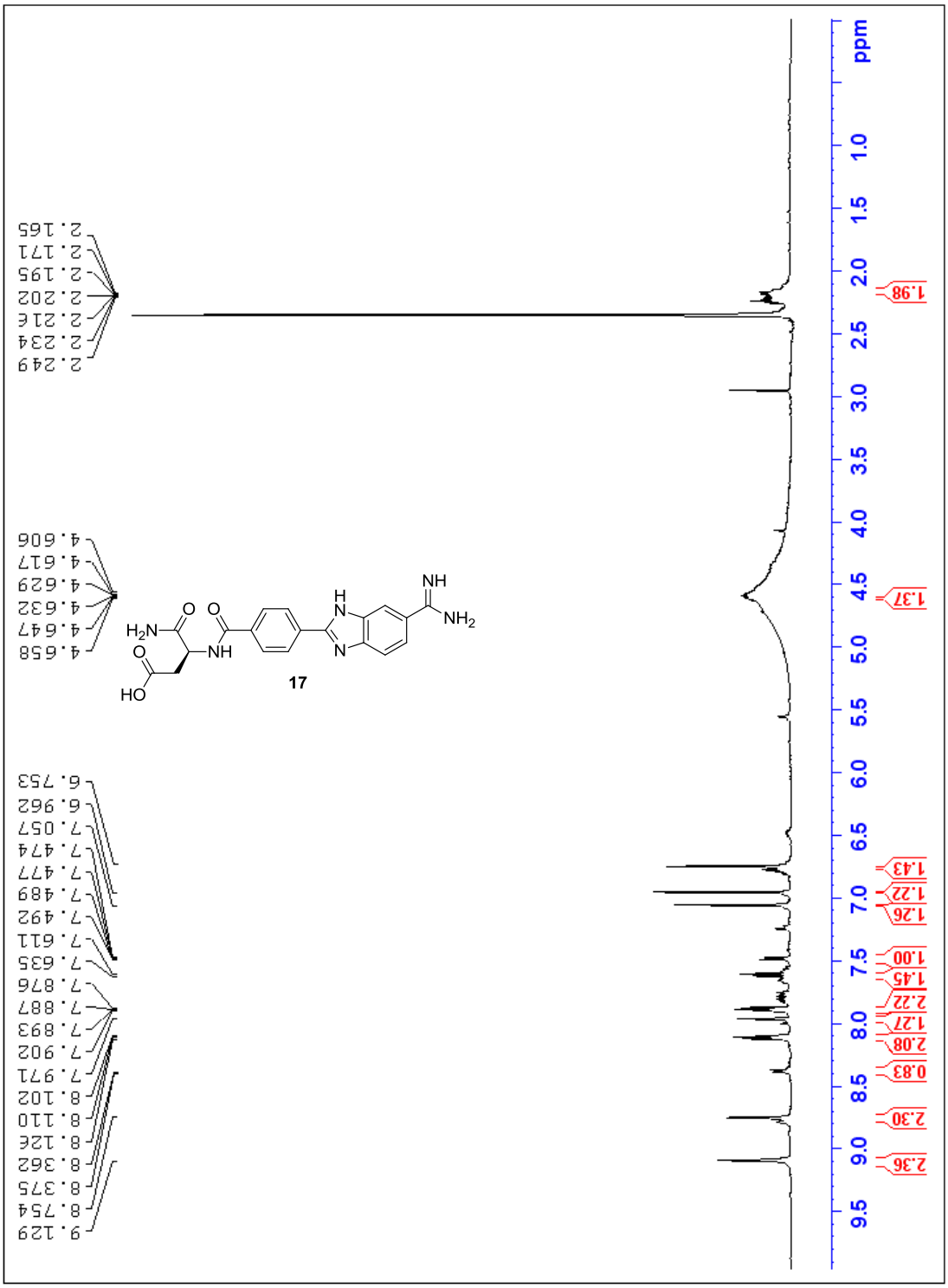
ppm
9.5
9.0
8.5
8.0
7.5
7.0
6.5
6.0
5.5
5.0
4.5
4.0
3.5
3.0
2.5
2.0
1.5
1.0
1.98
1.37
1.43
1.22
1.26
1.00
1.45
2.22
1.27
2.08
0.83
2.30
2.36
2.249
2.234
2.216
2.202
2.195
2.171
2.165
4.658
4.647
4.632
4.629
4.617
4.606
6.753
6.962
7.057
7.474
7.477
7.489
7.492
7.611
7.635
7.876
7.887
7.893
7.902
7.971
8.102
8.110
8.126
8.362
8.375
8.754
9.129
H2N
O
O
NH
O
HO
H
N
N
NH
NH2
17

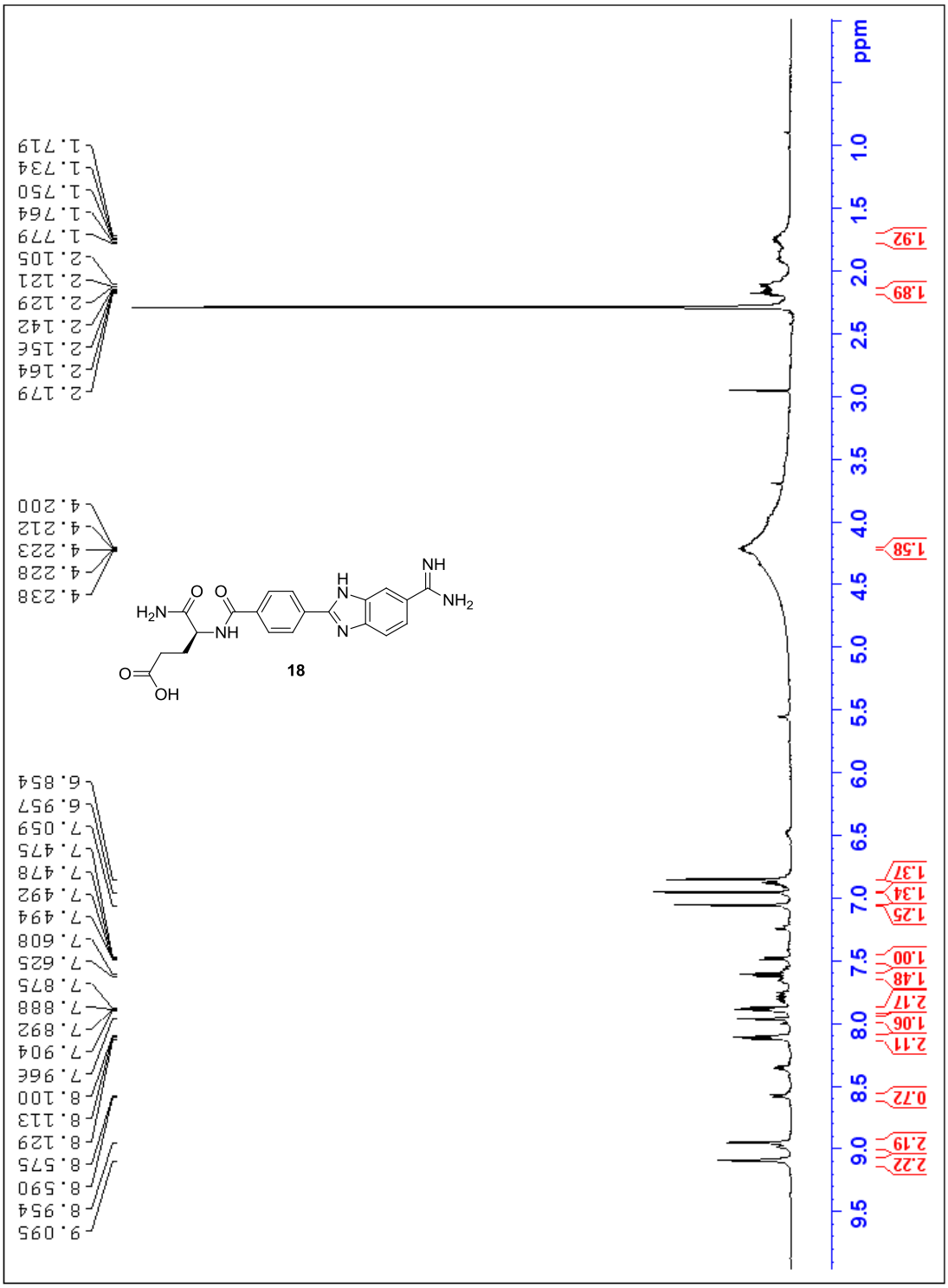
18
ppm
1.92
1.89
1.58
1.37
1.34
1.25
1.00
1.48
2.17
1.06
2.11
0.72
2.19
2.22
1.719
1.734
1.750
1.764
1.779
2.105
2.121
2.129
2.142
2.156
2.164
2.179
4.200
4.212
4.223
4.228
4.238
6.854
6.957
7.059
7.475
7.478
7.492
7.494
7.608
7.625
7.875
7.888
7.892
7.904
7.966
8.100
8.113
8.129
8.575
8.590
8.954
9.095

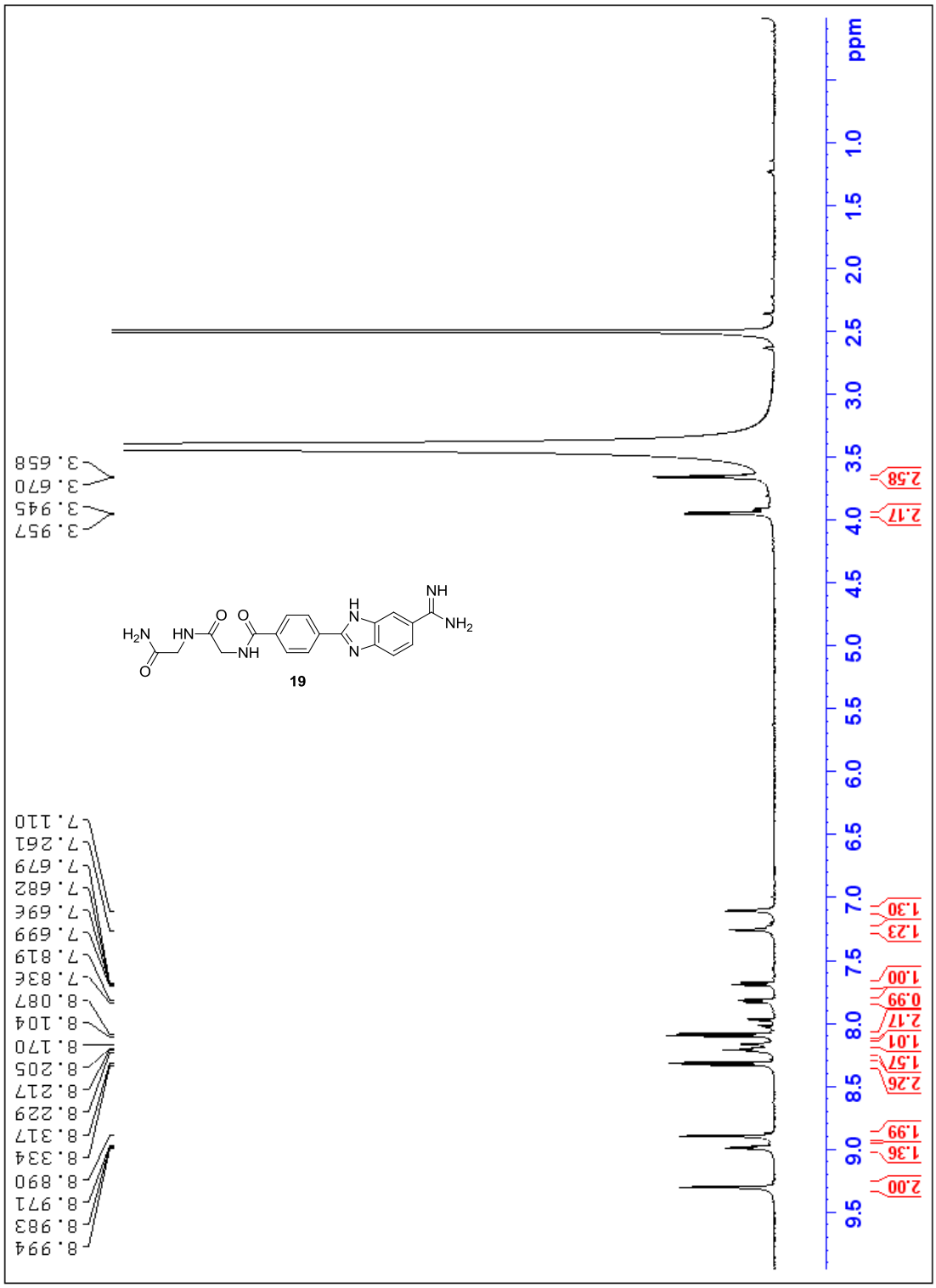
19
ppm
9.5
9.0
8.5
8.0
7.5
7.0
6.5
6.0
5.5
5.0
4.5
4.0
3.5
3.0
2.5
2.0
1.5
1.0
2.00
1.36
1.99
2.26
1.57
1.01
2.17
0.99
1.00
1.30
1.23
2.58
2.17
3.957
3.945
3.670
3.658
8.994
8.983
8.971
8.890
8.334
8.317
8.229
8.217
8.205
8.170
8.104
8.087
7.836
7.819
7.699
7.696
7.682
7.679
7.261
7.110

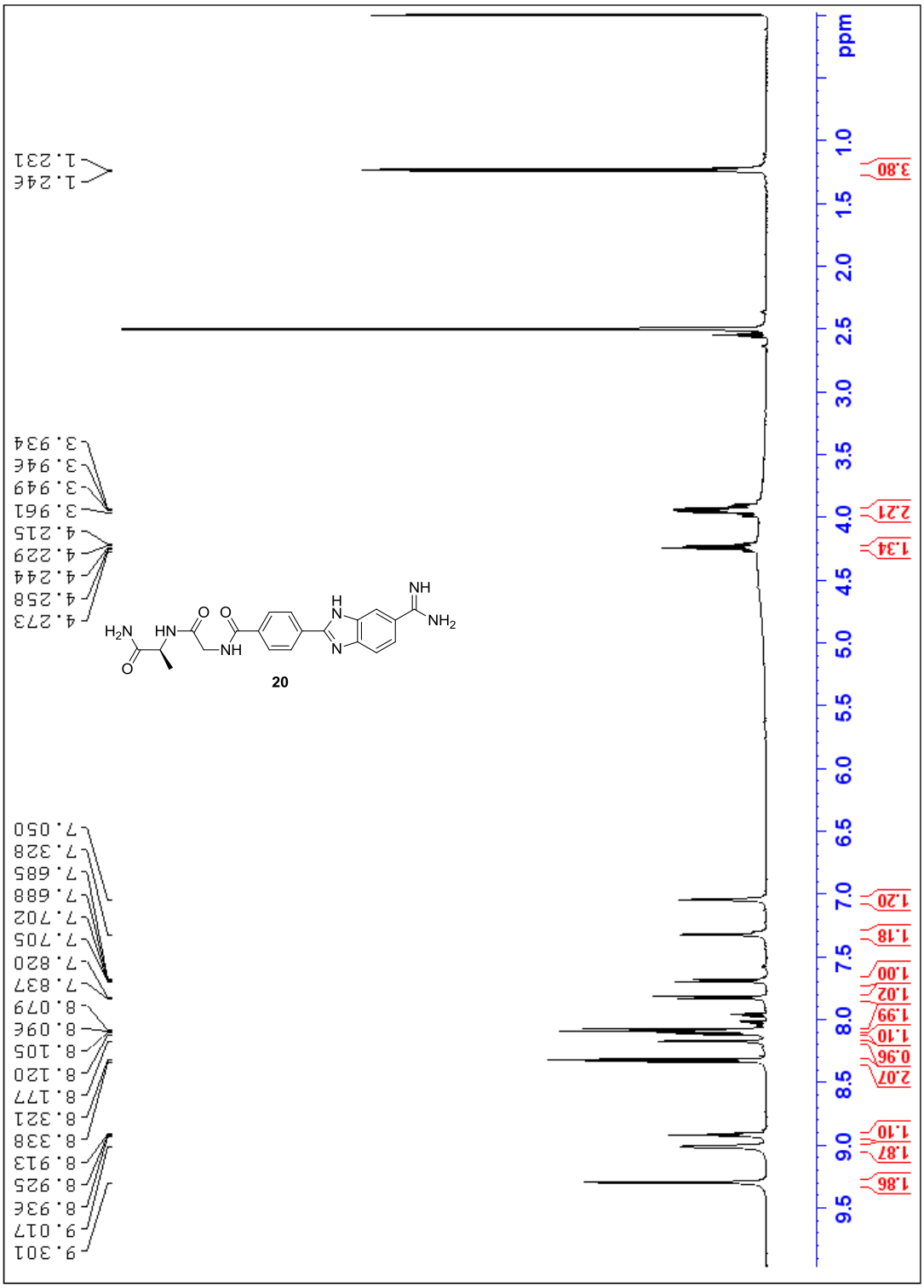
ppm
1.0
1.5
2.0
2.5
3.0
3.5
4.0
4.5
5.0
5.5
6.0
6.5
7.0
7.5
8.0
8.5
9.0
9.5
3.80
2.21
1.34
1.20
1.18
1.00
1.02
1.99
1.10
0.96
2.07
1.10
1.87
1.86
1.231
1.246
3.934
3.946
3.949
3.961
4.215
4.229
4.244
4.258
4.273
7.050
7.328
7.685
7.688
7.702
7.705
7.820
7.837
8.079
8.096
8.105
8.120
8.177
8.321
8.338
8.913
8.925
8.936
9.017
9.301
NH
NH2
H
N
N
HN
O
NH
H2N
O
20

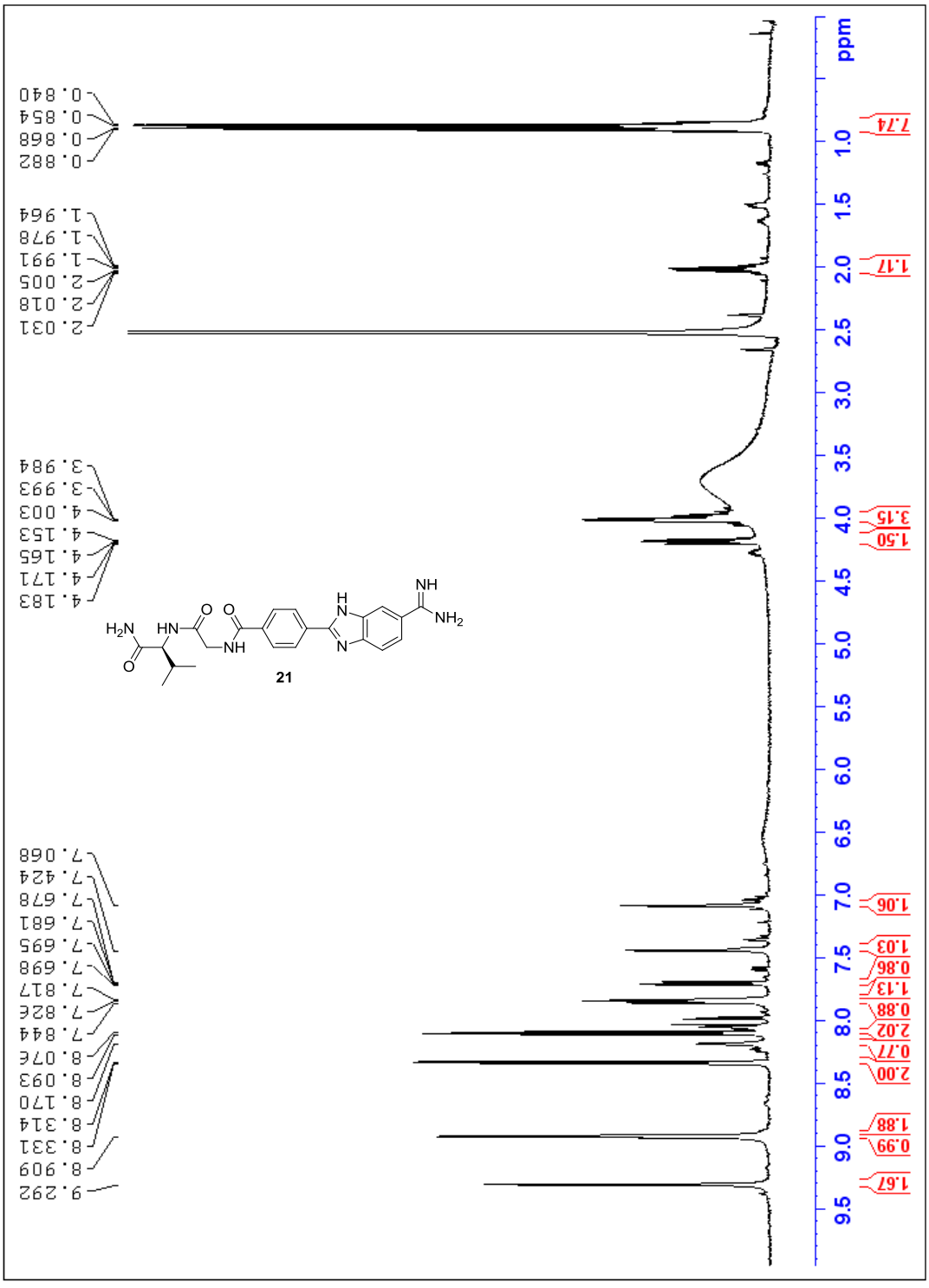
21
ppm

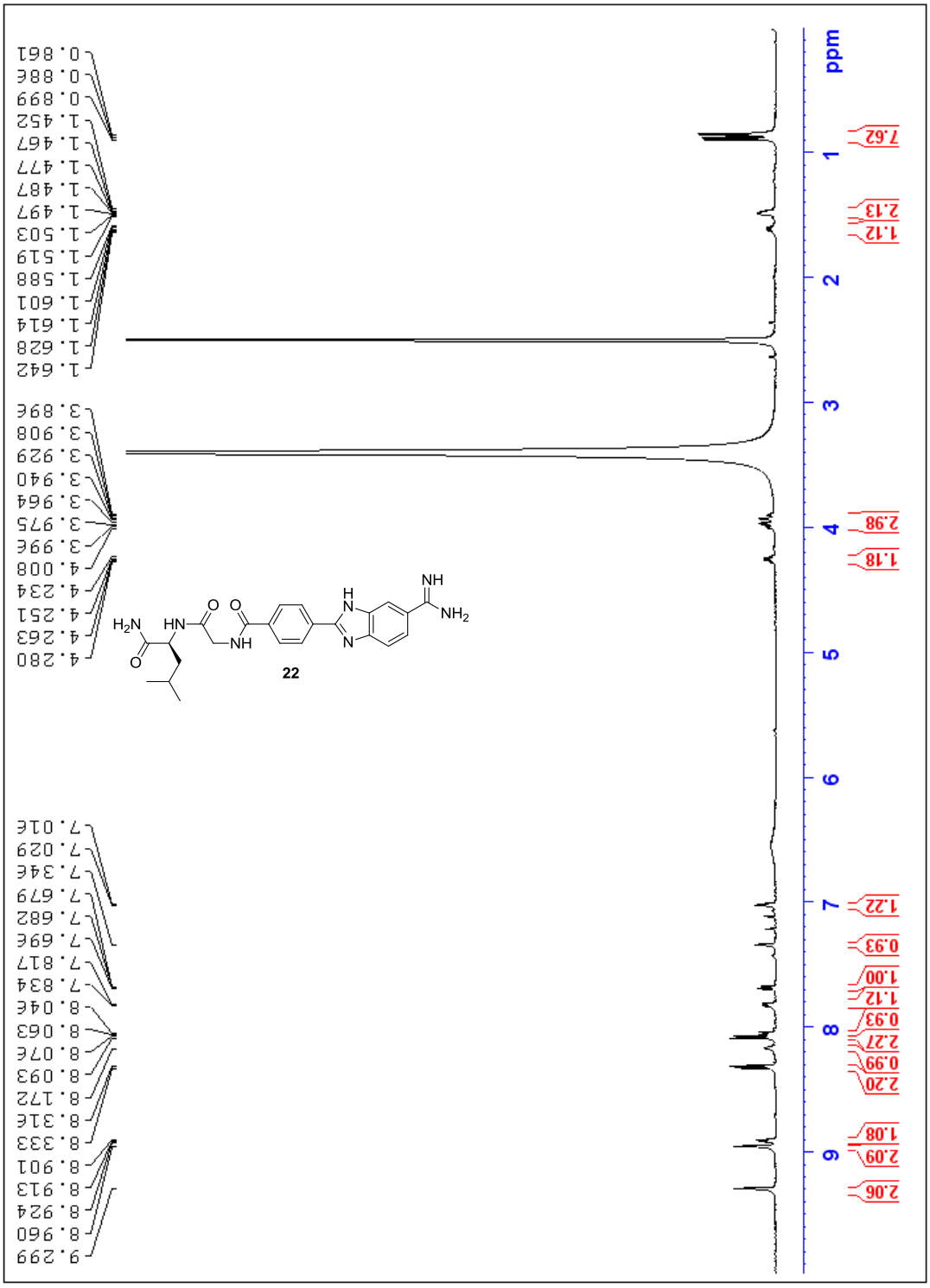
ppm
1
2
3
4
5
6
7
8
9
7.62
2.13
1.12
2.98
1.18
1.22
0.93
1.00
1.12
0.93
2.27
0.99
2.20
1.08
2.09
2.06
0.861
0.886
0.899
1.452
1.467
1.477
1.487
1.497
1.503
1.519
1.588
1.601
1.614
1.628
1.642
3.896
3.908
3.929
3.940
3.964
3.975
3.996
4.008
4.234
4.251
4.263
4.280
7.016
7.029
7.346
7.679
7.682
7.696
7.817
7.834
8.046
8.063
8.076
8.093
8.172
8.316
8.333
8.901
8.913
8.924
8.960
9.299
H2N
HN
O
O
NH
NH
N
H
N
NH2
22

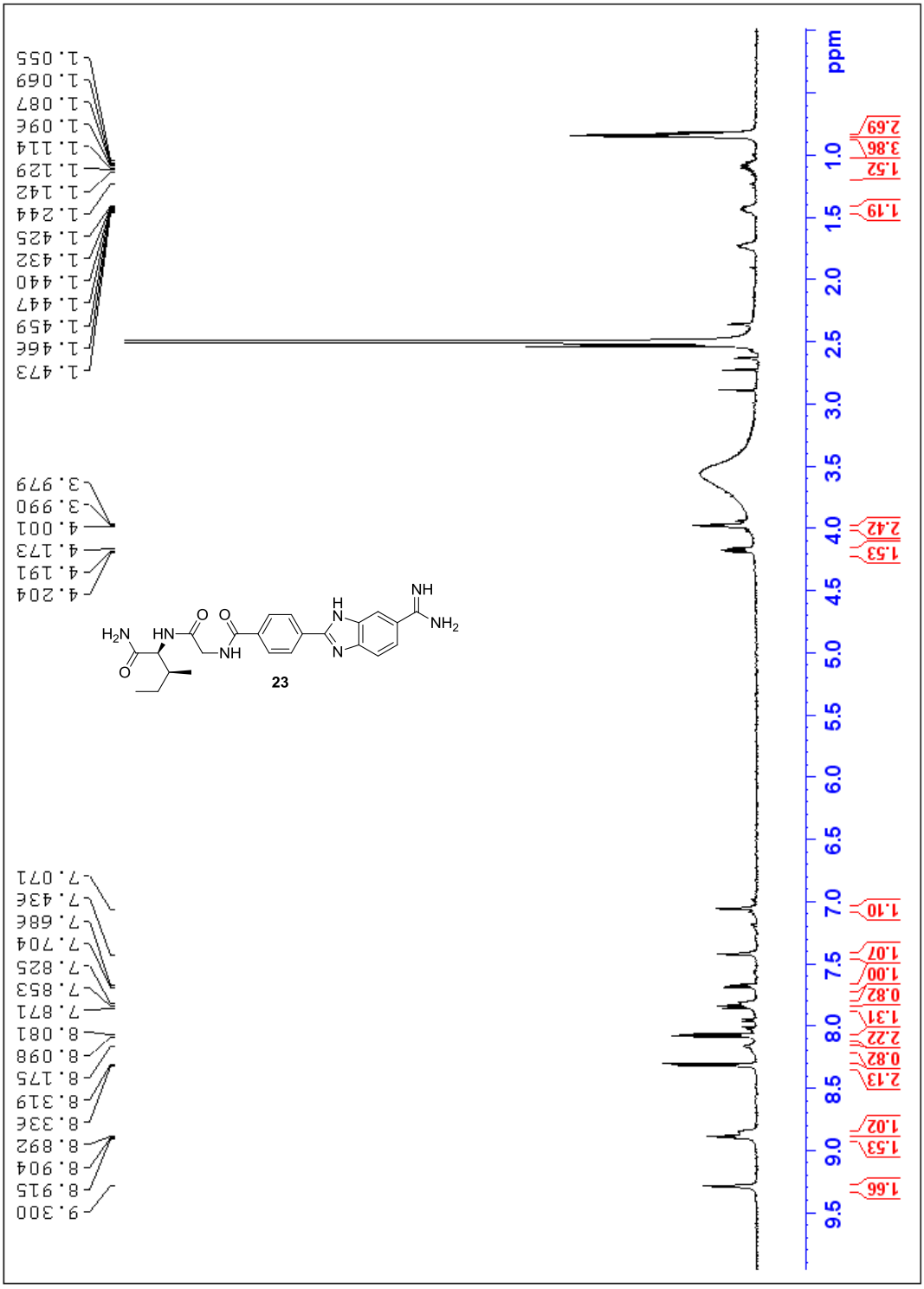
23

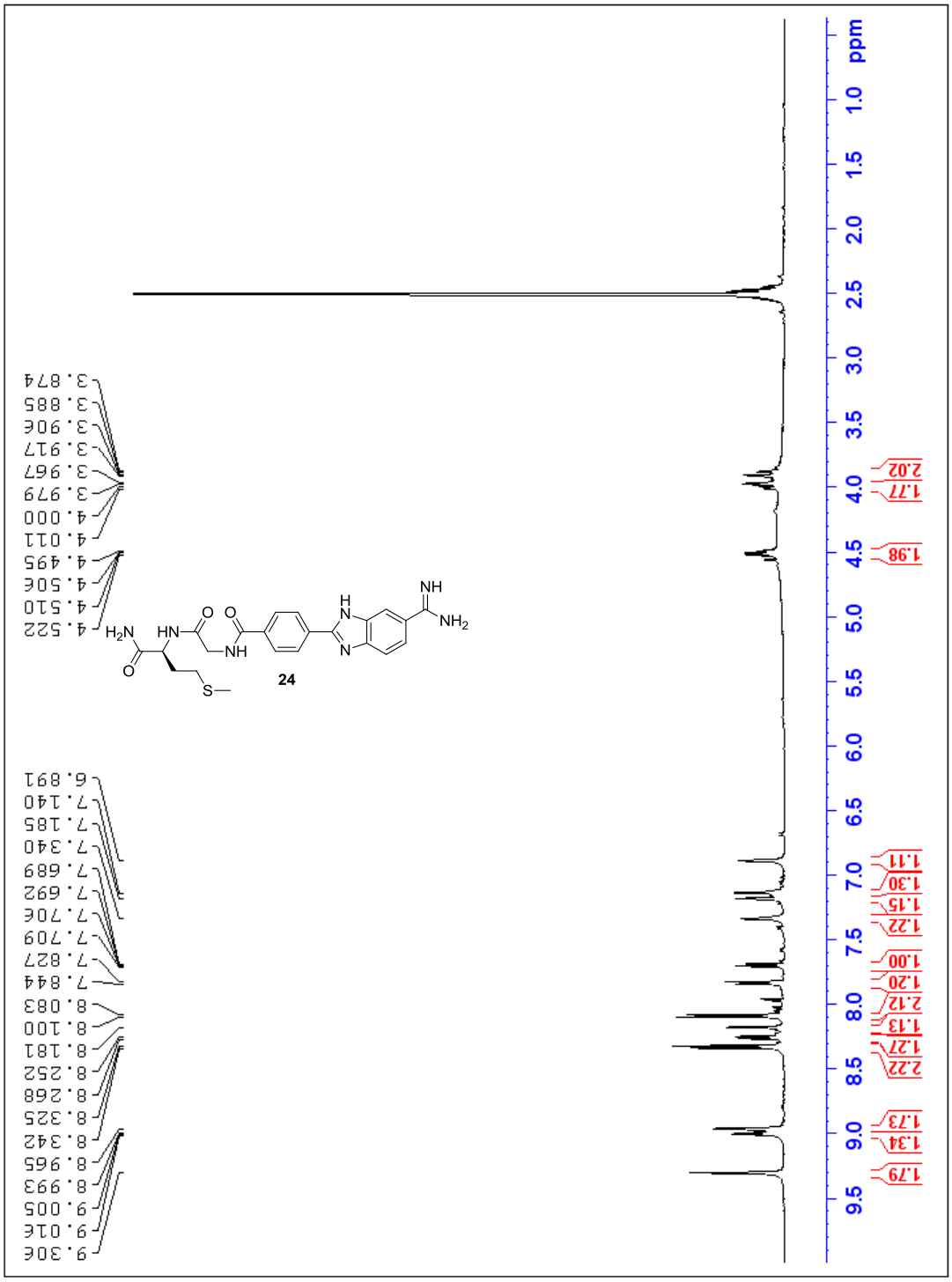
24

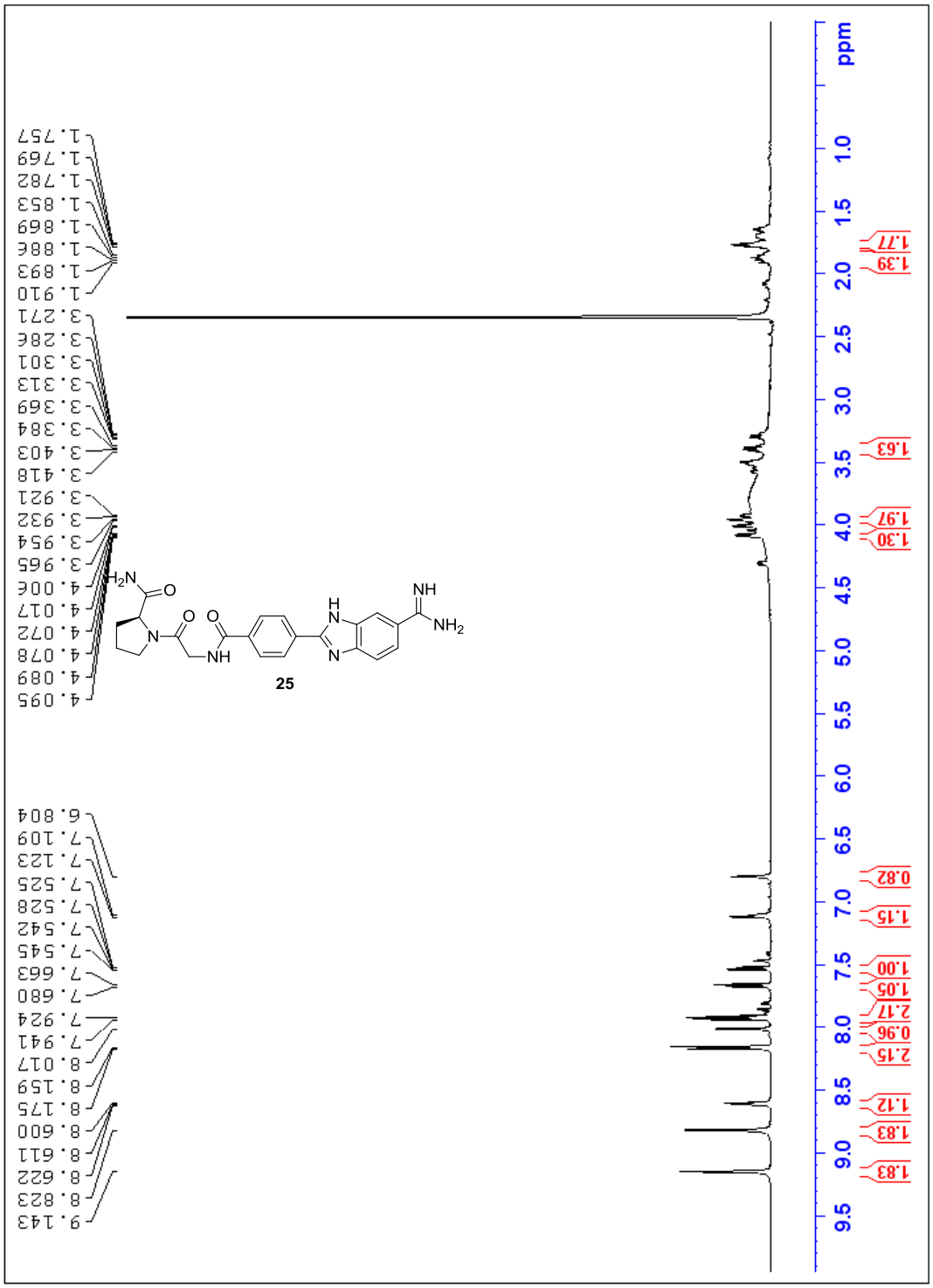
25
ppm
1.83
1.83
1.12
2.15
0.96
2.17
1.05
1.00
1.15
0.82
1.63
1.97
1.30
1.39
1.77

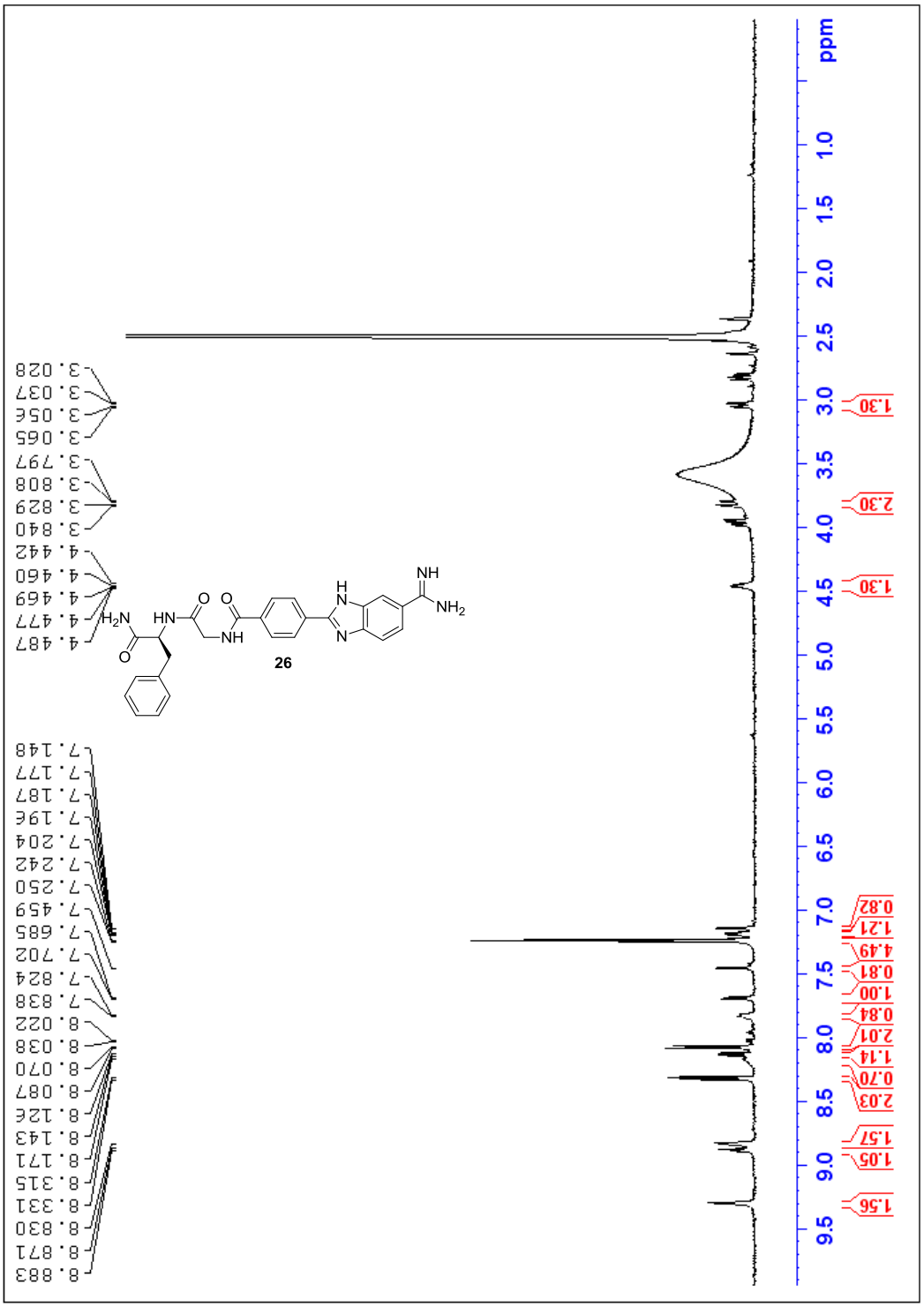
ppm
9.5
9.0
8.5
8.0
7.5
7.0
6.5
6.0
5.5
5.0
4.5
4.0
3.5
3.0
2.5
2.0
1.5
1.0
1.56
1.05
1.57
2.03
0.70
1.14
2.01
0.84
1.00
0.81
4.49
1.21
0.82
1.30
2.30
1.30
8.883
8.871
8.830
8.331
8.315
8.171
8.143
8.126
8.087
8.070
8.038
8.022
7.838
7.824
7.702
7.685
7.459
7.250
7.242
7.204
7.196
7.187
7.177
7.148
4.487
4.477
4.469
4.460
4.442
3.840
3.829
3.808
3.797
3.065
3.056
3.037
3.028
H2N
HN
O
O
HN
O
NH
H
N
N
NH
NH2
26

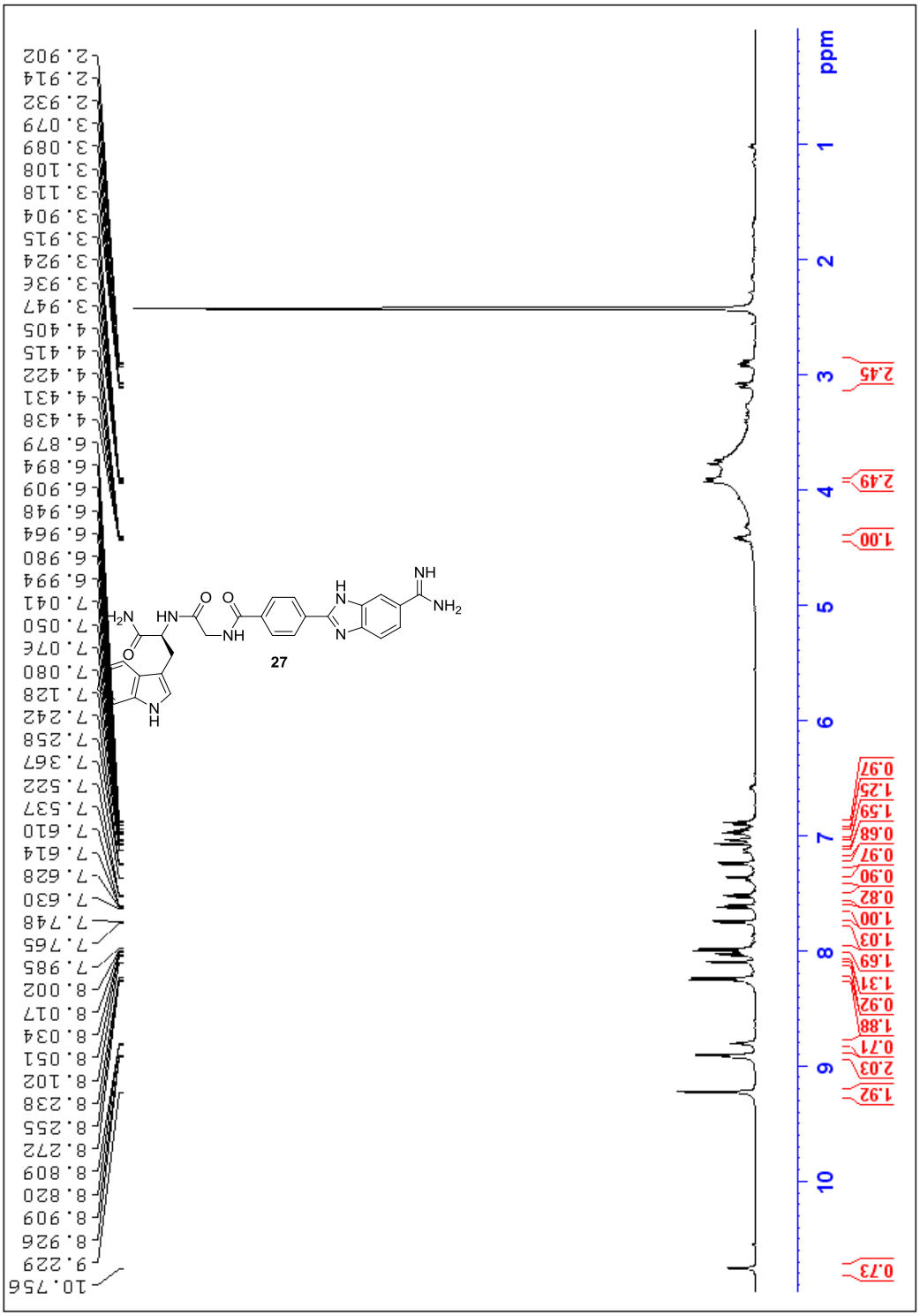
27
ppm
1
2
3
4
5
6
7
8
9
10
0.73
2.45
2.49
1.00
1.92
2.03
0.71
1.88
0.92
1.31
1.69
1.03
1.00
0.82
0.90
0.97
0.68
1.59
1.25
0.97
10.756
9.229
8.926
8.909
8.820
8.809
8.272
8.255
8.238
8.102
8.051
8.034
8.017
8.002
7.985
7.765
7.748
7.630
7.628
7.614
7.610
7.537
7.522
7.367
7.258
7.242
7.128
7.080
7.076
7.050
7.041
6.994
6.980
6.964
6.948
6.909
6.894
6.879
4.438
4.431
4.422
4.415
4.405
3.947
3.936
3.924
3.915
3.904
3.118
3.108
3.089
3.079
2.932
2.914
2.902

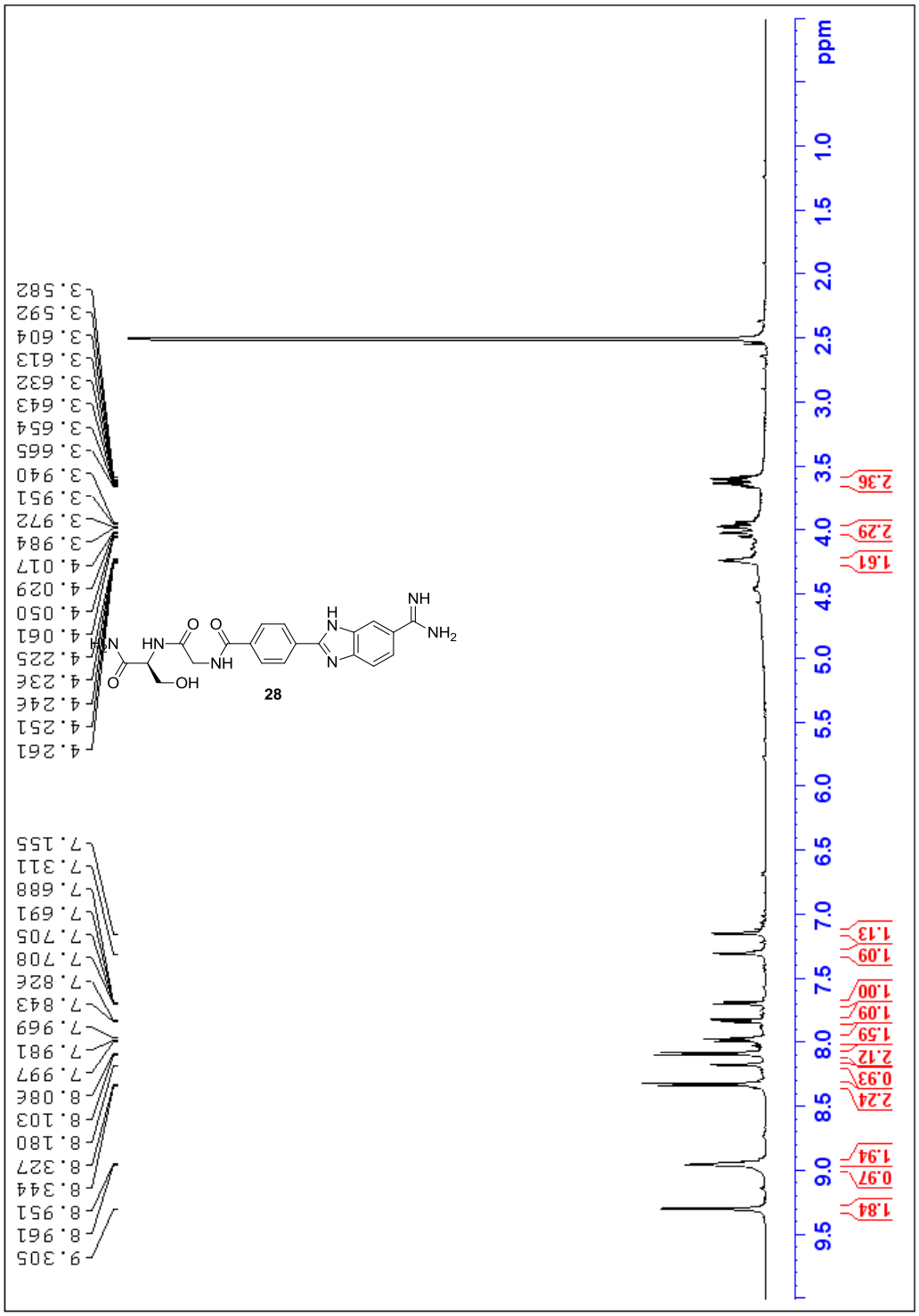
9.305
8.961
8.951
8.344
8.327
8.180
8.103
8.086
7.997
7.981
7.969
7.843
7.826
7.708
7.705
7.691
7.688
7.311
7.155
4.261
4.251
4.246
4.236
4.225
4.061
4.050
4.029
4.017
3.984
3.972
3.951
3.940
3.665
3.654
3.643
3.632
3.613
3.604
3.592
3.582
28
ppm
1.84
0.97
1.94
2.24
0.93
2.12
1.59
1.09
1.00
1.09
1.13
2.36
2.29
1.61

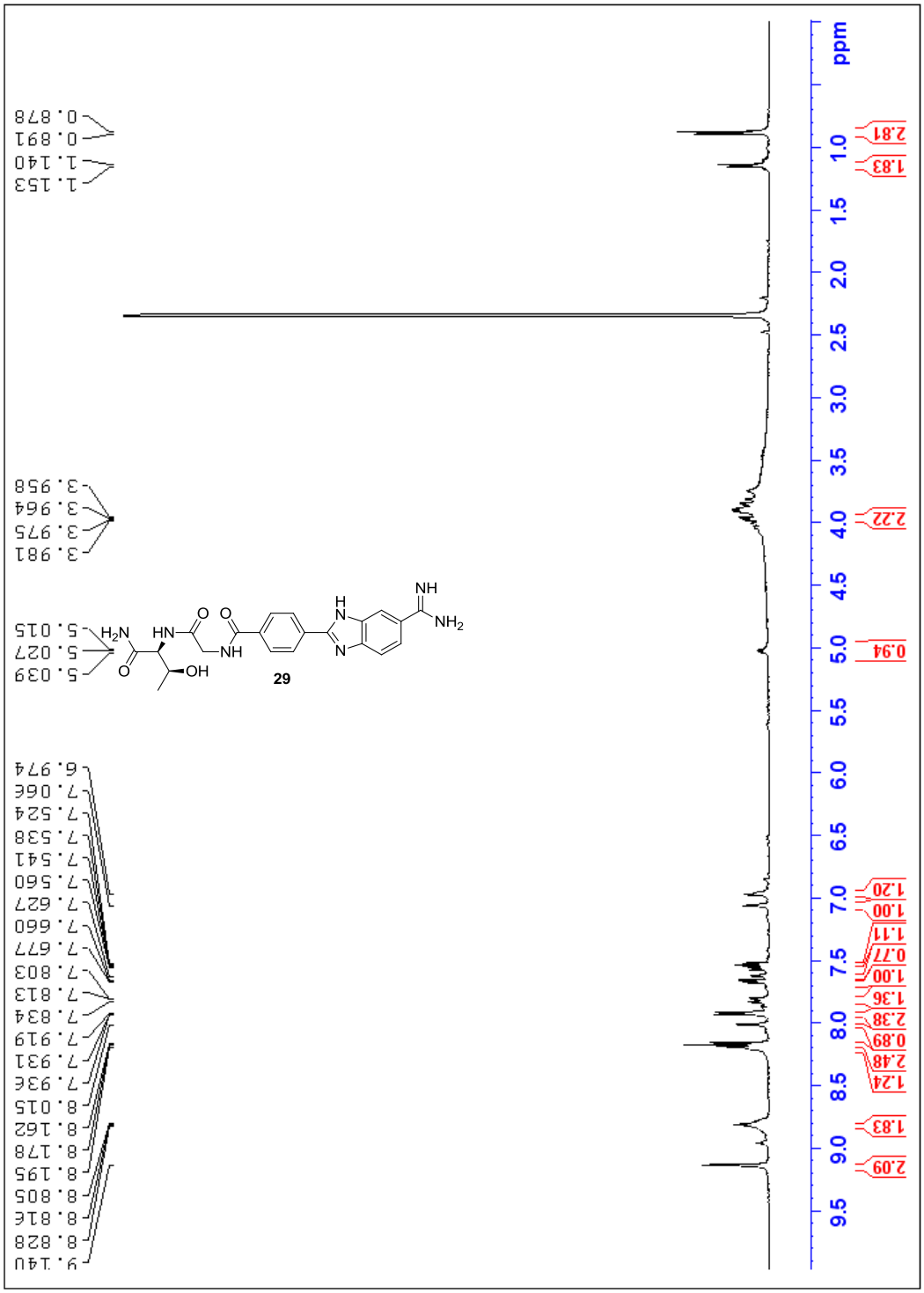
29

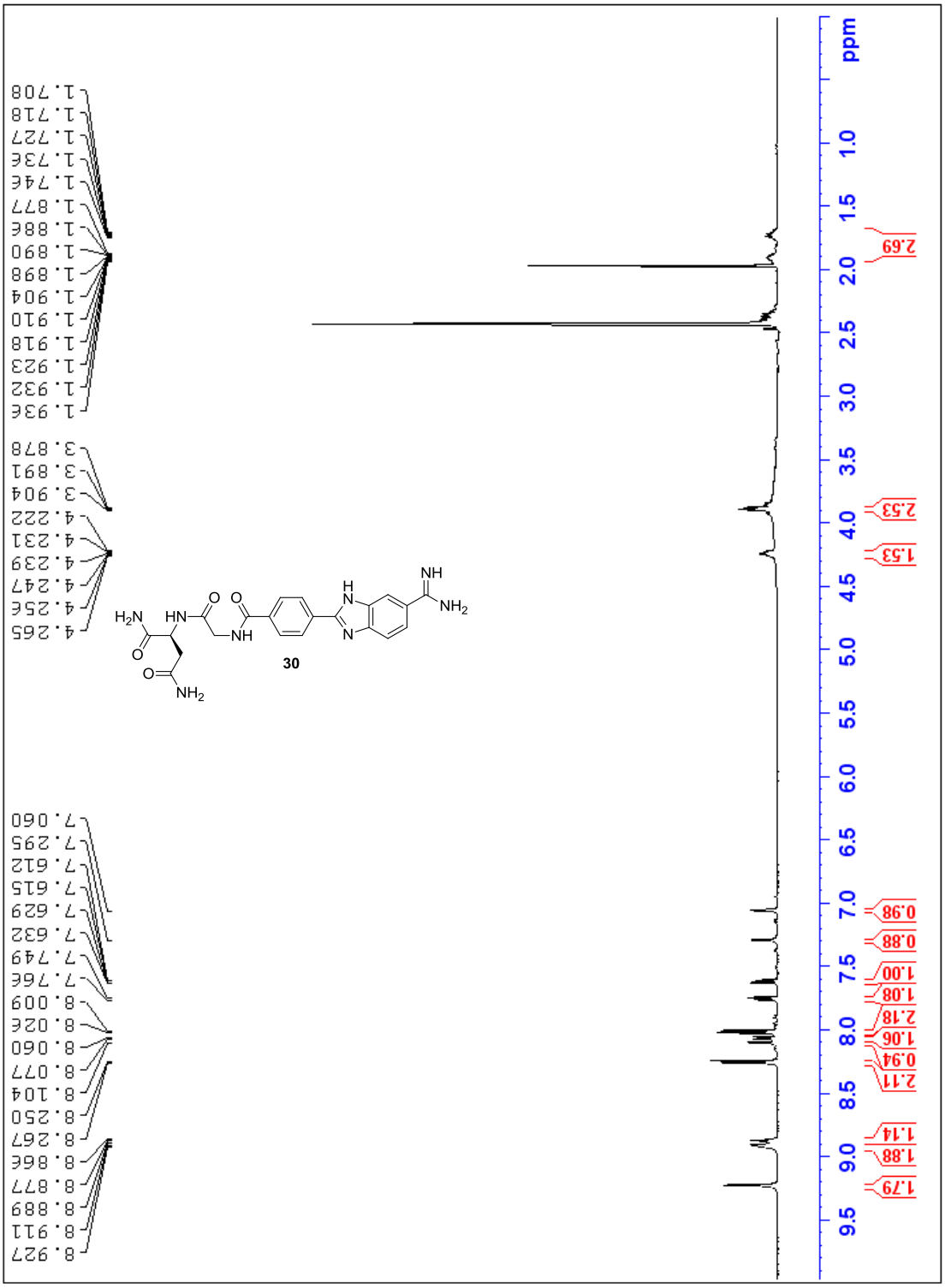
30
ppm
1.0
1.5
2.0
2.5
3.0
3.5
4.0
4.5
5.0
5.5
6.0
6.5
7.0
7.5
8.0
8.5
9.0
9.5
2.69
2.53
1.53
0.98
0.88
1.00
1.08
2.18
1.06
0.94
2.11
1.14
1.88
1.79

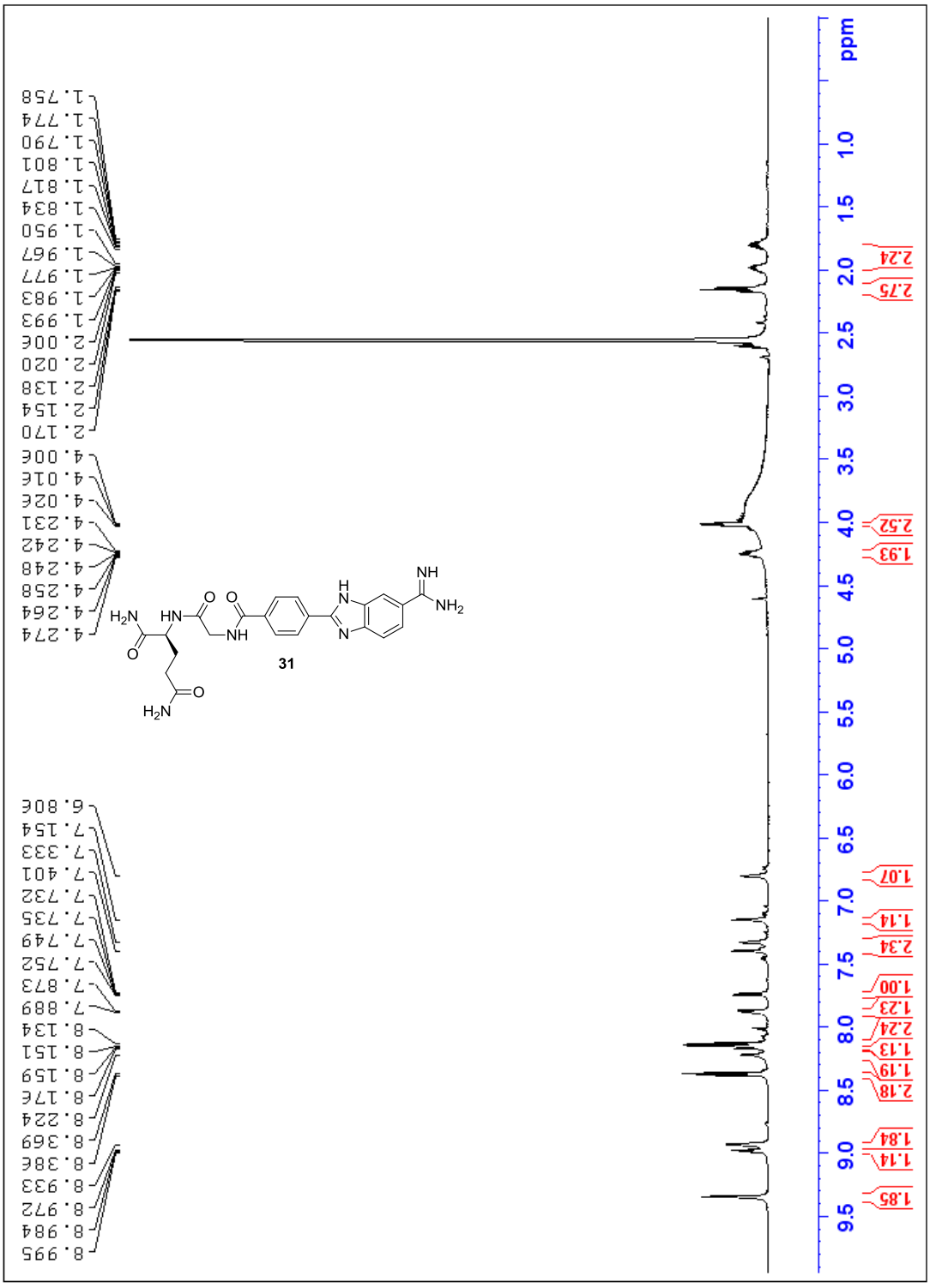
ppm
9.5
9.0
8.5
8.0
7.5
7.0
6.5
6.0
5.5
5.0
4.5
4.0
3.5
3.0
2.5
2.0
1.5
1.0
1.85
1.14
1.84
2.18
1.19
1.13
2.24
1.23
1.00
2.34
1.14
1.07
2.52
1.93
2.75
2.24
8.995
8.984
8.972
8.933
8.386
8.369
8.224
8.176
8.159
8.151
8.134
7.889
7.873
7.752
7.749
7.735
7.732
7.401
7.333
7.154
6.806
4.274
4.264
4.258
4.248
4.242
4.231
4.026
4.016
4.006
2.170
2.154
2.138
2.020
2.006
1.993
1.983
1.977
1.967
1.950
1.834
1.817
1.801
1.790
1.774
1.758
H2N
HN
O
O
NH
H
N
N
NH
NH2
O
H2N
O
31

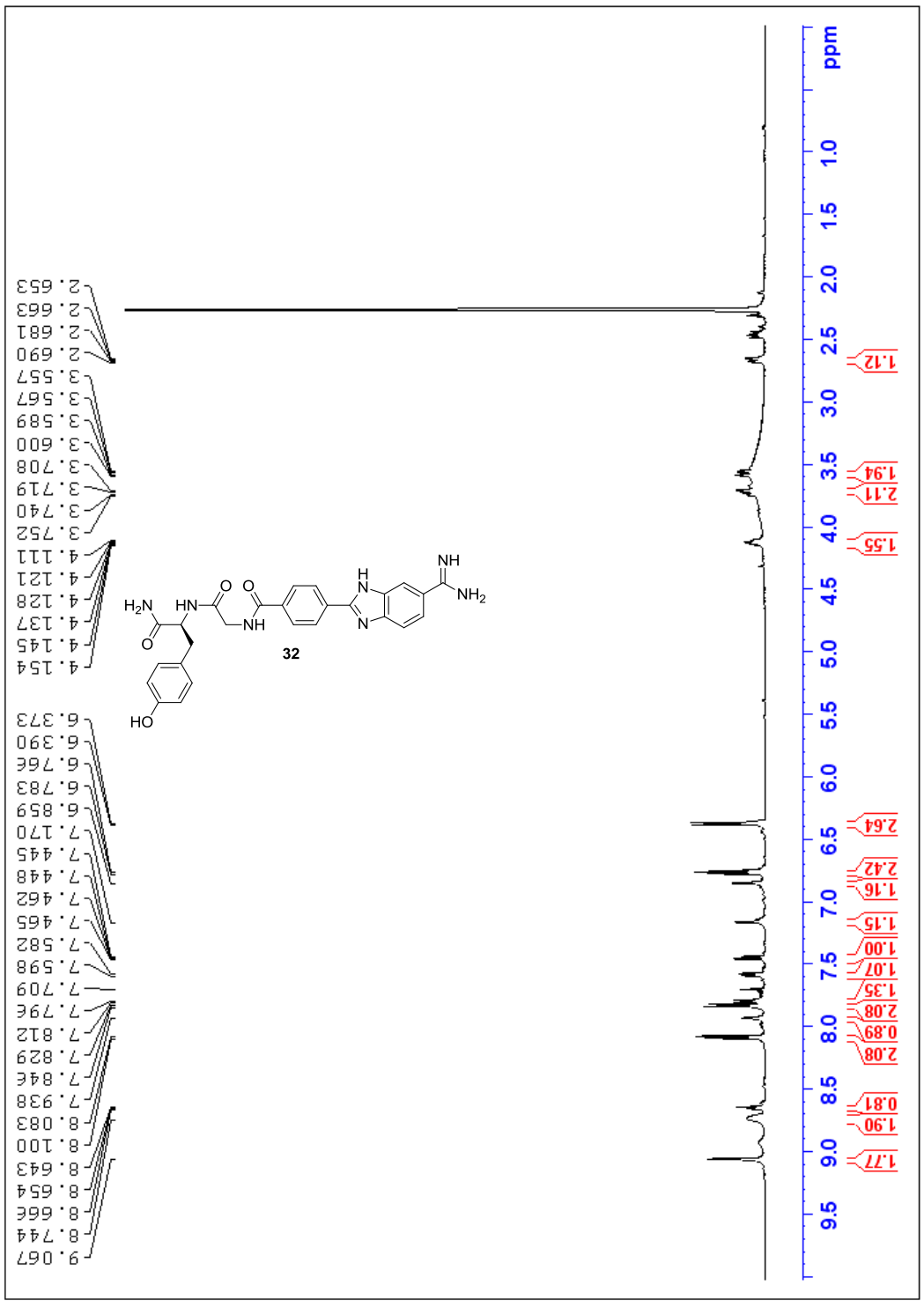
9.067
8.744
8.666
8.654
8.643
8.100
8.083
7.938
7.846
7.829
7.812
7.796
7.709
7.598
7.582
7.465
7.462
7.448
7.445
7.170
6.859
6.783
6.766
6.390
6.373
4.154
4.145
4.137
4.128
4.121
4.111
3.752
3.740
3.719
3.708
3.600
3.589
3.567
3.557
2.690
2.681
2.663
2.653
H2N
HN
O
O
HN
O
NH
H
N
N
NH
NH2
HO
32
ppm
9.5
9.0
8.5
8.0
7.5
7.0
6.5
6.0
5.5
5.0
4.5
4.0
3.5
3.0
2.5
2.0
1.5
1.0
1.77
1.90
0.81
2.08
0.89
2.08
1.35
1.07
1.00
1.15
1.16
2.42
2.64
1.55
2.11
1.94
1.12

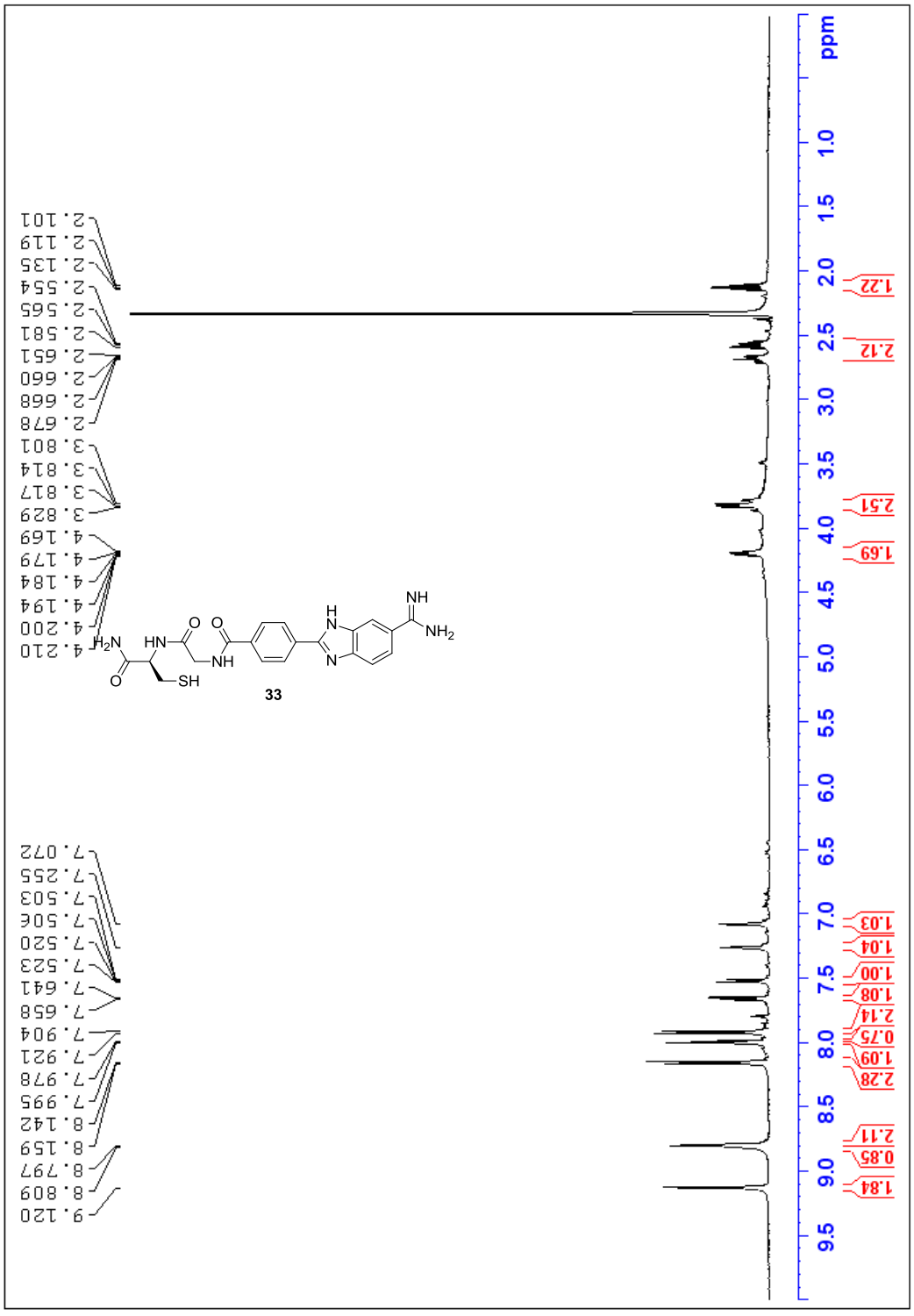
ppm
9.5
9.0
8.5
8.0
7.5
7.0
6.5
6.0
5.5
5.0
4.5
4.0
3.5
3.0
2.5
2.0
1.5
1.0
1.84
0.85
2.11
2.28
1.09
0.75
2.14
1.08
1.00
1.04
1.03
1.69
2.51
1.22
2.12
9.120
8.809
8.797
8.159
8.142
7.995
7.978
7.921
7.904
7.658
7.641
7.523
7.520
7.506
7.503
7.255
7.072
4.210
4.200
4.194
4.184
4.179
4.169
3.829
3.817
3.814
3.801
2.678
2.668
2.660
2.651
2.581
2.565
2.554
2.135
2.119
2.101
33

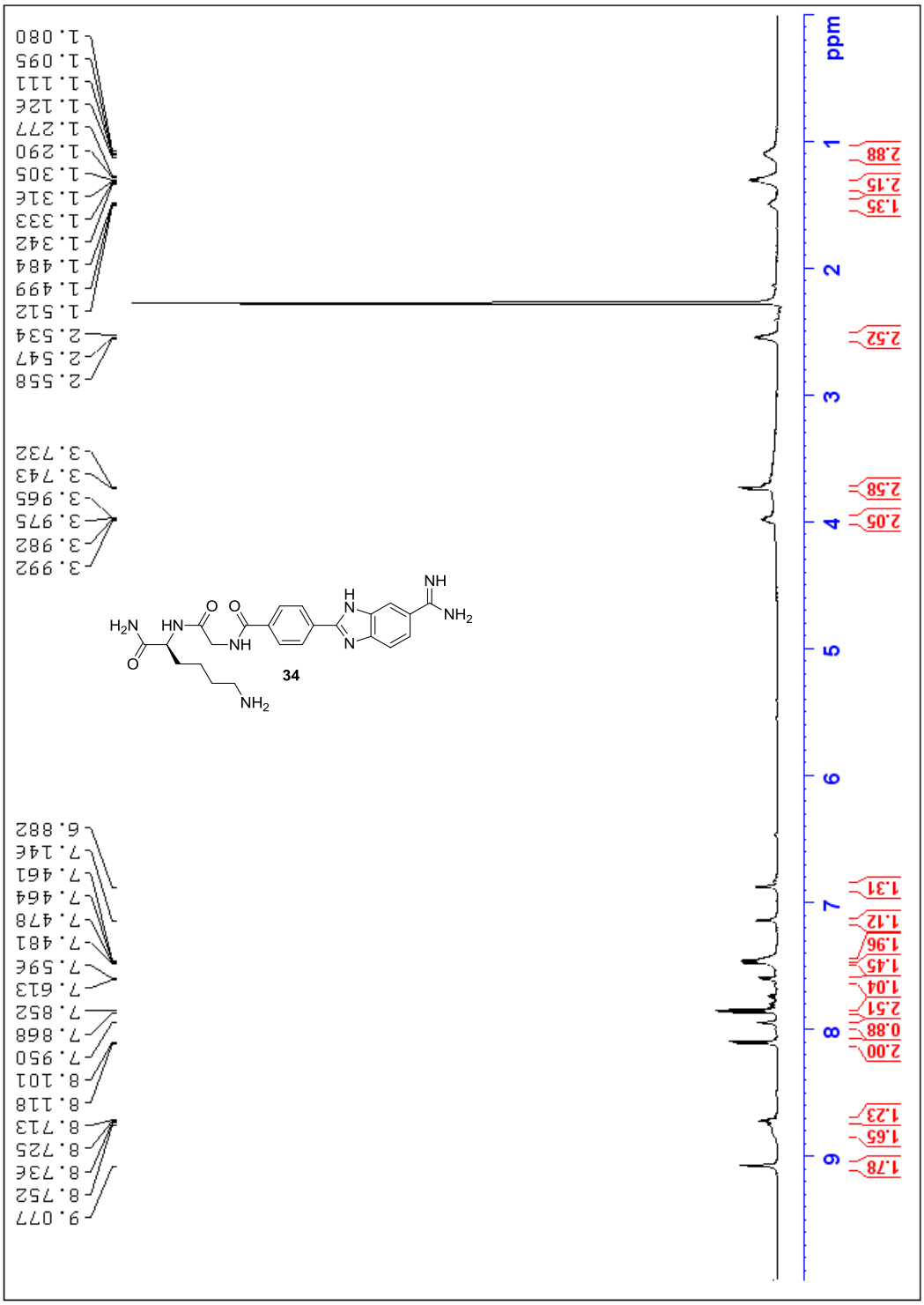
ppm
1
2
3
4
5
6
7
8
9
2.88
2.15
1.35
2.52
2.58
2.05
1.31
1.12
1.96
1.45
1.04
2.51
0.88
2.00
1.23
1.65
1.78
1.080
1.095
1.111
1.126
1.277
1.290
1.305
1.316
1.333
1.342
1.484
1.499
1.512
2.534
2.547
2.558
3.732
3.743
3.965
3.975
3.982
3.992
6.882
7.146
7.461
7.464
7.478
7.481
7.596
7.613
7.852
7.868
7.950
8.101
8.118
8.713
8.725
8.736
8.752
9.077
H2N
HN
O
O
NH
NH
H
N
N
NH
NH2
NH2
34

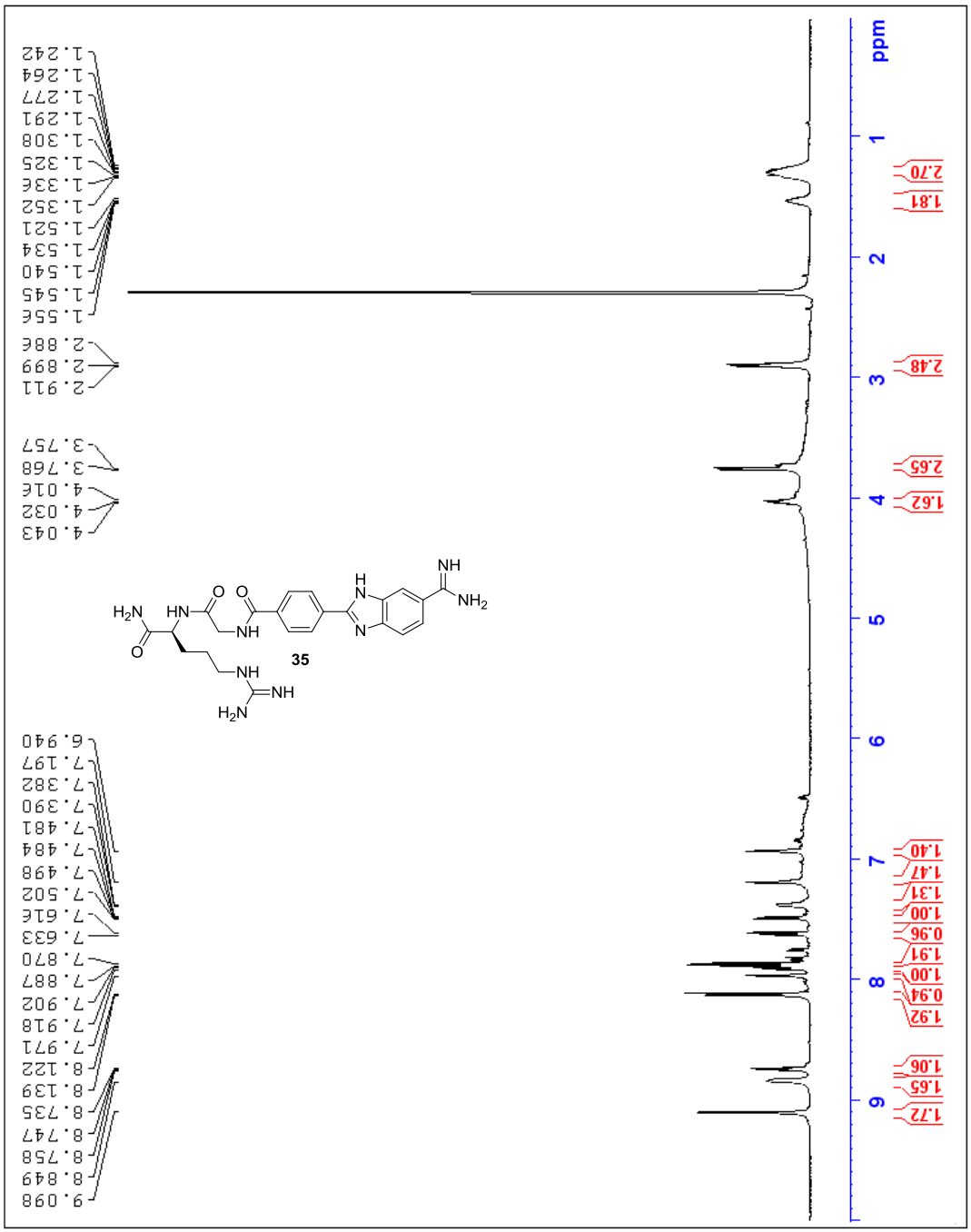
35
ppm

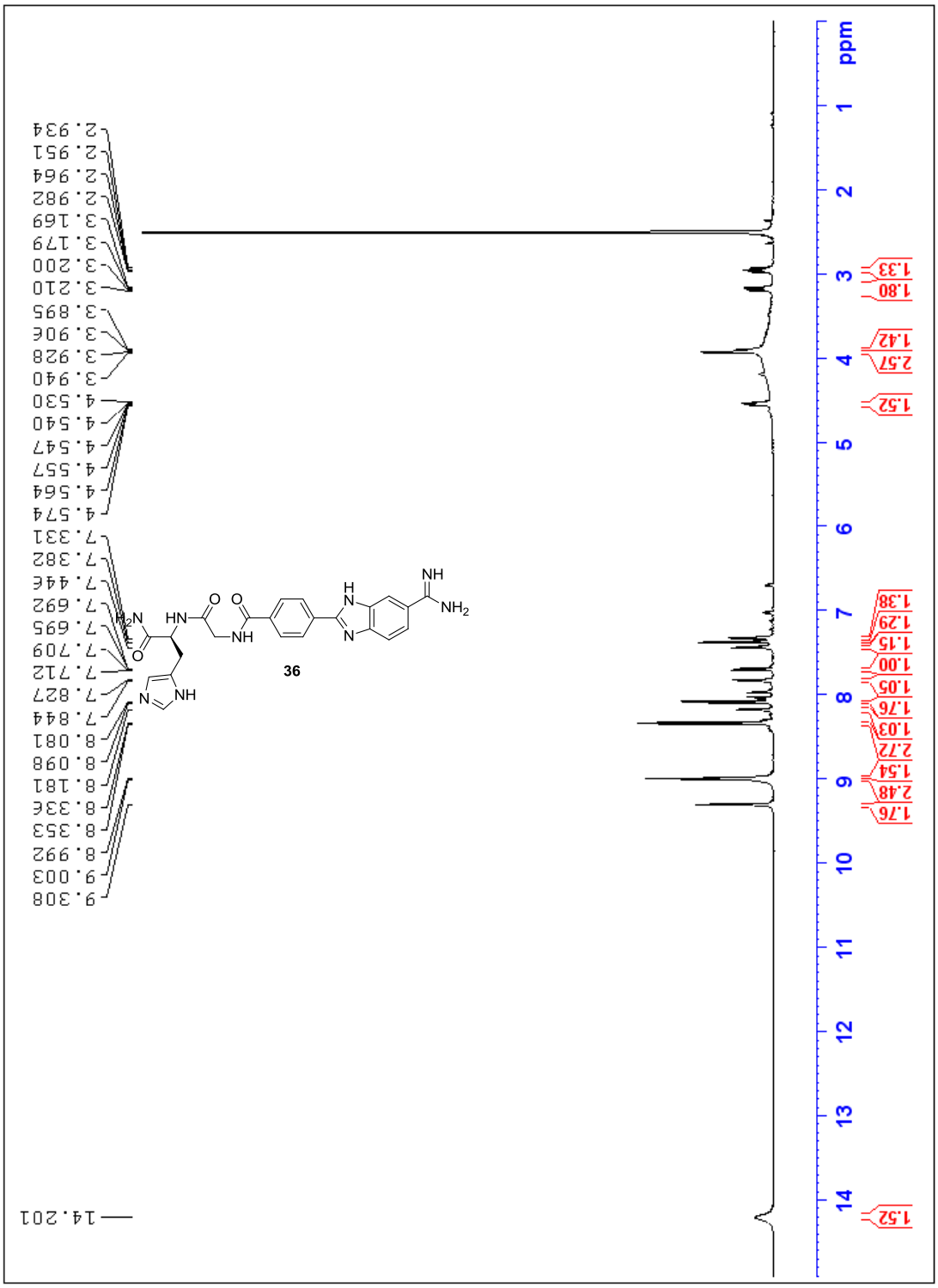
36

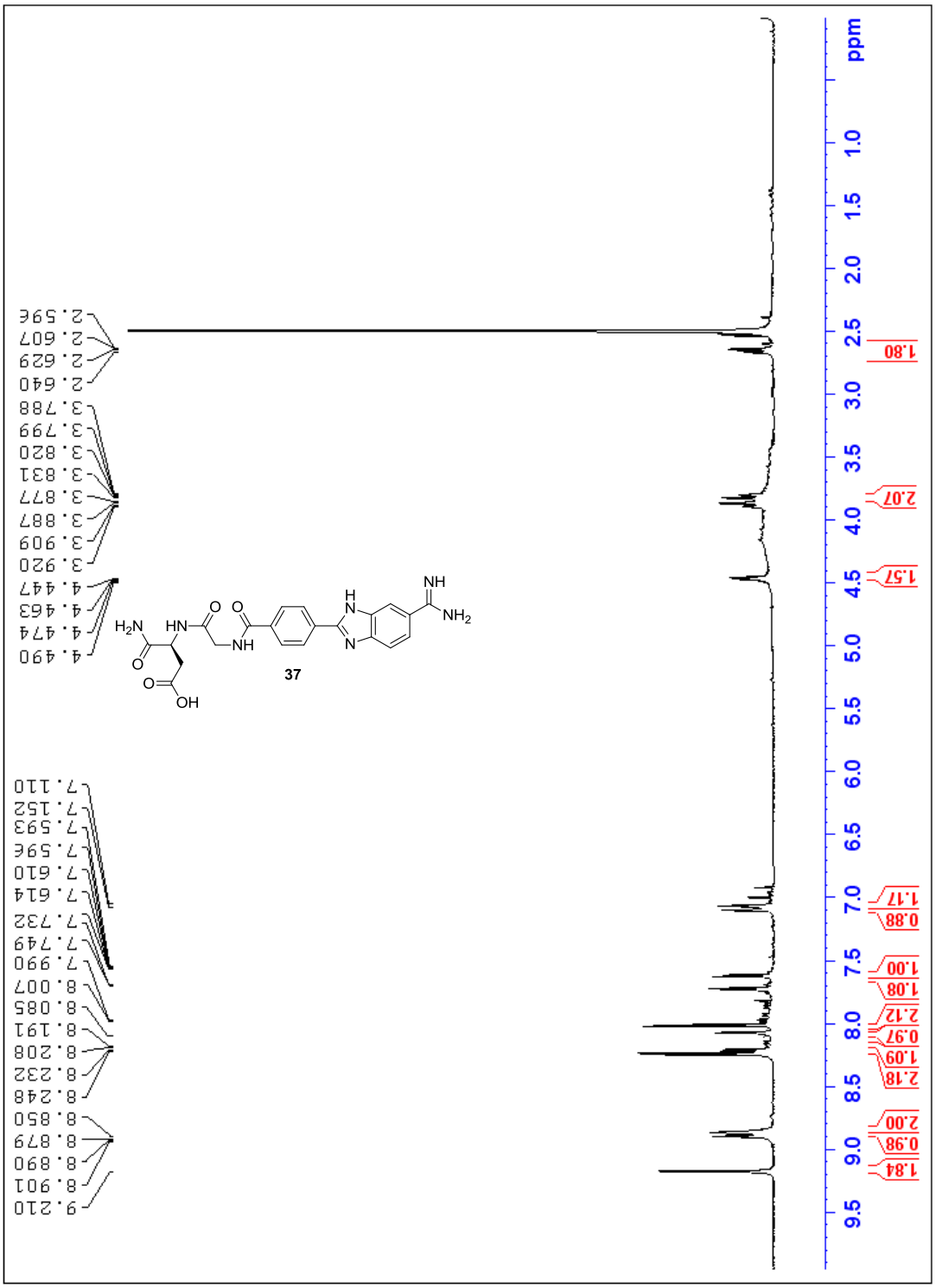
ppm
9.5
9.0
8.5
8.0
7.5
7.0
6.5
6.0
5.5
5.0
4.5
4.0
3.5
3.0
2.5
2.0
1.5
1.0
1.84
0.98
2.00
2.18
1.09
0.97
2.12
1.08
1.00
0.88
1.17
1.80
2.07
1.57
9.210
8.901
8.890
8.879
8.850
8.248
8.232
8.208
8.191
8.085
8.007
7.990
7.749
7.732
7.614
7.610
7.596
7.593
7.152
7.110
4.490
4.474
4.463
4.447
3.920
3.909
3.887
3.877
3.831
3.820
3.799
3.788
2.640
2.629
2.607
2.596
H2N
HN
O
O
NH
O
O
OH
H
N
N
NH
NH2
37

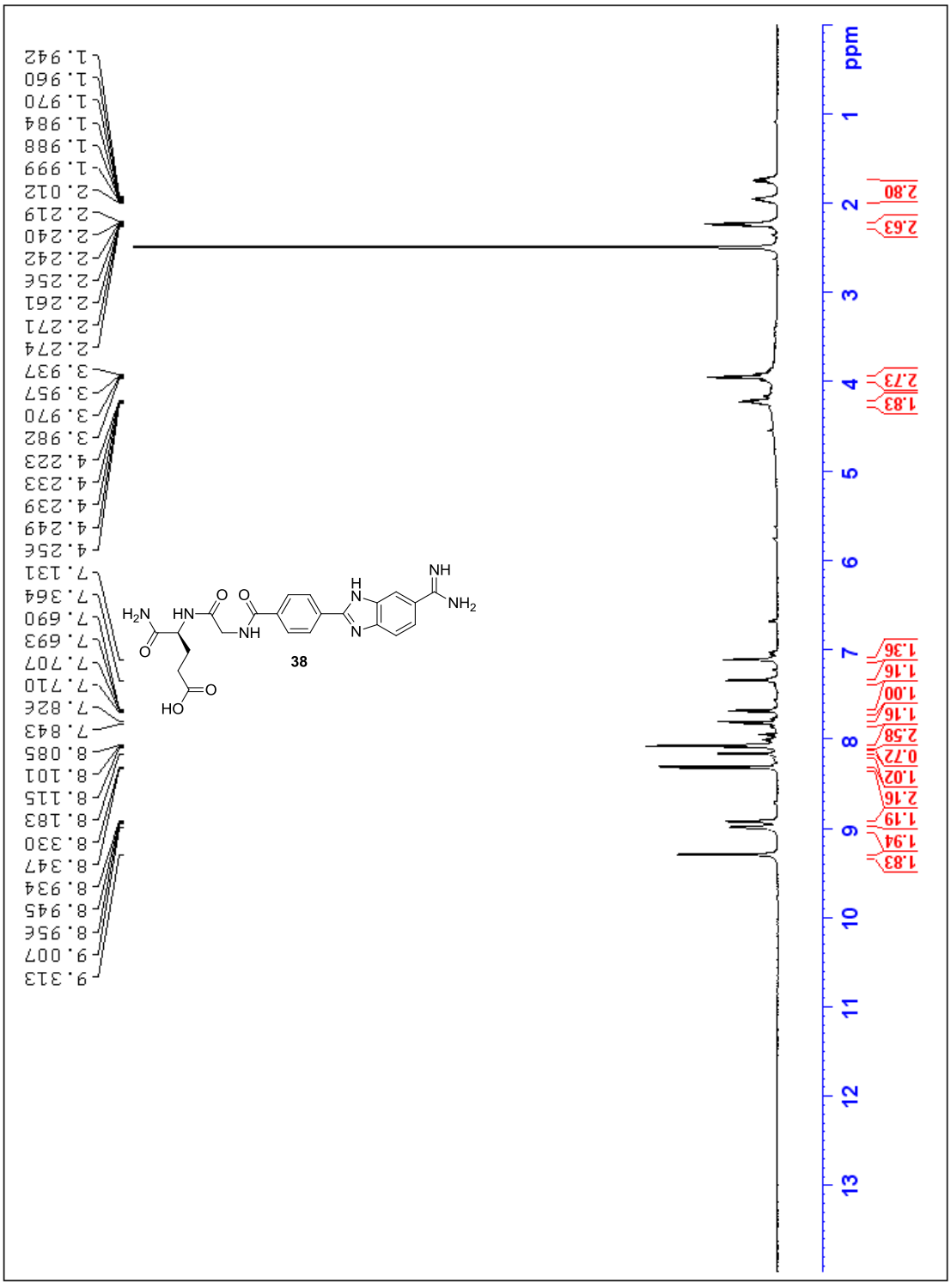
38
ppm
1 2 3 4 5 6 7 8 9 10 11 12 13
2.80
2.63
2.73
1.83
1.36
1.16
1.00
1.16
2.58
0.72
1.02
2.16
1.19
1.94
1.83
1.942
1.960
1.970
1.984
1.988
1.999
2.012
2.219
2.240
2.242
2.256
2.261
2.271
2.274
3.937
3.957
3.970
3.982
4.223
4.233
4.239
4.249
4.256
7.131
7.364
7.690
7.693
7.707
7.710
7.826
7.843
8.085
8.101
8.115
8.183
8.330
8.347
8.934
8.945
8.956
9.007
9.313

Appendix B. Mass Spectra

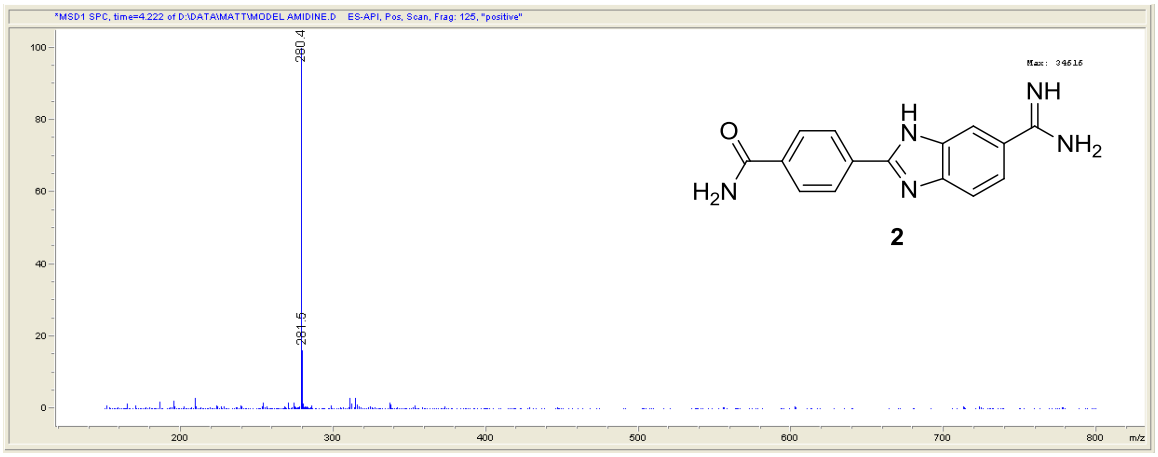

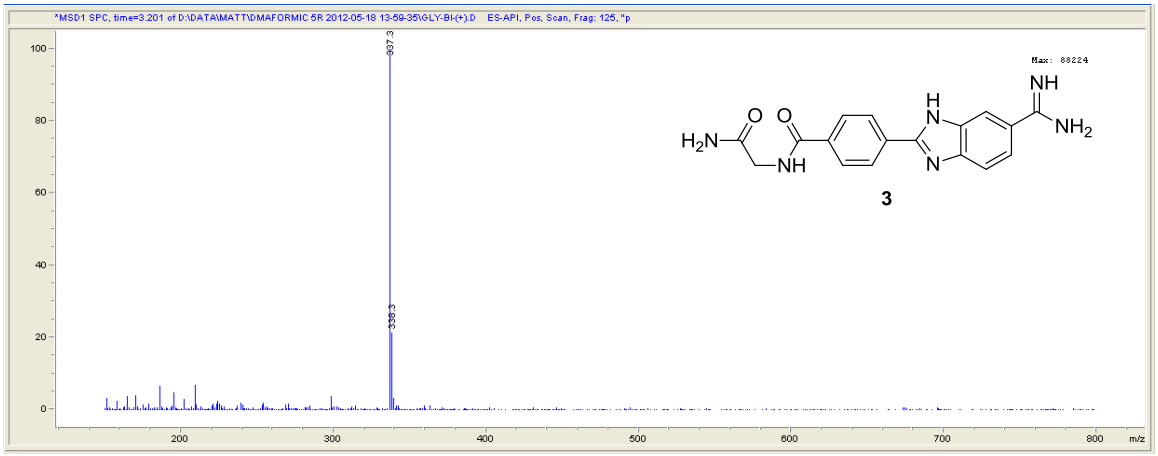

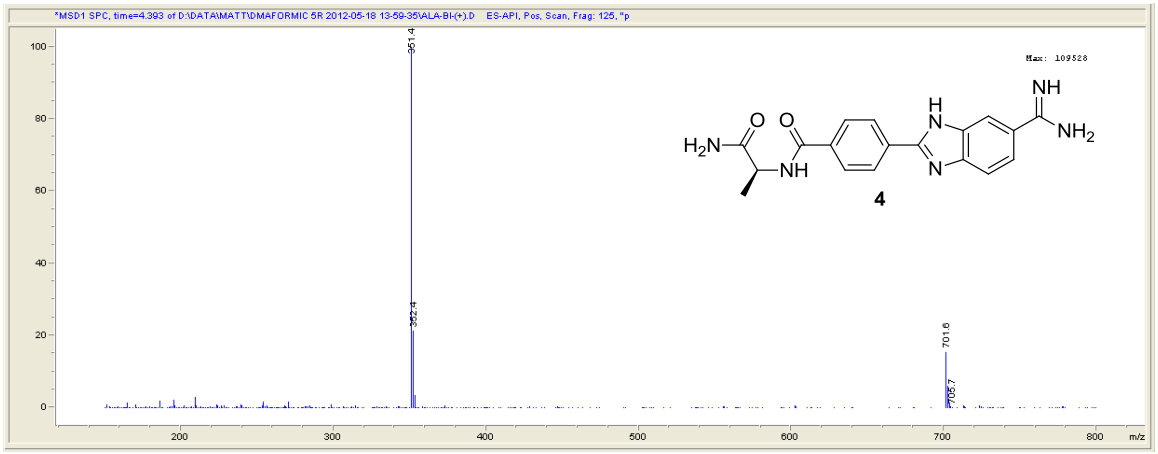

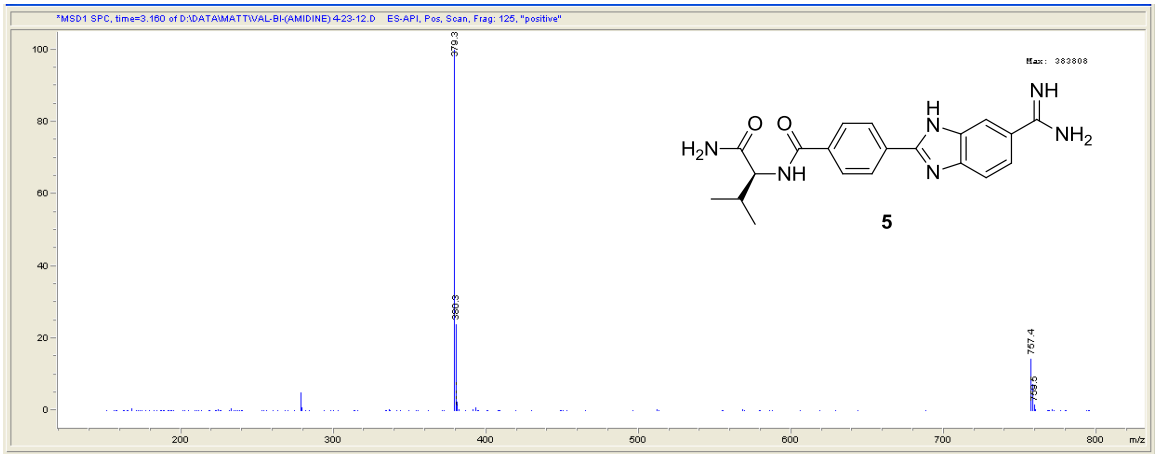
*MSD1 SPC, time=3.160 of D:\DATA\MATT\VAL-BI-(AMIDINE) 4-23-12.D ES-API, Pos, Scan, Frag: 125, "positive"
Max: 383808
379.3
380.3
757.4
NH
H
N
O
O
H2N
NH
N
NH2
5
m/z

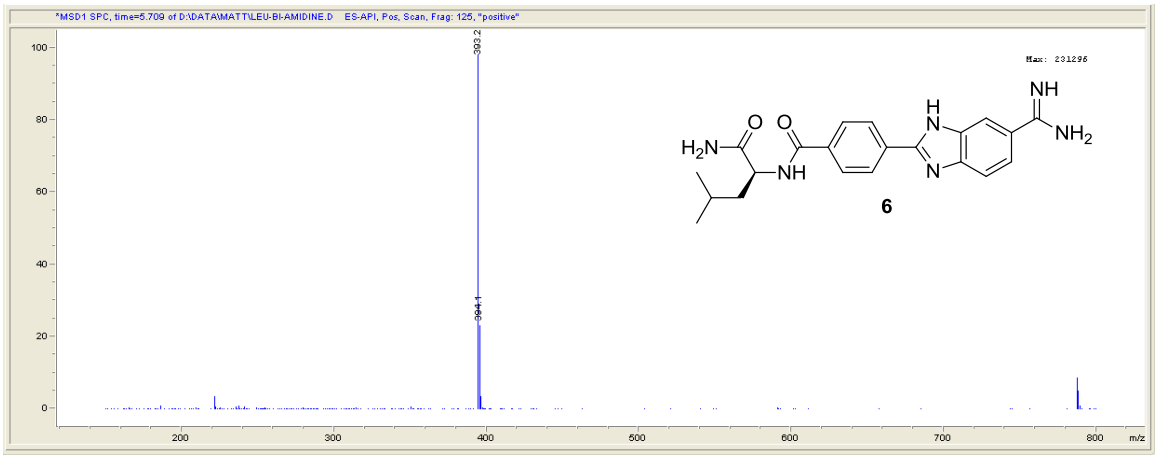
*MSD1 SPC, time=5.709 of D:\DATA\MATT\LEU-BI-AMIDINE.D ES-API, Pos, Scan, Frag: 125, "positive"
Max: 231296
393.2
394.1
NH
H
N
O
O
H2N
NH
N
NH2
6
m/z

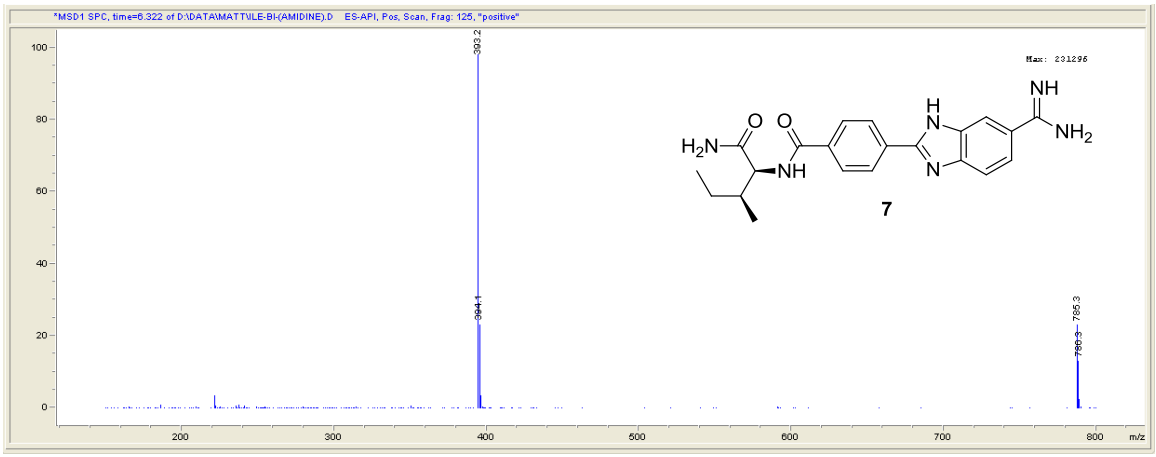
*MSD1 SPC, time=6.322 of D:\DATA\MATT\ILE-BI-(AMIDINE).D ES-API, Pos, Scan, Frag: 125, "positive"
Max: 231296
393.2
394.1
785.3
NH
H
N
O
O
H2N
NH
N
NH2
7
m/z

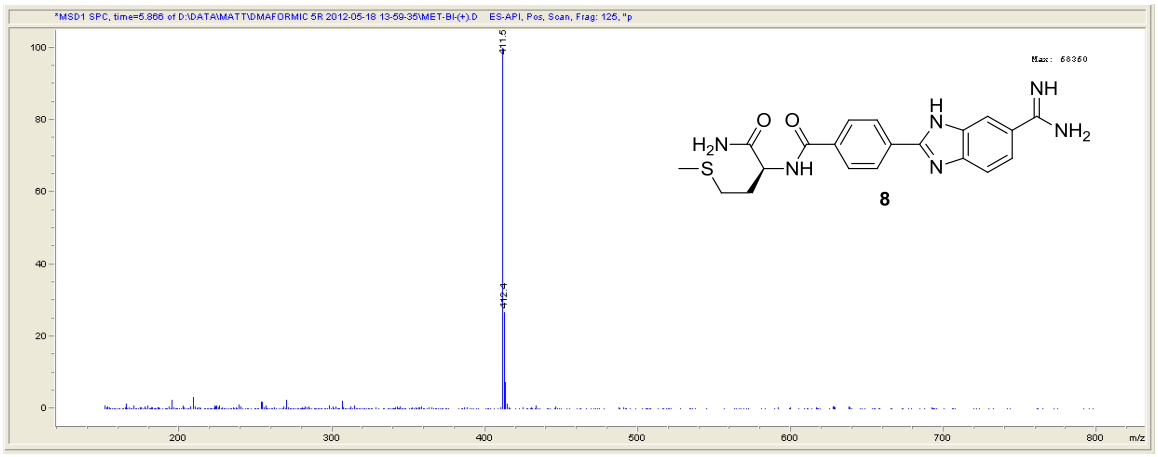
*MSD1 SPC, time=5.866 of D:\DATA\MATT\DMAFORMIC 5R 2012-05-18 13-59-35\MET-BI-(+).D ES-API, Pos, Scan, Frag: 125, "p
Max: 68360
411.5
412.4
8

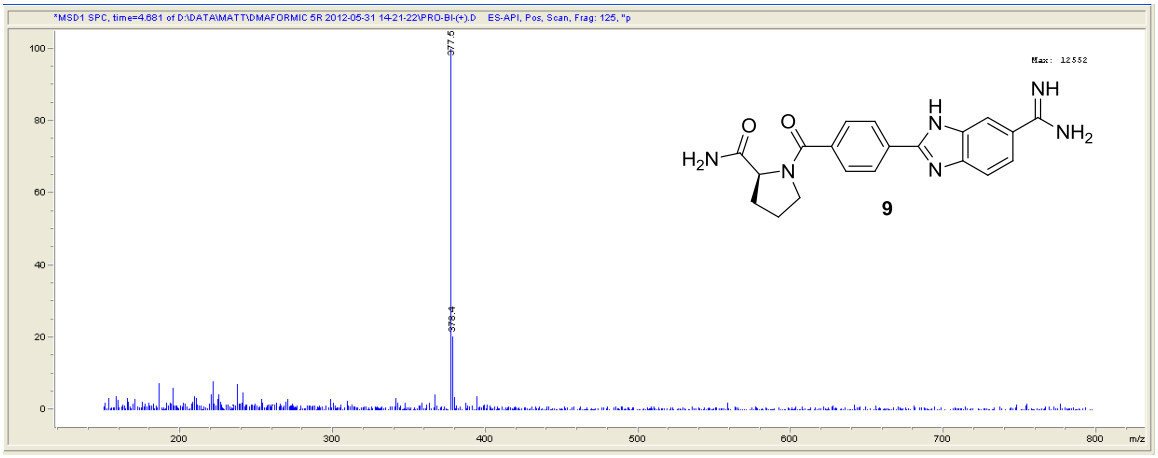
*MSD1 SPC, time=4.681 of D:\DATA\MATT\DMAFORMIC 5R 2012-05-31 14-21-22\PRO-BI-(+).D ES-API, Pos, Scan, Frag: 125, "p
Max: 12552
377.5
378.4
9

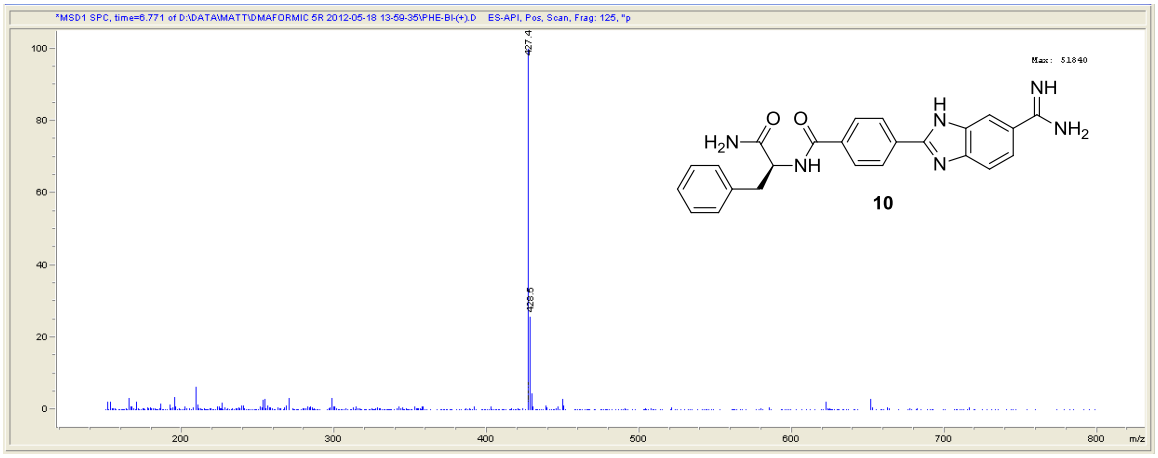
*MSD1 SPC, time=6.771 of D:\DATA\MATT\DMAFORMIC 5R 2012-05-18 13-59-35\PHE-BI-(+).D ES-API, Pos, Scan, Frag: 125, "p
Max: 51840
427.4
428.5
10

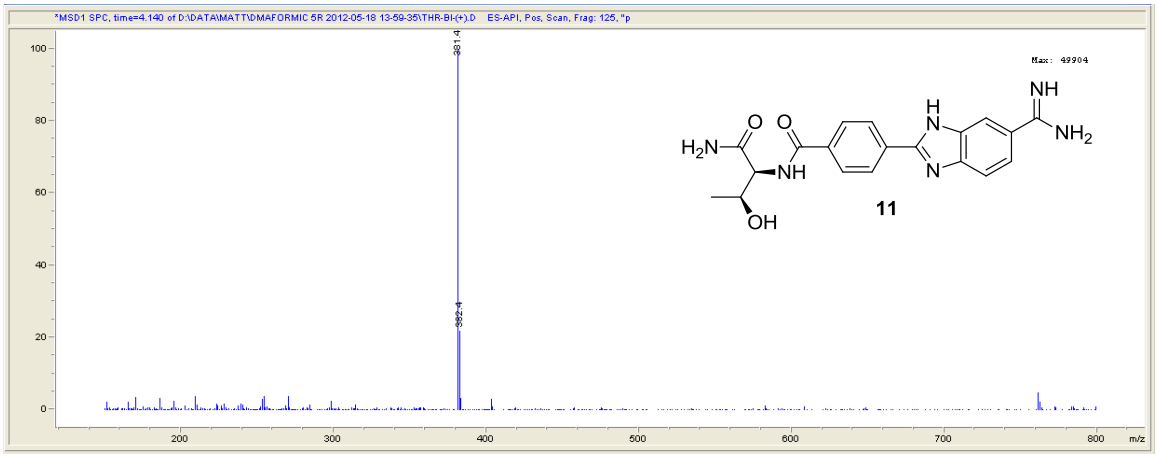
*MSD1 SPC, time=4.140 of D:\DATA\MATT\DMAFORMIC 5R 2012-05-18 13-59-35\THR-BI-(+).D ES-API, Pos, Scan, Frag: 125, "p
Max: 49904
381.4
382.4
11

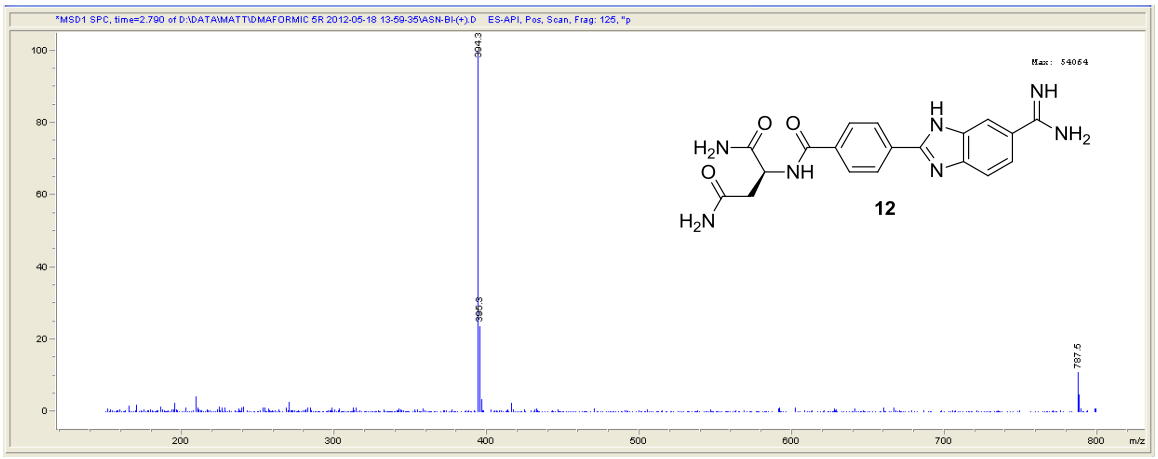
*MSD1 SPC, time=2.790 of D:\DATA\MATT\DMAFORMIC 5R 2012-05-18 13-59-35\ASN-BI-(+).D ES-API, Pos, Scan, Frag: 125, "p
Max: 54064
394.3
395.3
787.5
12

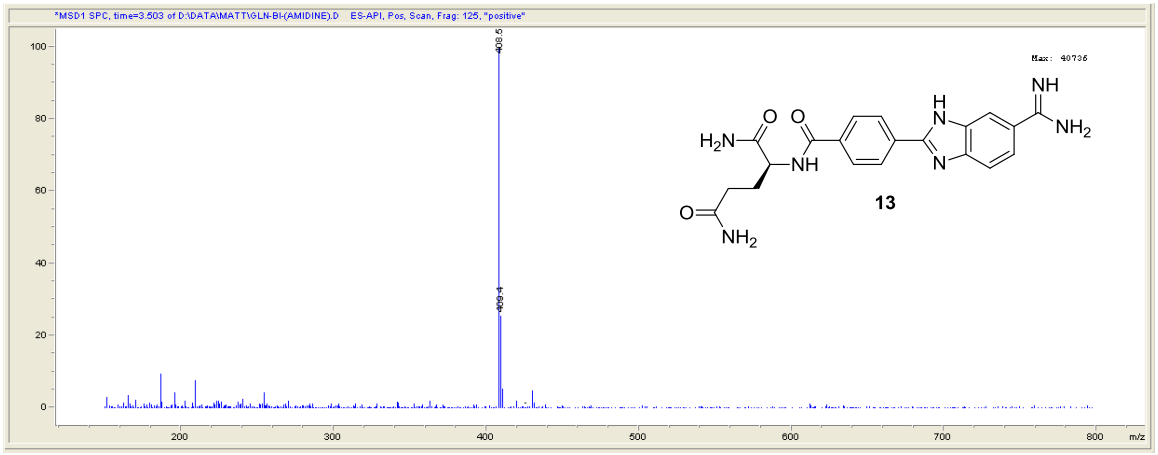
*MSD1 SPC, time=3.503 of D:\DATA\MATT\GLN-BI-(AMIDINE).D ES-API, Pos, Scan, Frag: 125, "positive"
Max: 40736
408.5
409.4
13

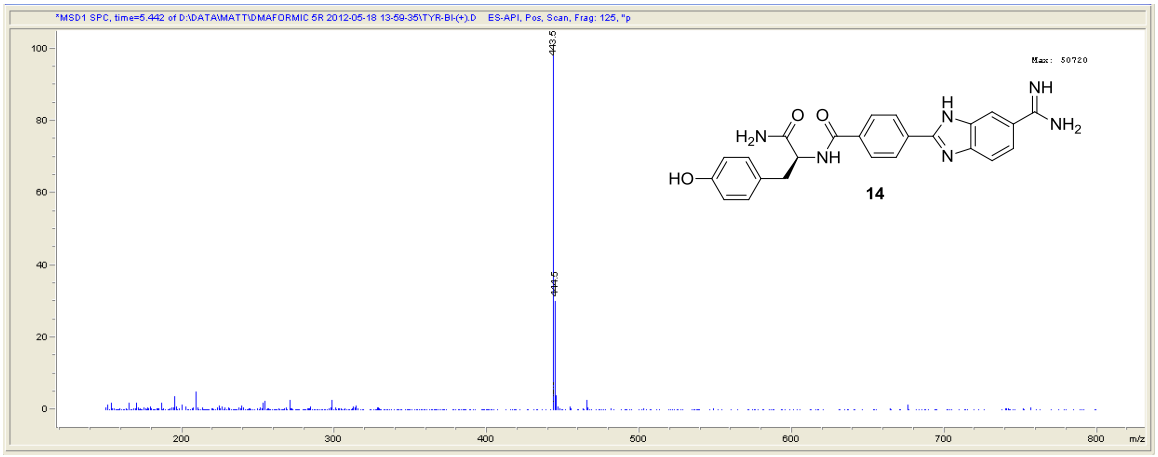
*MSD1 SPC, time=5.442 of D:\DATA\MATT\DMAFORMIC 5R 2012-05-18 13-59-35\TYR-BI-(+).D ES-API, Pos, Scan, Frag: 125, *p
443.5
444.5
Max: 50720
14
m/z

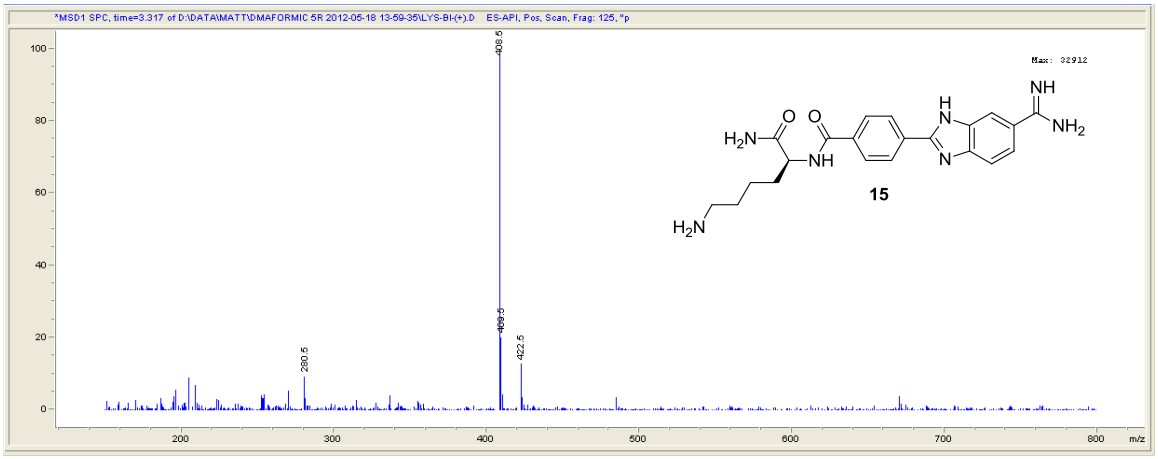
*MSD1 SPC, time=3.317 of D:\DATA\MATT\DMAFORMIC 5R 2012-05-18 13-59-35\LYS-BI-(+).D ES-API, Pos, Scan, Frag: 125, *p
408.5
409.5
422.5
280.5
Max: 32912
15
m/z

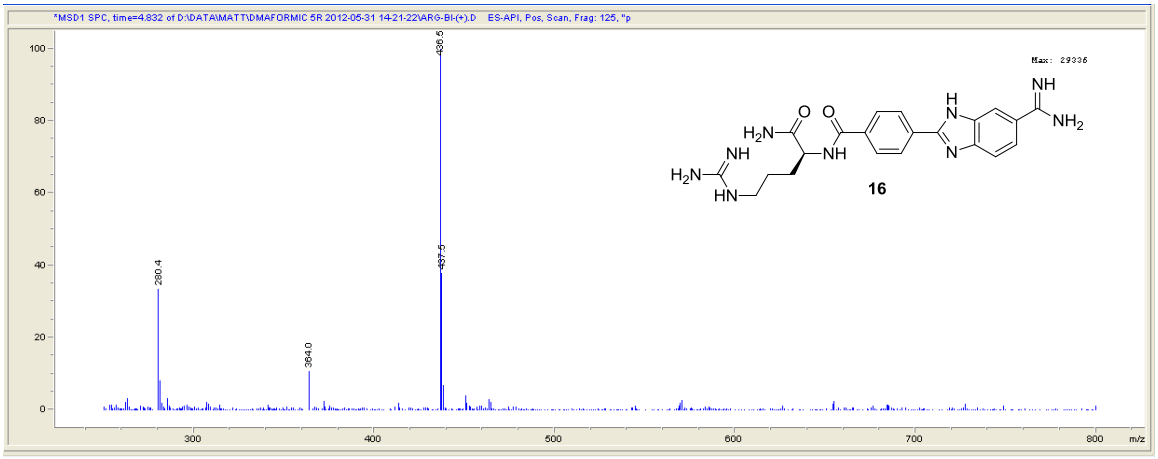
*MSD1 SPC, time=4.832 of D:\DATA\MATT\DMAFORMIC 5R 2012-05-31 14-21-22\ARG-BI-(+).D ES-API, Pos, Scan, Frag: 125, *p
436.5
437.5
280.4
364.0
Max: 29336
16
m/z

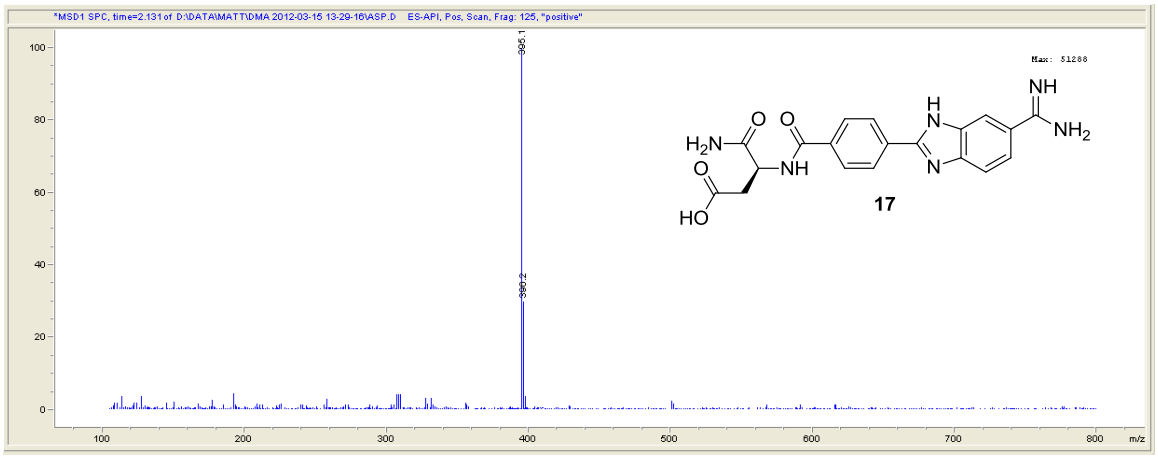
*MSD1 SPC, time=2.131 of D:\DATA\MATT\DMA 2012-03-15 13-29-16\ASP.D ES-API, Pos, Scan, Frag: 125, "positive"
395.1
397.2
Max: 51288
17

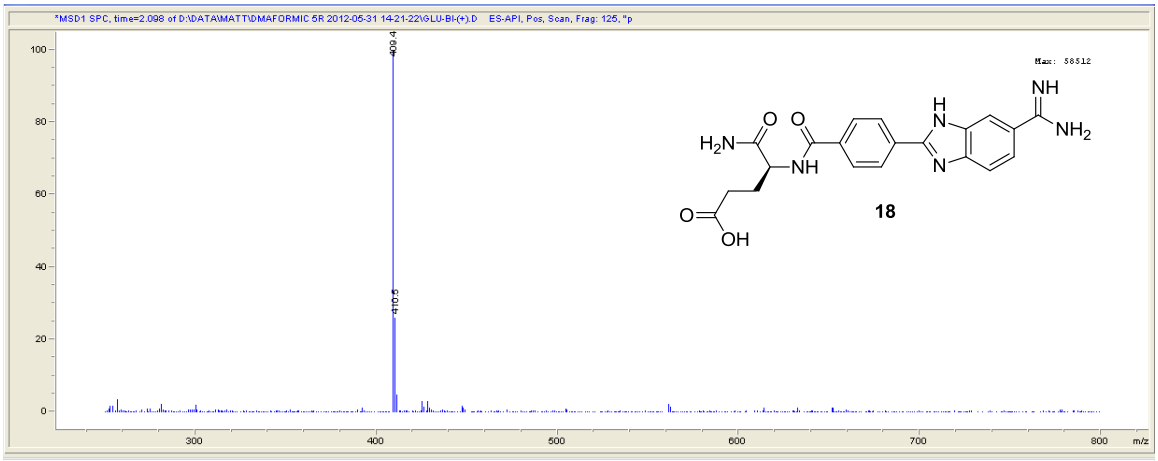
*MSD1 SPC, time=2.098 of D:\DATA\MATT\DMAFORMIC 5R 2012-05-31 14-21-22\GLU-BI-(+).D ES-API, Pos, Scan, Frag: 125, "p
409.4
410.5
Max: 58512
18

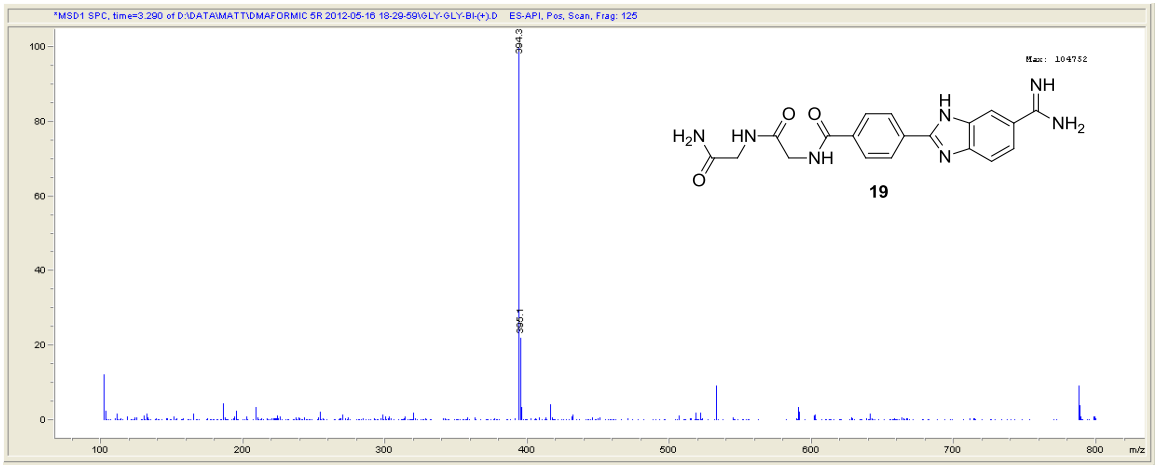
*MSD1 SPC, time=3.290 of D:\DATA\MATT\DMAFORMIC 5R 2012-05-16 18-29-59\GLY-GLY-BI-(+).D ES-API, Pos, Scan, Frag: 125
394.3
395.1
Max: 104752
19

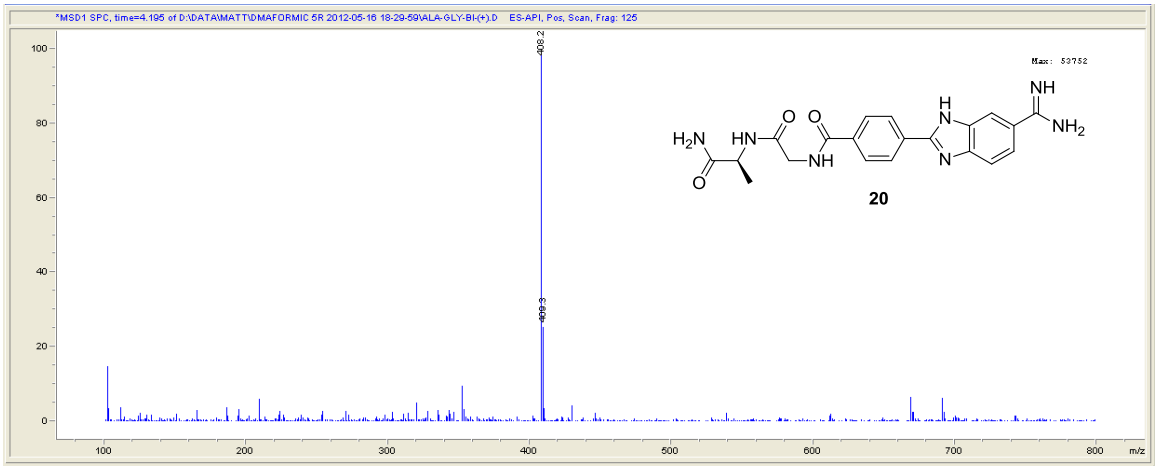
*MSD1 SPC, time=4.195 of D:\DATA\MATT\DMAFORMIC 5R 2012-05-16 18-29-59\ALA-GLY-BI-(+).D ES-API, Pos, Scan, Frag: 125
Max: 53752
408.2
409.3
m/z
20

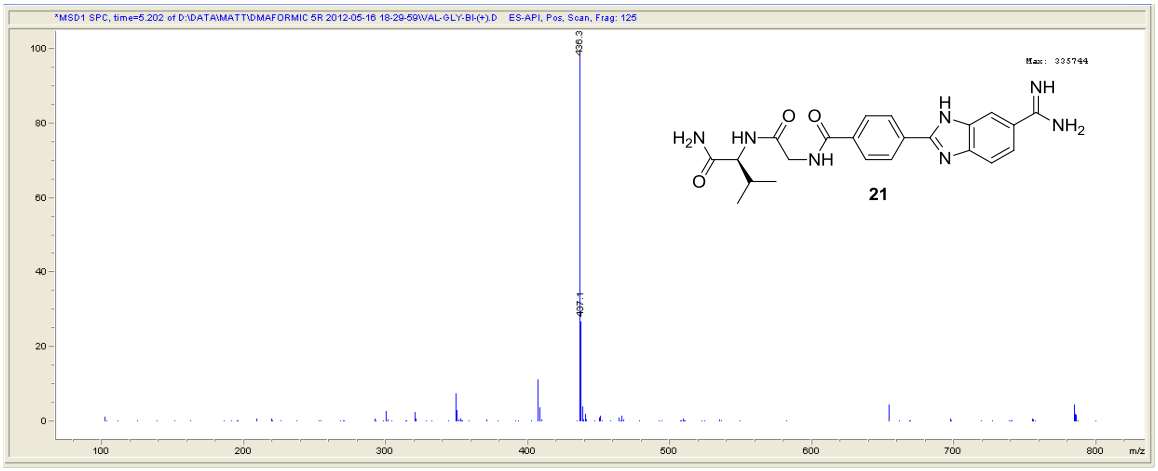
*MSD1 SPC, time=5.202 of D:\DATA\MATT\DMAFORMIC 5R 2012-05-16 18-29-59\VAL-GLY-BI-(+).D ES-API, Pos, Scan, Frag: 125
Max: 335744
436.3
437.1
m/z
21

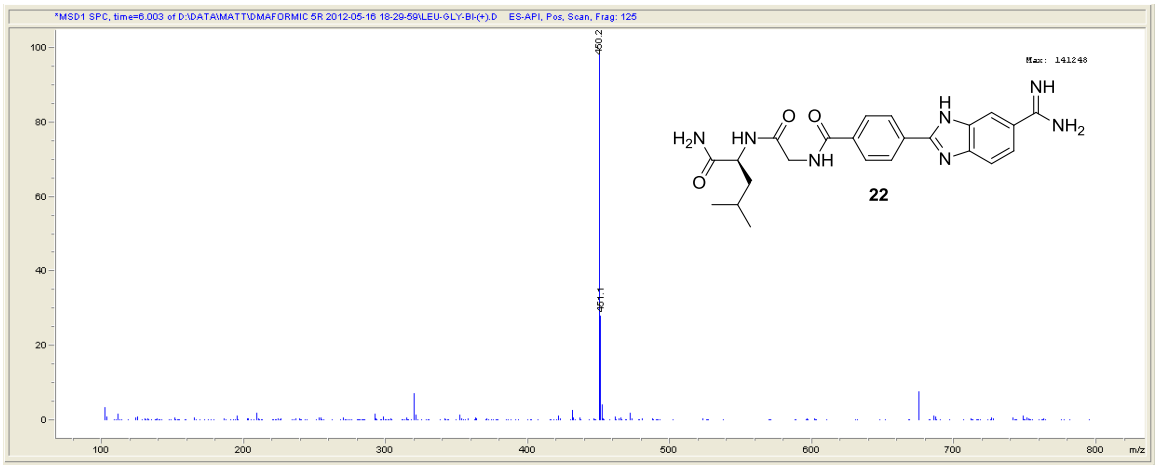
*MSD1 SPC, time=6.003 of D:\DATA\MATT\DMAFORMIC 5R 2012-05-16 18-29-59\LEU-GLY-BI-(+).D ES-API, Pos, Scan, Frag: 125
Max: 141248
450.2
451.1
m/z
22

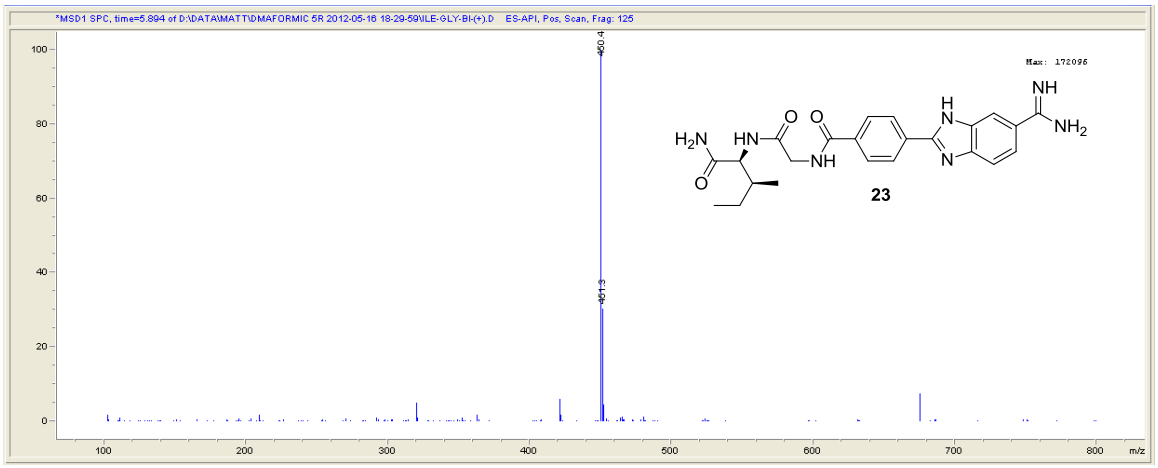
*MSD1 SPC, time=5.894 of D:\DATA\MATT\DMAFORMIC 5R 2012-05-16 18-29-59\ILE-GLY-BI-(+).D ES-API, Pos, Scan, Frag: 125
Max: 172096
460.4
461.3
23
m/z

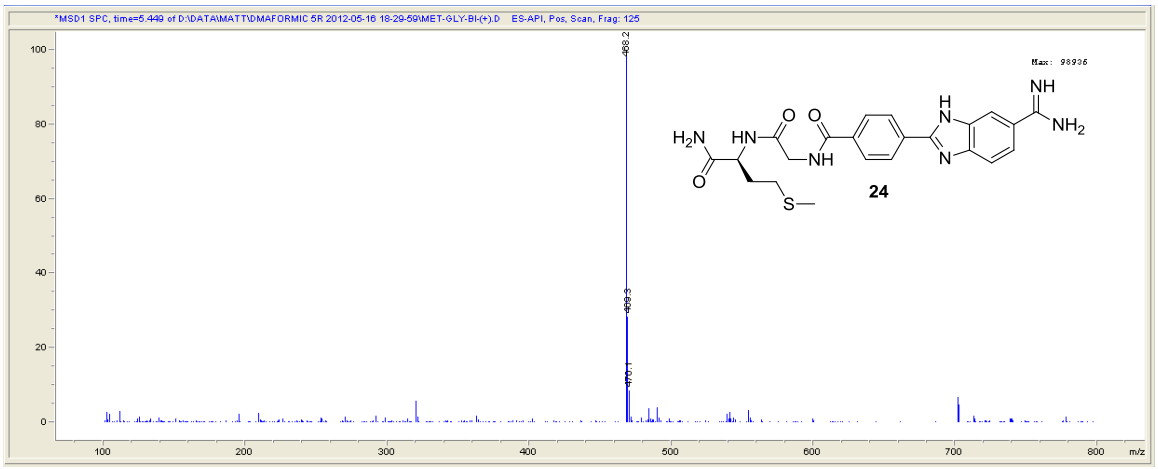
*MSD1 SPC, time=5.449 of D:\DATA\MATT\DMAFORMIC 5R 2012-05-16 18-29-59\MET-GLY-BI-(+).D ES-API, Pos, Scan, Frag: 125
Max: 98936
468.2
469.3
470.1
24
m/z

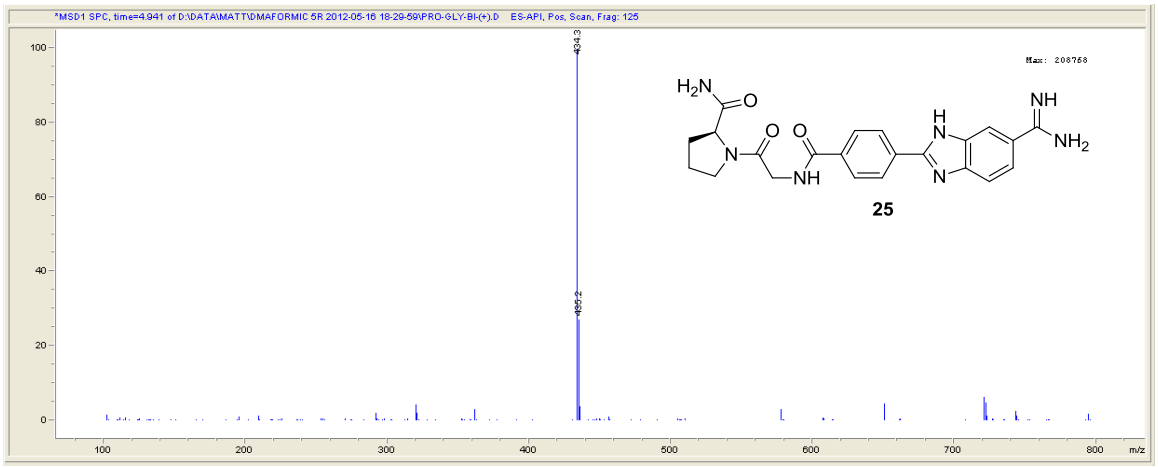
*MSD1 SPC, time=4.941 of D:\DATA\MATT\DMAFORMIC 5R 2012-05-16 18-29-59\PRO-GLY-BI-(+).D ES-API, Pos, Scan, Frag: 125
Max: 208768
434.3
435.2
25
m/z

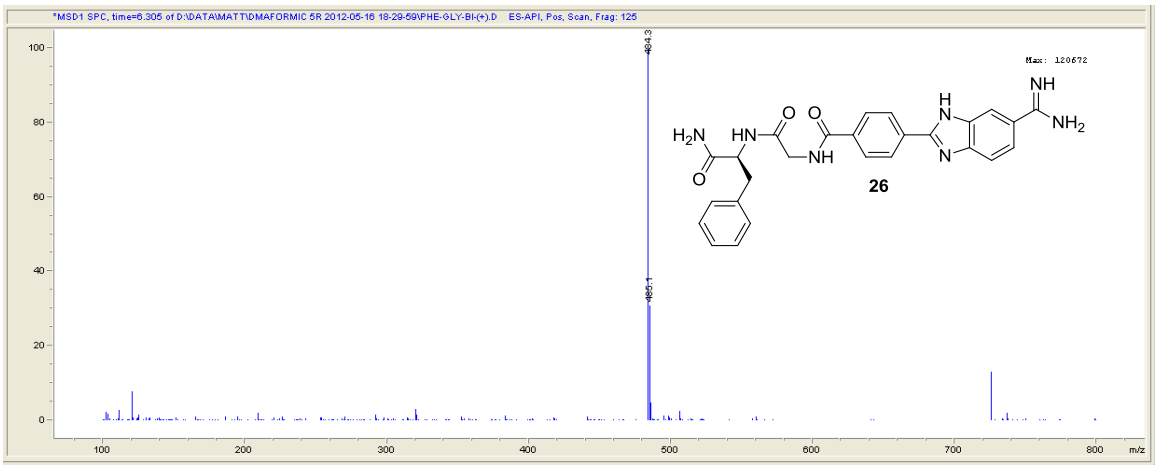
*MSD1 SPC, time=6.305 of D:\DATA\MATT\DMAFORMIC 5R 2012-05-16 18-29-59\PHE-GLY-BI-(+).D ES-API, Pos, Scan, Frag: 125
Max: 120672
484.3
485.1
26
m/z

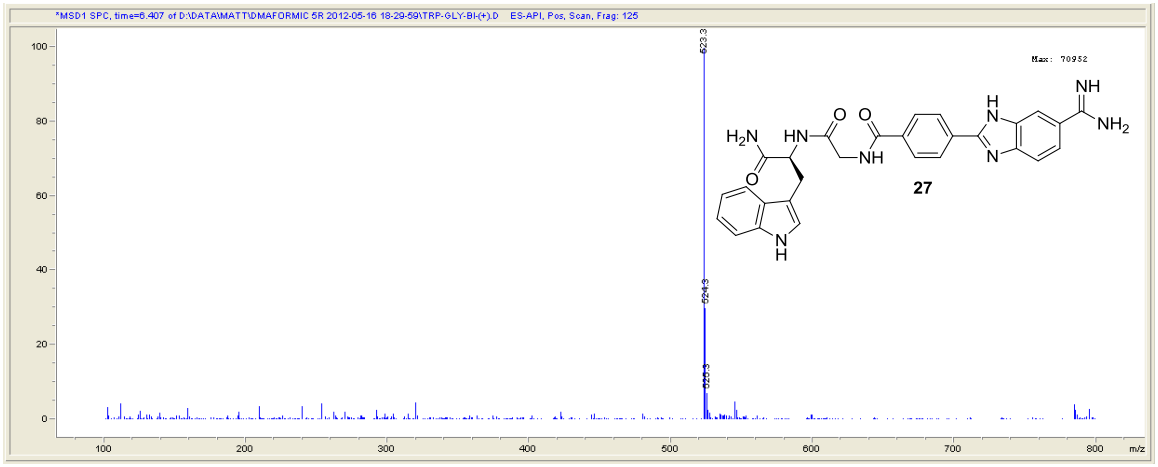
*MSD1 SPC, time=6.407 of D:\DATA\MATT\DMAFORMIC 5R 2012-05-16 18-29-59\TRP-GLY-BI-(+).D ES-API, Pos, Scan, Frag: 125
Max: 70952
523.3
524.3
27
m/z

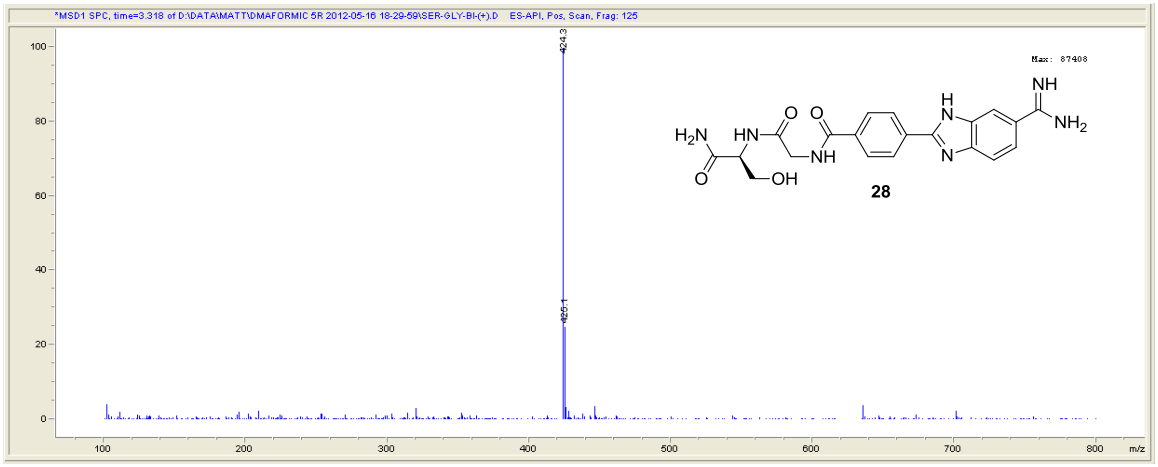
*MSD1 SPC, time=3.318 of D:\DATA\MATT\DMAFORMIC 5R 2012-05-16 18-29-59\SER-GLY-BI-(+).D ES-API, Pos, Scan, Frag: 125
Max: 87408
424.3
425.1
28
m/z

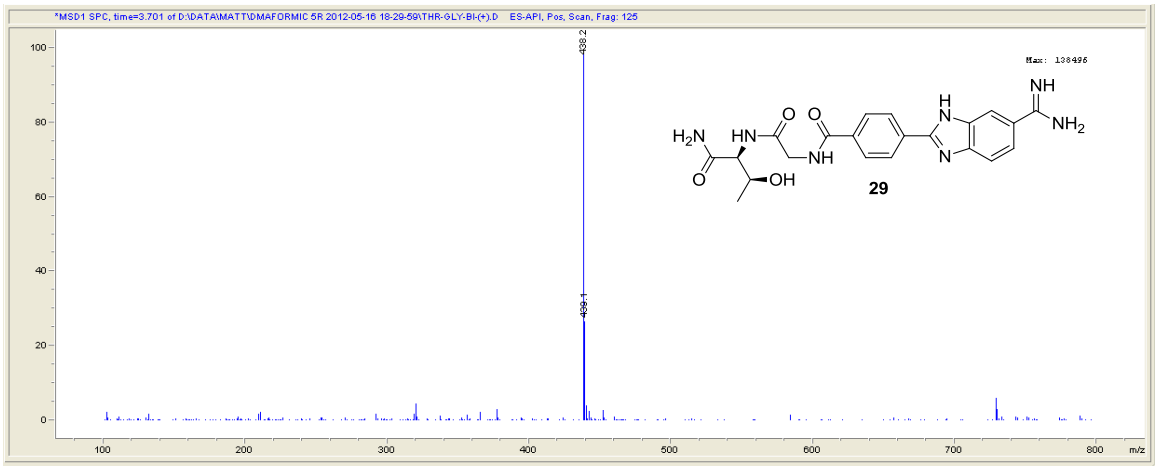
*MSD1 SPC, time=3.701 of D:\DATA\MATT\DMAFORMIC 5R 2012-05-16 18-29-59\THR-GLY-BI-(+).D ES-API, Pos, Scan, Frag: 125
438.2
439.1
Max: 138496
29

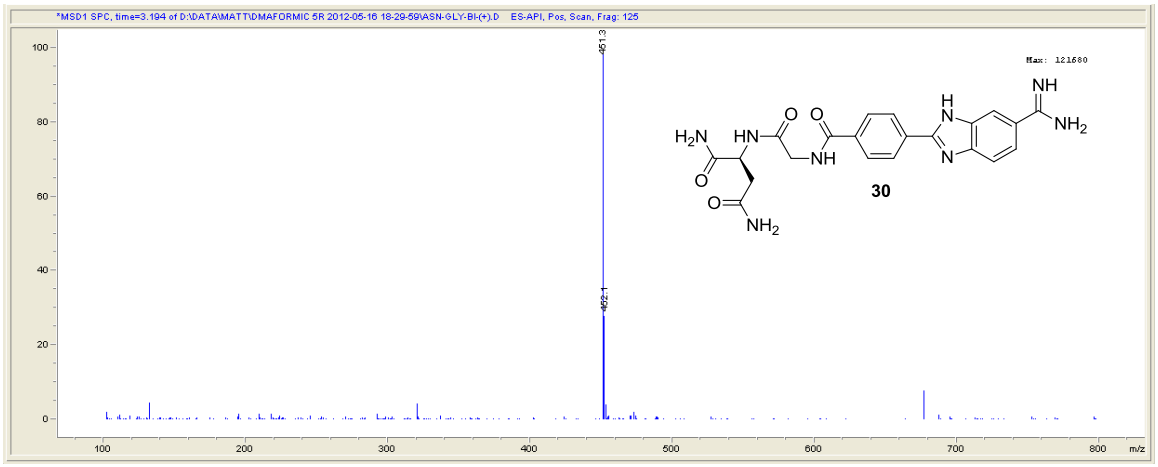
*MSD1 SPC, time=3.194 of D:\DATA\MATT\DMAFORMIC 5R 2012-05-16 18-29-59\ASN-GLY-BI-(+).D ES-API, Pos, Scan, Frag: 125
451.3
452.1
Max: 121680
30

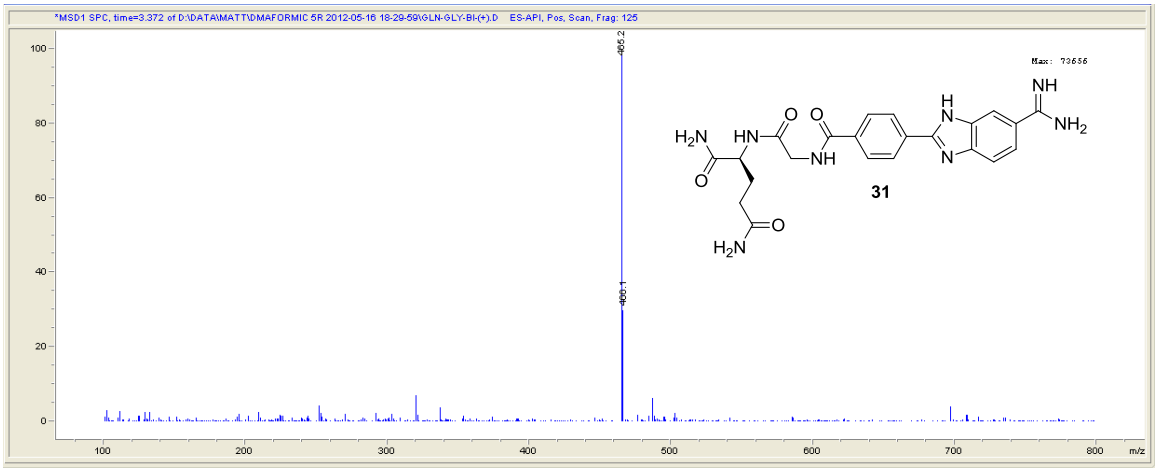
*MSD1 SPC, time=3.372 of D:\DATA\MATT\DMAFORMIC 5R 2012-05-16 18-29-59\GLN-GLY-BI-(+).D ES-API, Pos, Scan, Frag: 125
465.2
466.1
Max: 73656
31

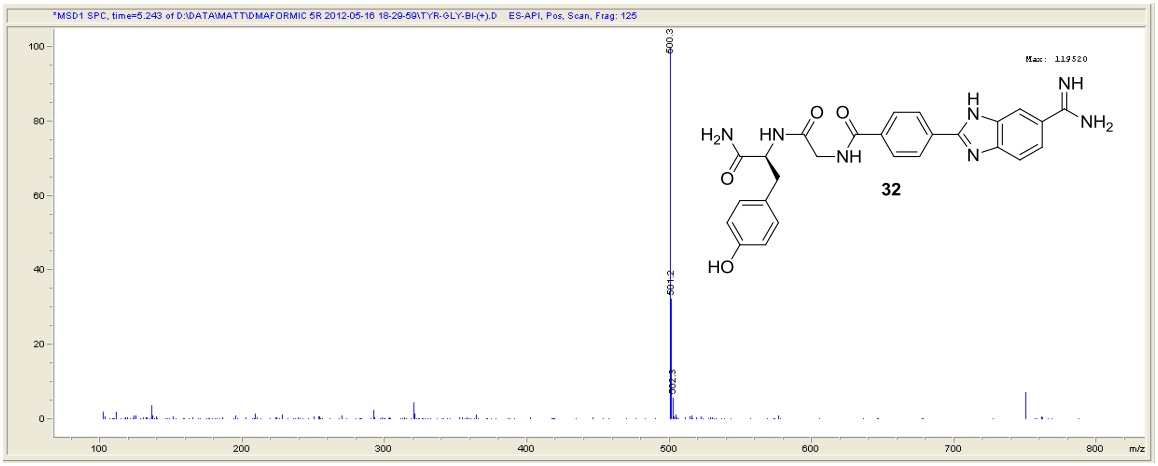
*MSD1 SPC, time=5.243 of D:\DATA\MATT\DMAFORMIC 5R 2012-05-16 18-29-59\TYR-GLY-BI-(+).D ES-API, Pos, Scan, Frag: 125
Max: 119520
600.3
591.2
602.3
m/z
32

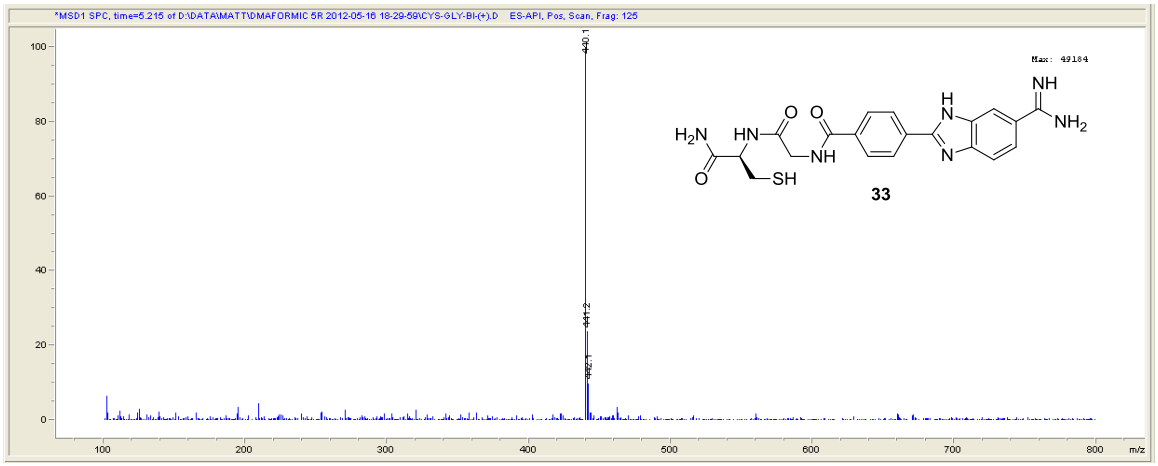
*MSD1 SPC, time=5.215 of D:\DATA\MATT\DMAFORMIC 5R 2012-05-16 18-29-59\CYS-GLY-BI-(+).D ES-API, Pos, Scan, Frag: 125
Max: 49184
440.1
441.2
442.1
m/z
33

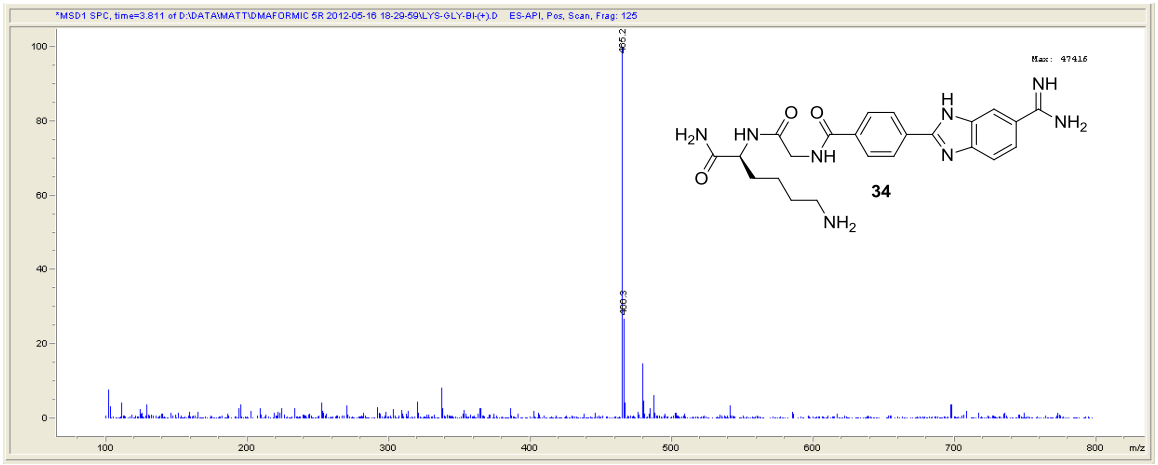
*MSD1 SPC, time=3.811 of D:\DATA\MATT\DMAFORMIC 5R 2012-05-16 18-29-59\LYS-GLY-BI-(+).D ES-API, Pos, Scan, Frag: 125
Max: 47416
465.2
466.3
m/z
34

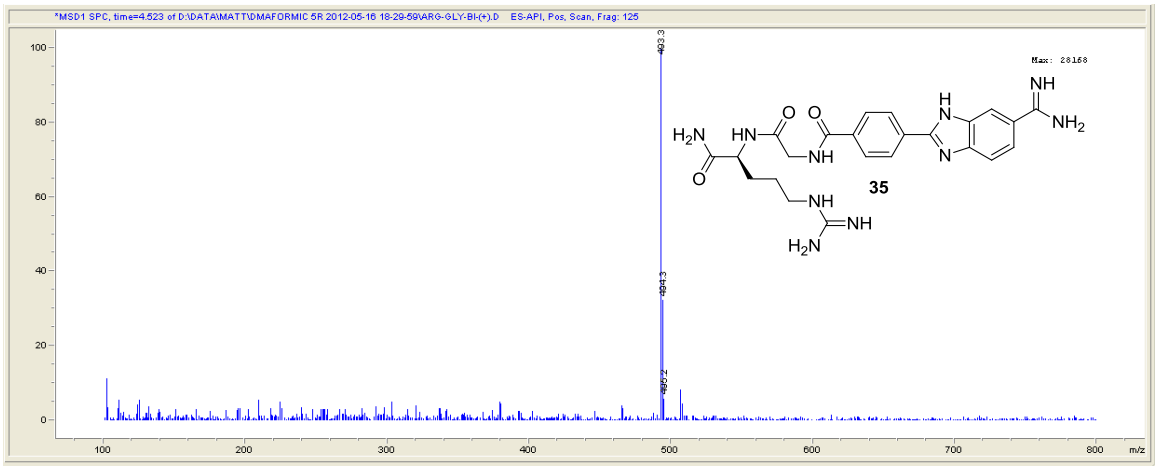
*MSD1 SPC, time=4.523 of D:\DATA\MATT\DMAFORMIC 5R 2012-05-16 18-29-59\ARG-GLY-BI-(+).D ES-API, Pos, Scan, Frag: 125
Max: 28168
493.3
494.3
496.2
35
m/z

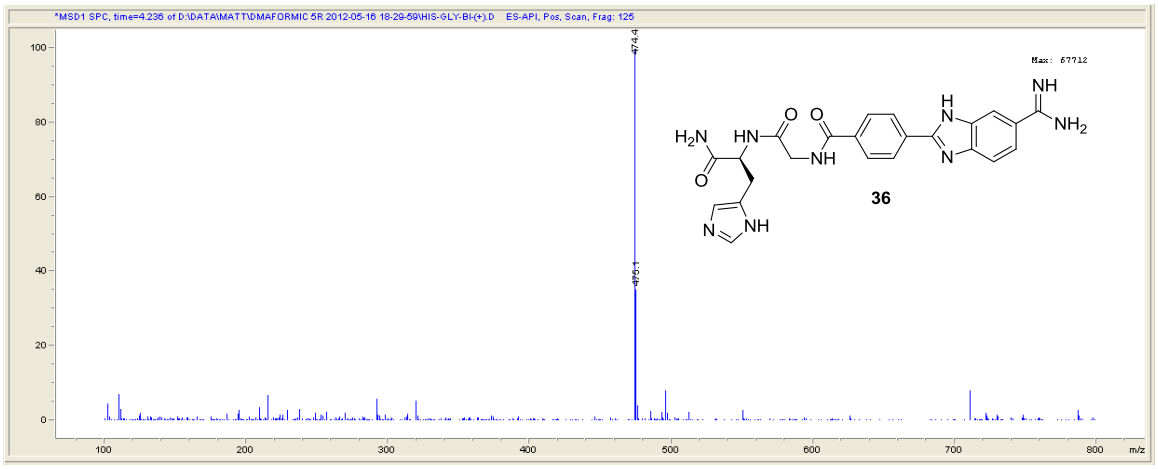
*MSD1 SPC, time=4.236 of D:\DATA\MATT\DMAFORMIC 5R 2012-05-16 18-29-59\HIS-GLY-BI-(+).D ES-API, Pos, Scan, Frag: 125
Max: 67712
474.4
475.1
36
m/z

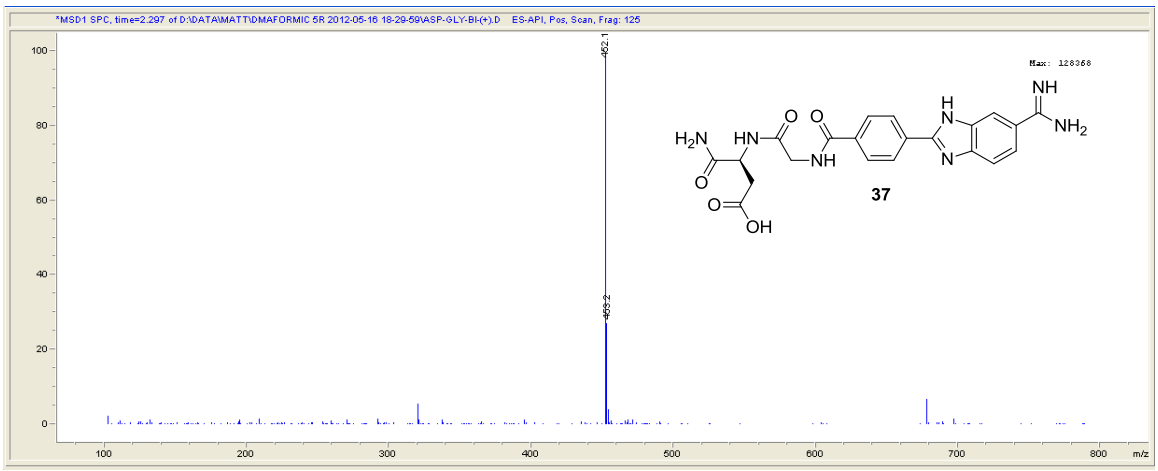
*MSD1 SPC, time=2.297 of D:\DATA\MATT\DMAFORMIC 5R 2012-05-16 18-29-59\ASP-GLY-BI-(+).D ES-API, Pos, Scan, Frag: 125
Max: 128368
452.1
453.2
37
m/z

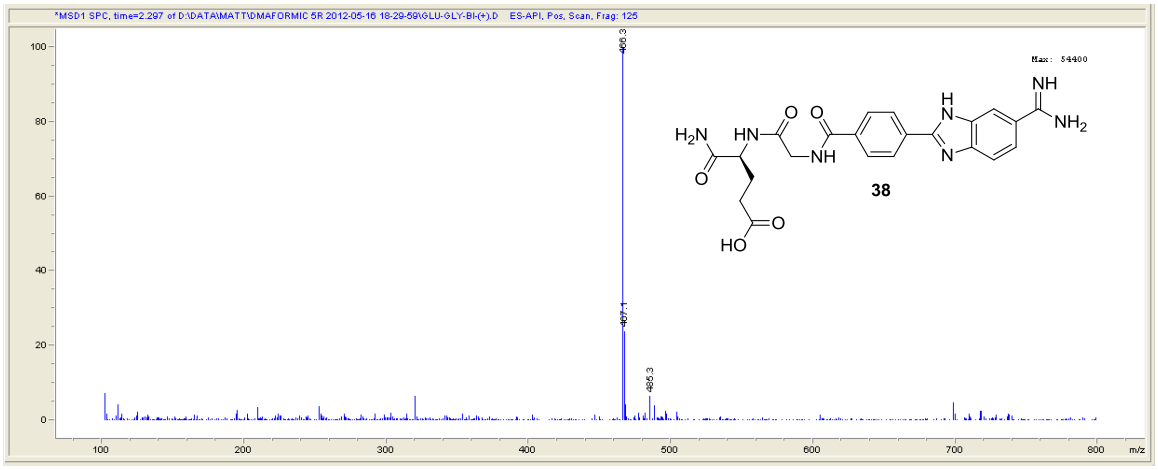
*MSD1 SPC, time=2.297 of D:\DATA\MATT\DMAFORMIC 5R 2012-05-16 18-29-59\GLU-GLY-BI-(+).D ES-API, Pos, Scan, Frag: 125
Max: 54400
406.3
407.1
485.3
100
80
60
40
20
0
100
200
300
400
500
600
700
800
m/z
38